KØBENHAVNS UNIVERSITETS INSTITUT FOR GEOFYSIK

The International Union of Geodesy and Geophysics
The International Association
of Seismology and Physics of the Earth's Interior

Papers Presented at the Ninth Assembly of

THE EUROPEAN SEISMOLOGICAL COMMISSION

Held 1-7 August 1966 in Copenhagen

Edited by HENRY JENSEN

AKADEMISK FORLAG København 1967

E.S.C.
COPENHAGEN
1966

KØBENHAVNS UNIVERSITETS INSTITUT FOR GEOFYSIK

The International Union of Geodesy and Geophysics
The International Association
of Seismology and Physics of the Earth's Interior

Papers Presented at the Ninth Assembly of

THE EUROPEAN SEISMOLOGICAL COMMISSION

Held 1-7 August 1966 in Copenhagen

Edited by HENRY JENSEN

AKADEMISK FORLAG København 1967

Published by the Organizing Committee
with the support of
the Ministry of Education and the Geodetic Institute

POLYTEKNISK TRYKKERI

C O N T E N T S

C O N T E N T S

C O N T E N T S

C O N T E N T S

P R E F A C E

The Ninth Assembly of the European Seismological Commission was held in Copenhagen 1-7 August 1966. The Commission is a body under the International Association of Seismology and Physics of the Earth's Interior, the International Union of Geodesy and Geophysics, and was as such invited to Denmark by the Royal Danish Geodetic Institute under which institution the seismic service for Denmark and Greenland is run.

An Organizing Committee was set up consisting of the following scientists:

Professor Einar Andersen, Director of the Geodetic Institute, President,

Professor Henry Jensen, the Institute of Geophysics, Secretary,

Magister J.V.Hjelme, Head of the Seismic Department of the Geodetic Institute, Treasurer,

Dr.Erik Hjortenberg, the Seismic Department of the Geodetic Institute.

The transactions of the meeting, including the synthetic reports, are intended to be published as an UGGI monograph under the editorship of the Secretary General.

In accordance with a resolution adopted at the Seventh Meeting at Jena in 1962 the host country will be responsible for the publication of the individual scientific contributions presented during the meeting. The Organizing Committee has acted as an editorial board in preparing this publication, the economic background being partly the technical facilities placed at our disposal by the Geodetic Institute, partly a generous grant from the Ministry of Education. The Organizing Committee wishes to express their sincere gratitude for this.

Manuscripts are presented in the form in which they were submitted to the Committee. In a few cases obvious errors and misprints have been corrected, but we hope that the meaning of the texts has in no case been changed.

For the Organizing Committee

Henry Jensen

Opening address by the Minister of Defence,
Mr. Victor Gram.

Ladies and Gentlemen!

On behalf of the Danish Government I am glad to extend a cordial welcome to Copenhagen to you all for the Meeting of the European Seismological Commission.

International meetings take place with increasing frequency, and I find this kind of meetings of very great value, especially when - as in the present case - there is a pronounced working programme. We have no doubt that such meetings, in the best possible way, contribute to the advancement of understanding and friendship between the nations.

From the very beginning Denmark has participated in the international collaboration in this field. Even if earthquakes fortunately do not directly interfere with the life of this country, we understand how important the scientific study of this force of nature is, and we are glad that we are able to contribute to this work in Denmark proper as well as our three stations in Greenland.

We have with pleasure noted the interest of UNESCO in this matter, not only through assistance to devastated areas, but also through a certain prevention of great damages and losses of human life through engineering improvements of buildings in threatened areas, and finally through a more scientific study of the nature and extension of the earthquakes.

I am convinced that this meeting will be important and successful. However, I also hope that the participants and the ladies will get an opportunity of receiving an impression of the country and the Danish people.

With these words and the best wishes I declare the Meeting of the European Seismological Commission open.

Victor Gram

Opening address by Professor, dr.phil. Jannik Bjerrum, vice-rector of the University.

Your Excellency, Mr.President, Ladies and Gentlemen!

As a representative of the Rector of the University, Professor Iversen, I have the honour of welcoming all the participants in the 9th Meeting of the European Seismological Commission here at the Ørsted Institute of the University.

The University of Copenhagen now disposes of chairs of different geophysical subjects: theoretical meteorology, physical oceanography, and the physics of the solid earth, and the last mentioned chair is just occupied by a seismologist who for some years has been a member of the E.S.C. - But Denmark has already for a long time been occupied with seismology, as in 1926 Professor N.E.Nørlund, at that time Director of the Geodetic Institute, through the aid of the Carlsberg Foundation, succeeded in establishing the Seismological Station in Copenhagen, which the participants later on will get an opportunity of visiting. Dr. Inge Lehmann was Chief of the Station and of the Seismological Division of the Geodetic Institute until 1953, Dr.Henry Jensen was Chief until 1965, when he became a professor at the University. Thus even if the seismological work has been done outside the University, there has constantly been a close connection, as the former Director of the Geodetic Institute, Professor Nørlund was, and the present Director, Professor Einar Andersen is attached to the University as a full professor.

Therefore the University is particularly glad to be able to provide a setting for a geophysical meeting with participation from about 25 different countries.

Seismological research is a science of great importance to mankind, considering the great catastrophes caused now and then by earthquakes at many places in the world, and it is also a science which is important as a tool to identify nuclear explosions all over the world. By studying the programme I have understood that the main subject of this meeting will be conditions concerning the Upper Mantle, but being no expert myself I shall not go into details. I should like to conclude by expressing my whishes that the lectures will give rise to lively discussions, and a hope that all the participants will return to their home countries with a scientific as well as a social profit from this meeting in Copenhagen.

Jannik Bjerrum

Discours fait par le Professeur E.Andersen.

Votre Excellence, Monsieur le Prorecteur, Monsieur le Président, Mesdames et Messieurs!

À titre de Président du Comité National Danois de Géodésie et de Géophysique et à titre de Directeur de l'Institut Royal de Géodésie de Danemark je vous souhaite cordialement les bienvenus à la réunion de la Commission Séismologique Européenne. Je remercie le Ministère de Défense de l'autorisation à inviter à cette réunion, et je remercie la Commission d'avoir accepté cette invitation. Je remercie Monsieur le Ministre de Défense d'être venu et de faire l'ouverture de notre réunion particulièrement solenelle. Je remercie l'Université de Copenhague pour la permission d'emprunter des salles de réunion ici à l'Institut H.C.Ørsted et je remercie Monsieur le Prorecteur d'être présent pour nous adresser des paroles de bienvenue. Je vous prie de transmettre nos remerciements au Recteur, Monsieur le Professeur Iversen, quand il sera de retour de ses vacances dans la Grèce.

Quelques-uns de vous seront peut-être étonnés que la séismologie au Danemark soit administrée par l'Institut Géodésique, mais sans doute il a été au bénéfice de la séismologie d'appartenir à un grand institut, travaillant intensivement, avec toutes les fascilités que cela implique. En effet, comme une curiosité je tiens à mentionner qu'il y a un peu plus de 40 ans j'ai commencé ma propre carrière dans l'Institute par du travail séismologique.

Comme il a été dit déjà, notre station à Copenhague fut établie en 1926, mais il y a un commencement danois de date encore plus ancienne, car le savant naturaliste, M.Porsild établit déjà en 1910 une station séismologique primitive à sa station arctique à Godhavn sur l'île de Disco à l'ouest du Groenland. Cette station arctique appartient maintenant à l'Université de Copenhague. Ses instruments étaient très primitifs, et surtout il y avait des difficultés à faire le service horaire, car c'était avant l'époque du radio.

Ainsi, l'intérêt du Danemark à la séismologie est à la fois vieux et intensif. Il nous fait donc bien du plaisir de collaborer avec des séismologistes partout dans le monde et de contribuer au développement de cette science.

Je finis mes paroles de bienvenue en exprimant mes meilleurs voeux pour l'importance scientifique de notre réunion.

Einar Andersen

PRESIDENTIAL ADDRESS

by

A.Zátopek

Excellences, Magnificence, Mr.Chairman, Ladies and Gentlemen, Dear Colleagues!

Following the kind invitation, generously extended to the European Seismological Commission by the competent Danish authorities, the foregoing VIIIth General Assembly, held in Budapest in September 1964, decided to organize the IXth General Assembly, which we are going to open, in Copenhagen from 1st till 7th August 1966. Allow me please to use the privilige to express, in the name of the E.S.C., our deeply felt gratitude for this invitation and to thank the representative of the Government of the Kingdom of Denmark, His Excellence, Minister of National Defence, Victor Gram, His Magnificence, Professor Dr. Jannik Bjerrum, Vice-Rector of the University of Copenhagen, and the President of the Organizing Committee, Professor Dr. Einar Andersen, Treasurer of the I.U.G.G., for their kind and cordial words of welcome and their good wishes addressed to our Assembly. I have the honour and pleasure to extend our most cordial greetings to Professor Rothé, Secretary General of the International Association of Seismology and Physics of the Earth Interior, to Professor Knopoff, Secretary General of the International Upper Mantle Committee, and to Dr. Fournier d'Albe, representative of UNESCO.

The local E.S.C. Organizing Committee has prepared for us quite excellent living and working conditions. It was an enormous work done by Professor Andersen as President, Professor H.Jensen as Secretary and the staff of the Committee and we are very much indebted to all of them.

We are happy that we were given the opportunity to come to this lovely land and old culture country and to pay a visit to this beautiful capital which has also a rich and living tradition in developing Science. From the number of famous scientists of this country I would remember only three names, which, in my opinion, are quoted among the

greatest one of the world: Tycho Brahe, the best observer of all times, whose life, work and death are connected also with my own country, and Hans Christian Oersted, discoverer of the interaction of the electric current and the magnetic field and founder of a systematic study of the electromagnetic field as a new branch of Physics, and Niels Bohr who opened with his atom model a new epoch in the history of mankind. And when speaking of Seismology, may I express our admiration for the splendid work of our honoured and beloved Miss Lehmann, who was one of the founders of the E.S.C.

In view of all this, we feel a heavy burden of responsibility; therefore we will and must do our best to have an Assembly, the level of which would be as high as possible. That represents a rather difficult task because of the programme, too rich relatively to the time at our disposal.

There are the following subjects on: We are to control the stage of implementation of Resolutions adopted in Budapest and to review the research work done by E.S.C. Sub-Commissions and Member Countries. Thereafter, we shall hear and discuss the reports and original scientific contributions, as presented to our Assembly. Further, it will be necessary to summarize our conclusions and fix the lines for the future work of the E.S.C. in resolutions which should facilitate the realization of the programme adopted. Moreover, there are administrative and organizational matters to be dealt with.

Therefore, some measures have been taken which appeared unavoidable: The working time set down for several days is longer than usually, and some parallel sessions of Sub-Commissions are foreseen in our time table; in addition, the time for reports and scientific communications has been strictly limited. I would like to ask the participants of our Assembly for understanding in point of these unpopular necessities. Our Secretary General has done his best to minimize these collisions which are a consequence of the great increase of the E.S.C. activities, while the length of time foreseen for the General Assemblies remained practically unchanged.

In order to ensure more time for discussions, a system of invited reporters, combined with presentation of individual scientific contributions, was suggested for this Assembly, already in Budapest. One presumed a necessary selection of papers to be made by the Presidents of the Sub-commissions or Working Groups in consideration.

The correctness of this idea was called in question by Professor Caloi who expressed his doubts regarding the possibility to include or exclude a contribution on the basis of a summary of some 15 lines only. He warned also against an excessive specialization of the E.S.C. Sub-Commissions and Working Groups because it could be, in opinion of Professor Caloi, the cause of loosing large horizons of Seismology as a whole. He recommended to have, from time to time, somewhat like discussion meetings related to actual questions, but without scientific communications. Another question was rised by President Hodgson whether it would not be better to organize the E.S.C. as a body independent of the Association of Seismology and Physics of the Earth's Interior, as e.g. the Seismological Society of America. There were also some organizational proposals by Dr.Ritsema. The Bureau of the E.S.C. highly appreciated these critical comments because they contained several correct and constructive ideas and were motivated by the purest interest in the benefit of the E.S.C., and aimed the maximal effectiveness of its activities. Therefore, the Assembly should carefully discuss these questions, too.

A further important subject should be a discussion about the development of a closer co-operation with UNESCO, and also, perhaps, some further steps to be taken in connection with the Upper Mantle Project in view of the progress made in deep seismic soundings during the last two years.

On the whole, the period since the Budapest Assembly was an active one, and the present Assembly in Copenhagen should become a further milestone at the way ahead of the European and the World Seismology. Now I have the honour and pleasure to declare the IXth General Assembly of the E.S.C. open, and address my best wishes of success to its participants.

S.I.Subbotin, V.B.Sollogub,
A.V.Chekunov, L.P.Livanova

CRUSTAL INVESTIGATIONS OF EAST CARPATHIANS AND ADJOINING REGIONS BY MEANS OF DEEP SEISMIC SOUNDING

Deep seismic sounding is at present the main method of crustal studies. This method provides us with the most exhaustive and precise information concerning the structure and physical properties of the Earth's crust and upper mantle. Deep seismic investigations not only allow to define the hypsometry and elastic properties of the main seismic interfaces, but also to trace the zones of deep fractures. These major geostructural elements are responsible for the discrete block character of the crustal structure. Their detection is especially important since they are usually the channels through which - from the mantle into the upper strata of the crust - the substance penetrates containing various useful mineral abundances.

In view of the great importance of deep seismic investigations the geophysical commission of the Carpatho-Balcan Geological association and the VII regional conference of the participant countries of the Euro-Asian region have laid down a program of investigations of the Earth's crust and upper mantle in the Carpatho-Balcan region and adjoining territories.

During the execution of the said plan the Research Institute of Geophysics of the Ukrainian Academy of Sciences in 1965 started investigations along the III international profile across the territory of the USSR, Hungary and Jugoslavia.

The studies have been carried out in the north-eastern part of the profile III crossing the Volyno-Podolski slope of the Russian Platform, Transcarpathian edge depression and partly the meganticlinorium of the East Carpathians.

In 1966 the investigations are being carried out in the region of the Carpathians, Transcarpathian depression, and zone of its junction with the Pannonian Middle Massif. In the last mentioned area the field works are being fulfilled as a collaboration between Hungarian and Soviet geophysicists. A unified system of travel-time curves has been compiled, the geophysicists of each country working on their own territories.

In 1965 investigations along the profile III were carried out by means of continuous longitudinal profiling giving travel-time curves for all main interfaces of the Earth's crust as well as its bottom - the Mohorovičić discontinuity (M). Distance between the shot-points in studies of the upper crustal layers is 10 - 30 km (Fig. 1) and in deep crustal studies 35 - 60 km. The length of the travel-time curves is correspondingly different: in the first case it was 90 - 110 km, in the second case it amounted to 170 - 200 km. In the zones of complex tectonics as, for instance, in the Forecarpathian depression and sections of its junction with the Russian Platform and folded Carpathians, the longitudinal profiling was supplemented by the non-longitudinal observations from the remote shot-points. A great number of spot soundings were performed in order to find depths to the Moho across the area.

The recording equipment consisted of geophones with $f_{resonance}$ = 10 - 11 cps and low frequency 60-channel seismic stations whose amplifiers transmitted frequencies 6 - 20 cps. Explosions were produced in boreholes having a depth about 30 metres; the charge at great distances from the shot-point to the recorder amounted to 300 - 700 kg, sometimes, under adverse conditions, it was 1,0 - 1,5 tons. Normally not more than 50 kg of TNT or 150 - 200 kg of powder were taken per one borehole. If the charge exceeded the said amount of the explosive matter the borehole grouping was used.

All the waves recorded can be classified in the following way:

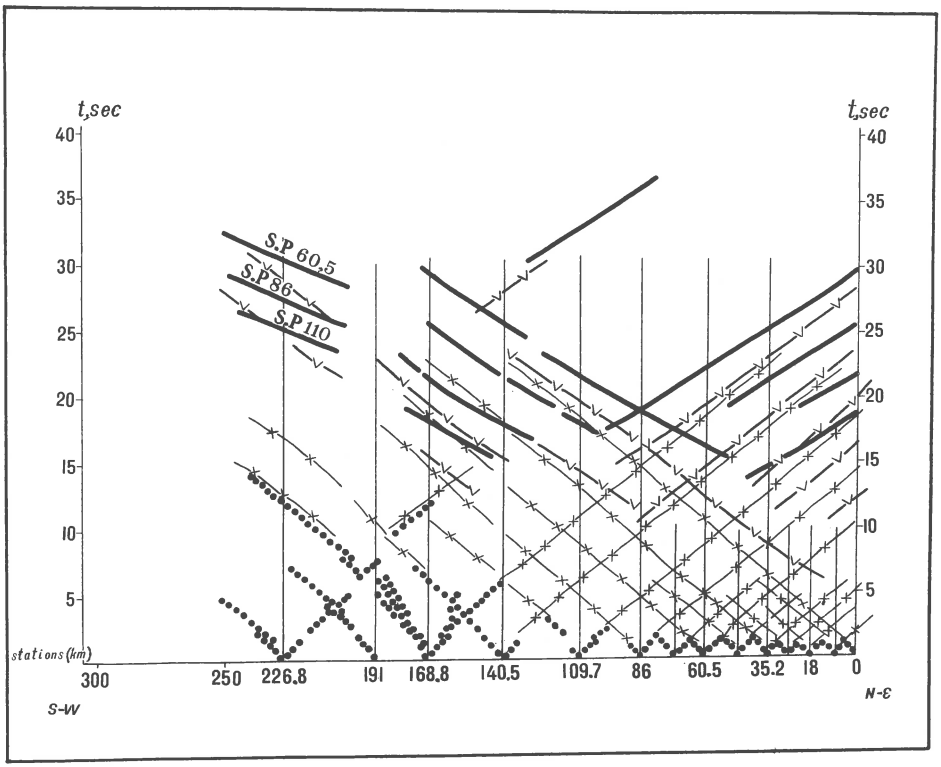

Fig. 1: Diagrammatic travel-time curves of the waves recorded on the profile Vishnevets-Dolina-Beregovo.

1) Waves from the interfaces within the sedimentary layer; 2) Waves from the surface of the "granitic" layer and from the interfaces within it; 3) Waves from the "basalt" surface; 4) Waves from the Moho discontinuity.

Waves from the seismic interfaces in the sedimentary cover;

waves from the basement surface and interfaces within the "granitic" layer;

waves from the surface of the "basaltic" layer and interfaces within it;

waves from the Moho discontinuity.

The character of the waves from the sedimentary cover varies from one region to another. On the south-west slope of the Russian Platform, where almost the whole sedimentary cross-section is represented by the platform-type palaeozoic deposits, a considerably weak velocity differentiation of the cross-section is characteristic with rather high values of the layer velocities. A number of reflectors are distinguished, the most typical of which are the Lower Silurian and Upper Devonian ones, having boundary velocities about 6 km/sec. The reflectors are dipping flatly to south-west towards the Forecarpathian depression.

In the Transcarpathian depression a series of low velocity waves (3 - 4 km/sec) appear which are associated with the seismic horizons in the younger deposits forming the depression.

In the folded Carpathians such velocities are very seldom observed; as the first arrivals at small distances from the shot-point the waves with velocities 4,5 - 5,5 km/sec are recorded which are characteristic of the Mesozoic-Palaeogenic complex. These waves attenuate sharply at the transition to the Forecarpathian depression which fact allows distinct location of the frontal part of the Skibian zone thrust fault of the folded Carpathians which thrust fault overlaps the inner zone of the depression. In the folded Carpathians the boundaries of the main structural zones can be clearly distinguished by the anomalous complications of seismic traces and due to the appearance of the local high-velocity waves.

The basement surface (of the "granitic" layer) is generally defined by the wave velocity of 6,0 - 6,2 km/sec. This wave is considered refracted head wave penetrating inside the basement crystalline cover due to the gradient increase of the velocity with the depth in its upper part.

Within the "granitic" layer several intermediate refractors with velocities of 6,3 - 6,5 km/sec are revealed. These horizons are not distributed throughout the "granitic" layer; but in crustal blocks, separated by the fractures, different

horizons are observed; in several blocks they are not distinguished at all. In most cases the kinematic characteristics of the waves from the "granitic" layer are almost identical which means that the corresponding kinematic criteria of the wave identification are losing validity. At the same time the dynamic features which cannot be neglected in the correlation and interpretation become of greater significance. Determination of nature and coordination of the waves is a complicated procedure which requires rather intricate systems of travel-time curves together with the continous profiling.

From the "basaltic" layer surface reflected waves are obtained which in the beyond-critical region are transformed into the head waves. The head waves from the "basalt" with the velocities of 6,8 - 7,0 km/sec are recorded as first arrivals at the distance of 165 - 170 km from the shot-point. Within the "basalt" the existence of several intermediate seismic interfaces is stated.

The Moho discontinuity is characterized by strong beyond-critical reflections which can be easily traced among the rest of the waves at distances 100 - 180 km from the shot-point. These reflections are recorded as a group of interference waves with frequent attenuation of certain phases and appearance of the others. In view of such a character of the records the phase correlation is strongly restricted. Total duration of recording a group of waves reaches 0,8 - 1,0 sec.

By the travel-time curves of the first arrivals as well as by numerous subcritical reflections (recorded in the vicinity of the shot-points at the times 3 - 15 sec) the velocity cross-section of the Earth's crust has been constructed. Calculation of velocities by the travel-time curves of the first arrivals was carried out on electronic computers using subcritical reflections. Velocities were determined by conventional techniques with help of statistical averaging. Mean velocity up to the "basalt" surface is 6,0 km/sec, and up to the Moho discontinuity 6,4 - 6,5 km/sec. Velocity differentiation of crustal layers is very small. The time-

depth curve thus obtained can be approximated either by a broken line or by a smooth curve. By the first method the Earth's crust is pictured as a homogeneous layered medium, by the second method as an inhomogeneous medium where the velocity increases continuously with depth. Most probably there is, in fact, a combination of both phenomena, that is, we deal with the inhomogeneous layered medium where small velocity jumps occur at interfaces between the layers, and in the layers themselves the velocity increases gradually with depth. The gradient of velocity is especially apparent for the upper consolidated crust.

According to the materials of investigations a preliminary seismogeological cross-section has been constructed (Fig. 2). It can be seen from the said cross-section that the Precambrian basement of the Russian Platform dips flatly in western direction from the depth 1,5 km in the extreme north-east of the profile, in the Vishnevets area, to 5,5 - 6,0 km in the region of the Dniester river. The smooth subsidence of the basement is complicated by a flexure bend in the vicinity of the stations 100 - 135 where the rate of the basement subsidence is considerably increased. At the boundary between the Russian Platform and the Forecarpathian depression a large fault is traced along which the basement dips sharply into the depression. The depth to the basement increases by 2 km, and in the outer zone of the Forecarpathian depression it is estimated to be 7,5 - 8,0 km. A still larger rupture dislocation is found at the boundary between the inner and outer zones of the depression. Here the basement, evidently represented by younger formations of palaeozoic age, subsides sharply by 3 - 4 km and the depths to it reach 10 - 12 km. Towards the folded Carpathians the basement uplifts ledgelike, in the meganticlinorium zone the depths amount to 3 - 6 km.

The "basaltic" layer surface within the south-west slope of the Russian Platform lies at depths of 19 - 22 km, being inclined in western direction, towards the Carpathians. In the eastern direction towards the Ukrainian shield an uplift of the "basaltic" surface is traced. The uplift seems

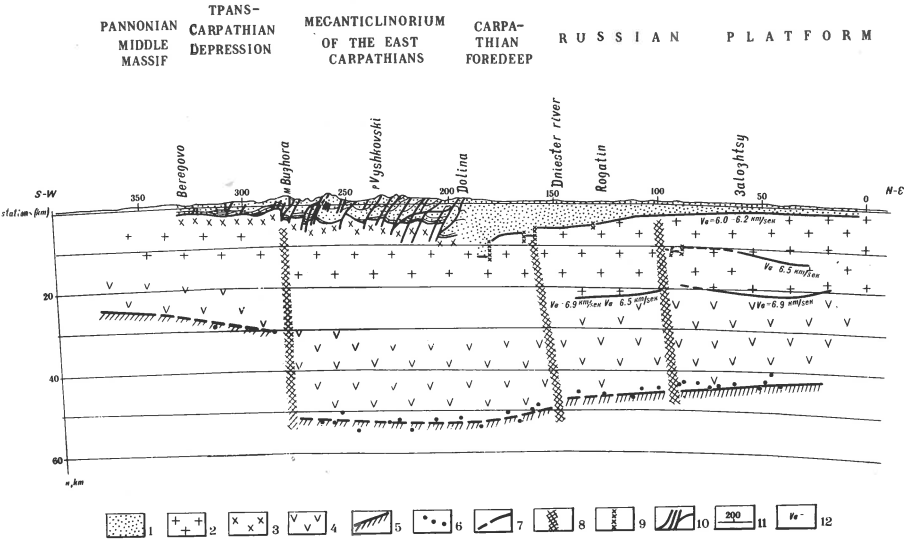

Fig. 2: Seismogeological cross-section of the Earth's crust along the profile Vishnevets-Dolina-Beregovo.

1) Sedimentary layer; 2) "Granitic" layer; 3) Metamorphic rocks of the Palaeozoic age in the "granitic" layer; 4) "Basaltic" layer; 5) Moho discontinuity; 6) Individual spot determinations of the depths to the Moho discontinuity; 7) Seismic interfaces; 8) Deep fractures; 9) Large fractures; 10) Fractures in the Carpathians according to some geological evidence; 11) Shot-points of the deep seismic sounding profile (in km); 12) Boundary velocity.

to continue farther in the eastern direction beyond the profile. Actually on the profile extension within the shield (the Korosten Pluto) the seismic horizon with the velocities of 6,6 - 7,0 km/sec is traced by means of our investigations at a depth of only 3 - 5 km. On the same area in the Korosten Massif the gabbro rocks constitute outcrops.

Subsidence of the Conrad discontinuity towards the Carpathians is complicated by a rupture dislocation in the region of the station 90; to the west from the dislocation the rate of subsidence increases. It is necessary to point

out that the rupture is located in the area where the above mentioned flexure begins along the basement surface. As a whole the "basalt" topography qualitatively coincides with the basement topography, echoing it. For that reason the thickness of the "granitic" layer on the south-west slope of the Russian Platform is practically unchanged.

The structure of the Moho surface has been studied not only along the profile, but throughout the area as well. This became possible due to the numerous "spot" determinations at various points, situated at a distance of 100-130 km from the shot-points of the main profile, i.e. at distances which are optimal for recording the beyond-critical reflections from the Moho discontinuity. Identification of the waves reflected from the Moho discontinuity presented no difficulty on account of their great dynamic expressiveness. The results obtained allowed compilation of a hypsometry scheme of the Moho discontinuity using the data gathered along the main profile (Fig. 3).

According to the scheme as well as to the cross-section (Fig. 2) one can see that from north-east and south-west the Moho discontinuity dips towards the folded Carpathians. At the beginning it dips smoothly. On the Russian Platform slope the depths increase slowly from 42 to 47 - 48 km in the Dniester area. Only in the region of the stations 85 - 90 the subsidence seems to be complicated by a fracture. In the area of the Dniester river along the large fracture the Moho discontinuity is faulted by 5 km towards the Carpathians. Beyond the fracture the depths increase to 52 - 53 km.

From the south-west - more exactly from the Pannonian Middle Massif towards the Carpathians - the depth to the Moho discontinuity at first also increases slowly from 25-30 km. In the link zone of the folded Carpathians and the Transcarpathian depressions the smooth subsidence is complicated by a very large deep fracture along which the Moho discontinuity dips under the Carpathians to the depths of 50 - 52 km. The vertical displacement of the Moho discontinuity along this fracture thus amounts to about 20 km.

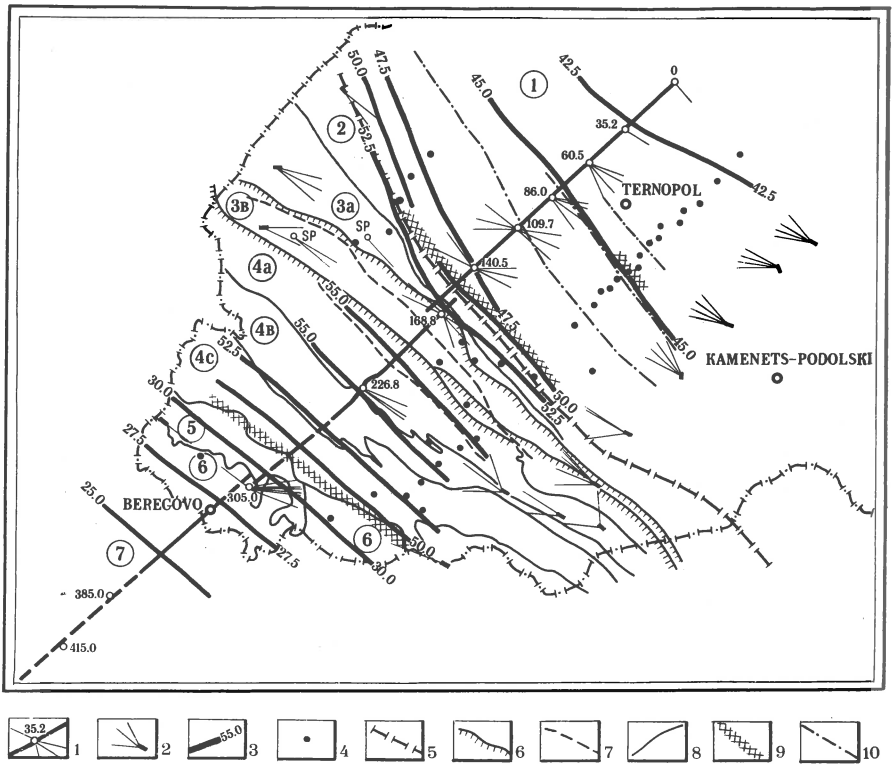

Fig. 3. Diagram of equal depths to the Moho discontinuity (M) in the East Carpathians and adjacent regions.

1-Deep seismic sounding profile with shot-points; 2-Encampments of individual seismic stations which recorded the waves from the Moho discontinuity outside the deep seismic sounding profile on basis of explosions on the said profile; 3-Equal depths to Moho (in km); 4-Points where depths to Moho have been determined outside the deep seismic sounding profile by records of individual seismic stations; 5-Boundaries of the Russian Platform; 6-Thrust line of folded Carpathians over the Forecarpathian depression and of the inner zone of the said depression over the outer one; 7-Position at depth of the boundaries between folded Carpathians and the inner and outer zones of the said depression; 8-Boundaries of individual tectonic zones; 9-Large abyssal fractures; 10-Ancient fractures of the Russian Platform.

Symbols in circles:

1-Russian Platform; 2-Buried caledonides; 3-Forecarpathian foredeep: a) outer zone, b) inner zone; 4-Meganticlinorium of the East Carpathians: a) outer anticlinal zone, b) central synclinal zone, c) inner anticlinal zone; 5-Vygorlat - Gutino volcanic ridge; 6-Transcarpathian depressions; 7-Pannonian Middle Massif.

Under the Carpathians the depths reach 55 - 57 km, sharp differences of values being observed throughout the area, sometimes at closely situated points which are indicative of the great diastrophism and fractured character of the Moho discontinuity. It is worth while mentioning that the area of maximum depths to the Moho discontinuity is displaced to the north-east with reference to the axial part of the meganticlinorium, which fact is in agreement with the position of the regional gravitational minimum of the Carpathians. The "root" formed by the Earth's crust is considerably wider than the mountain structure of the Carpathians, it encompasses also the Forecarpathian depression area.

The investigations performed make it possible to distinguish the largest deep fractures of the region. The fractures limiting the Carpathian "root" in south-west, Transcarpathian, and north-east, the Dniester river area, are undoubtedly related to such. These fractures intersect the Moho discontinuity and cause its sharp vertical displacement.

A large ancient deep fracture is traced also on the south-west slope of the Russian Platform, in the area of stations 90 - 100. This fracture is manifested as a flexurelike bend of the basement surface, a rupture of the "basalt" surface along which there is a vertical displacement and rupture of the Moho discontinuity. The fracture separates crustal blocks with different intermediate (in the "granite" and "basalt") seismic interfaces terminating in the dislocation zone or appearing after it. In the fracture zone magnetic anomalies are observed; the gravity field in the same area sharply changes its character from the mosaic into the strip-like type. The fracture dips steeply to the north-east far into the Russian Platform.

A similar dip is characteristic of a deep fracture breaking the Moho surface in the Dniester river area and reaching the upper crust in the link zone between the Russian Platform and the Forecarpathian depression. Comparing this evidence with the data obtained for the Crimea and the north-

western Forecaucasus, it is possible to state the general tendency: deep fractures of the south marginal part of the Russian Platform as well as of the adjoining regions dip everywhere to the north under the Platform.

Thus, the investigations along the III international profile proved the existence of the "roots" along the Moho discontinuity in the Carpathian area, presence of large deep fractures separating main geological megastructures, sharp variation of the crustal thickness, etc.

The last mentioned phenomenon may be ascribed as well to vertical movements of crustal layers as to physico-chemical processes occurring in the Earth's crust.

It is necessary to point out that the horizontal displacements in the upper part of the sedimentary cover in the Carpathians and Forecarpathian depression are probably associated with the deep fracture, whose amplitude reaches 20 km, and which separates the Carpathians from the Transcarpathian depression and Pannonian Massif.

Deep seismic investigations along the international profile III carried out in cooperation of the Soviet, Hungarian, and Jugoslavian geophysicists on their own territories make it possible to obtain a continuous cross-section of the crust from the ancient Russian Platform, across the East Carpathian meganticlinorium, Pannonian Middle Massif, folded construction of Dinarides to the Adriatic sea.

V.B.Sollugub, N.I.Pavlenkova, A.Y.Diachkova

PHYSICAL PECULIARITIES OF THE UKRAINIAN CRUSTAL BLOCKS

The Earth's crust of the Ukraine - from the Black Sea to Voronezh Massif - has been studied by means of deep seismic sounding. The profile crosses the Black Sea depression, the Alpine folding of the Mountaneous Crimea, the Hercynian platform, the Ukrainian shield, the Dniepro-Donetsk depression, and the Voronezh Massif.

The thickness of the Earth's crust and its layers is found to be in a certain relation to the upper crustal structure. The thickest crust and the maximum thickness of the so called "basaltic" layer with P-velocity from 7 to 8 km/sec are characteristic of the shield areas and the Alpine folded region of the Mountaneous Crimea, the minimum thickneses being in the regions of the Dniepro-Donetsk and Black Sea depressions. The total thickness of the sedimentary cover and the "granitic" layer (with the velocity from 6 to 7 km/sec) along the whole profile remains almost constant (except for the Bielozerka upheaved block), and the inverse dependence between thicknesses of the said layers is observed, namely, the more sediments the smaller the thickness of the "granitic" layer (see Fig. 1).

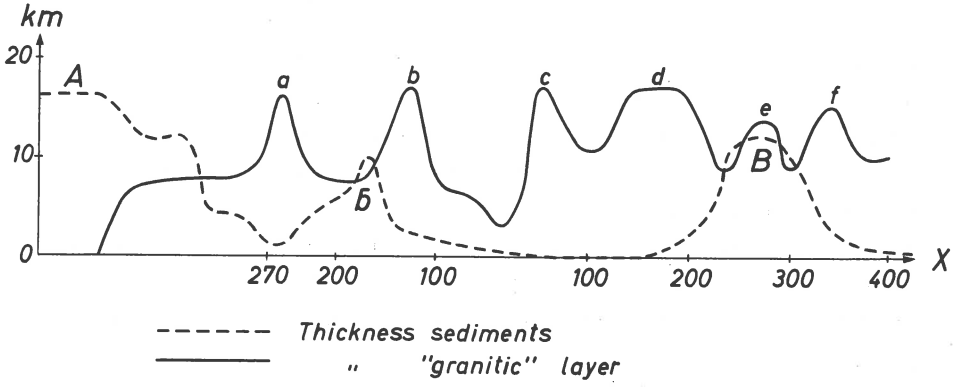

Fig. 1. Graph of sedimentary and "granitic" layer thickness variations.

Such dependence confirms to a certain degree the hypothesis of formation of granites from sediments. This hypothesis being considered true, a conclusion should be drawn that in the vicinity of the contemporary depressions ancient synclines with great thickness of sediments existed which were consequently transformed into the "granitic" layer. In this case sharp variations in thickness of the "granitic" layer observed on many deep seismic sounding profiles can be easily explained.

Formation of contemporary and ancient synclines and depressions took place because of existence of deep fractures. These are clearly defined in the course of seismic investigations by a number of characteristic features: seismic discontinuities, diffraction points, steep-dipping seismic boundaries etc. The detailed analysis of seismic data with consideration of gravimetry results allows not only to define deep fractures, but also to characterize physical properties of each block. For such specification we have investigated the following parameters of the medium: variation of mean velocities along the profile, boundary velocities at the transition from one block to another, intensities of waves refracted and reflected at the discontinuities, number of seismic interfaces, densities of rocks in the blocks according to gravimetry data, and elastic properties and densities of the crystalline and metamorphic rocks according to laboratory analysis.

A. For estimation of mean crustal velocities the first arrivals were used which were considered direct refracted waves and reflections from the Moho discontinuity.

In terms of the first arrivals velocities were defined by means of the well-known equations of Wiechert-Tchibissov and Kondratiev, where by a section of the travel-time curve, (characterized by arrival-time t, distance x from the shot-point, apparent velocity V^*, and t_o) it is possible to calculate the mean velocity to the maximum depth of the ray penetration $H = \frac{V_{mean}\, t_o}{2 \cos i}$, where $\sin i = \frac{V_{mean}}{V^*}$. By means of these equations for each shot-point a complete chart of mean velocities can be compiled.

Using reflected waves only the mean velocity to the Moho discontinuity can be defined.

For the more detailed characteristics of mean velocities of the "granitic" layer the misalignment curves of the first wave according to the overtaking travel-time curve were used; in terms of τ the gradient β of velocity increase with the depth is calculated.

All the velocity data obtained are presented on a velocity column (Fig.2) and a graph of mean velocity variations along the profile (Fig. 3B).

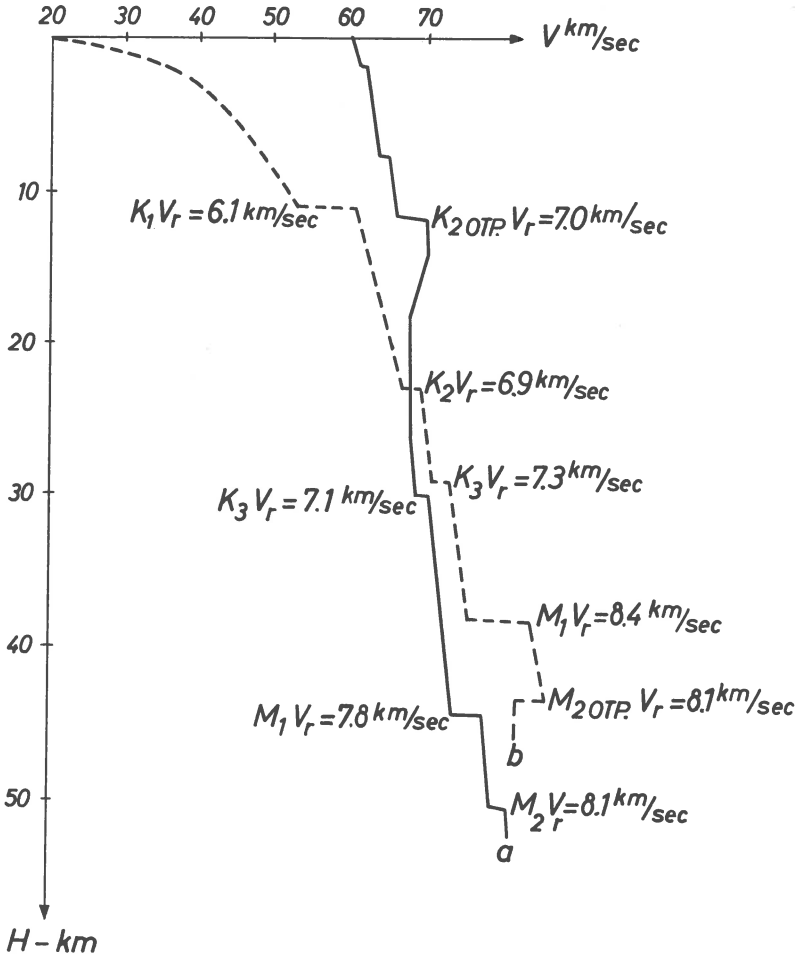

Fig. 2. Velocity column of the Earth's crust

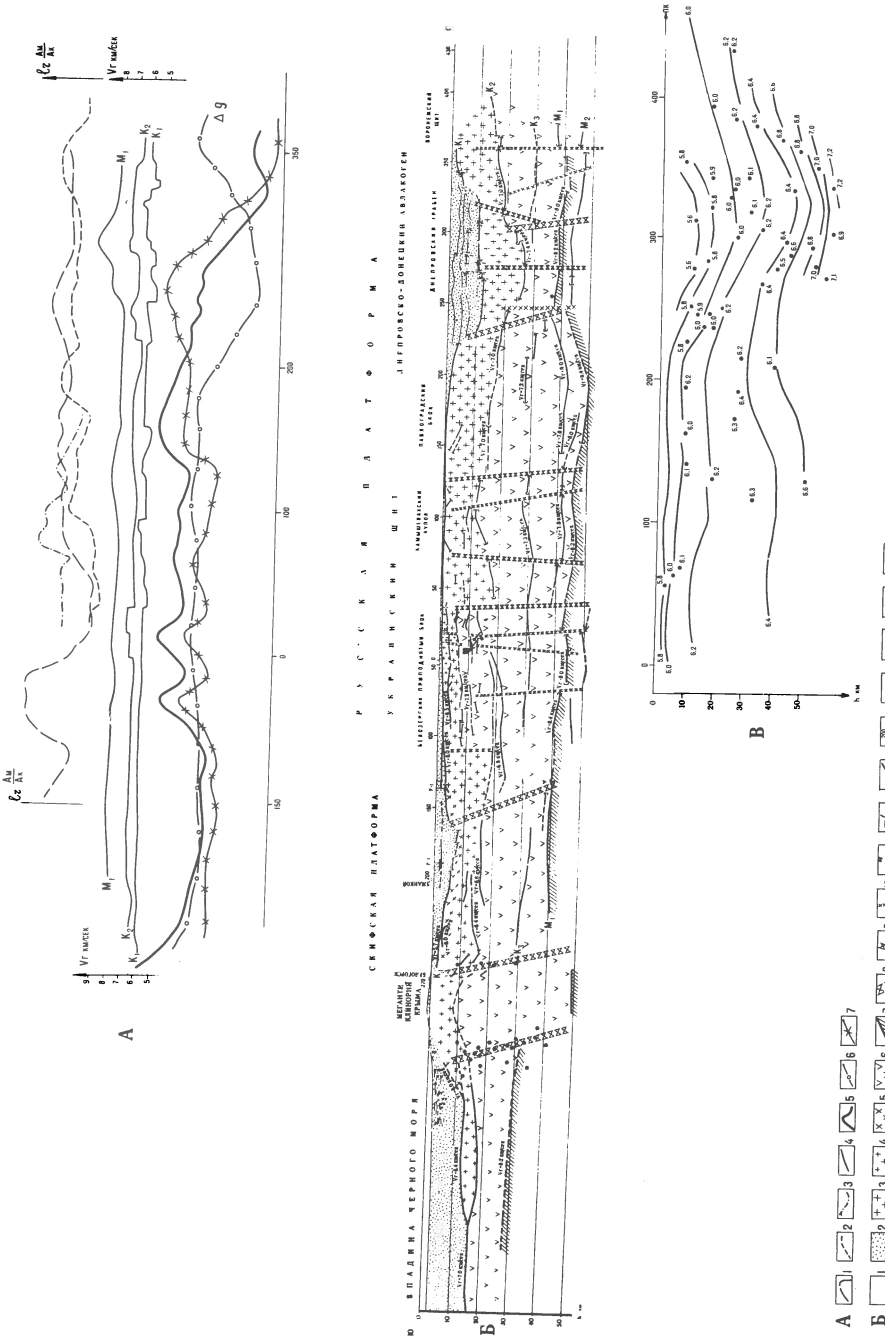
А
Б
В
Δ g
Vг км/сек
Vг км/сек
h, км
ВПАДИНА ЧЕРНОГО МОРЯ
СКИФСКАЯ ПЛАТФОРМА
УКРАИНСКИЙ ЩИТ
ДНЕПРОВСКО-ДОНЕЦКИЙ ПРОГИБ
РУССКАЯ ПЛАТФОРМА

Fig. 3

Fig. 3, А. 1) Curves of amplitude ratios of the P^m and P_2^k waves by direct travel-time curves. 2) Same for the counter travel-time curves. 3) Ratio graph of amplitudes of P_1^k and P^k converted waves. 4) Graphs of boundary velocities for the interfaces K_1, K_2 and M. 5) Observed gravity curve. 6) Calculated gravity curve by the topography of seismic interfaces. 7) Difference gravity curve.

Б. 1) Water table. 2) Sedimentary layer. 3) "Granitic" layer. 4) Metamorphic rocks of the Byelozerka series in the "granitic" layer. 5) Metamorphic rocks of the palaeozoic-trias-jurassic age in the "granitic" layer. 6) Basaltic layer. 7) Mohorovičić discontinuity. 8) Deep fractures, separating main regions. 9) Deep fractures, subdividing separate crustal blocks. 10) Same with less certainty. 11) Fractures within separate blocks. 12) Dislocations along the basement surface and sedimentary cover. 13) Seismic interfaces. 14) Points of the profiles (in km). 15) Boundary velocity. 16) Boreholes. 17) Earthquake foci. 18) Difraction points.

В. 1) Mean velocity values. 2) Lines of equal mean velocities.

The velocity column has been compiled in the following way. The general character of mean velocity variations with the depths is derived on the basis of mean velocities calculated from the first arrivals. Seismic interfaces were represented on the graph as velocity jumps, being taken larger for the reflecting discontinuities than for the refracting ones. If the wave associated with a certain layer is a refracted one, and not a head wave, the said layer has a gradient of velocity increase with depth.

From Fig. 2 it can be seen that the greatest contrasts of crustal velocities occur in the lower layers; for the Ukrainian shield (A) we have a smooth increase of velocities with depth, in the Dniepro-Donetsk depression (B) they increase more rapidly and the depth of 45 km in the bottom of the crust a layer with the increased velocity of 8,2 - 8,4 km/sec is distinguished.

For the mantle substance, however, in the region of the Ukrainian shield velocities are probably larger than in the region of the Dniepro-Donetsk depression and Voronezh Massif.

On fig. 3B a graph of mean velocity variations along the profile is shown, the effect of the sediments during the compilation of the said graph being excluded.

It can be seen from the drawing that in the Earth's crust on the central part of the Dniepro-Donetsk depression a sharp change of mean velocities occurs: increased velocities are characteristic of the southern part of the profile - the Ukrainian shield, the lower velocities are observed in the Voronezh Massif region. Considering the behavior of the isolines of the mean velocities we can distinguish two main blocks of the Earth's crust, on the boundary of which blocks the Dniepro-Donetsk graben was formed.

A considerably sharp contrast of velocity values occurs also in the region of the Devladovo fracture which results in the increased velocities in the Pavlograd block. A velocity jump for the "granitic" layer is observed in the region of the Nikopol dislocation.

The relationship mentioned is well confirmed also by graphs of the boundary velocities (Fig. 3A): in the centre of the Dniepro-Donetsk depression V_b along the Moho discontinuity increases sharply from 8,1 to 8,4 km/sec. Other crustal blocks are also differentiated by boundary velocities: increased velocities 7,0 - 7,4 km/sec are characteristic of the "basaltic" layer of the Byelozerka block, while for the Moho discontinuity lower velocities of 7,8 - 8,0 km/sec are obtained. Velocity jumps along all the horizons are observed in the region of the Nikopol and Devladovo fractures.

B. To characterize different crustal blocks the dynamic properties of the depth waves were used, namely their variability along the profile. The variations of wave intensities are supposed to describe the change of physical properties of the discontinuity.

It is necessary to point out that in the territory of the Ukrainian shield where the thickness of sediments is small (10-200 m) the contacts of separate blocks represented by different petrographic varieties are very distinctly seen from the dynamic characteristics of the PSP - or PSS - type wave.

The amplitude-ratio curves of the waves from the Mohorovičić and Conrad discontinuities also give some grounds

for a characteristic of physical state of the crustal bottom. So the minimum points of these curves correspond, as a rule, to dislocated zones along the Moho discontinuity.

For characteristics of variations of the seismic interface peculiarities at the transition from one block to another the types of the recorded waves were considered. It is stated, for instance, that at the transition from the Pavlograd block to the Dniepro-Donetsk depression the features of the Moho discontinuity are changed, in the first case only the beyond-critical waves were recorded, in the second case head waves were also included. The same phenomenon is observed for the "basaltic" layer surface in the Byelozerka block region; from the said discontinuity distinct reflections are recorded; for other blocks reflections from the Conrad discontinuity were not obtained.

A similar important feature of the cross-section is its stratification. In this respect the blocks of the Ukrainian shield are sharply differentiated from one another. The Pavlograd block is characterized by a relative homogeneity and absence of seismic interfaces within the "granitic" layer, while the Byelozerka block is abundant in seismic interfaces. For this last mentioned block horizontal layering of the "granitic" and "basaltic" layers is peculiar. This starts at the depth of 3-4 km in spite of the fact that to the depth of 1-2 km, according to geological evidence, vertical layering is observed. The existence of vertical (upper level) and horizontal (lower level) layering is found in the regions of the young Alpine folding where this phenomenon can be explained by horizontal shifts of the surface layers. The analogous processes might occur in the shield.

With the purpose of studying elastic properties of the crystalline and metamorphic rocks of the Ukrainian shield a considerable amount of laboratory determinations of the elastic properties and densities on rock samples, taken from the bore-holes with the maximum depth of 2,1 km was undertaken.

On Fig. 4 the curves of longitudinal and Rayleigh waves and densities against depths for three bore-holes are shown.

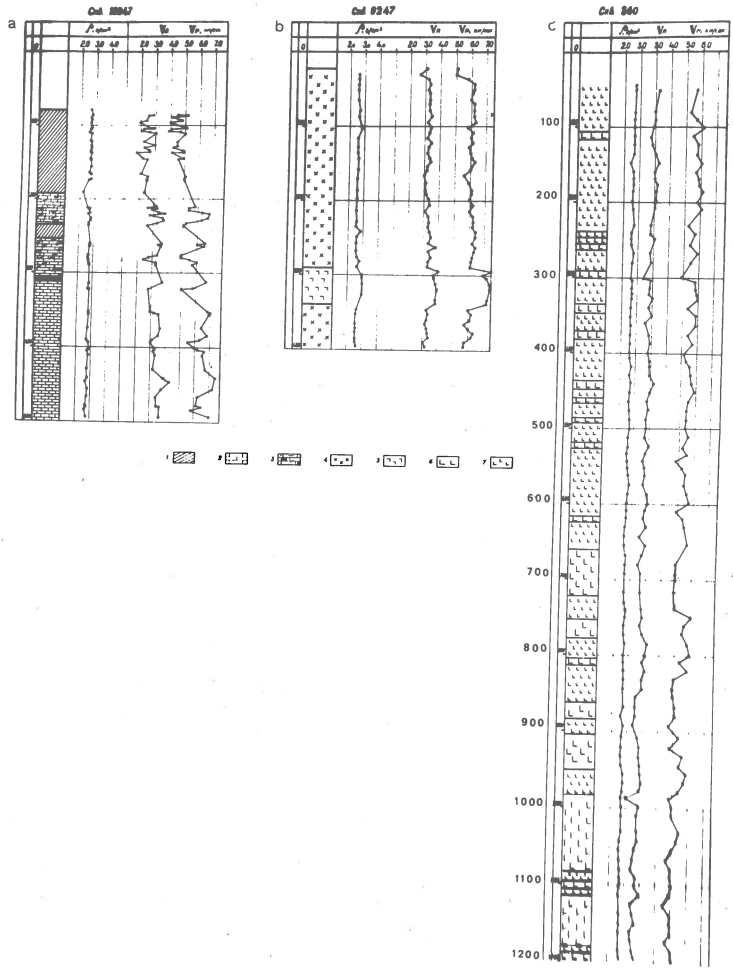

Fig. 4. Density, V_P, and V_R versus depth for three boreholes.

1) Quarts-biotite schists. 2) Dolomite marbles. 3) Marbles: dolomite, quartz, leached out, fissurred. 4) Migmatites. 5) Amphibolites. 6) Syenites, leucocratic, coarse-grained. 7) Syenites, melannocratic, medium-grained.

For the metamorphic rocks of the Krivoy Rog (a and b) the increase of velocities of longitudinal and Rayleigh waves with depth is clearly marked while the density value remains practically unchanged.

In the alkali syenites of the October Massif (c) velocity variations are in the immediate relationship with the petrographic composition of rocks.

Directly in the region of the deep seismic sounding profile metamorphic and enclosing rocks of the Byelozerka and Pavlograd blocks have been studied.

In the course of comparison of elastic characteristics of migmatites in the Byelozerka and Pavlograd blocks a contrast in velocity values of the longitudinal waves is observed. In the first case velocity values vary in a greater range from 5,3 to 6,2 km/sec and are characterized by a somewhat smaller mean value. For the Pavlograd block the velocity variation is less (5.8-6,3 km/sec) and the mean value higher.

Thus, the analysis of laboratory results indicates the difference of elastic properties of separate blocks of the Ukrainian shield.

Density characteristics of the blocks can be based on gravimetry data as well. Comparing the gravity anomaly curve with the seismic cross-section we can notice that in the majority of cases the shape of the Δg curve does not correspond with the topography of the main seismic interfaces. Even the deep Dniepro-Donetsk graben is not associated, as we might expect, with the gravity minimum. It may be supposed that the petrographic inhomogeneities of crustal substance have the main influence on the development of gravity anomalies. And in fact the Byelozerka block is associated with a marked gravity maximum; in the centre of the Dniepro-Donetsk depression a sharp drop of Δg coincides with a variation of the mean velocities, and only the maximum of Δg over the Crimean mountains coincides with the rise of the "basaltic" layer surface.

For a more precise correlation of crustal blocks with gravity data a gravity curve has been calculated which characterizes the total influence of all seismic interfaces. The difference in density values was taken equal to 0,1 g/cm^3 for each interface. The curve thus obtained was extracted from the observed one, and it is possible to consider the difference curve as characterizing the density inhomogeneity

of the crustal substance. Comparing this curve with the seismic cross-section we arrive at the conclusion that crustal blocks have a sharp density differentiation. Increased values of the "granitic" layer densities are characteristic of the Byelozerka block; in the Pavlograd block region increased values of the "basaltic" layer may be expected. The Voronezh block has lower densities. Density variations from one block to another are sharp at the transition through the fractured zone which is confirmed by the coordination of the fractures with gravity steps.

Thus, the deep seismic sounding data together with the results of gravity surveys can be used for studying the crustal substance and give a general outline of the physical state of its separate blocks.

E.Grigorova, D.Sokerova

A DETERMINATION OF THE DEPTH OF MOHOROVICIC'S BOUNDARY IN BULGARIA BASED ON BODY WAVES OF NEAR EARTHQUAKES

An attempt has been made to define the depth of Mohorovičić's boundary in the active seismic zones of Bulgaria by investigating the velocity cross section of longitudinal body waves of near earthquakes. Data has been taken from the bulletins of the Kew observatory and the Bureau Central Séismologique International as well as from available seismograms of 20 seismic stations with epicentric distances of less than 15° ($\Delta = 15°$).

Earthquakes having M = 4.5 which have occurred in Bulgaria and have had their focuses in the Earth's crust have been considered.

The method of work represents a discrete correlation of the longitudinal body waves for each separately considered earthquake.

Identification of the seismic waves has been carried out under the adoption of a two layer model of the Earth's crust: Mohorovičić's boundary, the imaginary boundary juxtaposed between the basalt and granite horizons. For that model the equation for the travel-time of seismic waves for comparatively small epicentric distances is termed as follows:

$$\Delta T = a + \frac{\Delta}{V} \qquad (1)$$

where a is the travel time of seismic waves at $\Delta = 0$; V is the velocity in the horizon in question, and Δ is the epicentral distance.

The computation of the velocities of the longitudinal refracted waves has been carried out by means of equation (1) from data of the separate waves taken from the seismic stations by the method of least squares. Data have been

taken also from stations situated around the epicenters of the earthquakes investigated.

The final processing of the earthquakes made it possible to investigate the velocities of the longitudinal waves of the earthquakes situated in the seismoactive zones of Bulgaria, i.e. Central West and Southwest Bulgaria, the Thrace plain along the course of the Maritza river as far as the town of Odrin (Fig. 1).

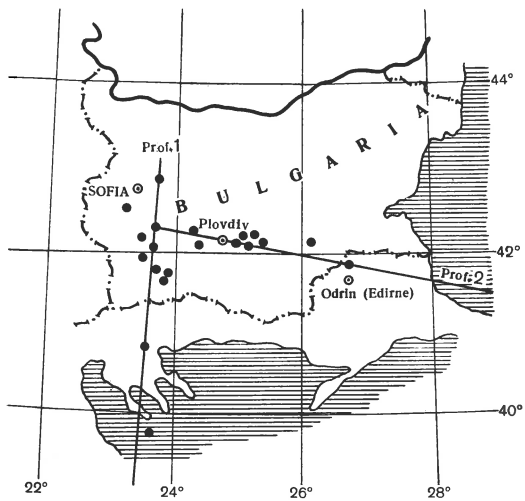

Fig. 1

Two profiles were drawn with distances from the epicenters not exeeding 30 km. The only exception is the earthquake of 28 I 1965 which occurred at a distance of 60 km. from profile I (Fig. 1).

The first profile having a North-South direction and length 350 km. begins from the town of Botevgrad and runs along the plain of Sofia, the Rila and Pirin mountains and the Halcides peninsula (Fig. 2).

Three horizons have been set up by the analysis of the travel-time-curves of the longitudinal waves:

The first horizon refers to the granite layer and has a velocity of the longitudinal waves of 5.50 to 5.66 km/sec, its boundary varies between 17-20 km and the horizon itself follows the behaviour of Mohorovičić's boundary.

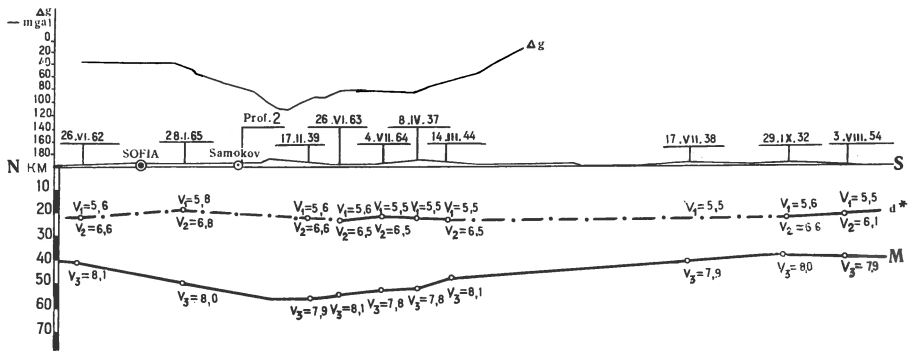

Fig. 2

The second layer is characterized with a velocity of the waves ranging from 6.12 to 6.62 km/sec and can be connected with the basalt layer.

The third horizon could be referred to the Mohorovicic's boundary with a velocity from 7.81 to 8.13 km/sec.

The thickness of the Earth's crust is 38 km near Botevgrad, comes to its greatest value 51 km under the Rila mountain and after that it grows smaller towards the Halcides peninsula where it reaches 35 km.

The earth relief and the anomalous gravitation field computed by Bouguer's reduction are plotted on the profile. Δg is in fair accordance with the changes in the thickness of the crust. The greatest value of the thickness corresponds to the most negative value of the Bouguer-anomaly.

The second profile having a direction West-East and a length of 270 km is drawn from Samokov along the course of the Maritza river as far as Odrin (Fig. 3).

The velocities of the longitudinal waves are as follows: from 5.52 km/sec to 5.65 km/sec for the granite horizon, from 6,36 to 6,76 km/sec for the basalt horizon and from 7.85 to 8.20 km/sec for the subcrustal substance.

The depth to the Mohorovicic-boundary on this profile varies in the following ranges: 50 km by Samokov, comes to 36 km by Pazardjik, then it goes down towards Plovdiv-

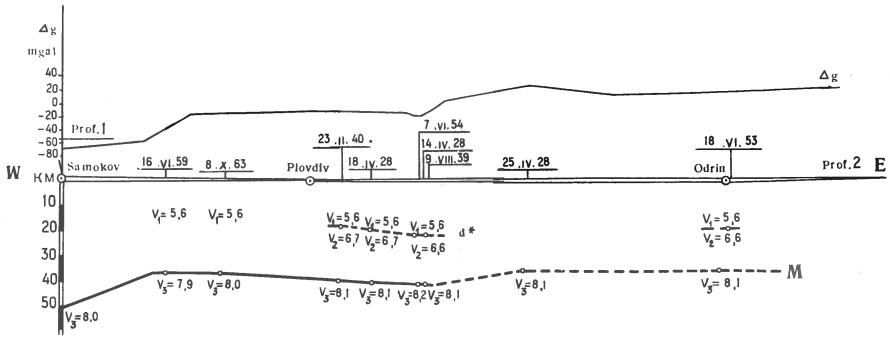

Fig. 3

Parvomai as deep as 40 km, which fairly well agrees with Bouguer's anomaly, and after that there is a rise up to 36 km.

The depth of the granite horizon comes to 17-20 km determined at three points. The results obtained from investigations like this make it possible to study the regional peculiarities of the depth structure by a limited number of seismic boundaries.

J.V.Pomerantseva, A.N.Moszhenko,
G.V.Egorkina, J.A.Sokolova

PRINCIPAL RESULTS OF CRUSTAL AND UPPER MANTLE INVESTIGATIONS WITH THE "ZEMLIA" RECORDING UNITS

In 1961 the All-Union Scientific Research Institute of Geophysical Exploration (VNIIGEOFIZIKA) started investigations for the development of the most effective technique of studying the crustal and upper mantle structure.

Records of compressional, shear, and surface waves from local earthquakes and explosions are used to determine velocities that are needed for conversion of time sections into depth ones for the purpose of locating zones of recent tectonic activity of the crust and upper mantle.

The present report describes the results of crustal and upper mantle investigations conducted in the South-east of the Russian platform and in the Azov-Kuban depression. The investigations were made by a group of research workers of VNIIGEOFIZIKA: A.N.Moszhenko, J.V.Pomerantseva, J.A.Sokolova, G.V.Egorkina, L.P.Barskova, L.S.Shumilina, G.J.Ivanchenko, S.S.Tarasevitch and others.

In the area of the Russian platform investigations with the "Zemlia" recording units were located along the DSS (deep seismic sounding) and CMRW (correlation method of refraction waves) profiles that had been run by VNIIGEOFIZIKA earlier. In the Azov-Kuban depression the "Zemlia" profile was run simultaneously with a refraction (CMKW) survey.

Refraction, reflection, and DSS deep investigations as well as seismological observations with "Zemlia" units conducted on the same profiles made it possible to estimate advantages and limitations inherent in each of the methods.

The technique and equipment employed in the above mentioned deep crustal and upper mantle investigations have been reported earlier (5-8).

As a result of the investigations conducted in the areas significantly differing in the geological structure (Russian

platform and Azov-Kuban depression) new information has been obtained about the structure of the crust and upper mantle.

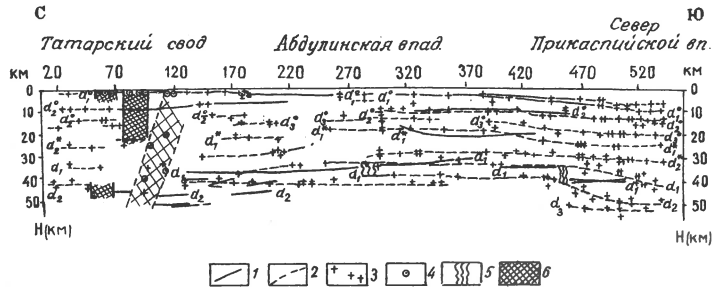

Fig. 1. Comparison of deep crustal sections obtained from refraction deep seismic sounding and "Zemlia" seismologic investigations. (Profile II from Tartar anticline to the North Caspian depression).

1) Interfaces in the crust from deep seismic sounding. 2) Interfaces in the crust from the "Zemlia" investigations (converted waves). 3) The locations of conversion interfaces. 4) Hypocenters of local earthquakes. 5) Fault zones from deep seismic sounding. 6) Fault zones from the "Zemlia" data.

d_1°- top of the basement. d_2°- top of the gabbro-diabase layer. d_3°- first interface in the gabbro-diabase layer. d_1^*- top of the Conrad layer. d_2^*- interface below the Conrad layer. d_1- first Moho discontinuity. d_2 and d_3- second and third Moho discontinuity.

1. Deep crustal and upper mantle sections have been obtained from records of distant earthquakes within the southeastern part of the Russian platform (6). Converted PS waves have been recorded at the following interfaces: top and bottom of the carbonate series, basement, M discontinuity and some interfaces within the crust and upper mantle (Fig. 1, 2, 3). The most distinct PS waves have been recorded from the basement and M discontinuity. Physical boundaries that have been identified within the crust divide the latter into layers 5 to 7 kilometers thick (Fig. 1, 2, 3). The interfaces are nearly flat extending for large distances. Horizontal crustal interfaces could not be traced within the areas incorporating foci of local

earthquakes. By means of conversion waves PS it was possible to locate distinct interfaces in the upper mantle, having the depth of 70-80 and 90-100 kilometers (Fig. 2).

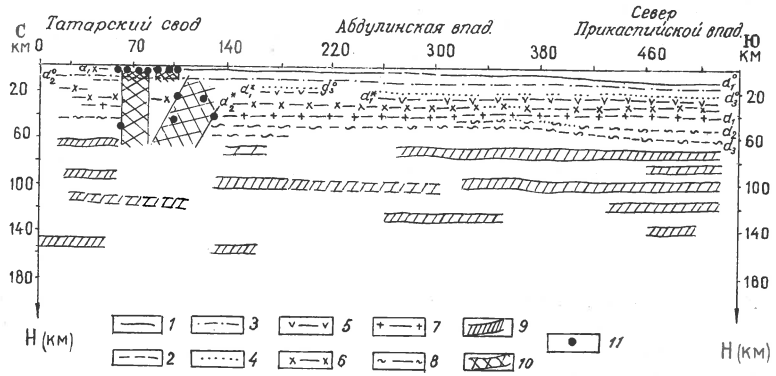

Fig. 2. Cross section of the crust and upper mantle along the profile from the Tartar anticline to the North Caspian depression.

1) Top of the crystalline basement from the proved data. 2) Top of the crystalline basement from the inferred data. 3) Top of the gabbro-diabase layer (d_3^g). 4) First interface inside the gabbro-diabase layer (d_3^g). 5) Conrad top (d_1^*). 6) Interface below the Conrad top (d_2^*). 7) First Moho top (d_1). 8) Second and third Moho tops (d_2 and d_3). 9) Interfaces in the mantle. 10) Fault zones located from the "Zemlia" investigations. 11) Epicenters of local earthquakes.

2. The analysis of seismograms from close earthquakes in the south-east of the Russian platform (4) resulted in making a location map of epicenters and locating seismicity zones to which the epicenters are confined (Fig. 4). Five zones containing earthquake foci have been located:

a) South top of the Tartar anticline,

b) South-east slope of the Zhigulevski-Pugachevski anticline,

c) The Ural's foredeep and west part of the folded Ural's,

d) Junction zone of the south-eastern part of the Russian platform and the North Caspian depression,

e) Zone of Zhigulevski dislocations.

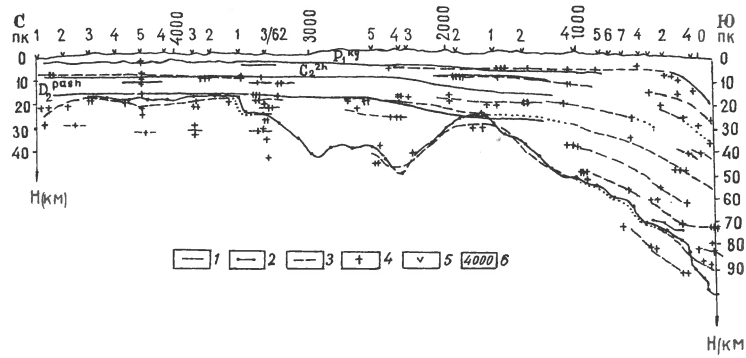

Fig. 3. Comparison of deep cross sections of the sediments and basement obtained from drilling, refraction and "Zemlia" investigations in the south-east of the Russian platform (profile II).

1) Interfaces in the sediments: top (P_1^{Kg}), bottom (D_2^{Pash}) of the carbonate formation and bottom (C^{2h}) of the coal-bearing formation from drilling data. 2) Top of the crystalline basement from refraction and drilling data. 3) Conversion interfaces from the "Zemlia" data. 4) Conversion points. 5) Location of the "Zemlia" stations. 6) Stations of the refraction and deep seismic sounding profile.

Epicenters of the first, second and third zones are within the crust with the depths of 20 to 50 kilometers. It is possible that epicenters of the fourth and fifth zones are within the mantle.

Zones of crustal and upper mantle activities coincide with fault zones derived from other geophysical investigations, such as gravity, magnetics, refraction, deep seismic sounding and drilling.

3. A composite travel-time graph of P and S waves has been obtained from the analysis of local earthquakes and explosion information for the distance of 20 to 700 kilometers for the south-eastern part of the Russian platform (Fig. 5). The following groups of waves could be distinguished from the graph:

a) Direct P and S waves recorded at the distances of 20 to 50 kilometers from the earthquakes having epicenters in

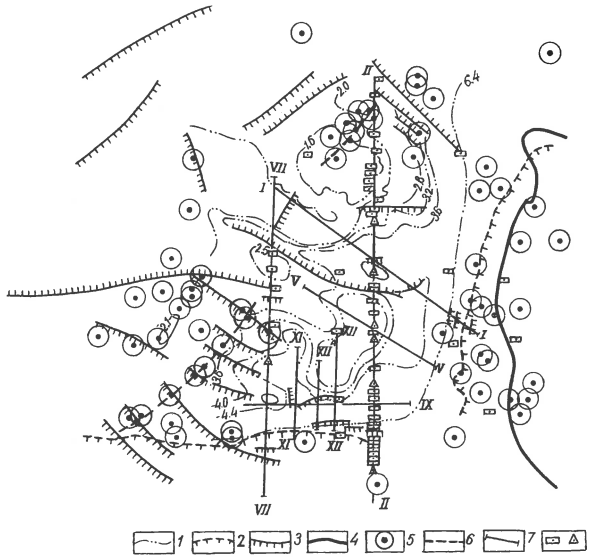

Fig. 4. Location of epicenters of local earthquakes shown on the sketch structural map of the crystalline basement of the south-eastern part of the Russian platform that had been prepared by P.A.Blokhin, Yn.N.Godin and others.

1) Contour lines of the basement surface. 2) Major regional faults (from gravity and magnetic data) separating the Russian platform from the North Caspian depression (in the south) and the Ural's (in the east). 3) Faults in the basement (from geological, refraction, gravity and magnetic data). 4) Area of the folded Ural's. 5) Epicenters of local earthquakes and explosions. 6) Faults located by the "Zemlia" records. 7) Previous refraction and deep seismic sounding profiles. 8) Stations of the "Zemlia" recording of 1963 and 1964, respectively.

the crust. Their travel-time graphs have a hyperbolic shape.

b) P_1° and S_1° waves considered as diving ones within the granite rocks with V_p = 5,9 - 6,0 km/sec and V_s = 3,3 km/sec recorded at the distances of 50 to 120 kilometers.

c) P_1^* and S_1^* waves with V_p = 6,4 km/sec and V_s = 3,6 km/sec comparable with the waves of the "basalt" layer, recorded at the distances of 120 to 200 kilometers.

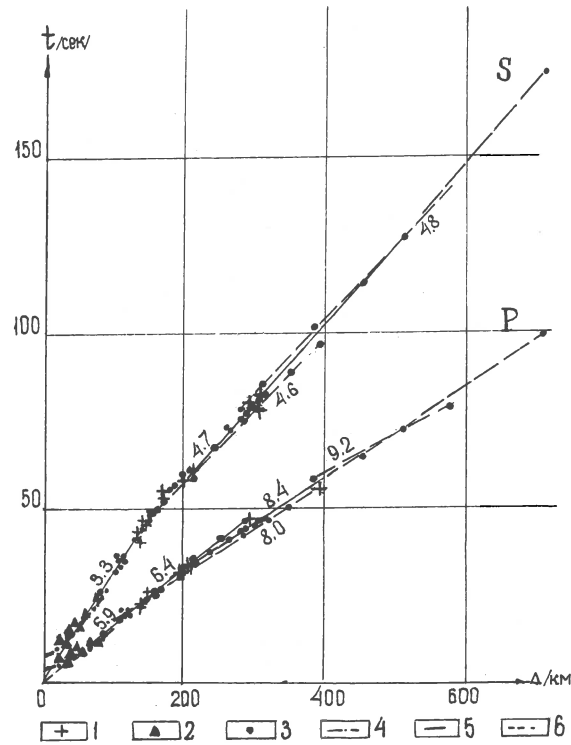

Fig. 5. Travel-time graph of P and S waves recorded as first arrivals in earthquake and explosion records.

1) Travel-times of the waves recorded from explosions. 2) Travel-times of the waves recorded from earthquakes with epicenter depths of 20 to 50 km. 3) Travel-times of the waves recorded from earthquakes and explosions without definitions of hypocenter depths. 4) Theoretical travel-time graphs of direct waves with the focus depth H = 23 km. 5) Proved areas of composite travel-time graphs. 6) Inferred areas of composite travel-time graphs.

d) A sharp change in the travel-time graph has been obtained at the distance of about 200 kilometers. P and S waves refracted from the M discontinuity with V_p = 8,0 km/sec and V_s = 4,6 km/sec have been observed at the distances of 200 to 400 kilometers.

e) Then, at the distances of more than 400 km, come P_{2-3}-waves associated with the mantle with the velocities of 8,4 km/sec and 9,2 km/sec respectively. S_{2-3} waves have

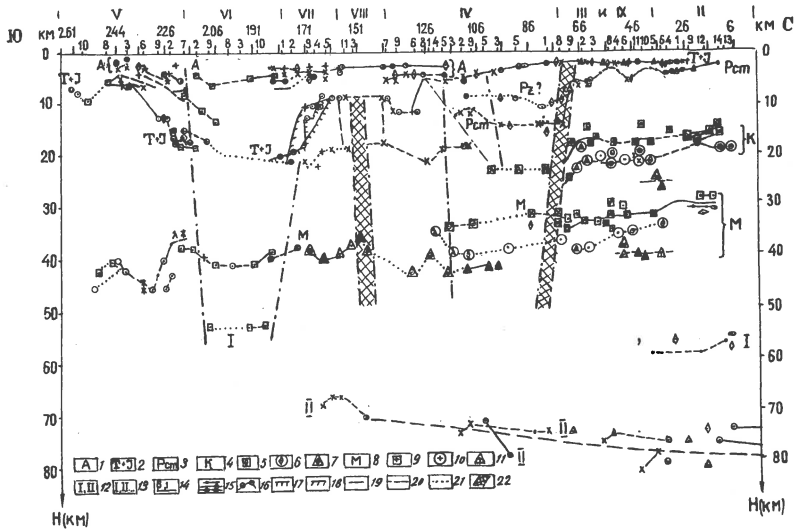

Fig. 6. Cross section of the crust and upper mantle from the "Zemlia" records obtained along the profile from Leningradskaya to F.Ghelendzhik.

1) Conversion interfaces in the sediments. 2) Top of the Triassic-Jurassic series. 3) Top of the crystalline basement. 4) Conrad layer. 5) First interface in the Conrad layer. 6) Second interface in the Conrad layer. 7) Third interface in the Conrad layer. 8) Moho discontinuity. 9) First interface in the M layer. 10) Second interface in the M layer. 11) Third interface in the M layer. 12) Conversion interfaces in the upper mantle. 13) Numbers of the "Zemlia" stations (at the top). 14) Numbers of the "Zemlia" stations with the location of seismometer pits and number of seismometers in them. 15) Conversion depths from different earthquakes projected normal to the line of the profile. 16) Conversion depths projected to the line of the profile from the interpretation of depths on both sides of the profile from different earthquakes. 17) Cross section of the Northern slope of the West-Kuban foredeep computed by means of approximation technique. 18) Cross section of the North slope of the West-Kuban foredeep computed from formulas available for a horizontally stratified medium. 19) Proved areas of conversion interfaces. 20) Inferred areas of conversion interfaces. 21) Supposed behaviour of conversion interfaces. 22) Faults and fault zones located by the "Zemlia" records.

the velocity of 4,7 km/sec and 4,85 km/sec. The analysis of the data obtained resulted in the determination of the coefficient $K = \frac{V_p}{V_s}$ in the crust which was used in further computations of the depth of conversion interfaces.

4. As a result of the investigations conducted in the Azov-Kuban depression crustal and upper mantle sections have been made along the main profile and some cross ones.

The most distinct conversion interfaces are the surface of the Triassic-Jurassic sequence, the surface of the Precambrian basement, the Mohorovičić discontinuity and some interfaces in the upper mantle (Fig. 6). Less persistent are intermediate boundaries in the crystalline and sedimentary rocks.

We may note here some features typical for the cross section obtained along the profile from Leningradskaya to Falshivii Ghelendzhik:

a) The presence of large regional crustal blocks having a latitudinal trend. The first of them is located in the north of the region investigated including part of the Skiffskaya platform and a zone of transition to the Azov-Kuban depression. The second incorporates the Belogorso-Berezanski macroswell and partly the Timashevskaya bench. The third block embraces nearly the whole of the Timashevskaya bench. The fourth block includes the West Kuban foredeep and the fifth block represents the Great Caucasus meganticlinorium.

b) Absence of continuous interfaces along the total of the profile. They are continuous only within the limits of some blocks. In the zones of the block-junctions the crustal interfaces are broken and in some places vertically displaced.

c) Regional lowering of the crystalline surface of the crust (surface of the transition zone) from the north to the south with the simultaneous uprising of all the crustal interfaces including the M discontinuity in the same direction.

d) Presence of transition zones from one crustal layer to another having a thickness of 3 or 4 km rather than flat

interfaces inside the crust, in the zone of transition from the crust to the mantle, and in the mantle.

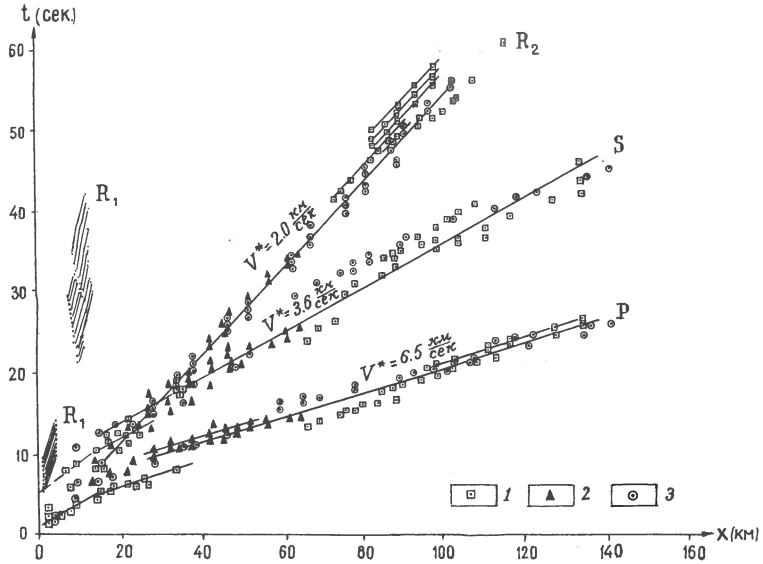

Fig. 7. A composite travel-time graph of P, S, and R waves, recorded from explosions.

1) Travel-times of the waves, recorded from the depth of crystalline basement changing from 2 to 5 km. 2) Travel-times of the waves, recorded from the depth of crystalline basement changing from 5 to 10 km. 3) Travel-times of the waves, recorded from the depth of crystalline basement changing from 10 to 20 km.

5. $\overline{K}(\overline{V}_p)$ and $K_1(V_{p1})$ curves and travel-time graphs for the P, S, R waves (Fig. 7) have been plotted from the results of explosion information obtained in the Azov-Kuban depression where $\overline{K} = \frac{\overline{V}_p}{V_s}$ and $K_1 = \frac{V_{p1}}{V_{s1}}$ (Fig. 8). The curves have later been used for making cross sections from converted waves of PS type recorded on seismograms of distant earthquakes.

6. Records of P and S waves from local earthquakes have given information about their epicenters that are mainly located along the Black Sea coast. (Fig. 9).

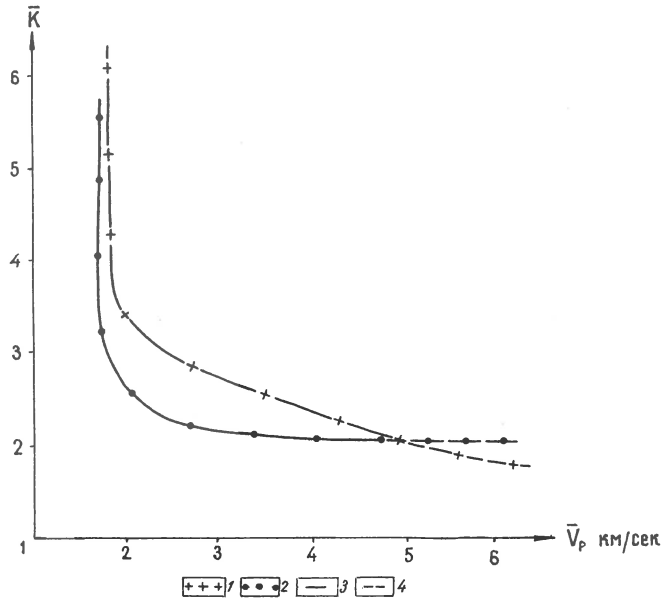

Fig. 8. $\overline{K}(\overline{V}_p)$ plots obtained from shots and local earthquakes within the south-eastern part of the Russian platform and Azov-Kuban depression.

1) Values of $\overline{K} = \overline{V}_p/\overline{V}_s$ obtained for the Russian platform. 2) Values of $\overline{K} = \overline{V}_p/\overline{V}_s$ obtained for the Azov-Kuban depression. 3) Proved areas of the $\overline{K} = (\overline{V}_p)$ curve. 4) Inferred areas of the $\overline{K} = (\overline{V}_p)$ curve

Thus, the investigations made with the "Zemlia" recording units in some regions of the USSR together with the development of the above described field technique and methods of interpretation of the data obtained have resulted in the following geological information:

1. Deep crustal and upper mantle structure has been studied in the regions of the Russian platform and Azov-Kuban depression with the total mileage of the profiles amounting to 1200 km.

2. Comparison of the cross sections obtained from "Zemlia" records with those of refraction, deep seismic sounding, and deep reflection surveys from the same regions made it possible to get a number of principally new ideas about the crustal structure and to estimate the possibilities of each method:

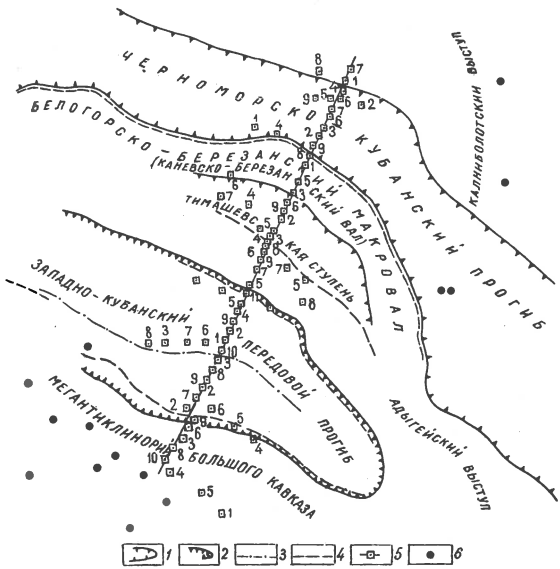

Fig. 9. Location of the "Zemlia" stations and epicenters of local earthquakes shown on the structural map of the North-West Fore Caucasus (that had been made by M.R. Pustilnikov, V.I,Korneyev, and V.R.Kripinevich).

1) Platform depressions. 2) Foredeeps. 3) Axes of foredeeps and depressions. 4) Inferred faults in the basement. 5) Line of the main north-south "Zemlia" profile with "Zemlia" stations. 6) Epicenters of local earthquakes recorded by the "Zemlia" units, time and number of recordings.

a) Investigations of the crystalline basement by means of a refraction technique do not enable one to study areas with dips exceeding 40°. As a result, sections plotted for large depressions and foredeeps generally do not correspond to the surface of the crystalline basement.

They reflect only the structure of the sediments. From the "Zemlia" records the basement surface must have a greater depth than from the refraction ones and must have a different structure.

b) In refraction and deep reflection surveys the medium investigated has to be averaged due to the fact that interfaces are investigated by rays of diving and reflection waves propagating nearly horizontally for great distances from shot points.

Whilst rays of PS waves recorded from distant earthquakes by means of the "Zemlia" equipment travel nearly vertically.

c) Flat continuous interfaces in the crust plotted from deep seismic soundings and deep reflection surveys appear to be arbitrary horizons.

From the investigations conducted with the "Zemlia" recording technique (Fig. 6) it is evident that transition zones rather than flat crustal interfaces are present between individual complexes of the crust, with these layers (zones) being continuously traceable only in some limited areas of the profiles within some of the crustal blocks.

As a matter of fact, if during the interpretation of the information obtained from conversion waves recommended here to be employed in such works (1-3) we resort to averaging the Δt_{ps-p} obtained at one station from different earthquakes, we also get flat interfaces and not zones in the crust, the same as in deep seismic sounding and deep reflection surveys (when flat phase travel-time graphs are made from a group of waves).

Bibliography

1. Andrejev, S.S.: "Izutjenije glubinnogo strojenija zemnoj kory pri posmostji obmennych woln PS, registrirujemych pri zemletrjasenijach" Izv. AN SSSR, ser. geofiz. nr. 1, 1957.

2. Bulin,N.K.: "Opredelenije glubiny skladtjatogo fundamenta pri pomostji obmennych prochodjastjich woln tipa PS registrirujemych pri zemletrjasenijach". Izv. AN SSSR, serija geofizitjeskaja nr. 6, 1960.

3. Bulin, N.K., Sytin, J.I.: "Opyt primenenija seismologitjeskich issledovanij dlja izutjenija glubinnogo strojenija zemnoj kory na territorii Turkmenii". Sbornik "Materialy po geologii i neftenosnosti zapadnoj tjasti Srednej Azii." VSEGEI Gostoptechizdat 1960 g.

4. Weschnjakov, N.V. i dr.: "Rukovodstvo po proizvodstvu i obrabotki nabljudenij na seismitjeskich stantsyjach SSSR". Izd. AN SSSR, 1952.

5. Mozzhenko, A.N.: "Apparatura magnitnoj zapisi dlja registratsyi zemletrasenij i udaljennych vzryvov". Izv. AN Turkm. SSR, ser. fiziko-techn., chimitj. i geolog. nauk nr. 3, 1961 g.

6. Mozzhenko A.N.: "Nizkotjastotnaja seismitjeskaja apparatura". Sb. "Glubinnoje seismitjeskoje zondirovanije v SSSR" 1961 g. Gostoptechizdat.

7. Pomerantseva, I.V., Mozzhenko, A.N., Sokolova, I.A. & Jegorkina G.V.: "Rezuljtaty regionaljnych issljedovanij s seismitjeskimi stantsyjami "Zemlja" i perspektivy ætich rabot."
"Regionaljnyje geologo-geofizitjeskije issljedovanija v bortovoj zone Prikaspijskoj vpadiny". Tr.Nizhnewolzhskogo NII Geologii i Geofiziki vyp. 2 Saratov 1964 g.

8. Pomerantseva,I.V., Mozzhenko, A.N., Sokolova, I.A. & Jegorkina, G.V.: "Primenenije seismologitjeskich stantsyj "Zemlja" pri izutjenii strojenija Jugo-vostoka Russkoj platformy." Doklady AN SSSR, tom 163, nr. 1, 1965.

9. Hasegawa, H.: "Die Wirkung der obersten Erdschicht auf die Anfangsbewegung einer Erdbebenwelle". Zeitschrift für Geophysik. Jahrgang VI, 1930, Heft. 2.

Jan Uchman

DEEP SEISMIC SOUNDINGS IN POLAND

The investigations carried out along two profiles since 1960 are reported. The results up to 1964 were presented at the ESC meeting in Budapest. Further more detailed measurements were carried out on the north half of the "A" profile (Radynia-Gdańsk Bay) and on the new profile "C" (Staracho-wice-Radzyn Podlaski). Both profiles intersect the marginal structure of the East-European Platform. North half of the "A" profile had a length of 230 km and profile "C" 136 km. Both had two terminal shot points. By means of two 60-channel apparatuses two reversal continuous lines of recordings were obtained; distance between channels equals 100 m.

As an example some results concerning profile "C" are here presented. Due to short profile length the interpretation of Moho and intermediate crustal discontinuities is based entirely on reflection waves. Here, cristalline bed surface, investigated in a rather dense network by Polish geological service, is not dealt with. The obtained seismograms have generally good quality; the best results, however, were obtained for distances above 100 km. A complex wave pattern was obtained; apart of the refracted wave group, three other wave groups were observed. Their apparent velocities vary with distance. The first two groups arrive from intermediate crustal discontinuities. At smaller distances they often fade out, while at the end of the section they appear very distinctly. The reflected waves from Moho (P^M refl) are the most intense waves between 80 and 136 km. In comparison with two other groups, the nature of these waves reflected from Moho is the most accurately defined by their kinematic and dynamic properties.

A number of stratified (homogeneous and heterogeneous) models of the Earth's crust was considered and theoretical distance curves compared with experimental ones. For the

model adapted as a result of consecutive approximations, the deviations between theoretical and experimental curves were explained assuming crustal block structure. The obtained image of the Moho discontinuity has feature of an anticline bounded at two sides by fractures. The Moho depth is considerable ranging about 48 km. The fractures in Moho, discovered by the absence of distinctive appearence of Moho reflection waves, may perhaps be connected with the marginal structure of the East-European platform. A similar anomalous fading of P^M refl. waves was observed on the adjacent, Ukrainian territories, as published by Sollogub.

It should be mentioned also that the Moho depth on the north part of profile "A" (between Konin and Gdańsk Bay) is of the order of 44 to 46 km as estimated from reflected and refracted waves. Another discontinuity 5 km below the Moho was discovered on the basis of the refraction wave.

Bibliography

1. B.Wojtczak-Gadomska, P.Guterch, J.Uchman: Ergebnisse der seismischen Tiefsondierungen in der VRP. Sonderband. Referate aus dem I. Internationalen Symposium über seismische Tiefsondierungen. Brno 1965.

2. K.Betlej, B.Gadomska, L.Gorczyński, A.Guterch, A.Mikolajczak, J.Uchman: Deep seismic sounding on the profile Starachowice-Radzyn Podlaski. Materialy i Prace Zakladu Geofizyki PAN, 1966.

3. A.Guterch, J.Uchman, B.Wojtczak-Gadomska: Investigations on the Earth's Crustal Structure in Poland by Means of Deep Seismic Soundings. Materialy i Prace Zakladu Geofizyki PAN, 1966.

V.I.Bune, A.A.Sorsky

SEISMOTECTONIC PRINCIPLES OF DISTINGUISHING ZONES OF PROBABLE ORIGIN OF STRONG EARTHQUAKE FOCI ON THE EXAMPLE OF THE CAUCASUS

According to the decision of the ESC in Budapest in 1964 and of the UNESCO conference in Tbilisi in 1965, preparations have been started for the compilation of a map of seismic regionalization of Europe.

Foci of many devastating earthquakes are located in the top structural layer of the Earth's crust. Therefore, for a map of regionalization it is necessary to use data provided by both seismology and tectonics. To compile a map of seismic regionalization it is necessary: 1. To distinguish zones of the origin of earthquake foci and to determine the maximum possible energy or magnitude of the earthquake, the epicentre of which can get into any point within the zone. 2. To estimate the probability for the occurrence of such an earthquake. 3. To determine the effect such an earthquake will have at the surface of the Earth. 4. To plot a map for the recurrence of maximum tremors.

On the example of the Caucasus the methods used for the solution of the first problem by a combination of seismological and tectonic data are demonstrated. For this purpose a tectonic map, an epicentre map of strong earthquakes, as well as data on the sizes of earthquake foci, on the zones of earthquake preparation, and on the depths of foci were used.

The tectonic map of the Caucasus distinguishes zones of uplifts and subsidences, zones of contrasting tectonic movements, deep faults, transverse flexures and uplifts. The zones of uplifts and subsidences are differentiated by age (Fig. 1).

The seismic map shows epicentres of earthquakes determined by instrumental and macroseismic data differentiated

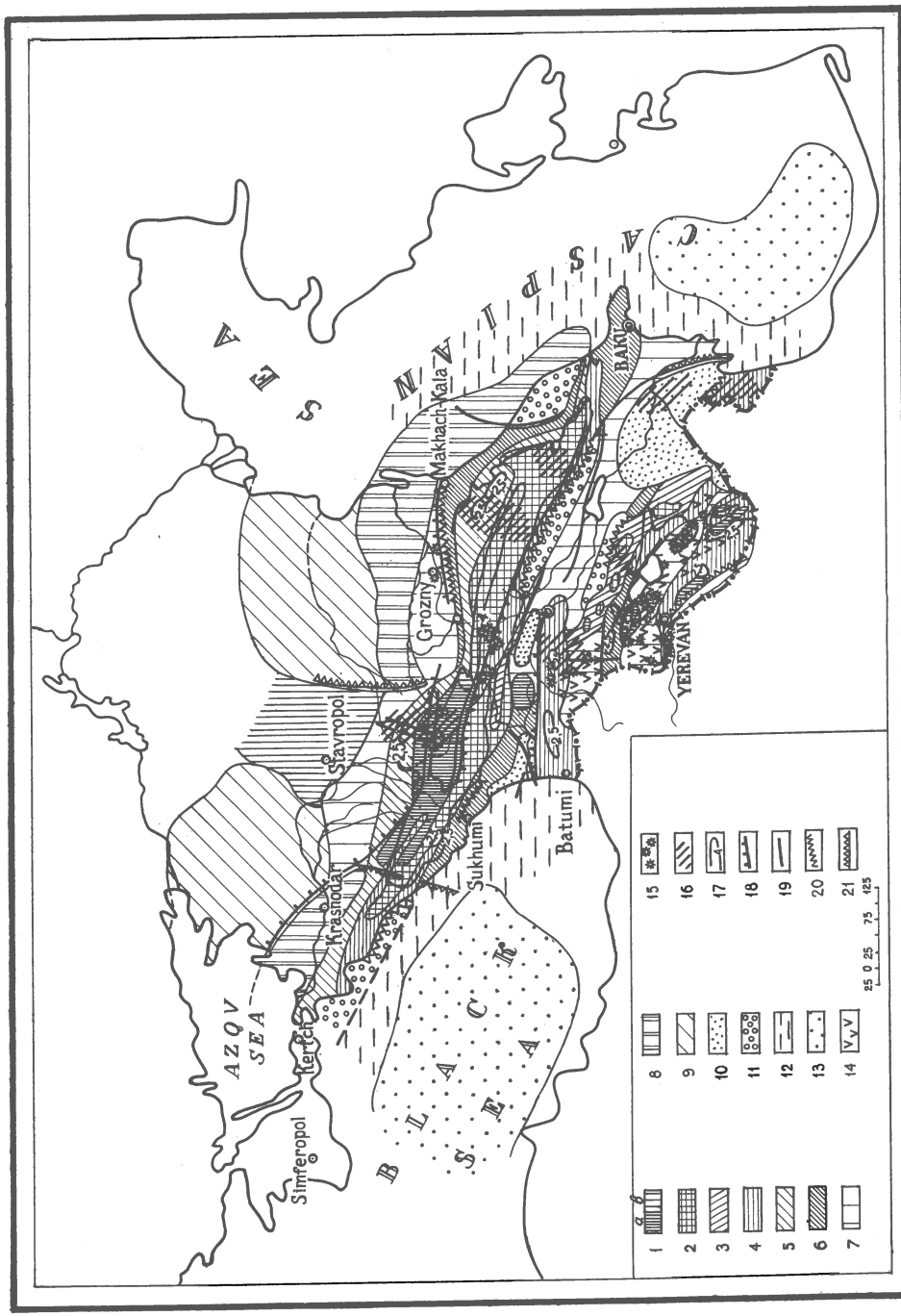
CASPIAN SEA
BAKU
Makhach-Kala
Grozny
Stavropol
Krasnodar
Kerch
Simferopol
AZOV SEA
BLACK SEA
Sukhumi
Batumi
YEREVAN
25
0 25 75 125

Fig. 1

Fig. 1: Tectonic basis for the seismotectonic map of the Caucasus.

I. Zones of folded uplifts formed at the place of geosynclinal depressions. 1) Pre-Alpine stable uplifts. a) subjected to disintegration during the Ng - Q, b) not subject to disintegration (edge of the platform). 2) Zones of Early Alpine intrageosynclines, transformed into uplifts during Early Mesozoic and developed as uplifts during the entire Meso-Cenozoic. 3) Zones of Early Alpine intrageosynclines, transformed into uplifts during the Middle Mesozoic-Early Tertiary time. 4) Zones of Middle Alpine intrageosynclines transformed into uplifts during the Early and Middle Tertiary time. 5) Zones of Middle Alpine parageosynclines transformed into uplifts during the Late Tertiary time. 6) Zones of Late Alpine parageosynclines transformed into uplifts before Late Pliocene.

II. Zones of subsidence formed at the place of Early Alpine intrageosynclines. 7) Zones of Neogene subsidences in the axial part of which uplifts had originated during the Pliocene-Quaternary time. 8) Zones of stable Miocene-Quaternary subsidence in foredeeps. 9) Marginal parts of platforms involved into moderate subsidences during the Late Alpine time. 10) Areas of recent subsidences within intermountain depressions. 11) Young (Pliocene-Quaternary) superimposed basins. 12) Zones of intense young subsidences within present seas. 13) Areas without a "granitic" layer. 14) Areas of young volcanicity (Pliocene-Quaternary). 15) Quaternary volcanoes. 16) Transverse uplifts. 17) Isolines of latest uplifts (in km). 18) Deep faults that cross the entire crust of the Earth up to the mantle. 19) Faults active during the Neogene-Quaternary time. 20) Zones of contrasting tectonic movements. 21) Transverse flexures.

by magnitude, intensity, and exactness of coordinate determinations (Fig. 2).

As a result of an analysis and a comparison of these maps a forecast map has been compiled for the zones of the possible origin of earthquake foci distinguished by their maximum energy into approximately two orders.

I. Character of tectonics

The tectonic map on Fig. 1 shows the main structural-historical zones formed during the Alpine cycle, as well as a number of structural elements genetically associated with seismicity.

On a rough scheme present-day Caucasus can be divided into two fundamental big areas by the nature of tectonic movements - an area of predominant uplifts and an area of predominant subsidence.

Structurally meganticlinoria of Greater and Lesser Caucasus are distinguished in the area of uplifts, while in the area of subsidence there is the Pre-Caucasus piedmont depression and the Transcaucasian intermountain depression. Transverse uplifts (Stavropolsk and Dzirulsk) divide them into two depressions: Kuban and Terek depressions in the Pre-Caucasus depression and Rioni and Kura depressions in the Transcaucasian depression.

The meganticlinorium of Greater Caucasus in a heterogeneous and complex folded-block area. Even more heterogeneous in its structure is the meganticlinorium of Lesser Caucasus, within which very small zones are recorded.

The present distribution of uplift and subsidence areas has not always been the same. At the beginning of the Alpine cycle the place of highly uplifted mountain chains was occupied by intensely downwarping intrageosynclines surrounded by uplifts - intrageanticlines.

As result of an evolution of the Caucasian geosynclinal area there has been a complete reversal of geotectonic conditions, when the zones of former intrageosynclines became folded uplifts, while intermountain depressions and foredeeps were formed in the places of former intrageanticlines.

The earliest uplifts, which already existed at the beginning of the Alpine cycle (sign 1 of the legend on Fig.1) experienced a stable elevation during the entire Mesozoic and were subject to the effect of considerably more differentiated vertical tectonic movements during the Neogene-Quaternary time. At the beginning of the Alpine cycle the axial parts of the meganticlinoria (sign 2 of the legend) were zones of intense downwarping; in the middle of the cycle uplifts were originating within these zones that grew especially extensive and experienced a sharp elevation at the end of the Alpine cycle (on the map this uplift is shown by isolines).

Narrow zones fringing the axial part represented intrageosynclines of a later generation. They experienced an uplift and folding in the middle of the Tertiary (for instance the intrageosyncline on the southern flank of Greater Caucasus). To a still later uplift depressions formed along the periphery of these zones were subjected. Thus, on the northern flank of Greater Caucasus these depressions were involved into an uplift at the end of the Tertiary, while the most peripheral parts of these depressions experienced an uplift during the Pliocene-Quaternary.

In this way, the development of folded and folded-block structures was proceeding centripetally from the axial parts of former intrageosynclines towards the platform and the intrageanticline that existed at the place of the Transcaucasian intermountain depression. These movements were the actual cause of the formation of mountainous uplifts at the place of former intrageosynclines, whereas the areas of Early Alpine intrageanticlines became changed into foredeeps and intermountain depressions, which experienced an especially intense downwarping during the latest - Neogene-Quaternary time. During the Pliocene superimposed depressions were formed in a number of places that absorbed the marginal parts of old platforms.

It should be stressed that during the entire Alpine cycle the greatest subsidence of all intrageosynclines and a most intense subsequent differentiated uplift are characteristic for the eastern part of the Caucasus, which tectonically is most mobile.

In analysing the development of the Caucasian geosynclinal area, in addition to the zones mentioned, narrow stretches are established, where a junction is taking place of zones with sharply contrasting vertical movements of the latest time period. In the majority of cases deep-seated faults correspond to these zones. As indicated by geophysical data, these faults often cut the entire crust penetrating into the upper mantle. In the Caucasus two groups of deep faults can be distinguished: longitudinal, separating individual zones, and transverse faults that

are common for the geosynclines and adjacent platforms. The main longitudinal faults are divided into a number of age groups, the youngest of which with a great amplitude of contrasting movements being characteristic of Eastern Caucasus and certain localities on the southern flank of Western Caucasus. Especially pronounced in the relief is one of the largest zones of deep faults separating from the south the meganticlinorium of Greater Caucasus from the Transcaucasian intermountain depression. Transverse deep faults are also developed within Lesser Caucasus - along its northern and southern junction with the intermountain depressions, where the contrast between the movements is especially great.

As a rule, transverse deep faults originate on the steep flank of transverse uplifts. A most important uplift of this kind is the Transcaucasian elevation extending across entire Caucasus from the Russian platform up to the Arabian. On Greater and Lesser Caucasus with the transverse faults complicating this uplift are associated zones of young volcanism, which is especially developed in Lesser Caucasus. A big transverse fault is established in the eastern part of the Caucasus, where in the Kura intermountain depression it is perfectly expressed in the nature of the gravitation field as a zone of a distinct gravity gradient.

Geophysical investigations made it possible to establish the general features of the geological structure of the crust in the Caucasus. The greatest thickness of the crust and of its "granitic" layer is characteristic for the axial parts of the meganticlinoria (55-65 km). Within intermountain depressions and in foredeeps the thickness of the crust is considerably smaller (35-45 km). The sharp decrease in the thickness of the crust is mainly accounted for by a petering out of the "granitic" layer in the western and eastern parts of the intermountain depressions - towards the Black Sea and the South-Caspian basin, where the structure of the crust is close to a suboceanic one.

In this way both the surface and the deep structure of the Caucasus indicate its heterogeneity. Recent tectonic

movements are a continuation of a tectonic evolution that started millions of years ago and, on the whole, inherit the movements of the Neogene-Quaternary time. The most intense present uplift involves the axial zone of Greater Caucasus from Elbrus in the west up to Shemakha city meridian in the east. From the south and north this uplift is limited by narrow zones of sharply contrasting tectonic movements.

On Lesser Caucasus the zones of the most intense present uplifts are associated with previously formed brachymorph and quaquaversal portions consisting of young volcanogene rock masses.

II. Nature of seismicity

2.1. Earthquake classification by the intensity of tremors in the epicentral zone, by magnitude or energy of elastic waves

A scale by S.V.Medvedev, V.Karnik, and W.Sponheuer has been used in determining the intensity of earthquakes. However, in describing the seismic regime it is not enough to have intensity determinations only, because intensity not only depends upon the energy of the earthquake, but also upon the depth of the focus. When the epicentre is located in the sea it is impossible to determine the maximum intensity at the epicentre, I_o. Consequently, the determination of magnitudes or of the energy classes, K, is of great importance. Such determinations have not been made for all earthquakes. For an approximate appraisal of the energy of all earthquakes according to one scale, a correlation of M or K values with a maximum distance of the P-wave and an isoseist area of VII - IX earthquakes may be used, as it is done, for instance, in Table 1.

In correlating data on seismicity with the information on tectonic structures it is important to have at least an approximate idea on the sizes of the foci zones, on the aftershock areas, and on the areas participating in the preparation of earthquakes, as done in Table 2.

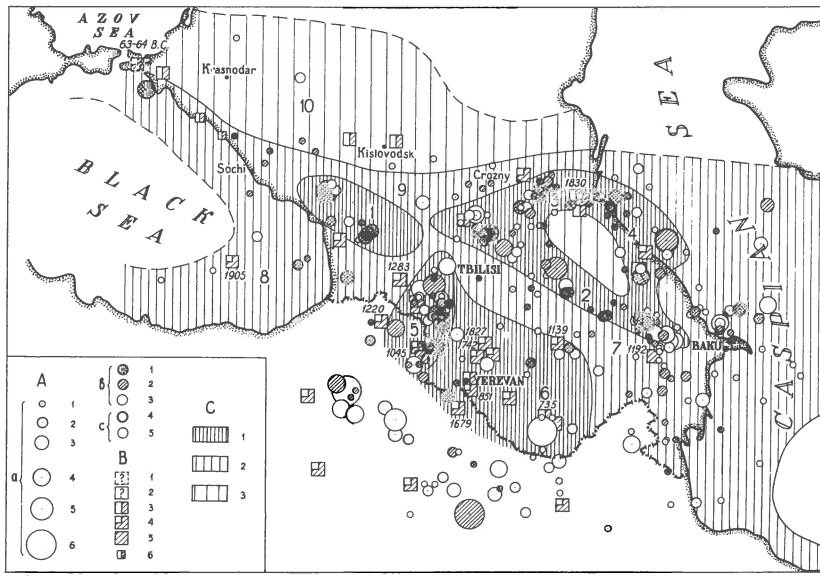

Fig. 2: Epicentre map of strong earthquakes in the Caucasus and a scheme of zones with a probable origin of strong earthquake foci. Zones: 1) Western zone of Greater Caucasus. 2) Eastern zone of Greater Caucasus. 3) North-eastern flank of Greater Caucasus. 4) Junction zone of the Caspian Sea basin with the north-eastern flank of Greater Caucasus. 5) Western zone of Lesser Caucasus. 6) Eastern zone of Lesser Caucasus. 7) Kura depression. 8) Junction zone of Black Sea basin with the Caucasus. 9) Northern Caucasus. 10) Junction zone of the Caucasus with the Russian platform.

A. Instrumental epicentres for the years 1910-1964.
a) Classification by magnitude: 1 - M = 4 - 4 1/4; 2 - M = 4 1/2 - 4 3/4; 3 - M = 5 - 5 1/4; 4 - M = 5 1/2 - 5 3/4; 5 - M = 6 - 6 1/4; 6 - M = 6 1/2 - 6 3/4.
b) Classification by the precision of determination: 1 - Class A - ± 25 km; 2 - Class B - ± 50 km; 3 - Classless.
c) Classification by the depth of focus: 1 - deep focus; 2 - focus in the crust.

B. Macroseismic epicentres.

Earthquakes before 1910: 1 - coordinates very indefinite; 2 - intensity unclear (VII-IX ?); 3 - I_o = VII; 4 - I_o = VIII; 5 - I_o = IX. 6 - earthquakes with I_o VII after 1910 for which no instrumental coordinates have been determined.

C. Zones of foci origin of strong earthquakes.
1 - zones of second category 6 1/4 ≦ M < 7 1/2. 2 - zones of third category 5 1/4 ≦ M < 6 1/4. 3 - zones of fourth category 4 1/2 ≦ M < 5 1/4.

Table 1: Scale for the classification of earthquakes by the energy of elastic waves

K	M	I_o	Area of tremors in th.sq.km. according to macroseismic data without consideration given to nature of ground			Distance of P wave recorded by general-type devices
			I over or equal to IX	I over or equal to VIII	I over or equal to VII	
18	$M > 8.1$	XII	10	10 - 30	30 - 100	
17	$7\frac{1}{4} < M \leqq 8$	X-XI	2	2 - 10	10 - 30	
16	$6\frac{1}{2} < M \leqq 7\frac{1}{2}$	IX-X	0.5	0.5 - 2	1 - 10	
15	$5\frac{3}{4} < M \leqq 6\frac{1}{2}$	IX	0.05	0.05-0.5	1.0	over 90°
14	$5\frac{1}{4} < M \leqq 5\frac{3}{4}$	VIII				45-90°
13	$4\frac{1}{2} < M \leqq 5\frac{1}{4}$	VII				30-45
12	$4 < M \leqq 4\frac{1}{2}$	VI				20-30
11	$3\frac{1}{2} < M \leqq 4$	V				7-20
10	$3 < M \leqq 3\frac{1}{2}$	IV				4-6.5
9	$2\frac{1}{2} < M \leqq 3$	III				5.5-4°

Table 2: Sizes of focus, areas of aftershocks, and area of the preparation of the earthquake

K	12	13	14	15	16	17	18
M	$4\frac{1}{2}$	5	$5\frac{1}{2}$	6	$6\frac{1}{2}$ - 7	$7\frac{1}{2}$ - 8	$8\frac{1}{2}$
				Focus of earthquake			
km	3	6	10	20	30 - 60	100-200	300-900
				Area of aftershocks			
km^2	6	20	60	200	600-2000	$2 \cdot 10^3$-$2 \cdot 10^4$	$6 \cdot 10^4$-10^5
				Area of the preparation of earthquakes			
km^2	30	140	650	$3 \cdot 10^3$	$1{,}4 \cdot 10^4$	$6{,}5 \cdot 10^4$	$8 \cdot 10^5$

In distinguishing zones with different maximum energy (magnitude) it is advisable as a first step to distinguish zones, between which the maximum energy of earthquakes will differ approximately two orders. In this connection all earthquakes are divided into six categories:

$$M_I > 7\frac{1}{2} \geqq M_{II} > 6\frac{1}{4} \geqq M_{III} > 5\frac{1}{4} \geqq M_{IV} > 4\frac{1}{4} \geqq M_V > 3\frac{1}{4} \geqq M_{VI}.$$

In estimating seismic danger earthquakes of the I-III categories (see Table 3 and Fig. 2) are of greatest interest.

2.2. Specific features in the distribution of earthquake foci in space

Nearly all the earthquakes of the Caucasus take place within the crust. On Fig. 2 only one earthquake of April 9, 1935 has its focus at a depth of 150 km. The majority of earthquake foci are located in marginal parts of the meganticlinoria of Greater and Lesser Caucasus. The greatest number of foci concentrated into definite groups are located within the eastern part of Greater Caucasus (east of meridian 44°E). The most distinct groups of earthquake foci are distinguished on the southern flank of Greater Caucasus in the area of Shemakha, Zakataly, and Kazbek; on the northern flank there are many epicentres in the area of Grozny-Makhachkala-Derbent; in the Caspian Sea they are recorded east of Derbent and north of Apsheron peninsula. On Lesser Caucasus the group of epicentres on Akhalkalaksk highland is especially distinct. In the past there have been many strong earthquakes in the areas of Sevan Lake, Erevan-Ararat, Nakhichevan (Zangezur and Aiozdzor mountains).

Foci of separate earthquakes occur also in junction places of the basins of the Black Sea and the Caspian Sea with the Caucasus as well as in the junction places of the Caucasus with the Russian platform.

III. Distinguishing zones of possible strong earthquake-foci on the basis of combined seismological and geotectonic data

By a comparison of the tectonic map with the distribution of the main epicentral zones relations have been established between seismicity and the history of the development of tectonic movements for individual blocks of the crust in the Caucasus.

Table 3

List of strong earthquakes in the Caucasus ($I_o \geqq$ VIII; $M \geqq 5\frac{3}{4}$)

Date	N.L.	E.L.	Class *) of precision	Zone	M	I_o	Region	Brief data
1	2	3	4	5	6	7	8	9
64-63 B.C.				8		VIII	Taman	Panticapaeum (Kerch), Phanagoria ruined.
735	39°,6	45°,5	?	6		VIII	Aiozdzor (Daralagez)	About 10 000 people perished
851,858,863, 869,893,894	40,0	44,6	?	6		VIII	Dvin (Artashat)	Dvin ruined. About 70 000 people perished
906	39,6	45,5	?	6		VIII	Aiozdzor (Daralagez)	Churches ruined
1045	40,6	43,3	?	5		VIII	Ani	Palaces ruined
22/IV-1088	41,4	43,3	?	5		VIII	Akhalkalaki, Tmogvi	City ruined
1132	40,6	43,3	?	5		VIII	Ani	Church ruined
1139				6		VIII	Gandzha (Kirovabad)	Gandzha and church in Akhpata (Alaverdi) ruined
1192	40,7	48,6	?	2		VIII	Shemakha	Destructions
1220	41,0	43,0	?	5		VIII	Ardagan	Church ruined
1235	40,7	46,3	?	6		VIII	Gandzha (Kirovabad)	

1	2	3	4	5	6	7	8	9
1283	41,7	43,2	?	5		VIII	Akhtsuri (Borzhomi region)	Churches ruined
1318	41,8	43,7	?	5		VIII	Mtskheta	Cathedral ruined
1319				6		VIII	Ararat, Ani, Sunik (Sision)	A number of cities ruined
1667, 1669, 1671	40,7	48,6	?	2		VIII	Chemakha	Devastations; about 80000 people perished
4/VI-1679	40,1	44,7	?	6		VIII	Ararat	A number of cities ruined
24/VII-1742	42,0	45,3	?	6		VIII	Alaverdi	Churches ruined
1827	40,5	44,8	?	6		VIII	Pambak, Sevan	Churches ruined
9/III-1830	43,0	47,0	?	3		VIII	Northern Daghestan	
2/VII-1840	39,6	44,5	?	6		VIII	Ararat	3000 houses ruined
11/VII-1859	40,7	48,4	B	2		VIII	Shemakha	Devastations; 100 people perished
2/IX-1869	40,6	48,7	B	2		VIII	Shemakha	Over 200 houses ruined
28/I-1872	40,6	48,8	B	2		VIII	Shemakha	City ruined
31/XII-1899	41,6	43,5	B	5		VIII	Akhalkalak upland	Destructions in three villages

1	2	3	4	5	6	7	8	9
13/II - 1902	40,7	48,6	B	2		VIII	Shemakha	About 7000 houses ruined
21/X - 1905	42,0	39,5	?	8			Black Sea	
20/II - 1920	42,0	44,1	B	5	$5\frac{3}{4}$ - 6	VIII	Adzharo-Trialeti, Gori	213 houses ruined on an area of 1000 sq.km
19/II - 1924	39,0	47,8	B		$5\frac{1}{2}$	VII	Ardebil	Buildings damaged
9/I - 1925	41,0	43,0	B	5	$5\frac{3}{4}$	VIII	Ardagan	Destructions in 43 villages
22/X - 1926	40,7	43,8	B	5	$5\frac{1}{2}$	VIII	Leninakan	1500 houses ruined
27/IV - 1931	39,3	46,0	B	6	$6\frac{1}{2}$	VIII	Zangezur	
9/IV - 1935	42,3	51,0	B	4	6	VI	Caspian Sea	Depth 150 km.
7/V - 1940	41,7	43,8	B	5	$5\frac{1}{2} - \frac{3}{4}$	VIII	Tabatskuri	
29/VI - 1948	41,9	46,4	B	2	$6\frac{3}{4}$	VII	Zakataly	
16/VII - 1963	43,2	41,8	A	1	$6\frac{1}{4}$	VIII	Chkhalta, West Caucasus	Buildings ruined
20/IV - 1966	41,8	48,2	A	4	$5\frac{3}{4}$	VIII	South Daghestan	
12/VII - 1966	44,7	37,2	A	8	$5\frac{1}{2} - \frac{3}{4}$	VI	Black Sea	

*) Classification by the precision of determinations of epicentres
A - ±25 km; B - ±50 km; ? - uncertain.

The strongest earthquakes originate in the intersection zones of deep faults of two directions (meridional and latitudinal). Earthquakes of an average intensity are associated with zones of longitudinal faults. Slight earthquakes originate practically everywhere. Using data on tectonics and seismicity it is possible to distinguish zones, within which earthquakes can originate with a varying maximum magnitude.

Table 3 shows that owing to a limited size of seismoactive zones in the Caucasus (not more than $5 \cdot 10^4$ sq.km) there can be no earthquakes here with $M_I > 7\frac{1}{2}$.

Zones of the second category are distinguished, where the origin of earthquakes with $6\frac{1}{4} \leqq M_{II} < 7\frac{1}{2}$ is possible. For instance several earthquakes with a magnitude of $6\frac{1}{2}$ are known on the southern flank of Greater Caucasus. Earthquake foci are located in one tectonic zone at a rather great distance from each other. Previously there have been no foci between them with a magnitude $6\frac{1}{2}$, but their appearance in future is quite probable inasmuch as we find here one direction of tectonic movements. In case of the origin of an earthquake with $6\frac{1}{4} \leqq M < 7\frac{1}{2}$ within the crust in the Caucasus, the zone of intensity VIII earthquakes can reach an area of 500-2000 sq.km and in the epicentre under unfavourable conditions of the ground there can be intensity IX devastations (Table 1). As a first stage it is necessary to distinguish zones, where foci of such earthquakes could originate according to a combination of seismological and geological data. This has been shown on Fig. 2.

Ten zones are distinguished in the concentration of earthquake foci of varying intensity. Zones of earthquakes of the II category: southern flanks of Greater Caucasus (1 and 2), northern (3) and north-eastern (4) flanks of Greater Caucasus; the western (5) and eastern (6) zones of Lesser Caucasus. Zones of earthquake concentrations of the III category: Kura depression (7), junction zone of the Black Sea basin with the Caucasus (8) and Northern Caucasus (9). Earthquakes of the IV category in the junction zone of the Caucasus with the Russian platform (10).

Table 4

Characteristics of the main seismoactive zones of the Caucasus

No	Name of zone	Zone area in 10^3 km^2	γ	A_{10}	Strongest earthquake observed			Category of possible maximum earthquake	Average period of recurrence M_{max} for 1000 years on area 1000 km^2
					M_{max}	I_{max}	Date		
1.	Western zone of Greater Caucasus	10	0,5	0,1	$6\frac{1}{4}$	VIII	16/VII-1963	II	0,1-0,3
2.	Eastern zone of Greater Caucasus	20	0,42	0,3	$6\frac{1}{4}$	VII	29/VI -1948	II	1-2
3.	North-eastern flank of Greater Caucasus	12	0,5	0,25	5	VII	2/III -1966	II	0,2-0,6
4.	Junction of Caspian Sea basin with north-eastern flank of Greater Caucasus	30	0,42	0,2	6	VI	9/IV - 1935	II	0,5-1
5.	Western zone of Lesser Caucasus	20	0,42	0,35	$5\frac{3}{4}$	VIII	7/V - 1940	II	1-2
6.	Eastern zone of Lesser Caucasus	40	0,46	0,10	$6\frac{1}{2}$	VIII	27/IV- 1932	II	0,2-0,3
7.	Kura depression	60	0,5	0,05	5	VI	5/III- 1946	III	0,1-0,3
8.	Junction of Black Sea basin with the Caucasus	60	-	-	$5\frac{1}{2}$	VI	12/VII-1966	III	-
9.	Northern Caucasus	25	-	-	$5\frac{1}{2}$	VII	14/I 1915	III	-
10.	Junction of the Russian platform with the Caucasus	60	-	-	$4\frac{1}{2}$ - $4\frac{3}{4}$	VII	19/IV -1926	IV	-

Table 4 gives the fundamental characteristics of the seismic regime in these zones and of the earthquakes with a maximum energy which already occurred in these zones. A conclusion on the possibility of earthquakes with M_{max} in Table 4 was arrived at on the basis of data on the sizes of the zones (Table 2 and Fig. 2) and on their activity (Table 3).

Distinguishing big zones is the purpose of forecasting the main zones of the probable origin of strong earthquakes, which is the first step in compiling a map of seismic regionalization.

In addition to the ten fundamental zones there are also local zones, like, for instance, the deep fault zone in the eastern part of Kura depression, the zone of Talysh mountains, the junction zone of Kura depression with the northern flank of Lesser Caucasus, the junction zone of Rioni depression with the southern flank of Greater Caucasus, etc. The establishment of these local zones is the purpose of the following stage of researches.

The authors thank most sincerely N.A.Vvedenskaia and I.V.Kirillova for their data and valuable advice used in the compilation of this paper.

R.Parks

CRUSTAL STRUCTURE OF THE BRITISH ISLES

A combined interpretation has been made for three separate explosion projects in the British Isles:

1962: A total of 21 depth charges (130 kg.) centred on Eskdalemuir, consisting of profiles to NE and SW, and an arc at 150 km. Some of these were also recorded at Rookhope, in northern England. An interpretation of this data has been published by Agger & Carpenter in 1964.

1965, Irish Sea: A joint project by the Universities of Edinburgh and Birmingham. 25 depth charges (130 kg.), fired on three profiles in the Irish Sea and recorded at three temporary stations in Wales and one in Ireland, covering distances from 4 to 230 km. Most of the shots were well recorded at Eskdalemuir, at distances from 220 to 400 km., and some also at the Rookhope site. Originally it was planned to use the Birmingham sonobuoys for short-range observations, but ultimately this was impossible because of changes in the shooting dates.

1965 Noordzee: A refraction study carried out by the Vening Meinesz Institute of Utrecht using the "velocity-depth" method. Charges ranged up to 2340 kg; most of the shots were recorded at Eskdalemuir and some also at field stations of the Irish Sea project.

Initially, interpretation has been concentrated on first arrivals, because of the greater uncertainties inherent in the identification of later arrivals. On first inspection, the observations appeared to fit two principal layers, with velocities around 6 and 8 km/sec and a cross-over around 120 km. - a model similar to that of Agger & Carpenter. However, the striking feature which emerges is that for the Irish Sea shots observed in Wales and Ireland, the first arrivals beyond 130 km. do not fit the velocity of 8 km/sec expected for P_n. Instead a value of 7.36 km/sec is indicated, with 95% confidence limits of $\pm$ 0.06 km/sec, and it

would seem that this corresponds to a well-defined layer. On the other hand, the long-range observations at both Eskdalemuir and Rookhope for all projects give satisfactory agreement with a velocity of 7.9 km/sec.

If the difference in velocities is to be explained as regional velocity variation, this would require variations of the order of 5% per 100 km. Although such large variations have been reported under the Rocky Mountains (Herrin & Taggart, B.S.S.A., 52, 1037-1046) it is considered unlikely that crustal structure in this area is equally complicated. On the contrary, preliminary results from the Skagerrak Project and from Norwegian shots observed at Eskdalemuir point to a high degree of uniformity, with virtually identical Pn velocities for both Jutland and the North Sea: 7.84 ± 0.04 km/sec.

The preferred interpretation is based on a velocity of 7.9 km/sec for the M-discontinuity under the entire area, with an intermediate layer of 7.4 km/sec appearing under the southern part. Some, but not all, of the Eskdalemuir records show a later phase which would correspond to the intermediate layer, and it may be that this layer changes horizontally in a manner related to the transition from continental to oceanic crust.

For the southern Irish Sea, where sufficient closely-spaced observations are available to provide information on the upper layer, the typical structure is:

Velocity, km/sec.	3.3	5.4	6.3	7.4	7.9
Depth, km		1.7	5.2	22-29	38

For the remainder of the region the details of shallow structure are less complete, but the depth to the M-discontinuity is estimated to be approximately 29 km for the vicinity of Eskdalemuir and 39 km for the Flamborough Head profile.

Alfonso Lopez-Arroyo and Gonzalo Payo

CRUSTAL STRUCTURE OF THE SPANISH CENTRAL PLATEAU

I. Introduction

The Spanish Seismological Survey has undertaken a broad program for investigating the crust-mantle structure in the Iberian peninsula. As part of such program one of us determined the velocity of crustal body phases (Payo 1964) and studied also the structure best fitting the data of surface waves dispersion from Toledo and Málaga records (Payo 1965).

Both studies refer to the peninsula as a whole. But the known tectonic features make very improbable the hypothesis of uniformity througout the region; on the contrary, there must be clear structural differences between, e.g., the Central Plateau and the Guadalquivir valley zone. Therefore, it becomes neccesary to make detailed studies of each one of the tectonic units composing the Iberian peninsula.

A program comprising three large refraction seismic profiles is in preparation for such study, to be developed in collaboration with institutions from other European countries. But it seems that some years will elapse before the program materializes. Then we thought it of interest to take advantage of large explosions in quarry blasts or of those produced for public works, for attempting the study of crustal structure of small regions. The present paper shows an example of this investigation.

II. Seismic data

As the Spanish Seismological Survey does not have yet portable seismographs the only explosions useful for our purpose are those produced near enough to an observatory to be recorded by the short period equipment of the station. The limestone quarry worked by "Cementos Asland" in Yepes,

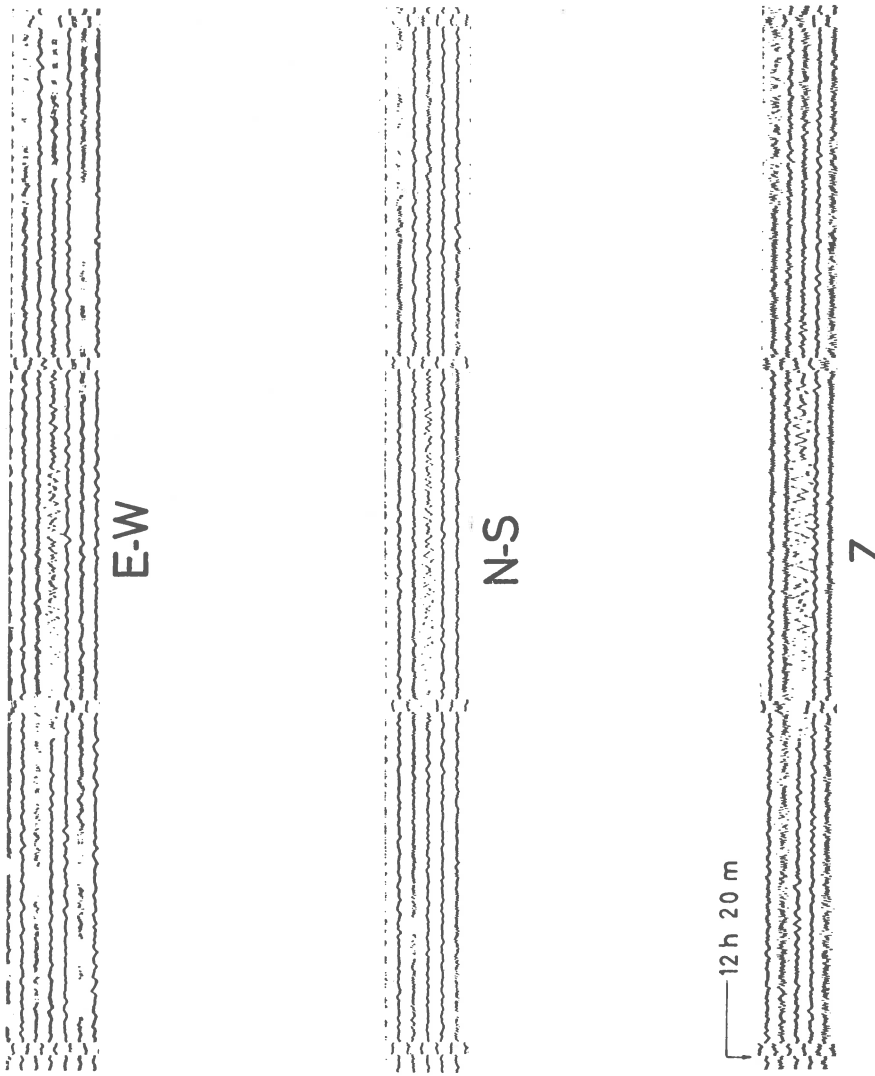

Fig. 1. Example of a blast recorded at Toledo by the short period Benioff seismographs.

31.625 km distant from Toledo observatory, provides frequent examples of this type.

A three component set of variable reluctance, Benioff type of short period seismographs, of the World Wide Standard Seismograph Network, are installed at Toledo.

A sample of the records obtained with such equipment of the Yepes quarry blasts is shown in Fig. 1. Paper speed is only 60 mm per minute and this limits the reading accuracy to about 0.1-0.2 sec. A similar accuracy was obtained for the firing time introducing a signal on the records using a telephone line from the quarry to the vault.

Nine records were selected from a total of 65 recorded blasts; they show quite clear onsets of the crustal body phases and well developed trains of Rayleigh waves.

III. Geological information

The Toledo observatory and Yepes are both placed in the Spanish Central plateau, between the great Guadarrama fault to the North and the Toledo mountains to the South. The formations outcroping in this zone are of two distinct types: highly metamorphed gneiss (basement rocks) and sedimentary rocks, mainly from Miocene and Holocene age with a few occurrences of Cenomanien. The contact between both rock types is represented by a wide fault system, to the South of the line Observatory-Yepes, with an approximate E-W trend.

Holocene formations are seen on the surface in the vicinity of the Observatory (Fig. 2). Sandy Tortoniense (feldspar sands with clay) predominates more to the East, passing later to gypsum and gypsy marls, and, still further East, near Yepes, Pontiense rocks (limestone, silex, sepiolite) rest on top of the Tortoniense formations; it is the Pontiense limestone that is worked at the Asland quarry.

The sedimentary layers fill up a large basin, the so-called tectonic basin of the Tagus river. An indication of the sedimentary layer thickness is provided by the borehole drilled by the Geological Institute near Alcalá de

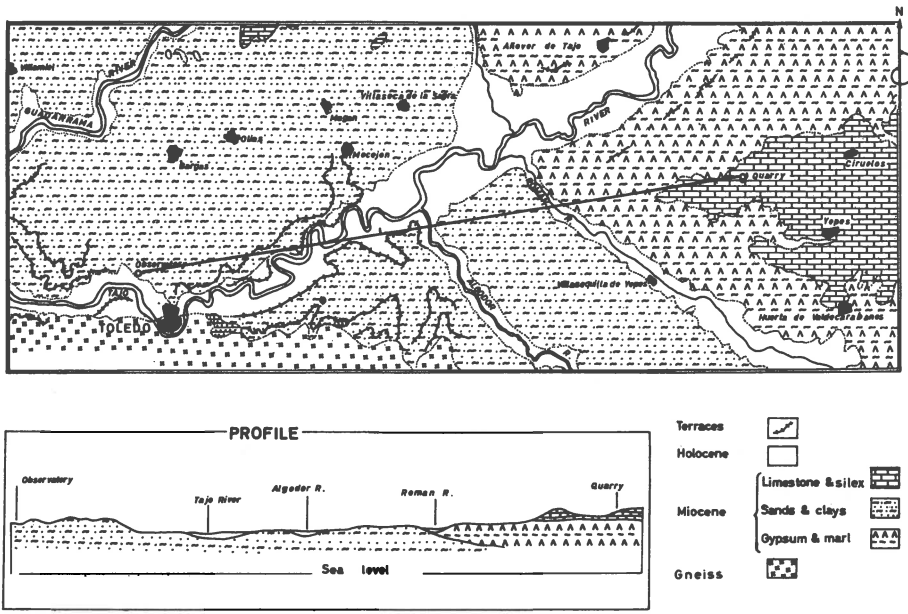

Fig. 2: Geologic map and section of the Observatory-Asland quarry area.

Henares (some 70 km to the NNE of Yepes) which went to a depth of more than 1.000 m without reaching the Eocene; another bore-hole drilled by Valdebro in Tielmes (about 50 km to the NE of Yepes) placed on a basement high, cut monzonitic granite at a depth of 2.212 from surface. The basin was formed as a large syncline when the Central Mountain Range and the Toledo mountains were raised by the Hercynian movement. It underwent several downward motions in later times and was differentiated as an interior lake at the beginning of the Miocene, a lake which was filled up with sediments apported by the rivers. The Miocene sediments were affected by the Neo-Alpine movement and tilted to the West, thus changing the base level of the rivers and starting a strong erosive action of them (Tagus, Tajo in Spanish, means cut).

A schematic profile from the Observatory to the Yepes quarry, is also shown in Fig. 2. It must be remembered however that it has only an indicative value.

IV. Results from body waves

Fig. 3 shows the average time and relative amplitude of the onsets which can be read in the blast records. The time deviation for a given onset in the different records considered does not exceed 0.2 sec for a given component; differences up to a maximum of 0.3 sec between the vertical and horizontal components have been read in a few cases. The relative amplitudes are very nearly the same for all recorded events, a result which is to be expected, since the explosion conditions are similar and the yielding of the blasts recorded varies in a fairly narrow range.

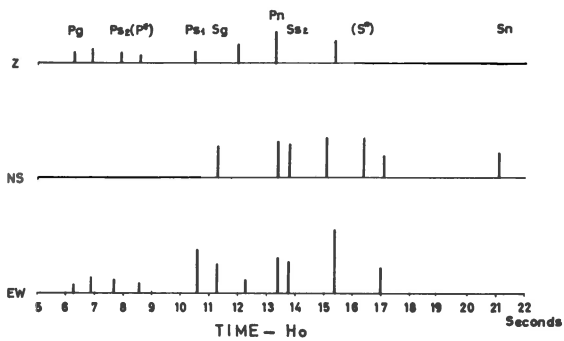

Fig. 3: Position and relative amplitude of recorded phases.

Pg and Sg waves are well recognizable on the records. Other onsets are not easy to identify. We used a trial and error and recurrence technique and arrived at the solution shown in the figure. The velocities, layer thicknesses and values corresponding to this solution are shown in Table 1.

In getting this solution we have considered that according to geologic data and the information available from bore-holes, in the sedimentary layer only the contact between the clayly rocks of the Cenozoic and the Upper Cretaceous formations presents an acoustic impedance contrast large enough to provide waves with energy recordable at the Observatory; thus, only two pairs of waves through the sedimentary section have been searched for. On the

Table 1

Model parameters

	Layer:	SEDIMENTARY	GRANITIC	BASALTIC	UP.MANTLE
MODEL 1	H	a. 1.2 b. 1.3			
	α	2.6	5.2		
	β	1.5	3.01		
	ρ	2.0	2.6		
MODEL 2	H	1.3			
	α	2.77	5.54		
	β	1.6	3.2		
	ρ	1.5			
MODEL 3	H	1.25			
	α	3.01	5.85		
	β	1.52	3.50		
	ρ	2.4	2.67		
MODEL from crustal phases	H	S1. 1.0 S2. 0.5			
	α	S1. 3.01 S2. 4.38	5.81		
	β	S1. 1.80 S2. 2.42	3.15		
MODEL IB 2	H	4.7	18.3	10.0	80.0
	α	3.94	5.9	6.6	8.1
	β	2.37	3.3	3.7	4.72
	ρ	2.34	2.8	2.85	3.3

other hand, the thickness of the sedimentary series should be smaller than that observed near Tielmes, since the Tagus basin thickens towards NNW and the basement rise at the bore-hole site is a gentle one; the adopted value must be taken as an average, because it is clear that the granite is much closer to the surface at the Observatory than under the Asland quarry. Finally, the relative amplitude on the three records has been taken into consideration in the

identification of phases; the relative position of the quarry with respect to the Observatory leads to expect that the dilatational waves will be recorded almost exclusively by the Z and N seismographs and it is also likely that the sedimentary phases have a large horizontal component.

Main features of the interpretation, apart from the sedimentary thickness, are the relatively high velocity of the materials in this upper formations (verified, by the way, by velocity log at a borehole in the basin) and the smaller velocity of the granitic layer as compared with the values given by the previous paper (Payo 1964).

V. Results from surface waves

All selected records show clear trains of Rayleigh waves guided mostly by the sedimentary layer. The trains are poorly dispersed (period-change from 1.6 to 2.5 sec) and the amplitudes also are fairly constant. The group velocity obtained from 5 records has been plotted in Fig. 4.

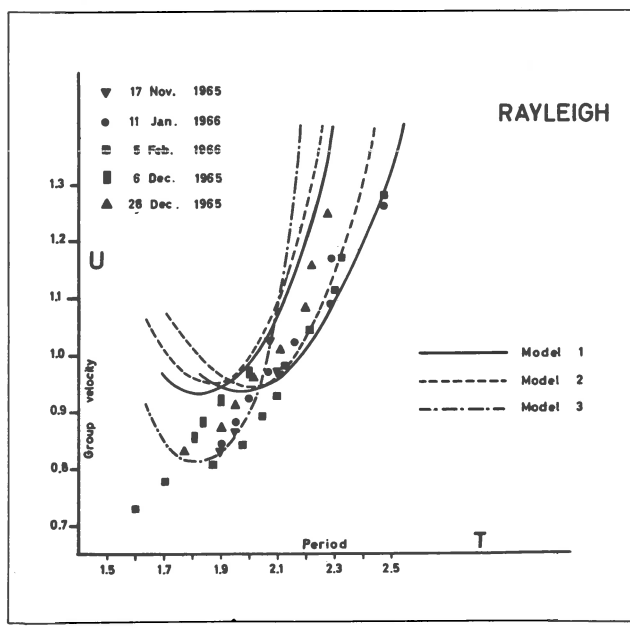

Fig. 4. Rayleigh wave dispersion data and theoretical dispersion curves for models 1, 2 and 3.

The scatter of points in the figure must be attributed to measurement errors, which cannot be avoided due to the low paper speed. But the general trend of the dispersation curve appears fairly well defined.

The tables of Mooney and Bolt (1964) have been used in order to obtain a simple structure with a dispersion curve coinciding with the data. As is known these tables allow the computation of dispersion curves corresponding to one-layer models with a wide variation of parameters. For the first model considered (model no. 1 in Table 1 and Figure 4) we kept a value of the shear wave velocity in the granitic layer similar to that obtained from the body wave analysis. Other models were considered for different values of velocity distribution and thickness of the sedimentary layer; two examples (models 2 and 3) are given in the table and the corresponding dispersion is shown in Figure 4. From these results it may be concluded that the thickness of the sedimentary layer is not larger than 1.4 to 1.5 km, in good agreement with the body wave data. It seems however that the dispersion data require a surface layer of very low velocity. On the other hand, the velocities obtained by the body wave analysis seem to be acceptable.

VI. Relation amplitude-charge

In Fig. 5 we have plotted the maximum record amplitude on the N-S component for different blasts of known size. It is clearly seen that in the range between 1500 and 4500 kgs of dynamite there is a linear relationship of the amplitude with the charge size. This relation may be expressed by the equation

$$A_r = 3.3 \times 10^{-3}\ C - 3$$

where A_r is record double amplitude in mm and C charge in kgs; since the maximum amplitude is usually shown by the Sg wave, with a period around 0.4 sec for which the instrument magnification is 35000,

$$A_g = 9.5 \times 10^{-5}\ C - 8.5 \times 10^{-2}$$

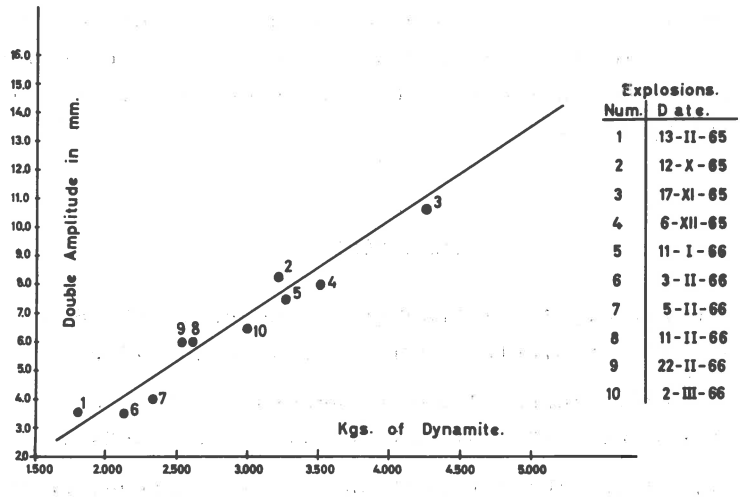

Fig. 5. Relation record amplitude to size of the charge.

where A_g is ground motion amplitude in microns and C is measured in kgs as before.

An interesting consequence of Fig. 5 is the capability of recording at Toledo observatory blasts from the Asland quarry of size as low as 1500 kgs to which corresponds a local Richter magnitude, M_L, of the order of 1.0. This is possible because the background noise on the short period instruments is mainly of larger period (1.5 to 2.0 sec) with the exception of that produced by trucks passing through the nearby road, which has a larger frequency (5 cps).

The situation is different at Málaga observatory, where another Benioff short period seismograph set is in operation; the noise on these instruments has a fairly large amplitude for periods of the order of 0.4 - 0.6 sec, then masking the records of small charge blasts (see Lopez Arroyo 1964).

Concluding remark

An example is given of crustal structure investigation carried out by the Spanish Seismological Survey using standard observatory equipment. Portable seismographs

have been ordered by the SSS and a large program with three long profiles will be developed in the near future. But in the meantime it seems worthwhile to make short studies like the one presented here because some information may be gained by them.

References

Lopez Arroyo, A., 1964: "Background noise on the SSS Standard instruments". Mem. I.G.C., v.33, 48 p.

Payo, G., 1964: "Crustal phases across the Iberian peninsula region". An. di Geof., v.17, 523-545.

Payo, G., 1965: "Iberian peninsula crustal structure from surface wave dispersion". B.S.S.A., v.55, 727-743.

Mooney, H.M. and Bolt, B.A.: "Dispersion tables for Rayleigh waves o a single surface layer". VESIAC Sp. Rep. 4410-102-X, 192 p.

G.Dohr, B.Hadjebi und K.Hehn

BEOBACHTUNGEN VON TIEFENREFLEXIONEN IN NORDDEUTSCHLAND

Auf der Tagung der CSE in Budapest im Jahre 1964 wurde über den Stand der Beobachtung und Auswertung von Tiefenreflexionen in der Bundesrepublik berichtet. Der Schwerpunkt der Beobachtungen lag damals im süddeutschen Raum, welcher zuerst durch umfassende Bearbeitungen, vor allem durch LIEBSCHER, ein vorläufiges, deutbares und geschlossenes Bild ergeben hatte.

Im vorliegenden Referat soll ausschliesslich über die Ergebnisse im norddeutschen Raum berichtet werden, in welchem nach früheren sporadischen Beobachtungen in den letzten Jahren von Hadjebi und Hehn über 5200 Seismogramme ausgewertet worden sind.

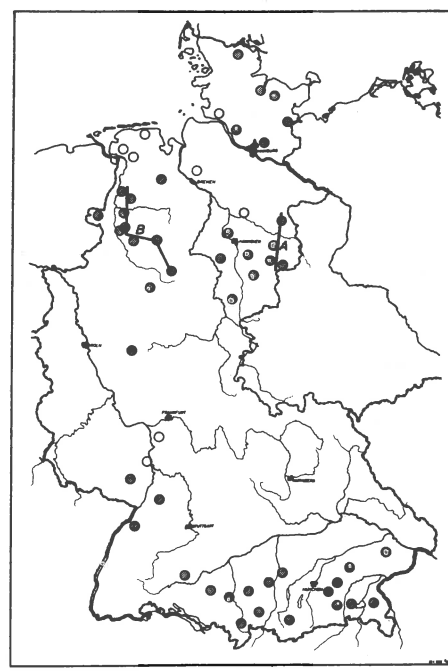

Figur 1: Übersichtskarte. Eingetragen sind durch schraffierte Kreise Arbeitsgebiete, in welchen gute oder brauchbare Tiefenreflexionen in der Bundesrepublik beobachtet wurden. Die offenen Kreise kennzeichnen Gebiete, welche mehrdeutige Ergebnisse lieferten

Abb. 1 gibt einen Überblick über die Beobachtungsgebiete in der Bundesrepublik. Man erkennt, dass sich die Messgebiete, in welchen Tiefenreflexionen beobachtet worden waren, vor allem auf 2 Räume konzentrierten, nämlich einmal den süddeutschen Raum südlich der Donau und das nordwestdeutsche Gebiet. Hier liegen die Messgebiete bevorzugt an dem Südrand des nordwestdeutschen Beckens. Ausserdem fallen eine Reihe von Registrierungen in den Raum von Schleswig-Holstein.

Zur Technik der Registrierung:
Einsatz von Magnetbandapparaturen der Firmen Seismos und Prakla. Hersteller: PRAKLA, SIE, GEOSPACE. Registriert wurde mit einer Verstärkereinstellung und Filterung, die für die Erfassung der für die Erdölproduktion interessierenden oberen Stockwerke optimal erschienen. Die Geophone hatten durchweg Eigenfrequenzen zwischen etwa 22 und 28 Hz. Erst in neuerer Zeit sind vereinzelt auch etwas tiefer abgestimmte Geophone bis herunter zu 14 Hz Eigenfrequenz zum Einsatz gekommen. Bündelung der Geophone zwischen 6- und 12-fach. Filterung allgemein etwa zwischen etwa 25 und 70 Hz.

Dieses alles bedingt, dass die Registrierung nicht mit den optimalen Bedingungen für die Erfassung von Reflexionen mit langen Laufzeiten erfolgte. Versuche mit sehr tief abgestimmten Refraktions-Geophonen (Eigenfrequenz ca. 2 1/2 Hz) ergaben keine Verbesserung der Aufzeichnung.

Wie bei früheren Bearbeitungen und den Ausarbeitungen im bayerischen Raum wurde auch in Norddeutschland zunächst wieder eine statistische Bearbeitung des anfallenden umfangreichen Materials durchgeführt und für jedes Messgebiet Häufigkeitsverteilungen der Tiefenreflexionen aufgestellt. In denselben ist, wie bereits mehrfach erwähnt, die absolute Anzahl der beobachteten Reflexionen als Funktion der Reflexionslaufzeit aufgetragen, wobei als Intervallbreite für die Auszählung der Reflexionen oder Reflexionsandeutungen im allgemeinen eine Intervallbreite von 0,2, in einigen Fällen auch von 0,1 sek., gewählt wurde. Verschiedentlich wurden auch Darstellungen mit einer Bewertung der Reflexionen gegeben, die indessen nur graduelle Unterschiede, jedoch keine sehr wesentlichen Änderungen in dem Erscheinungsbild der Häufigkeitsverteilungskurven bedingen. Statisti-

sche Teste bestätigten allgemein die Signifikanz der auffällig hervortretenden Maxima.

Während in Bayern die Häufigkeitsverteilungskurven durchweg recht scharfe Maxima lieferten, die sich zwanglos über viele Gebiete korrelieren liessen, ist das Erscheinungsbild dieser Kurven in Norddeutschland meist komplizierter. Dieses mag z.T. seine Ursache darin haben, dass die reellen Reflexionen von tieferen Unstetigkeitsflächen vielfach von multiplen Reflexionen überlagert sind, z.T. mag die Ursache aber auch tatsächlich in einer anderen Beschaffenheit der tiefen Grenzflächen bzw. der Übergangszonen zu suchen sein. Hierfür spricht, dass in verschiedenen Gebieten der Bereich der Maxima verschwommen erscheint oder aber, dass die Maxima eine beträchtliche Halbwertsbreite besitzen.

In den meisten Beobachtungsgebieten wurden brauchbare bis gute Reflexionen, bevorzugt bei einer Reflexionszeit von 5 - 6,5 Sekunden, registriert. Diese immer wieder beobachtete Anhäufung von Reflexionen wurde als Hinweis auf die Conrad-Diskontinuität angesehen. Auf die Problematik dieser Zuordnung und ihre Wertung als blosse Arbeitshypothese wird noch weiter unten eingegangen werden.

Mit grösserer Wahrscheinlichkeit dürfen die Maxima in den Häufigkeitsverteilungskurven bei zumeist etwa 10 - 12 Sekunden, welche z.T. recht markanten Reflexionseinzätzen korrespondieren, der Mohorovičić-Diskontinuität zugeordnet werden.

Nach der Zuordnung der Spitzen in den Häufigkeitsverteilungen zu tiefen Unstetigkeitsflächen erfolgte eine Umrechnung auf Teufen, einheitlich mit den plausibelsten Geschwindigkeitsannahmen. Die Wirkung der Sedimente bis zum Zechstein wurde mit Hilfe der Unterlagen der Erdölindustrie eliminiert, d.h. es wurde in jedem Messgebiet mittlere Teufe und Reflexionslaufzeit des Zechsteinbasisbereiches ermittelt. Unterhalb des Zechsteins wurde bis zum Bereich der Conrad-Diskontinuität mit einer durchschnittlichen Geschwindigkeit von 5900 m/sek. gerechnet, darunter wurde eine Intervallgeschwindigkeit von 6800 m/sek. angesetzt. Dort, wo mit dem Auftreten einer Inter-Diskon-

tinuität zwischen der Conrad- und Mohorovičić-Diskontinuität gerechnet werden kann, wurde an derselben nochmals ein Geschwindigkeitssprung von 6800 m/sek. auf 7100 m/sek. angenommen.

Die nachfolgenden 3 Abbildungen geben die Zusammenstellungen der Häufigkeitsverteilungskurven über grössere Gebiete. Dabei soll auf den unterschiedlichen Charakter der Maxima in den einzelnen Räumen hingewiesen werden. Abb. 2 zeigt die Kurven längs eines NS-Profiles östlich von Hannover, in welchem sich die Maxima einander recht gut zuordnen lassen. Die Lage dieses und des in Abb. 4 genannten Profiles ist in der Abb. 1 eingetragen.

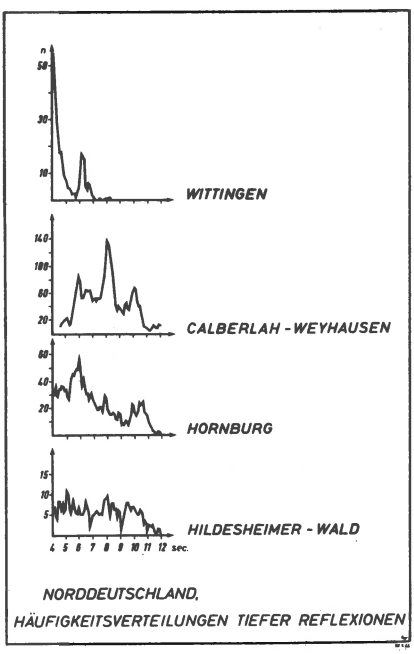

Figur 2: Häufigkeitsverteilungen tiefer Reflexionen aus mehreren Arbeitsgebieten im Raum Osthannover (Profillinie A).

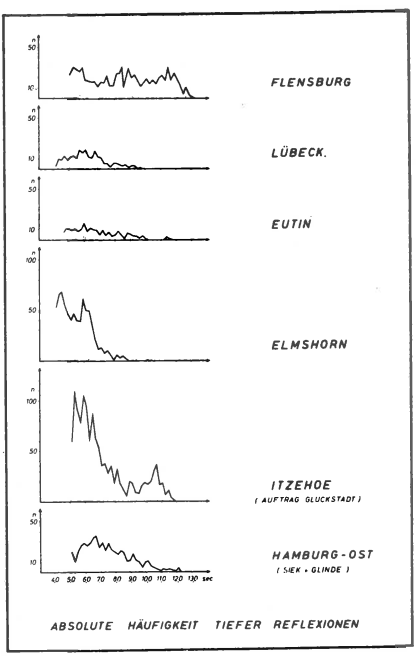

Figur 3: Häufigkeitsverteilungen tiefer Reflexionen im Gebiet Schleswig-Holstein.

Abb. 3 zeigt die Häufigkeitsverteilungen tiefer Reflexionen aus verschiedenen Arbeitsgebieten Schleswig-Holsteins.

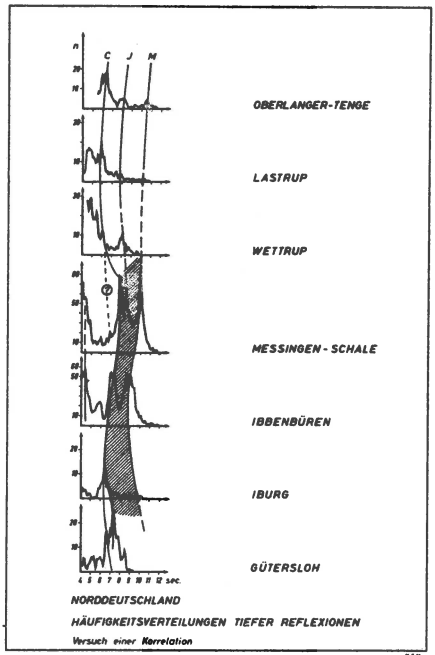

Figur 4: Häufigkeitsverteilungen tiefer Reflexionen im Gebiet des Ostemslandes (Profillinie B).

Abb. 4 zeigt die Verteilungskurven aus dem Gebiet des Ostemslandes. Hier liegen auf engem Raum verhältnismässig viele Beobachtungen vor, und aus diesem Grunde wurde hier auch versucht, aus dem vorliegenden Material detailliertere Aussagen über den Verlauf der Conrad-Diskontinuität - besser gesagt der dem Reflexionshorizont C zuzuordnenden Grenzfläche - zu machen. Hehn hatte bereits früher anhand des Materials aus 3 Arbeitsgebieten auf ein möglicherweise kräftiges Einfallen des Reflektors nach SW in diesem Gebiet hingewiesen.

In der Abb. 4 ist zugleich ein Korrelationsversuch der Maxima der Häufigkeitsverteilungskurven dieses Gebietes dargestellt. Es muss ausdrücklich betont werden, dass diese Darstellung nur ein Versuch und eine Deutung unter mehreren möglichen ist. Unter Hinzuziehung des Materials aus den umliegenden Gebieten, insbesondere dem südlich an-

grenzenden Raum, erscheint jedoch diese Korrelation als die z.Zt. plausibelste Deutung. Massgeblich für die getroffene Zuordnung war dabei die überraschende Ähnlichkeit in den Verteilungskurven der Gebiete Ibbenbüren und Messingen-Schale. Schliesst mann diese Messgebiete an die weiter südlich liegenden Beobachtungen an und legt zugleich die Realität der getroffenen Zuordnung in beiden Gebieten zugrunde, so folgert hieraus eine sehr kräftige Verbiegung der C-Grenzfläche zwischen den weiter nördlich liegenden Gebieten Oberlanger-Tenge, Lastrup und dem südlichen Raum. Es sei bemerkt, dass eine andere Deutungsmöglichkeit darauf hinzielen kann, das Auftreten dieser "Stufe" mit der Ablösung der Reflexionen von der Conrad-Diskontinuität im Norden durch einen tief liegenden "Instrusivkörper" weiter südlich zu erklären. In Anbetracht der Nähe des sog. Bramscher Massivs kann auch diese Deutung nicht ganz ausgeschlossen werden.

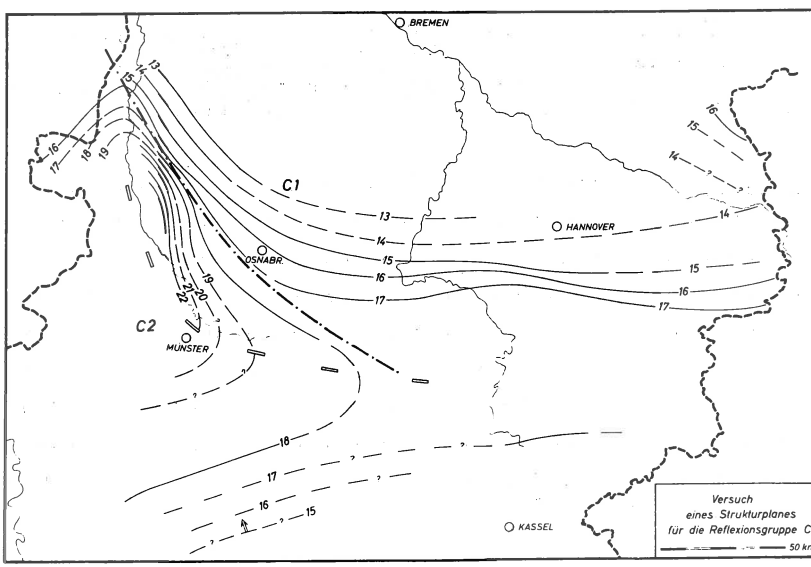

Figur 5: Der hier dargestellte Strukturplan für die Horizonte C 1 und C 2 beruht auf der versuchsweisen Korrelation der Maxima aller Häufigkeitsverteilungen in dem betrachteten Raum. Für das Gebiet westlich und nordwestlich von Münster und Osnabrück wird auf die Korrelation der Kurven nach Abbildung 4 verwiesen.

In der Abb. 5 ist versucht worden, aufgrund aller Beobachtungen am Südrand des nordwestdeutschen Beckens einen Strukturplan für den Reflektor C darzustellen. Man erkennt die auf der in der vorstehenden Abb. erläuterten Korrelation beruhende kräftige Absenkung des Reflektors im Gebiet des Ostemslandes. Bemerkenswert erscheint jedoch, dass sich auch weiter östlich ein, wenn auch nicht ganz so markantes Absinken längs einer WNW-OSO-verlaufenden Linie deuten lässt. So würde sich das bereits früher diskutierte, zu sehr unterschiedlichen Teufen führende Ergebnis der sehr benachbarten Gebiete Springe und Eldagsen (nahe Hannover) deuten lassen.

Auffallend ist, dass die hier aufgezeigte Streichrichtung weitgehend mit der grossregionalen tektonischen Richtung, insbesondere im Gebiet des Ostemslandes, zusammenfällt. Auch ein Zusammenhang mit den grossen magnetischen Anomalien bei Bramsche und bei Lingen steht möglicherweise im Zusammenhang mit dem Bau des tieferen Untergrundes, wie er sich hier andeutet. Die Buchstaben C1 und C2 sollen indessen andeuten, dass es sich bei der getroffenen Darstellung nicht unbedingt um geologisch gleiche Grenzflächen handeln muss. Auf die Möglichkeit, dass wir etwa in der Linie des "Abbruchs" von einem tiefer liegenden Horizont - Conrad-Diskontinuität - in einen höheren Reflektor gekommen sind, ist, wie bereits bemerkt, eine zweite Deutungsmöglichkeit.

Immerhin zeigt diese Darstellung, dass der diskutierte Raum, d.h. der ganze Südrand des nordwestdeutschen Beckens, noch eine Fülle von Problemen birgt und dass der Bau des tieferen Untergrundes hier sehr wohl gewisse Parallelen mit der bekannten Geologie der höheren Stochwerke aufzeigen kann. Vor allem aber erscheint es notwendig, dieses Gebiet und die hier aufgeworfenen Fragen durch weitere Messungen näher zu untersuchen.

Ein erster Schritt in dieser Richtung ist bereits durch die Mitregistrierung einer grossen Anzahl stärkerer Schüsse, welche im Rahmen eines grossräumigen Refraktionsprogrammes der Erdölindustrie erfolgt, getan.

So wurden durch die seismischen Apparaturen der geophysikalischen Institute der Universitäten Münster, Hamburg und Kiel im vergangenen Jahr über 600 Seismogramme zur Untersuchung des tieferen Untergrundes anlässlich der Refraktionsmessungen mitregistriert. Die Qualität des aufgenommenen Materials ist z.T. recht gut. Die Bearbeitung wird gegenwärtig in den Instituten der Universitäten Hamburg und Münster durchgeführt, und es ist zu erwarten, dass die ersten Ergebnisse, insbesondere aus den Registrierungen im Gebiet zwischen Oldenburg und Münster, welches für unsere Fragestellung besonders interessant ist, in Kürze vorliegen werden.

Im Zuge der oben erwähnten grossregionalen refraktionsseismischen Messungen der deutschen Erdölindustrie sind in diesem Jahre auch erstmalig Weitwinkel-Reflexionseinsätze und Refraktionseinsätze von der Mohorovičić-Diskontinuität registriert worden. Die Messung erfolgte südwestlich der Stadt Flensburg nahe der dänischen Grenze. Die Einsätze sind von guter Qualität und heben sich deutlich von den Refraktionseinsätzen höherer Horizonte ab. Eine vorläufige Teufenabschätzung führt auf eine Tiefe von 30 bis 31 km, ein Wert, der recht gut mit den Reflexionseinsätzen von Steilwinkelreflexionen aus dem Messgebiet Flensburg, wie sie aus den Häufigkeitsverteilungen abgeleitet wurden, übereinstimmt. Bemerkenswert ist jedoch, dass die Mohorovičić-Diskontinuität nach diesen Registrierungen einen kräftigen Einfall nach Norden zeigt. In Mittelholstein ist ebenfalls eine qualitativ gute Registrierung mit Refraktions- und Weitwinkel-Reflexionseinsätzen aus dem Bereich der Mohorovičić-Diskontinuität erfolgt. Hier ist ein Refraktor mit einer Refraktionsgeschwindigkeit von etwa 8000 m pro Sekunde erfasst worden, welcher bei einer Teufenlage von 26 bis 27 km nach Norden einfällt. Diese Beobachtung ergänzt bemerkenswert gut die oben genannte Registrierung eines reflektierenden Horizontes in ca. 30-31 km Tiefe nahe der dänischen Grenze. Aus diesen Registrierungen ist also im nördlichen Schleswig-Holstein ein kräftiger Einfall der Mohorovičić-Diskontinuität nach Norden abzuleiten.

Mit Ausnahme dieser Registrierungen ergibt sich für den Bereich der Mohorovičić-Diskontinuität in Norddeutschland ein annähernd gleichbleibender Teufenwert von 30 bis 32 km. Eine Ausnahme könnte in dem bereits oben diskutierten Gebiet Ibbenbüren vorliegen. Deutet man hier nämlich (vergleiche Abb. 4) die hintere Spitze in der Häufigkeitsverteilungskurve als Einsatz aus dem Bereich der Mohorovičić-Diskontinuität, so würde sich für dieselbe hier eine Teufe von nur etwa 26 km ergeben.

Diese Betrachtungen zeigen, dass die wenigen Aussagen, welche wir in Norddeutschland über die Mohorovičić-Diskontinuität aus den reflexionsseismischen Messungen gewonnen haben, noch kein zusammenfassendes Bild über eine mögliche Strukturierung dieser Grenzfläche ergeben. Die an einigen Stellen beobachteten ungewöhnlichen Neigungs- und Teufenwerte lassen zunächst die Frage offen, ob wir es im Bereich der Mohorovičić-Diskontinuität mit einem wesentlich komplizierteren Bau zu tun haben als bislang angenommen wurde.

Schliesslich ist noch darauf hinzuweisen, dass die Teufen für den Bereich der Conrad-Diskontinuität von den früher aus den Daten der Helgoland-Sprengung abgeleiteten Tiefenwerten abweichen. Es drängt sich hierbei der Verdacht auf, dass die früher ermittelten und der Conrad-Diskontinuität zugeordneten Einsätze von einem höheren Refraktor stammen könnten. Die Annahme eines Geschwindigkeitsgradienten an der Grenzfläche der Conrad- und auch Mohorovičić-Diskontinuität (in Analogie zu den Folgerungen, welche z.B. Giese aus den Refraktionsbeobachtungen im Kristallin der böhmischen Masse gezogen hat) würde die Diskrepanz der neuen Teufenwerte gegenüber den aus der Helgoland-Sprengung ermittelten Teufen nur vergrössern.

Zusammenfassend ist noch einmal darauf hinzuweisen, dass alle vorliegenden Beobachtungen darauf hindeuten, dass wir es zumindest im Bereich der sogenannten Conrad-Diskontinuität mit einem bewegteren Relief im Untergrund Norddeutschlands zu tun haben als dies früher angenommen werden konnte. Auch die Ergebnisse der Prospektionsseismik, insbesondere der Refraktion, deuten in diese Richtung. Der Name "Conrad-Diskontinuität" steht hierbei für eine immer wiederkehrende

Anhäufung von Reflexionseinsätzen aus einem annähernd gleichen Teufenbereich. Es ist nicht damit gesagt, dass es sich dabei stets um die gleichen geologischen Grenzflächen handelt. Insofern sollte der Name "Conrad-Diskontinuität" zunächst als rein seismischer Begriff gewertet werden.

Aufgabe dieses Referates war zunächst eine Bestandsaufnahme des vorliegenden Materials im norddeutschen Raum, wie es von der Reflexionsseismik für die Erforschung des tieferen Untergrundes geliefert wird, zu geben. Ein weiterer Ausbau unserer Kenntnisse wird zweifellos nur in Zusammenarbeit mit anderen geophysikalischen Methoden in Zukunft möglich sein. Der Kontakt mit der in immer grössere Teufen vordringenden Prospektionsseismik, die im Auftrage der Erdölindustrie durchgeführt wird, erscheint besonders notwendig.

Cl. Behnke

ÜBER GESCHWINDIGKEITEN SEISMISCHER WELLEN IM ZENTRALEN TEIL DER OSTALPEN

Die Vorstellungen über die Geschwindigkeiten wurden erarbeitet auf Grund der Messergebnisse auf einem refraktionsseismischen Gegenschussprofil in den Ostalpen. Das Profil bildet mit der Streichrichtung der Alpen einen Winkel von etwa 25°; die Schusspunkte liegen in Hochgebirgsseen, und zwar im Lago Bianco in den Tessiner Gneisen nahe dem St. Gotthard sowie im Lago Lagorai im Südteil der Dolomiten. Die Untersuchungen erstrecken sich somit auf den eigentlichen Alpenkörper als auch auf die Dinariden.

Um eine optimale Korrelation zu ermöglichen, wurden die Seismogramme in einer Montage zusammengestellt. In reduzierter Laufzeitdarstellung wurde für Schuss und Gegenschuss der gleiche Koordinatenursprung verwendet; diese Anordnung ermöglicht einen direkten Vergleich von Neigungen und Laufzeiten äquivalenter Einsatzgruppen.

In den Laufzeitkurven der schussnächsten Einsätze beider Profile zeigt sich eine deutliche Krümmung. Es liegt nahe, diese Krümmung als Folge eines vertikalen Geschwindigkeitsgradienten zu deuten. Zur Bestimmung des numerischen Wertes dieses Gradienten wurde eine Methode von Hagedorn (1955) verwendet. Man trägt die Laufzeiten von Tauchwellen der in Frage kommenden Schicht in einem doppelt logarithmischen, schiefwinkligen System auf (Abb. 1). Sodann bringt man die in einem gleichen System gezeichnete Kurve $x = 2 \sinh \frac{t}{2}$ optimal mit der Laufzeitkurve zur Deckung. Die Werte v_o und δ können dann an den Schnittpunkten der Nullachsen des Laufzeitsystems mit dem Koordinatensystem der Gradientkurve abgelesen werden. Nach dieser Methode ergeben sich für die Gradienten der obersten Schicht, vom Lago Lagorai gemessen 0,051 und vom Lago Bianco gemessen 0,063.

Zur Konstruktion von Modellen des tieferen Untergrundes dieses Teiles der Alpen wurde von hypothetischen Modellen

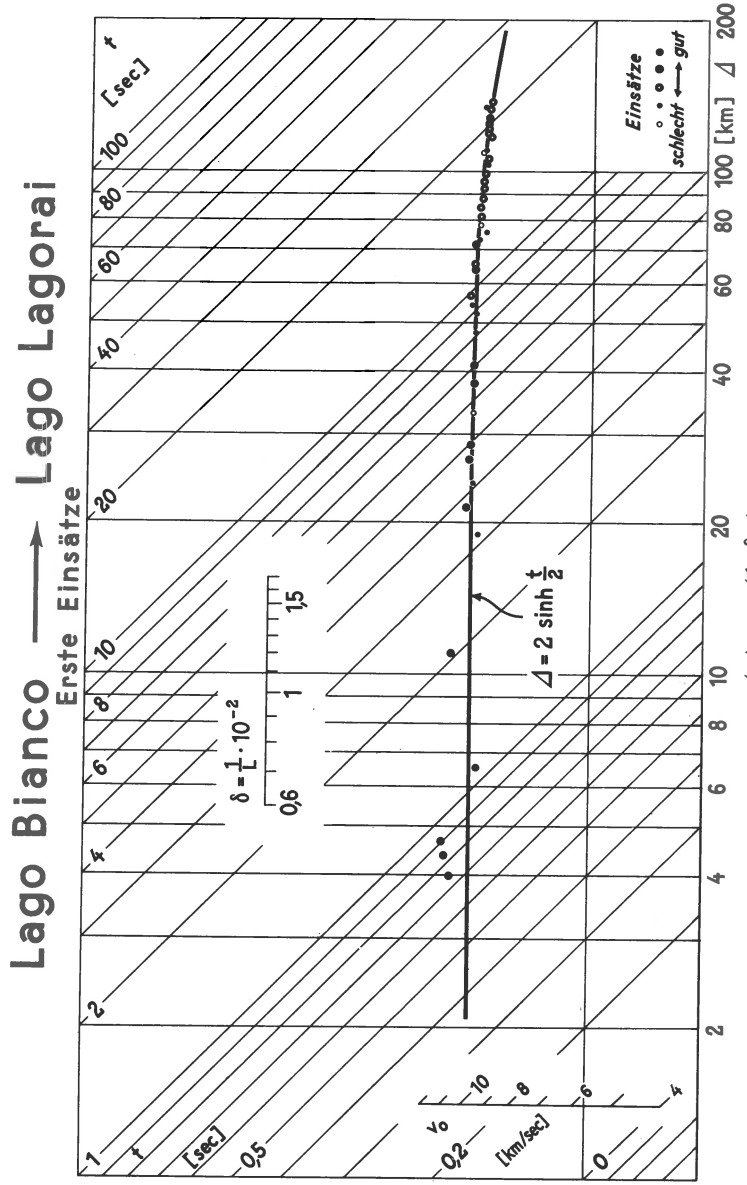
Lago Bianco ⟶ Lago Lagorai
Erste Einsätze
t [sec]
Δ [km]
Einsätze
schlecht ⟷ gut
$\delta = \frac{1}{L} \cdot 10^{-2}$
$\Delta = 2 \sinh \frac{t}{2}$
$v(Z) = v_0 (1 + \delta z)$
v_0 [km/sec]
$v_0 = 5{,}7$ km/sec
$v_0 \delta = 0{,}0627$
$\delta = 0{,}011$ km^{-1}
$L = 90{,}9$ km

Fig. 1

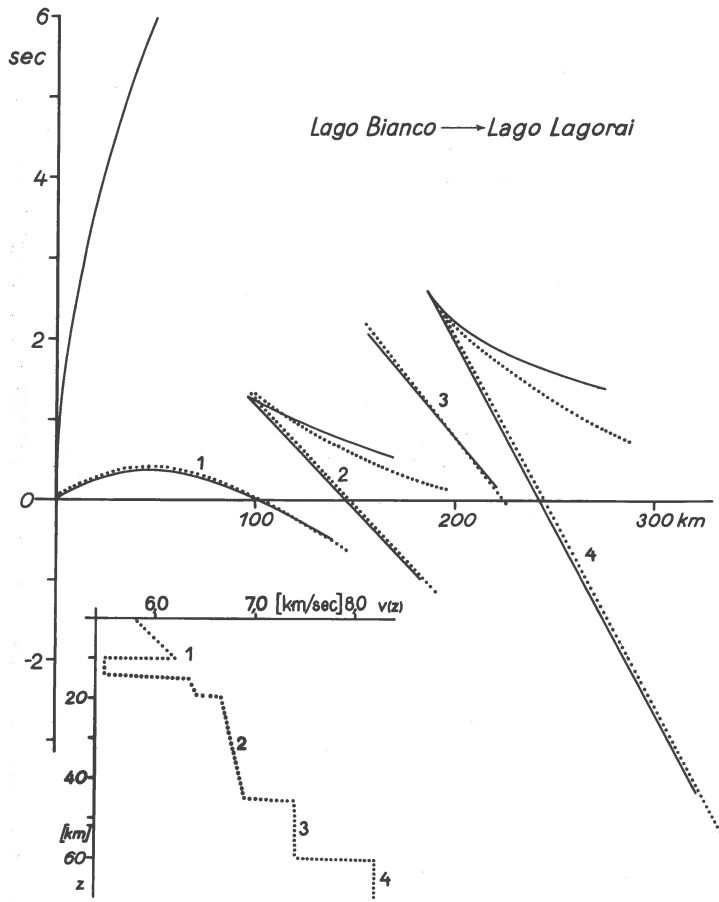

Fig. 2

ausgegangen, für die mit Hilfe einer elektronischen Datenverarbeitungsanlage die theoretischen Laufzeitkurven errechnet wurden. Nach einem Iterationsverfahren ergibt eine optimale Übereinstimmung des gemessenen mit dem errechneten Laufzeitkurvenbild die in Abb. 2 dargestellte vertikale Geschwindigkeitsverteilung. Unterhalb eines starken vertikalen Gradienten in der obersten Kristallinschicht liegt zwischen 10 und 15 km Tiefe ein low-velocity-layer. Sodann steigt die Geschwindigkeit langsamer an, nur von relativ geringen Sprüngen unterbrochen, bis im Grenzbereich

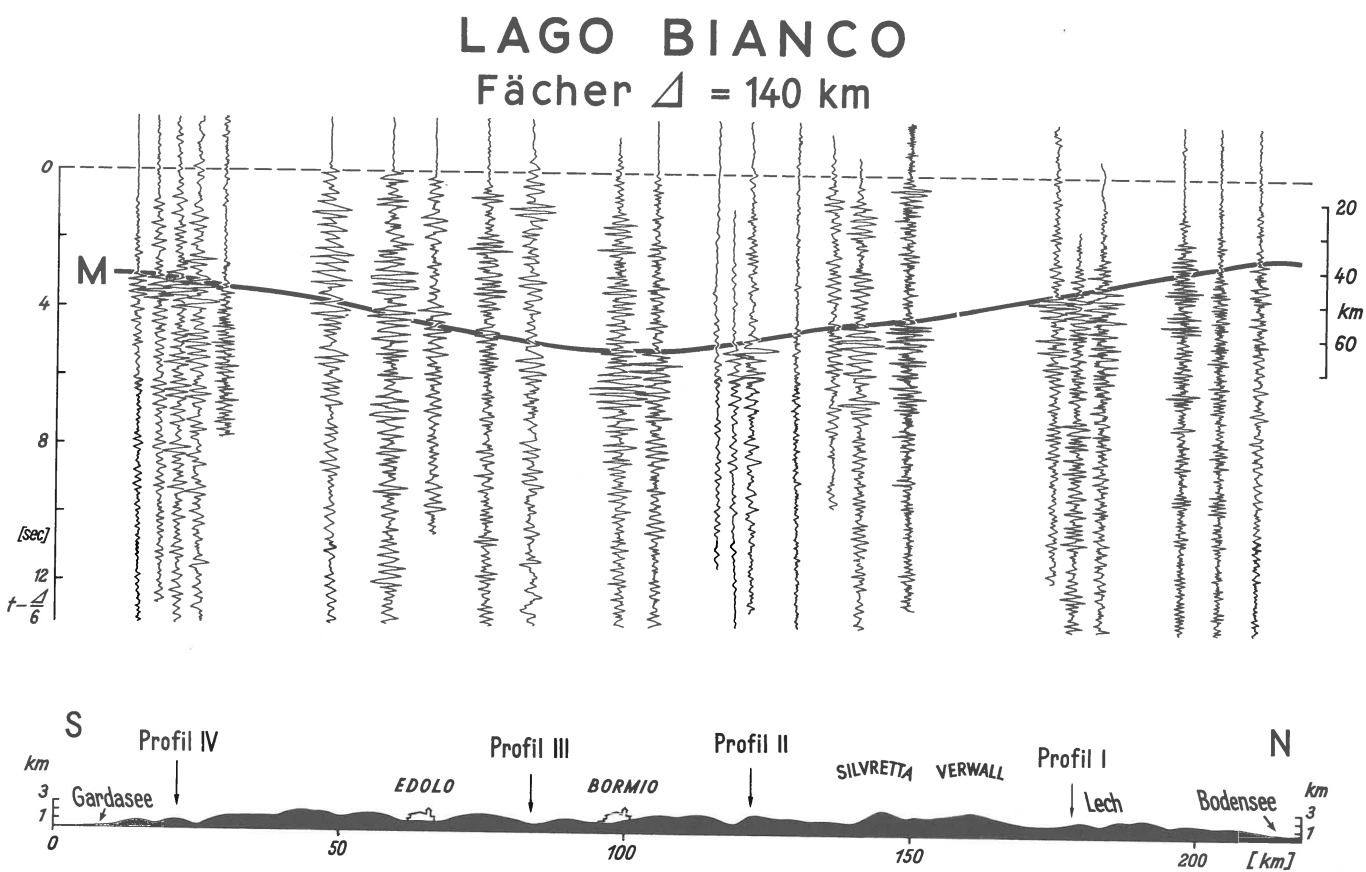
LAGO BIANCO
Fächer Δ = 140 km
0
4
8
[sec]
12
t−Δ/6
M
20
40
km
60
S
N
km
3
1
Gardasee
Profil IV
Profil III
Profil II
Profil I
EDOLO
BORMIO
SILVRETTA
VERWALL
Lech
Bodensee
0
50
100
150
200
[km]

Fig. 3

von Kruste und Mantel, der hier in einer Tiefe von etwa 60 km liegt, der konstante Wert von 8,2 km/sec erreicht wird. Den Grenzflächen im konventionellen Sinne kommt hiernach die Bedeutung von Grenzbereichen mit mehr oder weniger stetigem Geschwindigkeitsübergang zu.

In der Abb. 3 ist die Seismogrammontage eines Fächers in einer Entfernung von 140 km vom Lago Bianco dargestellt. Der Fächer reicht vom Bodensee bis zum Südende des Gardasees und überdeckt damit die gesamten Alpen. In den Seismogrammen kann zwanglos eine Linie korreliert werden, die den Einsätzen reflektierter Wellen von der Mohorovičić-Diskontinuität entspricht. Bei der Korrelation, die nach den Vorstellungen von Wellenwegen der geometrischen Optik durchgeführt wurde, erscheint eine charakteristische Wurzelzone unter den Zentralalpen.

Die seismischen Feldmessungen wurden im Rahmen des Schwerpunktprogramms "Untergrund Mitteleuropa" durchgeführt. Der Deutschen Forschungsgemeinschaft sei für die Förderung und Bereitstellung der erforderlichen Mittel gedankt.

Literatur

J.E.Hagedorn: Templates for fitting Smooth Velocity Functions to Seismic Refraction and Reflection Data. Geophys.Prosp. III (1955) 4.

K.Fuchs, St.Müller und M.Landisman

DER AUFBAU DER ERDKRUSTE IN MITTELEUROPA AUS SPRENGSEISMISCHEN UNTERSUCHUNGEN

Die Existenz eines Kanals reduzierter Wellengeschwindigkeit im oberen Teil der kontinentalen Erdkruste wurde vor kurzem von Müller und Landisman (1966) und Landisman und Müller (1966) gefordert. Dieser Kanal verursacht das Verschwinden der direkten P_g - Einsätze in etwa 120 km Entfernung vom Schusspunkt. Eine abrupte Geschwindigkeitszunahme an der Kanalunterkante erzeugt Zweiteinsätze mit starken Amplituden, die den P_g-Einsätzen etwa 0.5 bis 2.0 Sekunden später nachfolgen. Diese Einsätze sind mit dem Symbol P_c bezeichnet worden. Sie lassen sich hinter den P_g-Einsätzen bis zu Entfernungen zwischen 40 und 60 km vom Schusspunkt zurückverfolgen. Die Einführung des Kanals behebt die Wiedersprüche, die bisher bei der Auswertung von Reflexions- und Refraktionsmessungen bestanden. Mit ihm lassen sich ausserdem die starken beobachteten Reflexionen mit Echozeiten um 4 sec als Folge des ausgeprägten Geschwindigkeitskontrastes an der Kanalunterkante erklären.

Fuchs und Landisman (1966) konnten die Anwesenheit dieses Kanals auf dem System von Refraktionslinien Adelebsen-Süd, Hilders-Nord und Hilders-Süd in Westdeutschland nachweisen. Im tieferen Teil der Kruste oberhalb der Mohorovičić-Diskontinuität fanden sie ausserdem eine 10 km mächtige Schicht mit einer P-Wellengeschwindigkeit um 7.5 km/sec.

Ein zusätzliches Argument für die Anwesenheit eines Kanals verminderter Wellengeschwindigkeit ergibt sich durch den Vergleich von experimentell bestimmten Gruppengeschwindigkeitswerten seismischer Oberflächenwellen mit theoretisch berechneten Dispersionskurven. Die experimentellen Daten stammen von Beobachtungen kurzperiodischer Rayleighwellen, die den Weg von Merkers (Rhön) nach Stuttgart durchlaufen

hatten. Über die Gruppengeschwindigkeitsmessungen an den Rayleighwellen des seismischen Ereignisses von Merkers (29. Juni 1961) wurde bereits früher von Schneider (1962) und von Schneider, Müller und Knopoff (1966) berichtet. Eine Schwäche der bisher vorgeschlagenen Geschwindigkeitsmodelle war, dass die höchste beobachtete Gruppengeschwindigkeit nicht mit der Airy-Phase (Gruppengeschwindigkeitsmaximum) der zugehörigen theoretischen Dispersionskurve zusammenfiel. Diese Schwierigkeit konnte durch Einführung des Kanals verminderter Wellengeschwindigkeit behoben werden.

Die Dispersionskurven seismischer Oberflächenwellen sind im kurzperiodischen Bereich zwischen 2 und 10 sec stark abhängig von der Mächtigkeit und den elastischen Konstanten der Sedimentschichten. Auf der Linie Merkers-Stuttgart sind aber die Sedimente durch zahlreiche Tiefbohrungen und kurze Refraktionslinien gut bekannt, so dass der Verlauf der theoretischen Dispersionskurven nicht mehr durch Annahmen über die Sedimentdecke variiert werden kann. Verwendet man das für die Refraktionslinie Hilders-Süd von Fuchs und Landisman (1966) angegebene Geschwindigkeitstiefen-Modell mit einem Sedimentpaket, das den präziseren Angaben auf der Linie Merkers-Stuttgart entsprechend verfeinert werden konnte, so erkennt man, dass die Periode des theoretischen Gruppengeschwindigkeitsmaximums von 8 sec ohne Kanal nach etwa 5 sec verschoben wird. Damit ist eine ausgezeichnete Übereinstimmung zwischen den experimentellen Daten und den theoretischen Dispersionskurven erzielbar: die höchste beobachtete Gruppengeschwindigkeit fällt jetzt mit dem theoretischen Maximum zusammen (siehe Figur 1).

Es liegt die Vermutung nahe, dass man eine ähnliche Verschiebung der Airy-Phase zu kürzeren Perioden hin auch durch Einführen einer Schicht verminderter Mächtigkeit oberhalb der sogenannten "Granitschicht" erreichen kann. Dass dieser Schluss falsch ist, soll in Figur 2 aufgezeigt werden. Dort sind die Dispersionskurven für 3 verschiedene Geschwindigkeitstiefen-Verteilungen miteinander verglichen. Modell A (siehe Tabelle 1) ist die "klassische" Krustenstruktur für Mitteleuropa mit einer Dreischichten-Kruste. Modell B (siehe Tabelle 1) ist eine Variation des Modells

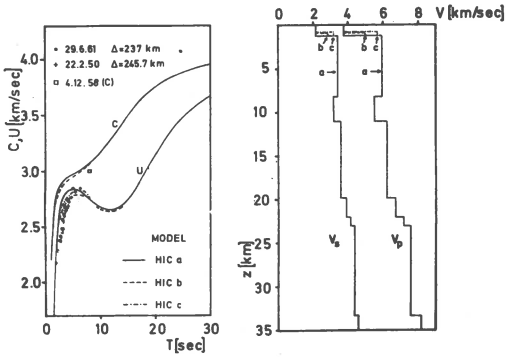

Fig. 1

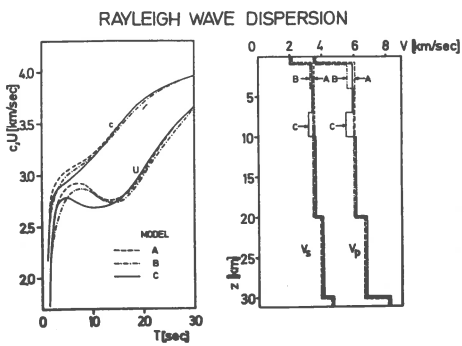

Fig. 2

Tiefe (km)	Mächtigkeit (km)	(km/s)	(km/s)	Dichte (g/cm^3)	
	1.0	3.50	2.00	2.50	
1.0	19.0	6.00	3.50	2.80	
20.0	10.0	6.70	4.00	3.05	Modell A
30.0		8.20	4.65	3.40	
	1.0	3.50	2.00	2.50	
1.0	3.0	5.60	3.30	2.75	
4.0	16.0	6.00	3.50	2.85	Modell B
20.0	10.0	6.70	4.00	3.05	
30.0		8.20	4.65	3.40	
	1.0	3.50	2.00	2.50	
1.0	6.0	5.90	3.40	2.80	
7.0	3.0	5.50	3.15	2.70	
10.0	10.0	6.10	3.60	2.90	Modell C
20.0	10.0	6.70	4.00	3.05	
30.0		8.20	4.65	3.40	

Tabelle 1: Krustenmodelle in Mitteleuropa

STUTTGART 2 (ref. Schneider, 1964, Abschnitt 3). In diesem Fall ist eine 3 km mächtige Schicht mit einer P-Wellengeschwindigkeit von 5.6 km/sec zwischen die Sedimente und die Schicht mit 5.9 km/sec eingeführt worden. Durch diese Massnahme wird zwar der Wert der Gruppengeschwindigkeit in der Airy-Phase verringert, gleichzeitig wird aber auch das Gruppengeschwindigkeitsmaximum zu höheren Perioden hin verschoben. Im Modell C (siehe Tabelle 1) ist ein Kanal verminderter Wellengeschwindigkeit unterhalb der 5.9 km/sec-Schicht eingeführt worden. Das Gruppengeschwindigkeitsmaximum verschiebt sich so zu niedrigeren Perioden zwischen 5 und 6 sec, wie es tatsächlich beobachtet wird.

Literatur

Fuchs, K. and M.Landisman: "Result of a re-interpretation of the N-S-refraction line Adelebsen-Hilders-south in Western Germany." Ztschr.f.Geophys., 32, 121-123, 1966a.

Fuchs, K. and M.Landisman: "Detailed crustal investigation along a north-south-section through the central part of Western Germany." Amer.Geophys.Union Geophys. Monograph Series, No.10, 1966b.

Landisman, M. and St.Mueller: "Seismic studies of the Earth's crust in continents; Part II: Analysis of wave propagation in continents and adjacent shelf areas." Geophys. Journ.R.A.S., 10, 539-554, 1966.

Mueller, St. and M.Landisman: "Seismic studies of the Earth's crust in continents; Part I: Evidence for a low-velocity zone in the upper part of the lithosphere." Geophys. Journ. R.A.S., 10, 525-538, 1966.

Schneider, G.: "Oberflächenwellen bei Nahbeben in Mitteleuropa." Veröff.Inst.f. Bodendynamik u. Erdbebenf. in Jena, 77, 151-162, 1962.

Schneider, G.: "Die Erdbeben in Baden-Württemberg 1955-1962." Veröff. d. Landeserdbebendienstes Baden-Württemberg, Stuttgart, 46 p., 1964.

Schneider, G., St.Mueller und L.Knopoff: "Gruppengeschwindigkeitsmessungen an kurzperiodischen Oberflächenwellen in Mitteleuropa." Ztschr. f. Geophysik, 32, 33 - 57, 1966.

P.Giese

DER GRENZBEREICH ZWISCHEN ERDKRUSTE UND ERDMANTEL*)

Die Seismogramm-Montagen von Refraktionsprofilen der seismischen Tiefensondierung der Erdkruste und des oberen Erdmantels zeigen im Entfernungsbereich zwischen etwa 70 und 250 km späte Einsätze, die sich im allgemeinen durch grosse Amplituden auszeichnen. Die Einsätze dieser Wellengruppe ordnen sich auf einer deutlich zur Entfernungachse konkav gekrümmten Laufzeitkurve an. Das dem Neigungsintervall dieser Kurve entsprechende Geschwindigkeitsintervall liegt zwischen den Werten 8,4-7,8 km/s und 6,6-6,2 km/s. Im mittleren Teil der Kurve können die Amplituden kleiner als am Anfang und Ende sein. Da der Anfang dieser Laufzeitkurve von einer annähernd geraden Laufzeitkurve, deren Neigung einer Geschwindigkeit von 8,4-7,8 km/s entspricht, tangiert wird, liegt die Deutung als überkritische Reflexion an der Mohorovičić - Diskontinuität nahe. Ergebnisse entsprechender modellseismischer Versuche scheinen diese Deutung zu bestätigen. Dennoch muss die Frage gestellt werden, ob diese Erklärung die einzig mögliche ist. Nicht nur eine reflektierte Welle besitzt eine konkave Laufzeitkurve, sondern auch eine Tauchwelle aus einer Zone mit einem starken Geschwindigkeitsgradienten. Beide Kurven sind rückläufig. Allein die Tatsache, dass diese Wellengruppe mit unterschiedlicher Deutlichkeit auftritt, zeigt an, dass der untere Krustenbereich und der obere Mantel regional verschieden aufgebaut sein müssen.

Da diese Laufzeitkurve mit den vorangehenden nicht zusammenhängt, kann das Herglotz-Wiechert-Verfahren nicht angewendet werden. Mit Hilfe der folgenden Näherungsformel

*) Gemeinschaftsarbeiten der deutschen geophysikalischen Institute im Rahmen der Schwerpunktprogramme der Deutschen Forschungsgemeinschaft "Geophysikalische Erforschung des tieferen Untergrundes in Mitteleuropa" und "Unternehmen Erdmantel", Beitrag Nr. 54.

lässt sich jedoch die Transformation in die Geschwindigkeit-Tiefen-Funktion vornehmen.

$$z \approx \frac{x}{2} \sqrt[2]{\frac{v \cdot t}{x} - 1} \Big/ \sqrt[4]{1 + \frac{\Delta v/\Delta z}{dv/dz}}$$

Es bedeuten:
z : Tiefe, x : Entfernung, v = dx/dt : Scheitelgeschwindigkeit, $\Delta v/\Delta z = (v-v_o) / dz$: mittlerer Geschwindigkeitsgradient, dv/dz : Geschwindigkeitsgradient an der Stelle z.

Die Formel muss iterativ gebraucht werden, d.h. man beginnt bei $\Delta v/\Delta z = 0$. Aus dieser ersten Näherung erhält man $\Delta v/\Delta z$ und dv/dz. Mit diesen Werten wird der zweite Näherungsschritt durchgeführt. Nach drei Schritten ist im allgemeinen bereits eine befriedigende Näherung erreicht worden.

Um zu untersuchen, welche Form die Geschwindigkeit-Tiefen-Funktion speziell im Grenzbereich zwischen Kruste und Mantel, in Arealen mit unterschiedlicher geologischer Entwicklung besitzt, ist ein Profil vom variskischen Kristallin der Böhmischen Masse über die Ostalpen bis in die Südalpen in dieser Weise ausgewertet worden. Dieses etwa 500 km lange Profil setzt sich aus mehreren einzelnen Refraktionsprofilen zusammen (Voggendorf-SE, Böhmischbruck-Eschenlohe, Eschenlohe-Lago Lagorai, Lago Lagorai NE und E). In keinem der ausgewerteten Profile ergab sich eine sprunghafte Zunahme der Geschwindigkeit von 6,2-6,6 auf 8,2 km/s. Lediglich zwischen 7,5 und 8,2 km/s kann ein Übergang von Tauchwellen zu reflektierten Wellen auftreten.

Die einzelnen Geschwindigkeit-Tiefen-Funktionen sind zu einem Profilschnitt mit Linien gleicher Geschwindigkeit zusammengestellt worden (Abb. 1). Für diese Betrachtungen ist das Geschwindigkeitsintervall zwischen 6,6 und 8,2 km/s von Interesse. Während im Nordteil des Profils dieser Bereich nur 8 km mächtig ist, verbreitert er sich nach Süden auf über 20 km. Eine besondere Scharung der Geschwindigkeitslinien bei 7,0 km/s ist nicht zu erkennen.

In ähnlicher Weise sind die Registrierungen aus den Westalpen des Jahres 1958 (Lac Nègre) einer Re-Interpretation unterzogen worden. Die m-Phase, von der Strassburger Aus-

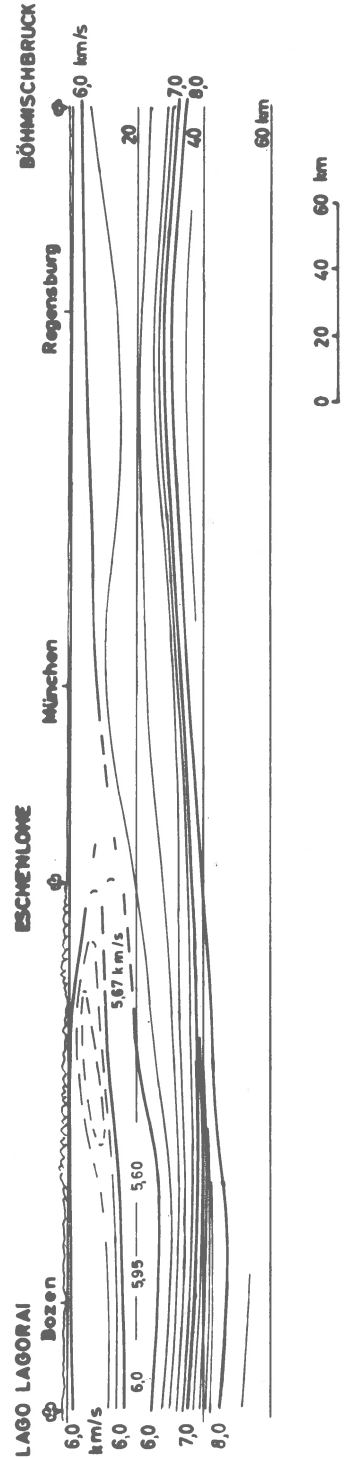
LAGO LAGORAI
Bozen
ESCHENLOHE
München
Regensburg
BÖHMISCHBRUCK
6,0 km/s
6,0
km/s
6,0
6,0
7,0
8,0
6,0
5,95
5,60
5,67 km/s
20
40
7,0
8,0
60 km
0
20
40
60 km

Fig. 1

wertegruppe als sPp-Welle gedeutet, muss der Übergangszone zwischen Kruste und Mantel zugeordnet werden. Dies gilt auch für den Bereich der Ivrea-Zone. Allerdings erstrecken sich hier die Gesteine, in denen sich die Longitudinalwellen mit einer Geschwindigkeit von 7,2 km/s ausbreiten, nicht bis zum Mantel, sondern nur etwa bis in 20 km Tiefe. Zwischen 20 und 30 km liegt eine extreme Geschwindigkeitsverringerung bis auf 4 km/s vor. Diese Aussagen beziehen sich auf die südliche Hälfte der Ivrea-Zone. Wie die Verhältnisse in der Nordhälfte aussehen, kann noch nicht diskutiert werden.

Für die Geologie ist die Frage von Bedeutung, wie sich dieser grosse Gradient petrographisch deuten lässt. In einem homogenen Gestein, gleich ob basisch oder sauer, kann in Tiefen zwischen 20 und 40 km keine Druck- und Temperaturverteilung einen derart grossen Gradienten zur Folge haben. Es bestehen daher nur zwei extreme Möglichkeiten zur Deutung. Entweder liegt ein kontinuierlicher Übergang von sauren zu basischen Gesteinen vor oder es findet innerhalb eines basischen Gesteins ein Phasenwechsel statt, der sich innerhalb einer mehr oder minder breiten Zone abspielt. In dem oberen Teil dieser Zone werden wohl Mischgesteine vorliegen, im unteren Teil dagegen dürften Phasenumwandlungen, gedacht wird in erster Linie an die Transformation Gabbro-Eklogit, stattfinden. In Arealen mit erhöhtem Temperaturgradienten verschiebt sich der Umwandlungsbereich in grössere Tiefe und vielleicht verbreitert er sich gleichzeitig. Diese Verhältnisse scheinen unter den Alpen vorzuliegen.

Die bisherige Mohorovičić-Diskontinuität entspricht der Geschwindigkeitslinie 8,2 km/s, nur darf sie in dieser Deutungsweise nicht mehr als Diskontinuität 1. Ordnung aufgefasst werden. In derselben Weise muss auch die Conrad-Diskontinuität gesehen werden. Identifiziert man diese Fläche mit der Grenze zwischen sialischem und simatischem Gestein, so muss man sie im Alpenvorland und in den Alpen an die Oberseite der Übergangszone legen. Damit beantwortet sich von selbst die Frage nach der Existenz der immer wieder in Zweifel gestellten Conrad-Diskontinuität. Zusammenfassend kann also gesagt werden, dass zwischen

Kruste und Mantel ein kontinuierlicher Übergang besteht, dessen Breite von der geotektonischen Position des Krustenteils anhängig ist.

Literatur

Giese, P. u. G. de Visintini, 1964
Ergebnisse des Lago Lagorai E-Profils.
I U G G Monographs no. 29
Commission Séismologique Européenne,
Réunion de Budapest Sept. 1964 : IV E 2.

Giese, P. 1966: Versuch einer Gliederung der Erdkruste im nördlichen Alpenvorland, in den Ostalpen und in Teilen der Westalpen mit Hilfe charakteristischer Refraktion-Laufzeitkurven, sowie eine geologische Deutung. Habil.Schrift; Math.Naturw. Fakultät der Freien Universität Berlin, 1-142.

Giese, P. 1966: Neue Gesichtspunkte zur Gliederung der Erdkruste auf Grund refraktionsseismischer Messungen. D G G - Tagung, Kiel, Nr. 15.

O.G.Schamina

DIE ABHÄNGIGKEIT DER P-WELLEN-AMPLITUDE VON DER HERDTIEFE
(seismologische, rechnerische und Modellangaben)

Bei Untersuchungen von Wellenleitermodellen des oberen Erdmantels wurde von uns festgestellt, dass in der Schattenzone die Abhängigkeit der P-Wellen-Amplitude von der Ursprungstiefe dem Geschwindigkeitsprofil der Modelle qualitativ ähnlich ist [1]. Daraus folgt, dass die Amplituden der Wellen tiefer Erdbeben eine nicht unwichtige Rolle bei der Entdeckung des Wellenleiters spielen können.

Angaben über die Abhängigkeit der P-Wellen-Amplitude von der Herdtiefe in verschiedenen Epizentralentfernungen sind in impliziter Form nur in den Diagrammen Gutenbergs und Richters zur Bestimmung der Magnitude tiefer Erdbeben enthalten [2]. Ihnen zufolge hat die Funktion A/T (H) (A - Amplitude, T - Periode, H - Herdtiefe) in einer Entfernung von etwa 1000 km ein Minimum bei H ungefähr gleich 160 km. Diese Tatsache spricht zugunsten der Hypothese Gutenbergs von der Existenz eines Wellenleiters in diesen Tiefen. Jedoch sind die Gutenbergschen Werte bekanntlich Mittelwerte einer Vielzahl von Erdbeben und einer grossen Anzahl von Stationen in verschieden Gebieten der Erdkugel. Man kann erwarten, dass sich die örtlichen Funktionen wesentlich von den mittleren unterscheiden können. Deshalb ist die Erforschung der Wellenamplituden von den in verschiedenen Tiefen einer Herdzone entstehenden Erdbeben von Interesse.

Als eine solche Zone wurde von uns die der Hindukusch-Erdbeben mit auf einer Fläche von ungefähr 100×100 km^2 (36,5 - 37,5 N; 70,5 - 71,5 E) konzentrierten Epizentren ausgewählt. Die mit der Messung der P-Wellen-Amplitude betrauten Stationen wurden so ausgewählt, dass sie zwei in westlicher und in nordöstlicher Richtung von den Epizentralzonen ausgedehnten Profile mit je ungefähr 2000 km Länge bilden. Es wurden die Aufzeichnungen der vertikalen

Komponente von Kirnos-Seismographen benutzt. Gemessen wurden die maximale Amplitude und die vorherrschende Schwingungsperiode in der Gruppe P mit einer Dauer von nicht mehr als 6 s. Die Frequenzscharakteristiken der Geräte wurden berücksichtigt.

Es wurden die Aufzeichnungen aller Erdbeben mit $M > 4$ bearbeitet nach Angaben die im Bulletin des seismischen Stationsnetzes der UdSSR für die Zeitspanne von 1952 bis einschliesslich 1964 enthalten sind. Für viele Erdbeben ist die vom Tadshikischen Institut für Seismologie nach einer von W.I.Bune [3] vorgeschlagener Methode bestimmte Energie bekannt. Wir entschliessen uns, diese Angaben zur Bestimmung der Abhängigkeit der Amplitude von der Herdtiefe für eine Reihe von Stationen zu benutzen. Für alle unsere Stationen erwies sich dies als unmöglich, weil die Zahl der registrierten Erdbeben nicht überall gleich ist und weil der Fehler bei der Bestimmung der gesuchten Funktion in einigen Fällen die zulässigen Werte überschreitet.

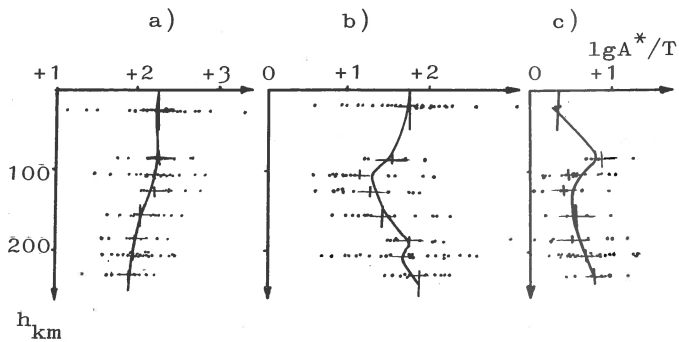

Abb. 1. Die Funktion lg A*/T für die Stationen Chorog (a), Kuljab (b) und Alma-Ata (c).
A* - maximale P-Wellen-Amplitude, auf Energiewerte von 10^{20} erg reduziert, T - vorherrschende Schwingungsperiode, H - Herdtiefe.

In Abb. 1 sind beispielsweise die Abhängigkeiten lg $A/T^*(H)$ (wobei das Zeichen * bedeutet, dass die Amplituden auf Energiewerte von 10^{20} erg reduziert wurden) für

die Stationen Chorog, Kuljab und Alma-Ata angeführt, für die die mittlere quadratische Abweichung des Mittels (horizontale Linien) 0,3 lg nicht überschreitet. Mittels vertikaler Linien wurden in der Zeichnung die Bereiche der mittleren Tiefen gezeigt.

Wir sehen, dass sich in Chorog die Amplitude gleichmässig mit der Tiefe verringert, was auch für die Epizentralenfernung 100-130 km zu erwarten war. In Kuljab jedoch wurde ein deutliches Minimum in mittleren Tiefen beobachtet. Die Epizentralentfernung beträgt hier rund 170 km und deshalb kann das Minimum nicht von den Besonderheiten des Geschwindigkeitsgefüges des Mediums hervorgerufen sein. Eher kann man dem Geschwindigkeitsprofil das Aussehen der Amplitudenkurve in Alma-Ata zuschreiben, das gerade in die Schattenzone fällt.

Das Aussehen der Kurve $\lg A/T^*(H)$ in Chorog gestattet diese Station als Grundlage zur Bestimmung der relativen Amplituden zu nehmen, indem man alle registrierten Erdbeben benutzt und nicht nur die, für die die Energie bekannt ist.

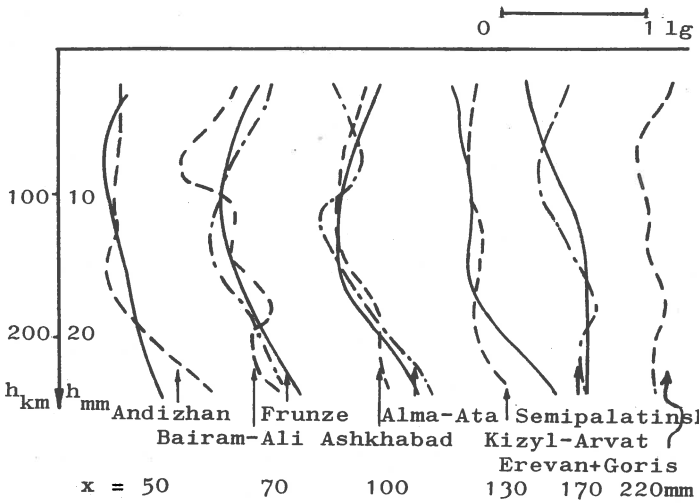

Abb. 2. Zusammenfassende Grafik der Funktion $\lg \frac{(A/T)_K}{(A/T)_{Chorog}} (H)$ für alle Stationen. Die Station Chorog wurde als Grundlage genommen. Ununterbrochene Linien sind Modellkurven.

In Abb. 2 ist eine zusammenfassende Grafik der Funktion $\lg \frac{(A/T)_K}{(A/T)_{Chorog}}$ (H) für alle Stationen dargestellt. Hier überschreitet die Abweichung des Mittels in allen Fällen nicht 0,3 lg. In der gleichen Zeichnung sind mit ununterbrochene Linien die Kurven $\lg \frac{(A/T)_K}{(A/T)_{20}}$ (das Zeichen 20 bezeichnet die Epizentralentfernung 20 mm - entspricht in der Natur 200 km) eingetragen, die auf einem Mantelmodell mit symmetrisch geformten Wellenleiter erhalten wurden, dessen Achse in einer Tiefe von 160-170 mm liegt (entspricht in der Natur 160-170 km). Das Mikromodell wurde aus einem Epoxydharz - Quarzsand-Gemisch durch Auftragen dünner Schichten mit verschiedenen Verhältnissen von Harz und Sand hergestellt [4, 5]. In einem solchen Modell hat das Absorptionsdekrement ϑ selbe Grössenordnung wie das des Mantels ($\vartheta \cong 0{,}06$). ϑ verringert sich im Modell mit wachsender Tiefe. Der Poissonsche Koeffizient σ verändert sich mit der Tiefe, wobei er seinen grössten Wert (0,36) nahe an der Oberfläche und auf der Wellenleiterachse erreicht, im weiteren verringert er sich in einer 300 km entsprechenden Tiefe bis 0,29. Qualitativ ist das dem Verhalten von σ in der Erde ähnlich.

Wie wir sehen, stimmen die Modell und natürlichen Kurven auf befriedigende Weise bis zu einer Entfernung von 1300 km überein. Beide haben ein gemeinsames charakteristisches Merkmal - das Minimum in mittleren Tiefen. (Wir möchten bemerken, dass bei Nichtwellenleitermodellen des Mantels (Modell Lehmann oder Jeffreys) ein solches Minimum nicht beobachtet wird). Die mit Berücksichtigung der Stationskorrekturen der Stationen Jerewan und Goris zueinander konstruierte summarische Kurve ist ebenfalls der Modellkurve für eine Entfernung vom "Epizentrum" von 200 mm (2000 km) ähnlich. In beiden Fällen verändert sich die Amplitude wenig mit der Tiefe. Auf der Grundlage der guten Übereinstimmung von Modell- und Natur - Amplitudenkurven kann man annehmen, dass das Geschwindigkeitsprofil im erforschten Gebiet qualitativ mit dem des Modells übereinstimmen muss. Um jedoch eine endgültige Schlussfolgerung

zu ziehen, muss untersucht werden, wie sich die Ausrichtung der Energiestrahlung der Herden auf die Amplitudenfunktionen auswirkt und ob das Minimum auf der Kurve lg A/T (H) nicht die Folge einer existierenden Ausrichtung ist. Mit diesem Ziel wurden von uns die Verschiebung in den Lagepunkten der Stationen für einzelne Erdbeben berechnet, für die aus Literaturangaben und mündlichen Mitteilungen [6] die Lage der Nodallinien bekannt ist. Ein grosser Teil des Materials wurde von der Aspirantin des Institutes für Geophysik der Akademie der Wissenschaften der UdSSR O.W. Sobolewa bereitgestellt, wofür der Autor zutiefst dankbar ist. Die Berechnungen wurden nach den Formeln von A.W. Wwedenskaja [7] angestellt.

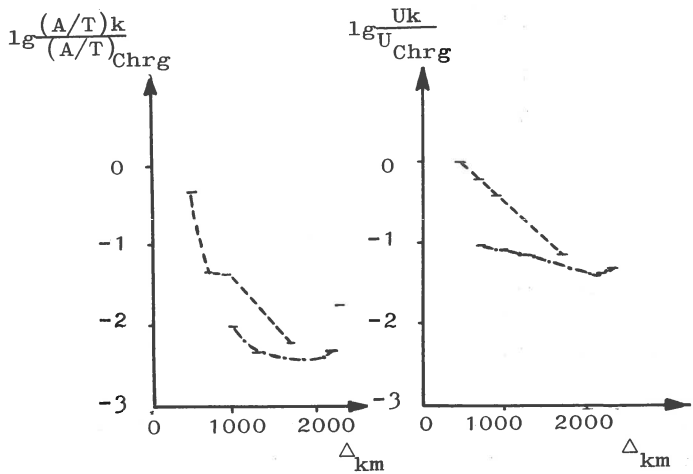

Abb. 3. Errechnete (a) und beobachtete (b) Funktionen $\lg \frac{(A/T)_K}{(A/T)_{Chorog}}$ (Δ) für Herdtiefen 200-210 km; - - - = westliche Richtung, - · - · = nordöstliche Richtung.

Die Berechnungen zeigten, dass die Amplitudenveränderung mit der Entfernung für unsere zwei Profile verschieden vorgehen muss. In Abb. 3 sind die errechneten und experimentellen Funktionen $\lg \frac{(A/T)_K}{(A/T)_{Chorog}}$ (Δ) für Herdtiefen von

200 km gezeigt. Aus Gegenüberstellungen beider folgt, dass man den Unterschied der experimentellen Kurven in westlicher und nordöstlicher Richtung vollständig mit dem Charakter der Herdausrichtung erklären kann, ohne dabei die mögliche Heterogenität des Mantels in Betracht zu ziehen.

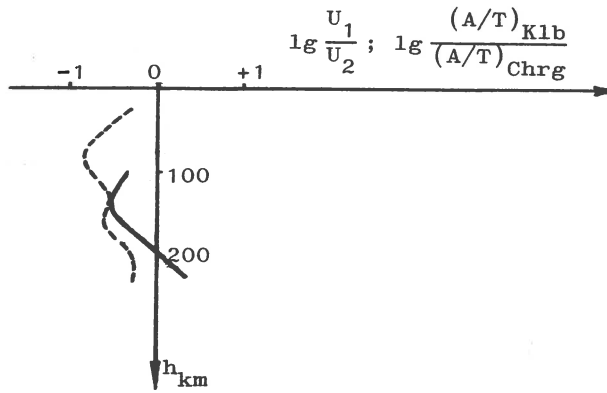

Abb. 4. Errechnete (———) und beobachtete (- - -) Funktion $\lg \frac{(A/T)_{Kuljab}}{(A/T)_{Chorog}}$

U = die Verschiebungsamplitude. 1 = Kuljab, 2 = Chorog.

Vergleichen wir die experimentellen und die errechneten Angaben für die Station Kuljab, für die ein anomales Verhalten der Amplitude mit wachsender Herdtiefe festgestellt wurde. In Abb. 4 sind die entsprechenden Grafiken $\lg \frac{(A/T)_{Kuljab}}{(A/T)_{Chorog}}$ (H) dargestellt. Zwischen den experimentellen und den errechneten Kurven besteht keine vollständige Übereinstimmung, jedoch ist das Minimum in mittleren Tiefen in beiden Fällen deutlich ausgedrückt. Das lässt annehmen, dass das anomale Verhalten der Amplituden in Kuljab in hohem Grade von der Herdausrichtung bestimmt wird. Das in einer Tiefe von ungefähr 80 km liegende Minimum auf der Experimentalkurve ist augenscheinlich von den besonderen geologisch-tektonischen Bedingungen im Gebiet Kuljab bedingt.

Bevor wir zur Gegenüberstellung der errechneten und der experimentellen Angaben für die für uns interessanteste, dem Schattengebiet entsprechende Entfernung von ungefähr 1000 km kommen, möchten wir folgende Bemerkung machen. Die von uns benutzte Berechnungsmethode ist ihrem Wesen nach für die Bestimmung der Verschiebungsamplitude in der Schattenzone nicht geeignet, weil sie auf der Vorstellung aufgebaut ist, dass die tieferen Erdschichten ein Medium sind, in dem sich die Geschwindigkeit mit wachsender Tiefe ununterbrochen vergrössert. Wenn deshalb die Schattenzone von einem Wellenleiter hervorgerufen wird, so wird sich das theoretische Verschiebungsfeld offenkundig vom beobachteten unterscheiden. Wenn folglich in unserem Falle ein Unterschied zwischen den experimentellen und den berechneten Kurven festgestellt wird, so zeugt das davon, dass die von uns gefundenen Funktionen $\lg \frac{(A/T)_K}{(A/T)_{Chorog}}$ (H) von dem Gefüge des Mediums (von der Existenz des Wellenleiters) und nicht von der Herdausrichtung bestimmt werden.

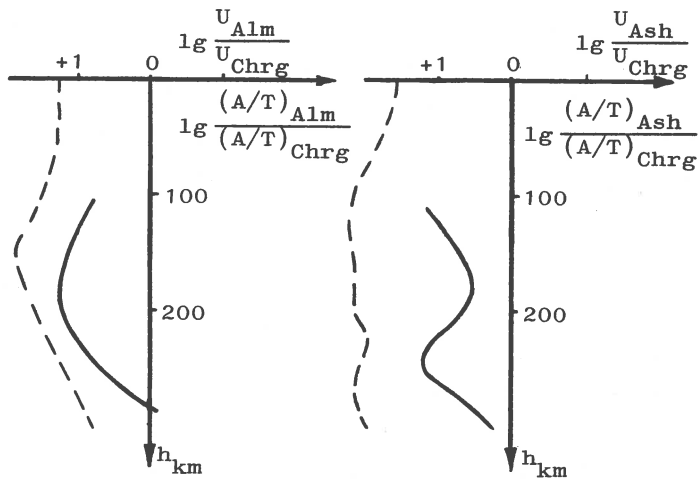

Abb. 5. Errechnete (——) und beobachtete (- - -) Funktion $\lg \frac{(A/T)_{Alma\text{-}Ata}}{(A/T)_{Chorog}}$ und $\lg \frac{(A/T)_{Ashchabad}}{(A/T)_{Chorog}}$.

In Abb. 5 sind die berechneten und die experimentellen Funktionen $\lg \frac{(A/T)_K}{(A/T)_{Chorog}}$ (H) für die Stationen Alma-Ata ($\Delta \sim 900$) und Ashchabad ($\Delta \sim 1100$) gezeigt. Die beobachteten Funktionen haben für beide Stationen ein und denselben Charakter - in mittleren Tiefen existiert ein Minimum. Für Alma-Ata ist es stärker ausgedrückt als für Ashchabad. Dabei sind die errechneten Kurven für diese Stationen ihrem Aussehen nach vollkommen gegensätzlich. Für Alma-Ata ist die errechnete Kurve der beobachteten sehr ähnlich, für Ashchabad hat sie entgegengesetztes Aussehen. Dort, wo die beobachtete Kurve ein Minimum hat, besitzt die errechnete ein Maximum. Folglich werden im gegebenen Fall die experimentellen Kurven $\lg \frac{(A/T)_K}{(A/T)_{Chorog}}$ (H) in ihrem Aussehen keineswegs von der Ausrichtung bestimmt. Die oben ausgesprochene Vermutung über die Existenz eines Wellenleiters erklärt das Vorhandensein des Minimums auf beiden Kurven. Die Strahlungsausrichtung "verbesserte" nur ein wenig, was das Gefüge bewirkte, indem es das Minimum in Alma-Ata vertiefte und das in Ashchabad abschwächte.

Wir bemerken, dass die von uns benutzten Formeln von Wwedenskaja für das erste Einsetzen (Schwingungsanfang) hergeleitet sind, wir jedoch die maximale Amplitude gemessen haben. Damit wird die im Vergleich mit der beobachteten Grafik grössere Streuung der Punkte auf der errechneten erklärt - bekanntlich erhält man immer für das erste Einsetzen stärkere Abhängigkeiten, als für die maximalen Amplituden.

Somit kommen wir auf der Grundlage der Gegenüberstellung der natürlichen, rechnerischen und Modellwerte zu dem Schluss, dass in dem erforschten Gebiet das Gefüge des oberen Mantels vom Vorhandensein eines Wellenleiters in einer Tiefe von ungefähr 170 km charakterisiert wird.

Zum Abschluss muss unbedingt betont werden, dass die von uns vorgeschlagenen Untersuchungsmethode des Geschwindigkeitsprofils des oberen Mantels keinen Anspruch auf Ausführlichkeit erhebt. Sie gestattet, die Frage nach der Existenz eines Wellenleiters zu beantworten und seine Tiefe

zu bestimmen. Wir möchten bemerken, dass die von A.A.Lukk [8] vorgenommenen Untersuchung der kinematischen Hodografen am Profil Pamir-Baikal ihn auch zu dem Schluss über die Existenz von Schichten mit verringerter Geschwindigkeit ungefähr in den gleichen Tiefen kommen liess.

Literatur

1. Ju.W.Risnitschenko, O.G.Schamina: Gegenüberstellung von auf Wellenleitermantelmodellen erhaltenen Amplitudenkurven mit seismischen Werten. Mitteilungen der Akademie der Wissenschaften der UdSSR, Serie Geophysik, Nr. 8, 1964.

2. B.Gutenberg, C.Richter: Magnitude and energy of earthquakes. Ann.geofis. 9. No.1, 1956.

3. W.I.Bune: Über die Verwendung der Golizynschen Methode zur ungefähren Einschätzung der Energie naher Erdbeben. Artikel- und Vortragssammlung. Arbeiten der Akademie der Wissenschaften der Tadschikischen SSR, Band 54, Ausgabe 1.

4. O.G.Schamina: Methodik des räumlichen Modellierens des Wellenleitermantels mit festen Stoffen. Mitteilungen der Akademie der Wissenschaften der UdSSR, Serie Geophysik, Nr. 7, 1965.

5. O.G.Schamina: Experimental investigation of necessary and sufficient characteristics of a wave-guide. Paper read on Symposium on seismic models, Liblice near Prague, Nov. 1965.

6. E.I.Schirokowa: Einige Angaben über den Charakter der Geschwindigkeitsveränderung in den oberen Schichten der Erdrinde. Mitteilungen der Akademie der Wissenschaften der UdSSR, Serie Geophysik, Nr. 8, 1963.

7. A.W.Wwedenskaja: Bestimmung der Verschiebungsfelder bei Erdbeben mit Hilfe der Dislokationstheorie. Mitteilungen der Akademie der Wissenschaften der UdSSR, Serie Geophysik, Nr. 3, 1956.

8. A.A.Lukk, I.L.Nersesow: Das Gefüge der oberen Erdrinde nach Beobachtungen von Erdbeben aus mittleren Herdtiefen. Vorträge der Akademie der Wissenschaften der UdSSR, mathematisch-physikalische Serie, Band 162, Nr. 3, 1965.

L.Antonova and V.Halturin

THE PERIODS OF SEISMIC WAVES DURING EARTHQUAKES

1. Data Used

This paper concerns the periods corresponding to maximum amplitudes in P, S, and surface waves (without differentiation of Rayleigh and Love waves). As many as 2000 SK-instrument records (V = const; T ranging from 0.5 to 10 sec) and a number of those taken by LP (T = 1 to 20-25 sec) and SP (T = 0.1 to 1.2 sec) have been investigated.

Data of the stations Moscow, Tashkent, Andijan, Frunze, Alma-Ata, Talgar, Alma-Ata-2, Garm, Ribatch'e, Irkutsk, Kyahta, and Kabansk as well as those of Budapest taken from the work of Bistrichan and Kiss (1962) have been considered.

The dependence of periods T upon the epicentre distance Δ (from 200 to 10000 km) and upon magnitude M (from 4 to 7.5) has been investigated. The effect of the recording station and the region of the earthquake epicentre on the character of the curve T-Δ has been studied as well.

2. The Structure of Scattering

All the regularities obtained appear against the background of widely scattered individual data.

The total scattering of particular points in the T-Δ graphs is summed up of the deviations due to level differences of curves for the earthquakes in this or that region, or recorded by different stations, as well as of shape variations of the curves defined by different mantle structures in different regions of the Earth. However, the main scattering is caused not by the just mentioned deviations, but by the so-called "casual" deviations. It seems that a considerable part is played by the irregular, impulse character of the body waves hampering measurements and sometimes making indistinct the conception of maximum phase period; interferentive character of the wave field; inaccuracies in determining the magnitudes of earthquakes; the

peculiarities of the spectral formation of the particular earthquake connected with the conditions of the epicentre. Average values σ of standard deviations of individual values $\lg T$ reflecting the effect of each of these factors (station, region, "casual") upon the total scattering of the points in curves $\lg T - \lg \Delta$ are given in Table 1.

Table 1

Standard deviation (in lg)

	Casual	Station		Region		Total
		Level	Shape	Level	Shape	
P	0.173	0.048	0.068	0.030	0.050	0.20
S	0.114	0.056	0.065	0.047	0.049	0.16
L	0.082	0.017	0.037	0.035	0.057	0.12

3. Surface Waves

Dependence of Their Periods upon Distance, Station, Region

Data upon which graphs $T - \Delta$ are based are reduced to one common magnitude $M = 5$ and in the summary graphs amends are made for region and station.

The dependence of the periods of surface waves upon the distance is of a step-like character (See Fig. 1). Periods of 7-8, 9-10, 12 and 16 sec are most common. Transition from one period to another is rather sharp. The steps are especially distincly noted in the graphs of particular stations. In the records of LP instruments the appearance of each typical period takes place at a shorter distance than in the records of SK instruments.

The typical periods depend upon the position of the extreme points of the dispersion curves of group speeds, and transition of the amplitude maximum from one period to another is the result of absorption.

The effect of conditions in the seismic station region upon the value of the maximum phase period is insignificant. The position of the epicentre has a greater effect. Thus earthquakes in the Baikal region are characterized by smaller

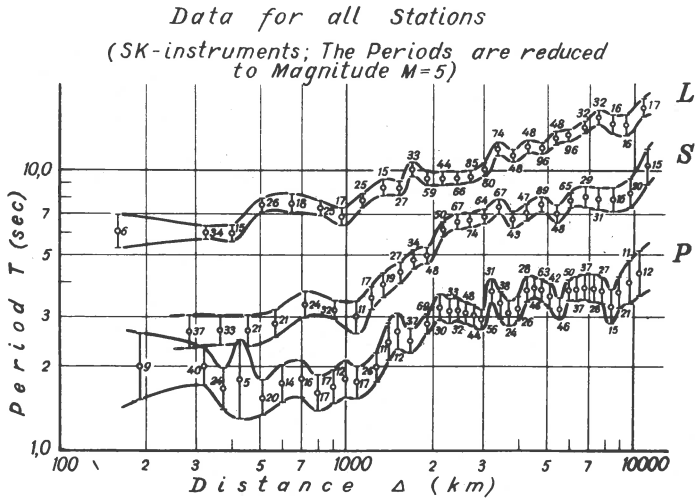

Fig. 1: The summary diagrams of the dependence of the period upon the distance for P-, S- and surface waves.

periods of surface waves as compared with the epicentres of Alps region, and earthquakes in Arctics, Far East and Indonesia are characterized by long periods.

4. Body Waves P and S Dependence of Their Periods upon Instruments, Distance, Region, Station

When comparing periods (Fig. 2) of waves P and S in records of SK and LP instruments made at the Talgar station, it is seen that: In 30-40% of the cases the spectrum of the longitudinal waves has at least two maxima, one of which is in the range of the plateau of the frequency characteristic of the SK instrument, and the second is often beyond it in the periods of the range of 10-20 sec. Therefore the periods of the maximum amplitudes of the earthquake waves P either coincide in the records of SK and LP, if the short-period peak of the spectrum is more intensive, or considerably differ, 2-3 times, if the long-period peak of the spectrum predominates. Maximum spectrum of the transverse

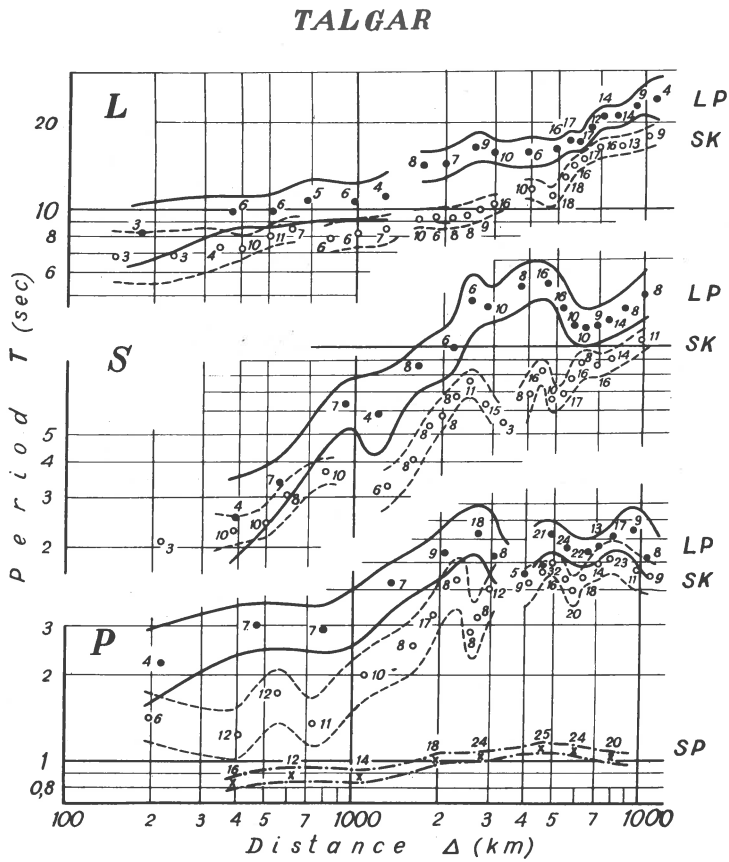

Fig. 2: The dependence of the visible periods in P-, S- and surface waves upon the distance in records with different instruments at the Talgar station.

waves falls into the periods of from 8 to 30-40 sec. As a rule, it lies beyond the frequency pass band of the SK instrument. That is why the records of S waves by SK and LP instruments at one point are not identical.

The change of the periods of body waves with the distance is the result of two reasons: of absorption and of chromatic aberration of seismic rays in the deep layers of the Earth. The first reason leads to the smooth growth of the periods with the distance, which is more or less intensive depending

upon the absorption properties of the substance at the depth to which the seismic rays penetrate. The second reason gives rise to the oscillations of curves on the background of this smooth growth.

At the distances of 200-1000 km periods $T_p \sim \Delta^{0.9}$; $T_s \sim \Delta^{1.1}$ is noted (Fig. 1), and in the teleseismic zone the periods are changed mush slighter ($T_p \sim \Delta^{0.1}$; $T_s \sim \Delta^{0.25}$). The value of the change of period with the distance was taken to evaluate the decrement of absorption (or the value of Q) in the upper and lower mantle. The following results were obtained (Table 2):

Table 2

	Upper mantle		Lower mantle	
Wave	ϑ	Q	ϑ	Q
P	0.015-0.025	125-200	0.001-0.002	1600-3200
S	0.025-0.040	80-125	0.003-0.006	500-1000

Curves of P and S wave periods both have the oscillating character. The following table gives epicentre distances (in thousands of km) to which the extremums of curves are timed:

Table 3

P	max	2.5		4.5		6.0-6.5		
	min		3.6-4.0		5.2-6.0		7-8	
S	max	2.5		4.5		6.0-6.5		
	min		3.3-4.0		5.5-6.0		7-8	

The positions of the extremums of the curves are nearly the same for stations that are located near to each other, but they differ to a certain extent for stations located at a distance, as in the case of stations of Central Asia and Baikal region (Fig. 3).

Minimums of the curves of periods correspond to maximums of the curves A/T, for example, of the Gutenberg calibra-

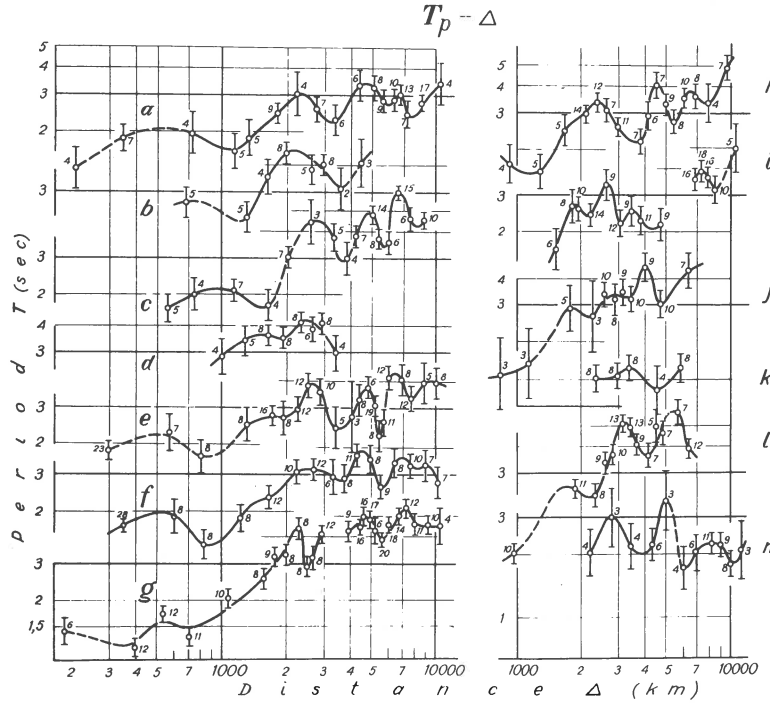

Fig. 3: The station dependence of the period of P-waves upon distance (the periods are reduced to magnitude M=5).

tion curve for m_p magnitude and to the positions of points of the bend of hodograph derivatives of waves P and S obtained by Bugaevsky (1957 and 1964). Thus the drop of the period of distances of 35-4000, 5200-6000 and 7000-8000 km is the result of the fact that the layers into which the seismic rays are penetrating and which correspond to these epicentral distances, focus more intensively a short-period component of the oscillation spectrum as compared to the long-period component. These layers must occur correspondingly at the depths of 800-900, 1200 and 1800 km. We may note the difference in the position of minimums and of their "depths" for curves drawn for earthquakes in different regions of the Earth (Fig. 4). This indicates the existence

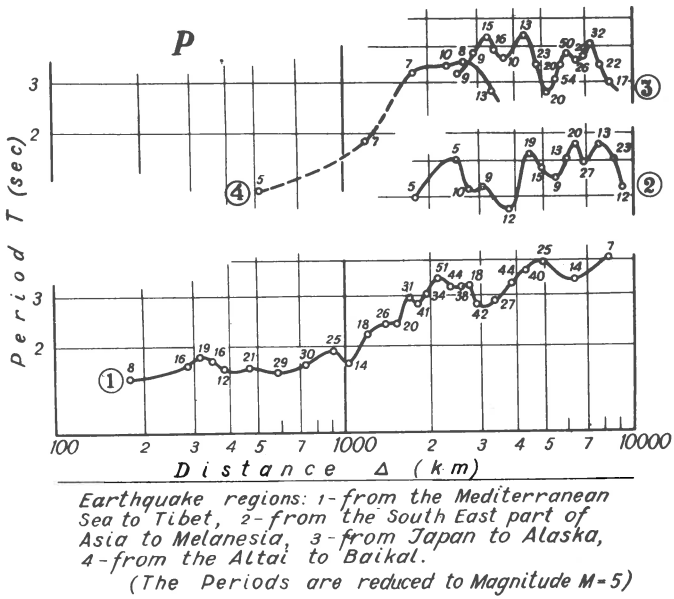

Fig. 4: The dependence of the periods of P-waves upon the distance for different focus regions.

of regional differences in the depth of occurrence, and may be, in the speed characteristics of these layers. Some unconformity in the position of these extremums in curves of P and S waves at the distances of about 2500 and 5500 km indicates the asymmetry of the in-elastic section of the upper mantle for P and S waves, and the presence in the upper mantle of a layer with a lowered speed only for S waves (which was registered by Nersesov and Lukk, 1965). It indicates also the impossibility of asymmetry of speed section along P and S waves at the depths in the range of 1200 km.

In comparing the levels of earthquake curves for different regions, the regional differences appear in the values of the earthquake periods with M = 5.0. The periods of body waves of Baikal earthquakes are in average 10-15% smaller and the periods of earthquakes in Japan and Arctic region are 7-12% larger than the periods of earthquakes in Alps zone (Fig. 4).

The differences in periods are also connected with peculiarities of stations. Thus Moscow station gives the smallest values of periods (3.50 in average) and stations of Baikal group and to the less extent stations of Alma-Ata and Frunze give large periods of body waves (Fig. 3).

5. Dependence of Periods upon Magnitude

The dependence of periods upon magnitude has been investigated in details for recording by instruments with frequency characteristics type SK flat in the interval of periods from 0.5 to 10 sec. For surface waves this dependence is slightly noticeable. For transverse waves it is more noticeable. And it is quite clearly noticeable and steady for longitudinal waves (Fig. 5).

The value of the derivative of the logarithm of period, taken with respect to magnitude, decreases with the distance and increases slightly with the magnitude. Table 4 contains average data from 11 stations taken with SK instruments.

Table 4

Wave	Thousands of km.	d lg T/dM with M	
		4 - 6	6 - 7.5
P	1 - 2	0.20	-
	2 - 4	0.17	0.16
	4 - 10	0.12	0.13
S	1 - 2	0.14	-
	2 - 4	0.08	0.10
	4 - 10	0.06	0.08
L	2 - 4	0.03	0.06
	4 - 10	0.02	0.05

The magnitude dependence of periods for S-waves in the SK instrument records is weakly manifested as compared with P waves and at some stations in teleseismic interval of distances it is scarely noticeable. In records made by long-

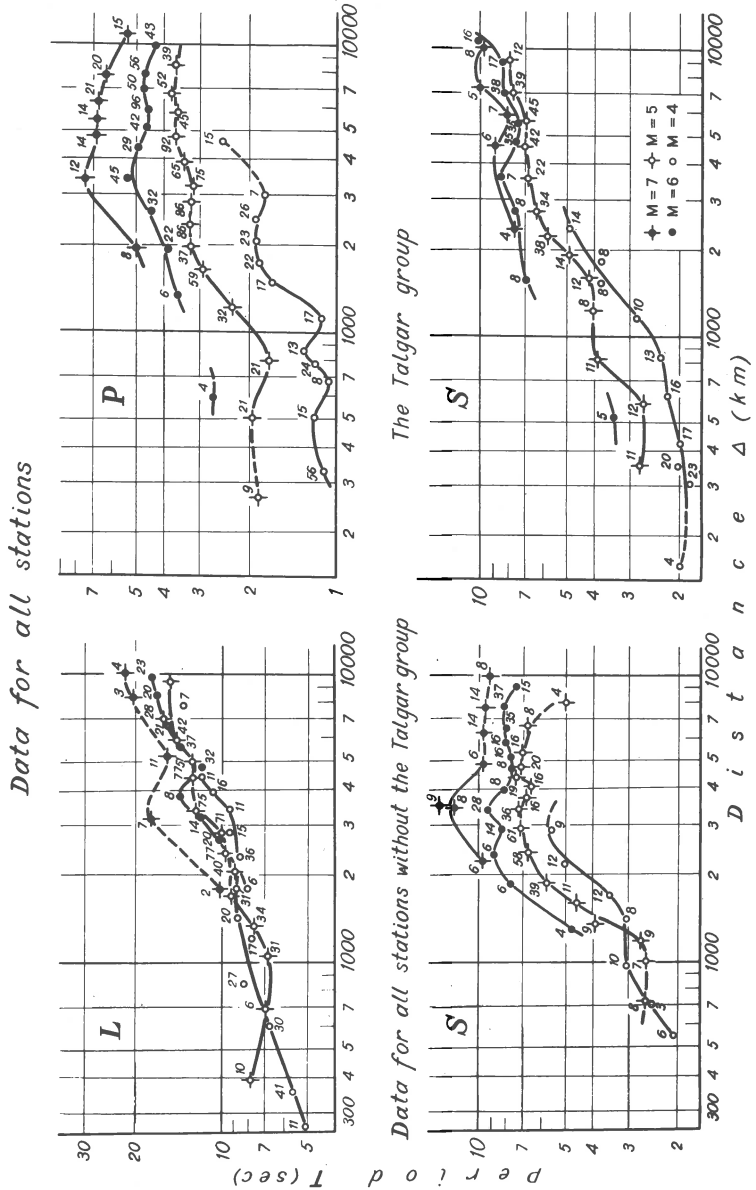

Fig. 5: The change of the T-Δ curves for P-, S- and surface waves in dependence upon magnitude (data for all stations).

period instruments this dependence is manifested much more intensively and the value of the derivative taken with respect to magnitude is equal to 0.14-0.16. On the one hand it is the result of a more intensitive absorption of transversal shear waves in the upper mantle, and on the other hand, the result of noticeable distortions of records made by SK instruments, which cut the main long-period component of the S-wave spectrum.

The value of the derivative of the P wave period taken with respect to magnitude is different for earthquakes with focuses in various regions of the Earth. (The magnitude dependence for S wave periods was not investigated from this point of view.) These differences correlate with the values of the periods themselves for the earthquakes with the magnitude M = 5. Thus for focuses in Arctic regions and Far East the derivative of period taken with respect to magnitude is minimum (0.12), and periods T_p for earthquakes with M = 5 in the teleseismic zone are maximum (3.5-4.0 sec.). Earthquakes in Baikal region and in China and Mongolia have maximum values of derivatives (0.16-0.17) and minimum values of periods (2.5-2.9 sec.). Data on earthquakes in the Mediterranean region of the Alps zone and Birma occupy intermediate positions (the derivative is equal to 0.13-0.14 and the periods to 2.9-3.2 sec.). This fact together with the tendency of the increase of period and decrease of derivative $\Delta \lg T/\Delta M$ with the distance is explained by absorption. The absorption properties of the mantle are not equal in the different regions of the world. In those regions, where the absorption is greater, the growth of the periods with the distance especially for more short-period and slight earthquakes is more intensive. This results in simultaneous diminution of the derivative and increase of the period. It follows that in the part of the world which we have examined the absorption property of the mantle is most intensive on the paths of the rays from Arctic region and Far East to Central Asia. Then in the order of diminution comes Alps zone, Birma and Indonesia. The minimum absorption in mantle is in China, Mongolia and Baikal regions.

Similar phenomena may be also connected with the increased absorption in the mantle in the region of the stations. Evidently, such is the case in the Tian-Shan region. For the stations located in this region lower values of the derivatives of periods taken with respect to magnitude are obtained for P waves as well as for S waves, higher values are obtained for the periods, and the noticeable growth of periods with distance is manifested even in the regions of teleseismic epicentral distances, while for the rest stations we can observe even some decrease in the period with the distance in the teleseismic zone, especially for intensive earthquakes. The last fact is evidently connected with some shortening of the way of the waves in the upper mantle with great epicentral distances and more steep angles at which waves pass the mantle.

References

Bisztricsany, E., Kiss, Z.: A body-wave magnitude equation for shallow-focus earthquakes. Ann.Univ.sei. Budapest, sec.geol. 1962.

Bugaevsky, G.: K voprosu o stroenij obolotchky Zemly. Bull. Soveta po Seismologii No. 6, Moscow, 1957.

Bugaevsky, G.: Godograph seismitcheskich voln i stroenije mantii. Sb. "Voprosy seismithnosty Sibiry", Trudy Inst. zemnoj kory, No. 18, 1964.

Gutenberg, B., Richter, C.: Earthquake magnitude, intensity, energy, and acceleration, II, BSSA 46, No. 2, 1956.

Nersesov, I., Lukk, A.: Stroenije verchnej tchasty obolochky Zemli po nabludenijam nad zemletryasenijamy s promejutochnoj glubinoy oschaga. DAN SSSR, 1965, 162, No. 3.

Halturin, V. i drugije (in press).: Osnovnye experimentalnye zakonomernosty dynamiki seismitcheskich voln. Nauka.

N.Canitez and S.B.Üçer

IMPROVED EPICENTERS IN AND NEAR TURKEY

(To be published in "Pure and Applied Geophysics")

Abstract

In recent years, many programs have been undertaken for relocation of epicenters using electronic computers. It is now quite possible that the earthquakes of Turkey and the Aegean Sea may be located accurately, because the existing recording stations show a good azimuthal distribution.

In the program written for the IBM 1620 the Sine-curve method of Gutenberg has been used. In this method which was first described by Gutenberg in an unpublished paper, residuals are plotted versus azimuths. The best fitting sine-curve is used to correct coordinates of epicenters and origin time.

The irregularities of the crustal thickness of the Earth and that of the velocities of seismic body waves in our region make the use of a standard travel-time table unsuitable. Because of this, a computational procedure has been employed which takes these changes in velocity into consideration. Therefore, in the relocation of each epicenter, we calculated a new travel-time equation to be used in subsequent iteration.

Between the years 1947-1960 improved values for 210 earthquakes have been obtained.

Pierre Mechler

MODELE DE CROUTE TERRESTRE DEDUIT DES DIFFERENCES DE TEMPS D'ARRIVEE DE SIGNAUX SEISMIQUES EN DEUX STATIONS VOISINES · APPLICATION A LA NORMANDIE

Le Laboratoire de physique de l'Ecole Normale Supérieure utilise en France cinq stations séismologiques ayant la particularité suivante: Chacune d'entre elles est constituée d'une station principale où sont enregistrées les trois composantes du mouvement du sol aussi bien en longue période qu'en courte période et de deux stations satellites éloignées de 30 à 40 km en général, équipées seulement d'un séismographe vertical courte période. Les deux stations satellites sont reliées par radio à la station principale et nous enregistrons les trois séismographes verticaux sur le même papier enregistreur. La vitesse de l'enregistrement étant de 2,5 mm par seconde, cette disposition nous permet d'avoir sans difficulté les différences de temps d'arrivée d'un signal dans les trois stations.

Cette disposition nous a conduit à étudier les différences de temps entre les arrivées d'un signal en fonction de l'azimut et de la distance du séisme. Si nous connaissons l'épicentre du séisme, il est possible à l'aide de tables de propagation de calculer les temps d'arrivée des signaux dans les trois stations et donc d'avoir des différences de temps d'arrivée théorique que l'on peut comparer aux différences de temps observées. Nous constatons qu'il existe un écart entre ces deux différences et c'est ce phénomène que nous voulons expliquer.

Nous devons d'abord vérifier que la méthode que nous utilisons n'introduit pas d'erreurs qui rendraient nos déterminations illusoires. Les coordonnées de l'épicentre étant supposées connues de façon parfaite des erreurs dans les temps de propagation pourraient s'introduire par l'utilisation de tables de propagation qui ne soient pas correctes. La comparaison des différentes tables montre que

les temps de trajet peuvent varier suivant la table utilisée mais que pour les séismes lointains (mettons plus de 2000 km) la vitesse de passage de l'onde est à peu près la même quelle que soit la table. Comme finalement sur des distances entre stations de l'ordre de quelques dizaines de kilomètres, c'est la vitesse de passage de l'onde qui compte pour la différence des temps d'arrivée, le choix de la table de propagation n'a pas d'importance. Supposons maintenant que le séisme ne soit pas bien connu. L'heure du séisme n'a pas d'importance puisque nous prenons une différence de temps entre deux stations. L'erreur sur les coordonnées de l'épicentre pourrait, elle, provoquer des écarts de temps, là encore l'expérience montre qu'il n'en est rien: la distance à une station varie mais la différence de distance entre le séisme et deux stations proches varie très peu et la vitesse de passage de l'onde variant peu avec la distance, nous n'introduisons que des erreurs inférieures aux erreurs de mesure sur la différence des temps.

Les considérations précédentes qui pourraient très facilement être étayées de façon quantitative montrent que l'écart entre les différences de temps calculées et observées entre deux stations proches doivent avoir une signification physique.

Les deux rais séismiques, issus du même séisme et devant arriver aux deux stations voisines, se propagent pendant la majeure partie de leur trajet à des distances très faibles l'un de l'autre. Il ne peut donc y avoir d'anomalies introduites au voisinage de la source. Notre étude de ces différences de temps doit donc mettre en évidence des anomalies au voisinage des stations. En d'autres termes, nous obtenons une façon nouvelle d'étudier la croûte terrestre et le manteau supérieur au voisinage des stations d'enregistrement.

Avant de montrer les conséquences géologiques que l'on peut tirer de cette étude des différences de temps dans des cas particuliers, il est utile de préciser comment nous utilisons ces différences de temps pour, d'une part avoir une localisation très rapide mais grossière de l'épicentre

et d'autre part mettre en évidence les anomalies dues à la croûte terrestre.

Supposons qu'une onde venant d'un séisme lointain passe sous les stations. Celles-ci étant proches, l'onde peut être supposée plane, elle dépendra donc de deux paramètres, son azimut θ et sa vitesse V de passage. Les différences de temps t_1 et t_2 entre les deux stations satellites 1 et 2 et la station principale se mettent sous la forme:

$$t_1 = \frac{a}{V}\cos\theta + \frac{b}{V}\sin\theta$$

$$t_2 = \frac{c}{V}\cos\theta + \frac{d}{V}\sin\theta$$

a, b, c, et d étant des paramètres géométriques dépendant de l'emplacement des trois stations. Nous pouvons en faire une représentation géométrique dans un plan rapporté à des axes obliques convenable pour que, V restant constant, la courbe $t_1 = f(\theta)$, $t_2 = g(\theta)$ représente un cercle dont l'angle au centre sera justement le paramètre.

Si nous supposons que la propagation se fait sans aucune anomalie, nous pouvons représenter, dans le plan précédent, les différences de temps t_1 et t_2 d'un séisme quelconque par un point M. La direction O M joignant le centre des axes au point M, nous donne immédiatement l'azimut sous lequel l'épicentre est vu de la station alors que la longueur O M nous donne, à un facteur près, l'inverse de la vitesse $\frac{1}{V}$ et, en connaissant la loi de variation de la vitesse en fonction de la distance, nous obtenons ainsi les coordonnées polaires de l'épicentre par rapport à la station.

Les mesures que nous avons faites montrent que la détermination précédente, qui peut se faire en quelques secondes, donne des azimuts à $\pm 5°$ près et des distances à 10% près, ce qui n'est pas si mal que cela.

Sur le diagramme précédent, nous pouvons porter non seulement les points expérimentaux mais aussi les points calculés, ce qui nous permet d'avoir de suite une vue des anomalies. Il est possible de corriger de façon expérimen-

tale le diagramme de façon à améliorer la détermination de l'épicentre.

Dans la dernière partie de notre exposé, nous allons donner des résultats expérimentaux obtenus dans une de nos stations en Normandie (dans l'Ouest de la France).

Les coordonnées de notre station principale sont:

F N	48°	45',750	N
	00°	28',916	W

et celles des deux stations satellites:

G N	48°	23',300	N
	00°	51',500	W
S N	48°	35',050	N
	00°	51',500	W

Nous avons choisi cette station pour tester notre méthode car c'est celle qui, a priori, était la plus homogène, les trois stations étant sur le même granite, à l'extrémité orientale du massif Armoricain.

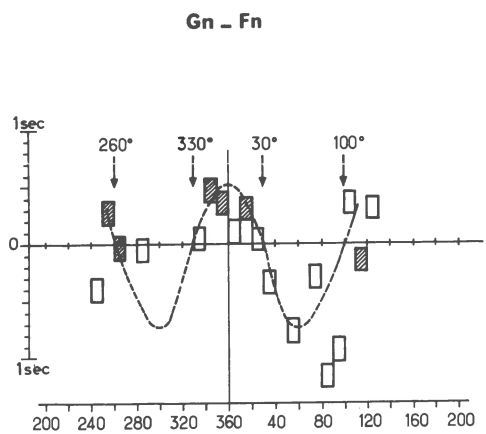

Figure 1

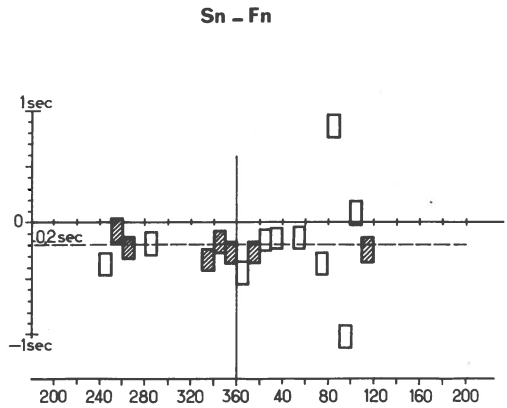

Figure 2

Les deux figures ci-jointes montrent les résultats d'une statistique faite sur nos enregistrements. Les séismes viennent principalement du Nord, exactement nous avons des signaux relativement nombreux entre 120° E et 120° W en passant par le Nord et très peu au Sud. Nous avons porté en abscisses l'azimut des séismes et en ordonnée la différence entre les différences de temps d'arrivée observée et calculée. Exactement en ordonnée, pour supprimer dans la mesure du possible l'influence des erreurs de lecture, nous avons fait des moyennes de tous les séismes dont les azimuts sont compris entre deux dizaines entières de degrés. Les rectangles dessinés ont un côté de 10° en abscisse, et de 1 dixième de seconde en ordonnée.

Les deux courbes, la première pour les stations G N et F N et la deuxième pour les stations S N et F N sont très différentes l'une de l'autre. A l'exception de deux points aberrants dans les deux courbes qui correspondent à une direction où nous n'avons observé qu'un seul séisme, les points de l'une des courbes s'alignent assez bien sur la droite t = -0,2 sec (S N, F N) tandis que pour l'autre (G N, F N) les points se placent sur une sinusoïde.

Les écarts observés entre les deux différences sont assez grands, plusieurs dixièmes de seconde. La précision de nos lectures étant au moins de 1 dixième de seconde, nous voyons que cet effet quoique faible, ce qui était prévisible vu la proxomité de nos stations est très réel.

Nous avons indiqué plus haut que l'explication de ces écarts doit être cherchée dans la croûte terrestre, ou dans le manteau supérieur, au voisinage de la station. A priori il y a deux explications possibles, soit entre les deux stations il y a une variation de vitesse dans les terrains, soit une variation dans la géométrie de ces terrains. Si en effet la croûte terrestre restait identique entre les stations, on ne saurait observer de tels écarts.

En prenant des valeurs nouvelles pour la structure de la croûte terrestre et du manteau supérieur, on calcule facilement que la variation de vitesse, dans une zone d'épaisseur convenable (de l'ordre de 20 à 30 km) doit être d'environ 10% pour expliquer une anomalie de 3 dixièmes de seconde dans les différences. Il me paraît difficile d'admettre que la vitesse du manteau supérieur puisse passer de 8 à 7,2 km/s sur une distance de 20 km environ. Par contre des variations d'épaisseur de la croûte sont beaucoup plus probables: une variation d'épaisseur de 2 à 6 km suivant les pendages pris pour les discontinuités, expliquent fort bien le même écart de 3 dixièmes de seconde, si on prend cette variation d'épaisseur sur une couche de 6 km/s surmontant une couche à 8 km/s. Bien que les pentes obtenues pour la discontinuité soient fortes, elles sont encore raisonnables et ce phénomène constitue certainement le paramètre principal de la variation entre les temps d'arrivée entre deux stations proches.

Notre méthode nous permet donc d'avoir une bonne approximation des variations d'épaisseur de la croûte terrestre au voisinage d'une station d'enregistrement.

A l'aide de ce qui précède, nous pouvons interpréter les écarts obtenus expérimentalement en Normandie. Sans vouloir rentrer dans tous les détails de calcul qui alourdiraient cet exposé que nous avons sciemment fait assez bref disons que la sinusoïde représentant les écarts entre les stations G N et F N s'explique très bien en supposant que la discontinuité de Mohorovičić n'est pas plane mais ondulée à la façon d'une tôle ondulée, la "longueur d'onde" du plissement étant de l'ordre de 30 km et l'amplitude d'environ 3 km. L'écart constant entre F N et S N s'expliquant, lui, en

supposant que la discontinuité de Moho ondule, n'est pas plane mais inclinée d'un peu moins de 10°, remontant sous la station S N.

Ces considérations sur Moho peuvent paraître arbitraires, surtout qu'elles sont très difficiles à vérifier par d'autres méthodes géophysiques, mais nous pouvons les comparer aux données de la géologie de surface. La direction du plissement de Moho correspond très exactement avec la direction du plissement du Massif Armoricain sur lequel se trouve nos stations (une longueur d'onde de 30 km se retrouve d'ailleurs aussi dans ce plissement géologique mais dans la partie Sud du Massif et non dans la partie Nord-Est où sont nos stations). D'autre part, la station S N étant à l'extrémité Est du Massif alors que les deux autres stations sont plus à l'intérieur du Massif, une remontée sous S N correspondrait à la présence de racines sous le Massif Armoricain.

Nous espérons donc avoir montré de façon claire que notre procédé d'étude des différences de temps d'arrivée entre deux stations très voisines permet d'obtenir d'une part une localisation peut-être grossière mais très rapide des séismes et surtout d'ajouter à la connaissance de la croûte terrestre au voisinage de stations d'enregistrement.

M.A.Choudhury et G.Perrier

ANOMALIE DU MANTEAU SUPERIEUR EN FRANCE

Les résultats obtenus à partir des durées de propagation et des vitesses apparentes des ondes longitudinales P par l'enregistrement de séismes provoqués dans le Sud-Algérien (profils Sud-Nord et distances comprises entre 19° et 24°) et aux Iles Aléoutiennes (profils Nord-Sud et distances comprises entre 80° et 85°) ont permis de préciser la structure du manteau supérieur dans le Centre de la France.

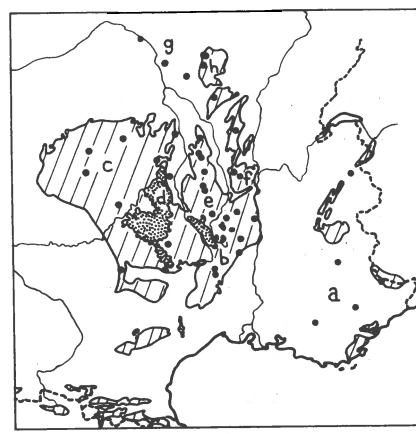

Figure 1

La carte générale (fig. 1) donne sur un fond géologique simplifié - terrains cristallins (hachures) et volcaniques (pointillés) - le réseau de 39 stations d'enregistrement. Celles-ci comprennent 15 stations permanentes d'observatoire (vitesse de déroulement: 12 cm/mn) et 24 stations mobiles à enregistrement rapide (2,5 à 6 cm/s) avec signaux horaires enregistrés simultanément dans l'un et l'autre cas. Les différentes régions étudiées étaient: les Alpes occidentales françaises (a), les Cévennes (b), le Limousin (c), les volcans d'Auvergne (d), le Forez (e), le Vivarais et le Beaujolais (f), le Nivernais (g) et le Morvan (h).

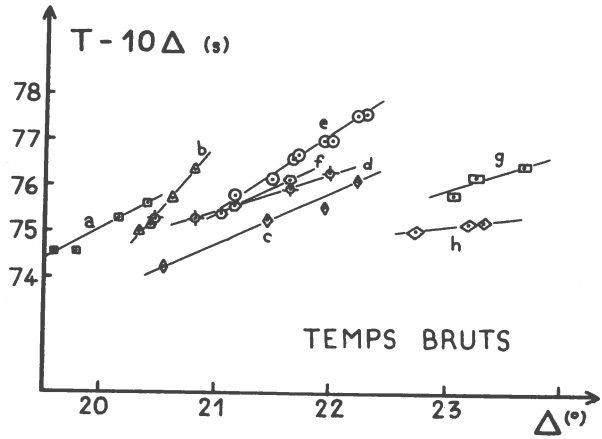

Figure 2

La figure 2 montre, en fonction de la distance Δ, les durées brutes de propagation réduites T - 10 Δ relatives à l'Algérie. Elle met en évidence:

1° - les alignements des données d'observation suivant les différentes régions;

2° - deux anomalies dans les vitesses apparantes pour les Cévennes (8,3 km/s) et le Forez (9,5 km/s);

3° - des écarts entre les durées de propagation pouvant varier, dans un même domaine de distance et pour deux régions différentes, de 0,9 s à 1,5 s.

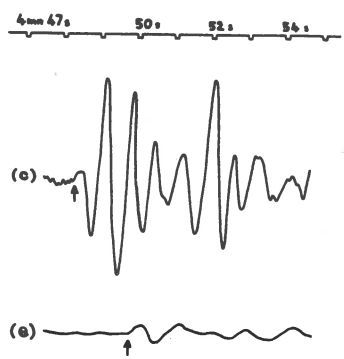

Figure 3

La figure 3 montre la reproduction de deux enregistrements obtenus, l'un dans le Limousin (c), l'autre dans le Forez (e) à des distances épicentrales voisines (21°,435 et 21°,473). On notera la différence d'aspect de ces deux enregistrements ainsi que l'écart existant entre les temps d'arrivée (δT = 0,96 s, après correction de la petite différence de distance entre les deux stations).

Nous avons appliqué aux durées brutes de propagation une correction destinée à éliminer l'effet des inégalités d'épaisseur de la croûte terrestre dans les diverses régions étudiées. Tous les résultats ont été ramenés à une croûte d'épaisseur moyenne égale à 24 km.

Ces corrections ont pu être faites grâce à l'étude systématique de la croûte terrestre dans le Massif Central, entreprise en 1961 et utilisant les tirs de carrière. Une partie des résultats obtenus a été publiée en 1963 [1] et 1965 [2].

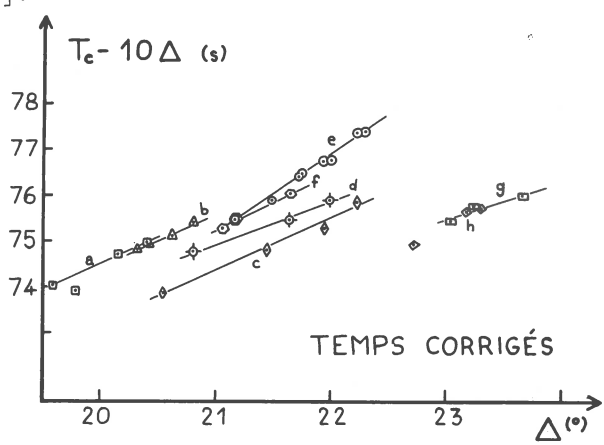

Figure 4

La figure 4 représente les durées réduites de propagation après correction $T_c - 10\Delta$ en fonction de la distance Δ. La comparaison de cette figure et de la figure 2 met en évidence les résultats suivants:

1° - l'anomalie de vitesse apparente observée dans le Forez (e) subsiste alors que celle des Cévennes (b) disparaît;

2° - autour de 21°,5, 3 groupes distincts apparaissent: Le Limousin (c), les volcans d'Auvergne (d) et le Forez (e);

3° - les durées de propagation relatives au Nivernais (g) et au Morvan (h), à des distances comparables, deviennent peu différentes et présentent une avance par rapport à l'ensemble des données.

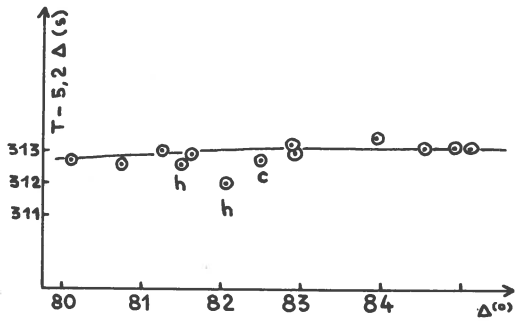

Figure 5

Par ailleurs, les durées de propagation des ondes P issues des Îles Aléoutiennes (fig. 5) varient en fonction de la distance suivant une loi presque linéaire entre 80° et 85°, à l'exception des 2 stations du Morvan (h) et de celle du Limousin (c) pour lesquelles on observe des avances respectives de 1, 0,4 et 0,4 s qui ne sont pas éliminées par une correction d'épaisseur de la croûte.

On ne peut donc attribuer les anomalies constatées (fig. 4 et 5) qu'à une hétérogénéité du manteau supérieur.

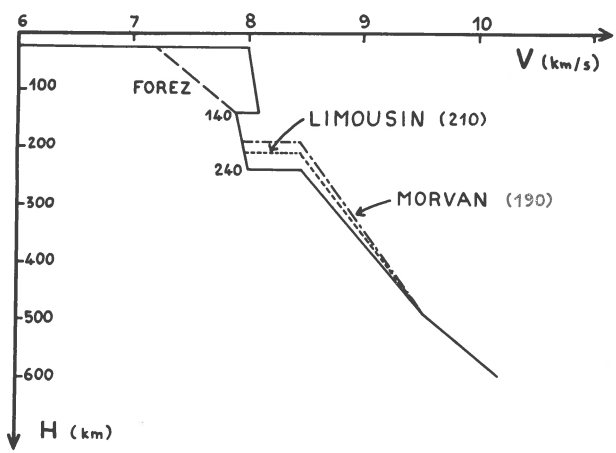

Figure 6

Nous avons déterminé un modèle de vitesse satisfaisant aux données expérimentales ci-dessus. Utilisant les résultats obtenus par B.Mohammadioun [3] à partir des spectres d'énergie des ondes de volume, nous avons assigné à la couche à faible vitesse du manteau supérieur, des limites supérieures et inférieures situées à des profondeurs respectives de 140 et de 240 km.

Les caractéristiques de ce modèle sont les suivantes:

a)

Vitesses (km/s)	Profondeurs (km)
6	de 0 à 24
8,0 à 8,1	de 24 à 140
7,9 à 8,0	de 140 à 240
8,47 à 9,54	de 240 à 493
9,54 à 10,20	de 493 à 600

b) les lois de variation de la vitesse en fonction de la profondeur sont du second degré;

c) la loi de variation entre 24 et 140 km est celle qui justifie le mieux les données d'observation entre 4° et 18° de distance épicentrale [4].

Ce modèle a été modifié du côté des stations afin d'expliquer les anomalies régionales:

A) Pour expliquer l'avance de certaines arrivées d'ondes, nous avons fait varier la limite inférieure de la couche à faible vitesse et nous avons trouvé, pour chaque massif géologique, les profondeurs suivantes: 190 km (Morvan), 210 km (Limousin) et 220 km (volcans d'Auvergne).

B) Pour expliquer l'anomalie de la vitesse apparente dans le Forez, nous avons tenu compte des résultats obtenus pour la croûte dans cette région [1], à savoir la mise en évidence d'une vitesse de 7,2 km/s pour les ondes P vers 26 km de profondeur (vitesse confirmée par un profil inverse) et l'absence d'une vitesse voisine de 8 km/s jusqu'à 250 km de distance.

Nous avons donc admis dans cette région une remontée de la couche à faible vitesse (V diminuant progressivement de

7,9 à 7,2 km/s entre 140 et 24 km). La valeur faible de la vitesse apparente s'explique alors par le fait que les rayons séismiques arrivant vers le Forez subissent une réfraction latérale due à ce changement de structure, le paramètre du rayon $p = \frac{r \sin i}{V}$ (r étant la distance entre un point P du rayon séismique et le centre O de la Terre, i l'angle de OP avec ce rayon) se trouvant ainsi augmenté.

Cette hypothèse concernant le Forez semble en accord avec les données des volcanologues [5]. Elle rejoint les préoccupations des géologues [6].

Des calculs d'hodochrones pour différents modèles de vitesse sont actuellement en cours avec l'aide d'un ordinateur électronique. Ils permettront d'examiner la possibilité d'autres hypothèses. Les résultats détaillés seront publiés ultérieurement.

En conclusion, nous pouvons affirmer que des alignements de stations, dans des régions géologiquement homogènes, ainsi qu'une grande précision sur les durées de propagation, permettent de mettre en évidence la cohérence des dispersions et d'en déduire des structures régionales précises, non seulement de la croûte mais aussi du manteau supérieur terrestre.

Bibliographie

[1] - G.Perrier. C.R.Acad.Sc. Paris, t.257, p.1321-1322, 1963, Séismologie. Ondes séismiques enregistrées dans les Monts du Forez.

[2] - G.Perrier. C.R.Acad.Sc. Paris, t.261, p.493-496, 1965, Séismologie. Variations d'épaisseur de la croûte terrestre dans le Centre et le Nord-Est de la France.

[3] - B.Mohammadioun. Thèse de doctorat d'Etat, Paris 1966. Structure du manteau et du noyau terrestres d'après les spectres d'énergie des ondes longitudinales.

[4] - M.A.Choudhury et J.P.Rothé. Ann.géophys., 21, fasc.2, 1965, p.266-272. Durée de propagation des ondes P; anomalie vers 20°.

[5] - A.Rittmann. Les volcans et leur activité, chap.IX, Masson, Paris, 1963.

[6] - J.Jung, M.Chichery et O.Vachias. Mém.Soc.Géol.Fr., n° 38, nouvelle série, 16, n° 4, 1939, p.1-28.

E.S.Husebye and B.Jansson

APPLICATION OF ARRAY-DATA PROCESSING TECHNIQUES TO ORDINARY SEISMOGRAPH STATIONS, WITH SPECIAL REFERENCE TO THE FENNOSCANDIAN NETWORK

Abstract

An efficient tool in seismic signal analysis is offered by array-data processing techniques, which are based on signal similarity in an array of seismometers. As the establishment and maintenance of an array are very expensive, it is natural to ask whether the array technique is applicable to ordinary seismograph stations, i.e. if a net of such stations can be considered as a super-large aperture seismic array (SLASA). We have shown previously that this is valid for the Swedish station net (Pure and Appl.Geophys., 63:82-104, 1966). These results encouraged us to further investigation of this problem, that is, to what extent does the P pulse shape depend on epicentral distance and crustal structure. We used hand-digitized seismograms of 12 earthquakes recorded by short-period seismographs in Fennoscandia. The sampling interval was 0.067 sec and for records digitized twice, the coherency in the period range of 0.8-3.0 sec was in average about 0.94.

In order to test signal similarity, some of the statistical properties of P pulses, like cross-correlation, coherency, phase shift and power spectra, were calculated. Another criterion is the gain in S/N obtained by applying array techniques and improved iP readings.

The results show that the correlation in average varies between 0.5-0.8, being significantly higher for signal lengths of 8 sec than for 16 sec, but does not exhibit a pronounced decrease for increasing station separation (relative to epicenter). The coherency calculations strongly indicate that the signal periods of about 1.5-2.5 sec correlate best, with correlations varying between 0.7 and 0.9. Simple delay and sum processing improved the S/N according to the $N^{-1/2}$ formula, and many readings of P phases could be improved.

Our conclusion is that the records from Fennoscandian stations in general exhibit the signal resemblance required by array-data processing techniques, although the station separation is in some cases as large as 1700 km. Since this network covers a large area with different crustal structures, ranging from sedimentary rocks to shield areas, and since also various types of seismographs are in operation, the results should be representative for other parts of the world too.

This research was carried out at the Seismological Institute, Uppsala, Sweden, with the sponsorship of the Air Force Cambridge Research Laboratories under Contract

AF 61(052)-702 through the European Office of Aerospace Research, OAR, United States Air Force, as part of the Advanced Research Projects Agency's project Vela-Uniform.

Markus Båth

PROPAGATION OF Sn AND Pn TO TELESEISMIC DISTANCES

Abstract

Sn and Pn waves propagated to teleseismic distances are investigated by means of short-period seismograph records of the Swedish network. Both phases have been found in the distance range of about 2400 km to 4700 km, but only provided the path is exceptionally homogeneous. Almost all paths are restricted to the Russian platform. There are probably very few areas in the world offering similar propagation paths. The velocities just under the Mohorovičić discontinuity are found to be 4.72 km/sec and 8.15 km/sec for transverse and longitudinal waves, respectively. The corresponding Poisson ratio is 0.248. These values are averages for the Russian Platform. Other properties, such as periods, dispersion, amplitudes, particle motions, propagation mechanism and comparisons with other related waves, are reported and discussed.

A complete report will appear in two papers in Pure and Applied Geophysics.*) This research was carried out at the Seismological Institute, Uppsala, Sweden, with the sponsorship of the Air Force Cambridge Research Laboratories under Contract AF 61(052)-702 through the European Office of Aerospace Research, OAR, United States Air Force, as part of the Advanced Research Projects Agency's project Vela-Uniform.

*) Vol.64, p.19-30 and Vol.65, p.5-11 (Editor's note).

H.Sima, E.Peterschmitt et C.Madureira

SUR LES ONDES REFLECHIES MULTIPLES

Abstract

Distinct phases appearing nearly at arrival time of Pa waves were examined for two earthquakes in the Kurile Islands region and two others near Japan. Travel times, particle motions, incident angles, and amplitude-distance relations were determined in order to identify these phases. From the results it follows that the waves are better explained to be multiple reflected waves. Moreover the value of Q is determined in medium of the upper mantle by spectral comparison between these distinct phases and the P phases.

Introduction

En de nombreuses stations en Europe on observe fréquemment à l'occasion de séismes éloignés à trajet continental des ondes bien caractérisées après les ondes réfléchies telles que PP ou PPP. La vitesse apparente de ces ondes, appelées ondes Pa, est voisine de 8,0 km/s d'après des observations italiennes comprises dans un intervalle de distance de 6000-10000 km. Caloi (1954) attribue ces phases à des ondes canalisées s'étant propagées avec la vitesse des P dans les couches à faible vitesse existant dans le Manteau supérieur. Magnitsky et Khorosheva (1961) ont déterminé le coefficient d'absorption des ondes Pa et Båth et Arroyo (1963) ont décrit en détail les observations faites en Suède. Plus récemment les ondes Pa de même que leurs analogues, les ondes Sa ont été utilisées comme une aide dans les recherches sur la structure du Manteau supérieur. A l'origine, la présente étude devait être consacrée aux ondes Pa provenant de séismes de l'Asie orientale, cependant l'analyse des données a conduit à admettre l'existence d'ondes différentes des ondes canalisées de type Pa.

Recherches des données

Afin de déterminer les séismes ayant donné lieu à des ondes de type Pa en Europe, nous avons examiné d'abord le bulletin séismique, puis les inscriptions Ewing-Press 30-90 de Strasbourg pour les années 1963-1964.

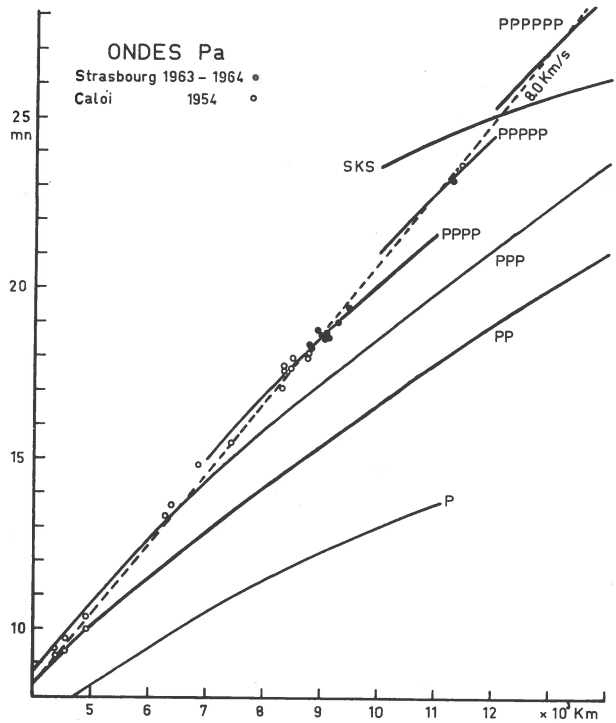

Figure 1: Hodochrones des ondes Pa d'après les bulletins de Strasbourg et les données de Caloi 1954.

Sur la figure 1 nous avons reporté les observations de Strasbourg de même que celles tirées du travail de Caloi 1954. Le nombre de données est insuffisant pour permettre la détermination des hodochrones précises. Mais il est possible cependant de faire une remarque importante: les observations, si elles correspondent bien à une vitesse apparente constante de 8,0 km/s, semblent s'accumuler dans des intervalles de distances où il est également possible en ce qui concerne les temps de propagation, d'interpréter ces

ondes Pa comme des ondes réfléchies multiples telles que PPP ou PPPP. Il se peut naturellement que cette observation soit due au manque de foyers séismiques dans le domaine de distance où la distinction entre les ondes de type Pa et les ondes réfléchies multiples est possible - par exemple pour des distances hypocentrales de l'ordre de 7500 km ou de 9800 km.

Afin d'éliminer cette hypothèse, nous avons sélectionné 4 séismes pour lesquels les ondes de type Pa étaient particulièrement nettes à Strasbourg et pour lesquels on pouvait espérer grâce au réseau World-wide de séismographes de type Ewing-Press obtenir des données homogènes, d'une part au point de vue instrumental, d'autre part du point de vue propagation. Les séismes étaient originaires des Kouriles et du Japon (Tableau 1). Les stations ont été choisies en Eurasie (Tableau 2) de façon à ne considérer que des trajets uniquement, ou du moins en très grande partie, continentaux.

Tableau 1

No	Date	Heure h mn s	Epicentre	Région	Profondeur (en km.)	Magnitude moyenne	Magnitude corrigée
1.	28 juin 1963	21 55 36.8	46°7N 153°3E	Iles Kouriles	12	6.6	6.8
2.	2 mai 1964	16 11 00.2	45°5N 150°3E	Iles Kouriles	35	6.4	- -
3.	16 juin 1964	04 01 44.3	38°3N 139°1E	Japon	53	7.3	7.2
4.	23 juin 1964	01 26 37.0	43°3N 146°1E	Japon	22	6.9	6.9

Tableau 2

Station	Abréviation	Coordonnées		Distance épicentrale (en km.)			
				1.	2.	3.	4.
Addis Abeba	AAE	9°02N	38°46E		10920	10280	10690
Copenhague	COP	55°41N	12°26E	8100	8130	8440	8210
Godhavn	GDH	69°15N	53°32W			8040	7430
Istanbul	IST	41°03N	28°59E	8850	8790	8730	8750
Kevo	KEV	69°45N	27°00E		6430	6840	6540
Kongsberg	KON	59°40N	9°40E		7820	8200	7930
Kap Tobin	KTG	70°25N	21°58W		7200	7860	7370
Malaga	MAL	36°44N	4°25W	10510	10560	10900	10660
New Dehli	NDL	28°41N	77°12E	6750	6530	5750	6240
Nord	NOR	81°36N	16°40W			6630	6120
Nurmijaervi	NUR	60°31N	24°39E	7270	7280	7550	7340
Porto	PTO	41°08N	8°36W		10200	10620	10320
Quetta	QUE	30°11N	66°57E		7200	6540	6950
Shiraz	SHI	29°39N	52°31E	8440	8280	7770	8080
Shillong	SHL	25°34N	91°53E	5850	5600	4630	5250
Strasbourg	STR	48°35N	7°46E	8950	8970	9260	9050
Stuttgart	STU	48°46N	9°12E	8890	8920	9180	8980
Toledo	TOL	39°53N	4°03W	10170	10220	10580	10320
Trieste	TRI	45°43N	13°46E	9050	9050	9230	9090

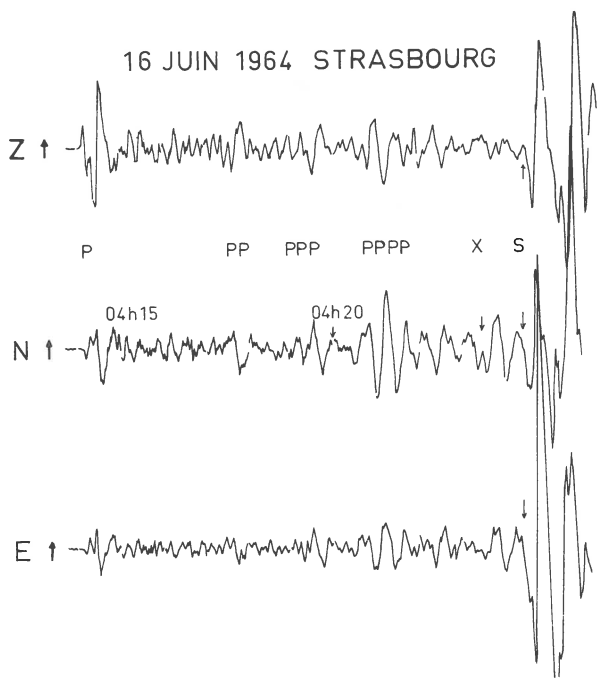

Figure 2. Ondes Pa ou PPPP enregistrées à Strasbourg. Séismographes Ewing-Press 30-90.

Résultats des observations

Aspect général des séismogrammes. La figure 2 donne un exemple d'enregistrement sur les Ewing-Press de Strasbourg des ondes de type Pa telles quelles ont été décrites par Caloi (1954). Entre les ondes classiques P, PP, PPP correspondant bien aux temps de propagation des tables et les ondes S apparaît une phase de grande amplitude notée PPPP sur la figure. On remarque la prépondérance croissante des composantes horizontales (en particulier de la composante NS, l'azimut étant N 37E) dans la succession P, PP, PPP, Pa ou PPPP. On remarquera également la diminution parallèle des fréquences plus élevées. Les amplitudes des phases Pa ou PPPP, souvent supérieures à celles des ondes P, PP, PPP qui les précèdent, sont à première vue difficilement explicables; c'est une des raisons qui ont conduit Caloi à admettre une propagation des ondes correspondantes le long du chenal à faible vitesse situé dans le manteau supérieur - l'asthenosphère.

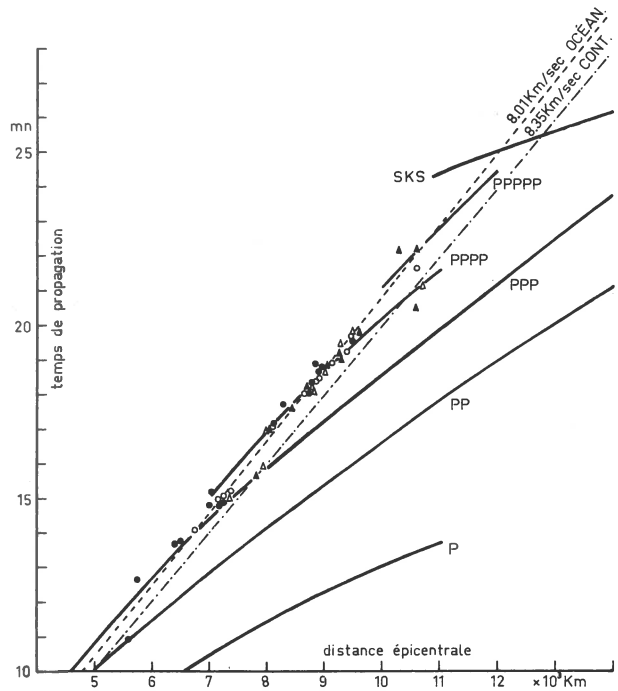

Figure 3. Hodochrones des ondes Pa ou nP à parcours eurasiatique pour 4 séismes originaires du Japon et des Kouriles.

Temps de propagation

Sur la figure 3, nous avons reporté les temps de propagation observés pour toutes les ondes de type précédent qui ont pu être mises en évidence pour les 4 séismes de la table 1 et pour les stations de la table 2. En dehors des hodochrones théoriques des ondes principales P, PP, PPP, PPPP, SKS, nous avons également tracé les deux droites correspondant aux vitesses de 8,01 et 8,35 km/s telles qu'elles ont été déterminées par Båth et Arroyo (1964) pour des trajets océaniques et continentaux de ces ondes. De façon analogue à la figure 1 on constate une accumulation de données pour des distances épicentrales comprises entre 6500 km et 8000 km d'une part, entre 8000 et 9800 km d'autre part. Pour le premier intervalle de distance, les phases étudiées peuvent être interprétées soit comme PPP soit comme Pa à trajet océanique; pour le deuxième intervalle l'interprétation conduit soit à une PPPP soit à une Pa à trajet également océanique. Or nous avons fait remarquer que les trajets étaient essentiellement continentaux; il en résulte que les hodochrones des phases conduisent à une interprétation en ondes réfléchies multiples PPP ou PPPP de préférence à celle d'ondes canalisées de type Pa.

Forme de l'onde

Afin d'étudier de plus près la forme de l'onde, les amplitudes ont été lues à la précision de 0,1 min. à l'aide d'un coordinatographe sur les enregistrements originaux - vitesse de déroulement généralement 15 mm/s - tous les 0,2 mm soit toutes les 0,8 secondes. Sur la figure 4, on a reporté le mouvement du spot du galvanomètre en suivant les composantes Z et $H = \sqrt{N^2 + E^2}$, ce qui est possible car pour toutes les composantes les courbes de grandissement sont les mêmes (à Strasbourg il faut multiplier les amplitudes Z lues par 2 pour obtenir des courbes identiques en Z et H). Les mouvements ne conservent pas une direction constante ni un sens de rotation constant; ceci est dû en partie à la présence des composantes à faible période et amplitude contenue dans les phases P et PP.

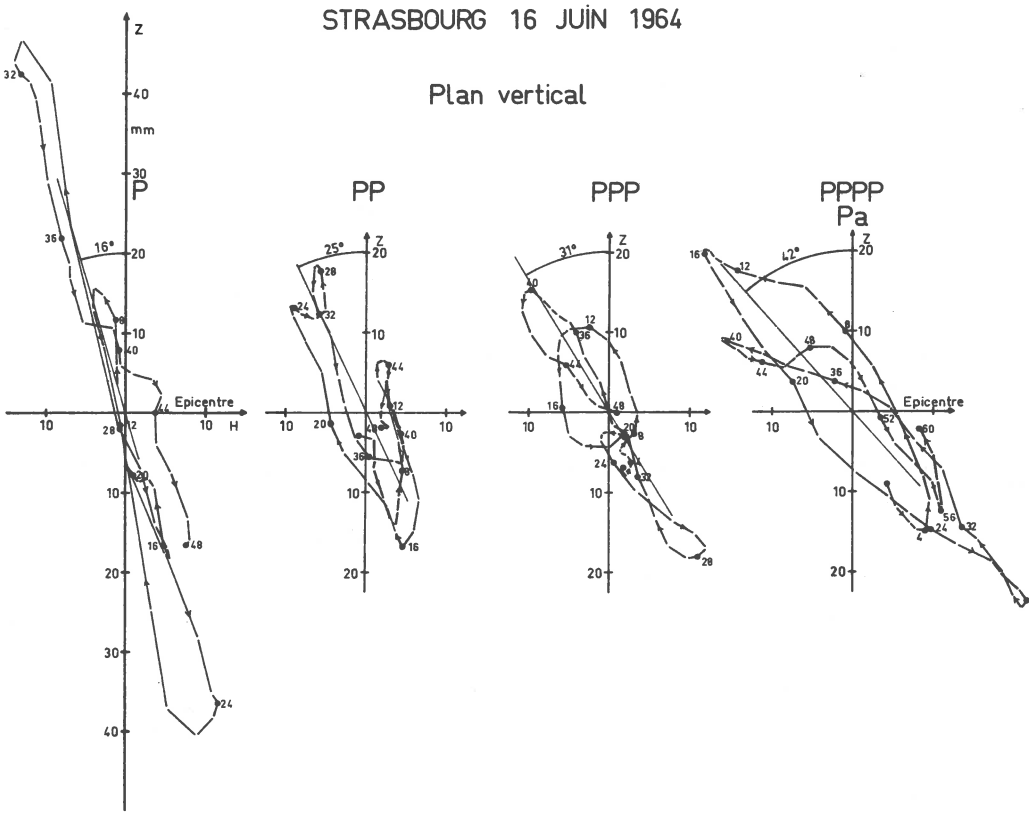

Figure 4. Ondes nP ou Pa: Mouvement du spot du galvanomètre.

Les mouvements pour les phases PPP et PPPP (ou Pa) sont rétrogrades dans une partie des grandes amplitudes et sont beaucoup plus simples que ceux des phases P et PP. Dans son ensemble le mouvement qui est pratiquement linéaire pour l'onde P devient de plus en plus elliptique. Ceci peut être la conséquence des changements de phase consécutifs aux réflexions successives.

On remarque également la variation continue de l'angle apparent d'incidence qui prend les valeurs respectives de 16, 25, 31 et 42° pour les ondes P, PP, PPP, PPPP ou Pa. On sait que pour un séisme superficiel - les profondeurs

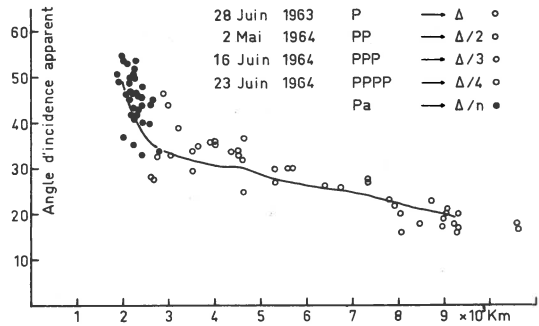

Figure 5. Variation de l'angle d'incidence apparent en fonction de la distance.

hypocentrales des 4 séismes sont assez faibles pour qu'il soit possible ici de les assimiler à des séismes superficiels - on a la relation générale $i(nP,\Delta) = i(P,\Delta/n)$ si l'écorce peut être considérée homogène de même que le manteau: cette relation est dans l'hypothèse précédente applicable aux angles vrais et aux angles apparents. Sur la figure 5 nous avons représenté les divers angles d'incidence apparents en reportant les points représentatifs de l'onde nP, distance réelle d'observation Δ, à la distance Δ/n. La ligne en trait plein - angle d'incidence apparent de l'onde P en fonction de la distance - a été déduite du schéma de répartition de vitesse de Gutenberg-Richter (Richter 1958, appendice V) pour une écorce standard. Les variations de constitution de l'écorce d'une station à l'autre produisent des variations des angles d'incidence apparents observées. Malgré cela la concordance entre les points observés et la courbe calculée est bonne dans l'ensemble. Elle conduit à penser que l'interprétation des phases étudiées en tant que produites par des ondes PPP ou PPPP est plus vraisemblable que celle d'une onde canalisée. Aux distances comprises entre 3500 et 5000 km pour l'onde P, 7000 et 10000 km pour l'onde PP, etc.., il semble y avoir une différence systématique entre la théorie et l'expérience.

Amplitudes

Afin de pouvoir comparer les amplitudes des diverses ondes de volume étudiées, il était nécessaire d'éliminer au préalable les variations relatives de magnitude des séismes utilisés. Dans un premier calcul nous avons déterminé la moyenne des magnitudes données par les diverses stations en ne conservant que les valeurs concordantes, nous avons ainsi obtenu les chiffres de 6,6; 6,4; 7,3 et 6,9 pour les séismes 1, 2, 3, 4 respectivement. Mais en comparant les amplitudes, il est apparu que la dispersion des valeurs observées pouvait pour les séismes 1, 3 être fortement réduite si en supposant la magnitude de moyenne 6,9 exacte pour le séisme 4, on adoptait les magnitudes de 6,8 pour le séisme 1 et 7,2 pour le séisme 3. Le séisme 2 de magnitude notablement inférieure n'a pas été utilisé pour cette partie de travail. Sur la base de ces magnitudes corrigées homogènes, les amplitudes observées - ou plus exactement les quantités A/T - pour les séismes 1 et 3 ont été multipliées par les coefficients 1,25 et 0,40 respectivement pour ramener la magnitude réelle à celle du séisme de magnitude 3 soit 6,9.

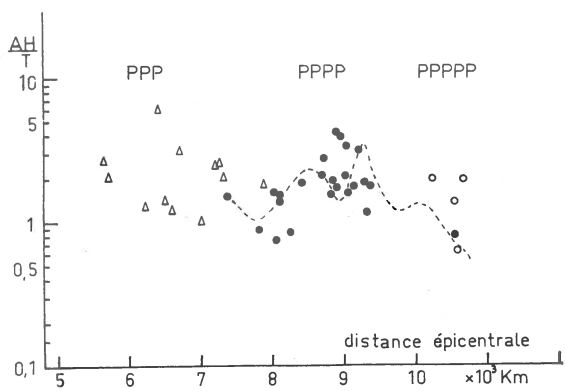

Figure 6. Rapport AH/T en fonction de la distance.

Sur la figure 6, nous avons reporté les valeurs A/T en admettant que les phases Pa étaient dues à des réflexions multiples. Nous nous attacherons spécialement aux phases

supposées PPPP. Elles sont identifiables entre des distances épicentrales de 8000 et 9500 kilomètres avec un maximum d'amplitude pour des distances voisines de 9000 kilomètres.

On sait que si la variation observée de l'amplitude des ondes superficielles en fonction de la distance épicentrale est en accord satisfaisant avec la théorie, il n'en est pas de même pour les ondes de volumes. Pour ces ondes, les variations de constitution du Manteau supérieur, introduisant des fluctuations dans les courbes log A/T pour les ondes telles que les P, PP, S, SS, Vanek (1959) et Vanek et Stelzner (1962) ont étudié en détail ces fluctuations. La courbe correspondant à P, composante horizontale, comprend deux maxima pour des distances de 2000 et 2500 km séparés par un minimum prononcé vers 2250 km. Pour l'onde PP, il existe dans les domaines des distances approximativement doubles des précédentes: deux maxima log A/T = 6,9 et 6,6 pour des distances de 4220 et 4700 km séparés par un minimum log A/T = 7,1 pour la distance de 4450 km. Ces variations sont attribuées à la structure de la discontinuité de 20°; la dissymétrie entre les ondes P et PP serait une conséquence des différences régionales de cette structure. Pour les ondes PPP et PPPP, une étude systématique me semble avoir été faite. Nous avons essayé de transposer la courbe de Vanek et Stelzner pour PPH à la distance double (Figure 6). Il est clair que cette transposition ne peut constituer qu'une approximation assez grossière en raison de la dissymétrie existant entre les courbes relatives à P et PP. Malgré cette restriction, on constate que la courbe établie ainsi répond assez bien aux observations. Il serait intéressant de compléter cette étude dans le domaine de distances comprises entre 9500 et 11000 kilomètres, domaine pour lequel nous n'avions qu'une seule donnée.

La présence d'un maximum net des amplitudes des phases étudiées pour une distance de l'ordre de 9000 kilomètres est inexplicable dans l'hypothèse d'une onde canalisée; par contre l'interprétation de ces phases en tant qu'ondes réfléchies multiples semble plus proche de la vérité.

Spectre

Les valeurs d'amplitudes lues sur les séismogrammes ont permis une analyse spectrale de diverses ondes P, PP, PPP, PPPP. Ces amplitudes, traduisant les phases inscrites en dehors des erreurs inévitables de pointés sur le coordinatographe, erreurs qui ne dépassent pas 0,2 mm - sont perturbées d'une part par le mouvement microséismique de période comprise entre 4 et 6 secondes et d'autre part par la réponse du séismographe.

Pour éliminer l'influence du séismographe il aurait été nécessaire d'opérer sur véritable déconvolution c'est-à-dire introduire dans le programme classique de calcul d'analyse spectrale, les constantes et les équations de l'ensemble séismographe-galvanomètre. Il n'a pas été possible de réaliser cette introduction; les résultats de l'analyse spectrale s'appliquent donc uniquement aux déplacements du spot de galvanomètre. (Nous tenonsà remercier vivement le

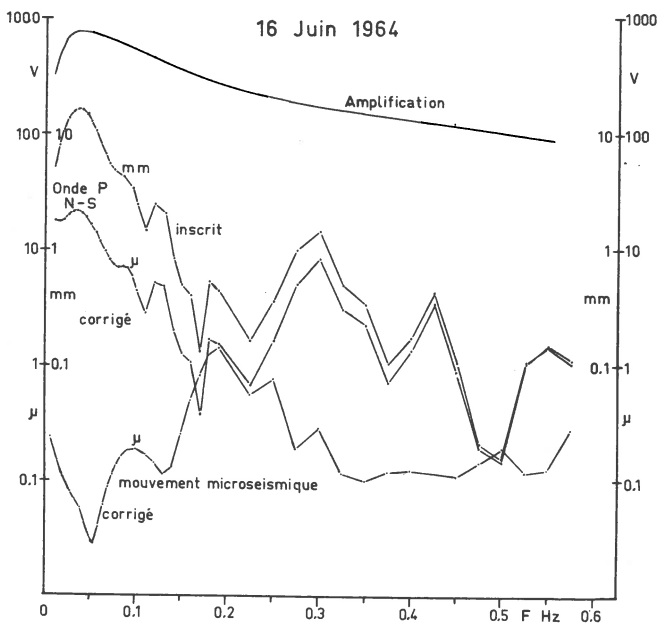

Figure 7. Analyse spectrale. Influence du mouvement microséismique et du séismographe.

personnel du laboratoire de Monsieur Jobert de l'Institut de Physique du Globe de Paris qui nous a permis le calcul de l'analyse spectrale sur la calculatrice UNIVAC 1107 de la Faculté des Sciences d'Orsay.) Nous avons tenté une correction de première approximation en supposant qu'il s'agissait d'ondes sinusoïdales entretenues et en divisant les amplitudes calculées par le grandissement du séismographe.

Les "mouvements du sol" ainsi calculés ne tiennent pas compte des réactions initiales. Sur la figure 7, nous avions représenté ainsi pour l'onde P la courbe de grandissement, la courbe d'analyse spectrale "inscrite" et la courbe corrigée qui s'en déduit, les échelles des amplitudes étant logarithmiques.

L'agitation microséismique est généralement faible à Strasbourg au cours des mois de mai et de juin, époque où ont eu lieu les 4 séismes étudiés. Néanmoins, nous avons tenu à vous rendre compte de son influence. Pour cela nous avons soumis les amplitudes de l'agitation microséismique du 16 juin 1964 pendant une durée de 3 minutes avant le début du séisme, à l'analyse spectrale. Les résultats de l'analyse ont été corrigées de l'influence de la réponse du séismographe.

L'agitation microséismique présente un maximum principal pour la fréquence 0,2 Hz soit pour une période de 5 secondes. Ce maximum se retrouve exactement sur l'onde P. Un deuxième maximum a lieu pour la fréquence 0,09 Hz soit pour la période de 11 secondes. Etant donné que l'amplitude pour cette fréquence est environ 10 fois plus faible que pour le maximum principal, cette fréquence plus élevée est absolument invisible directement. L'agitation microséismique de telle fréquence a été décrite par plusieurs auteurs, en particulier par J.Oliver. Dans le domaine des fréquences plus élevées supérieures à 0,3 Hz, il n'apparaît plus de maxima bien définis; il en résulte que certains maxima mis en évidence dans l'analyse des ondes longitudinales dans ce domaine de fréquence ne sont pas attribuables à l'agitation microséismique ni aux erreurs de pointés.

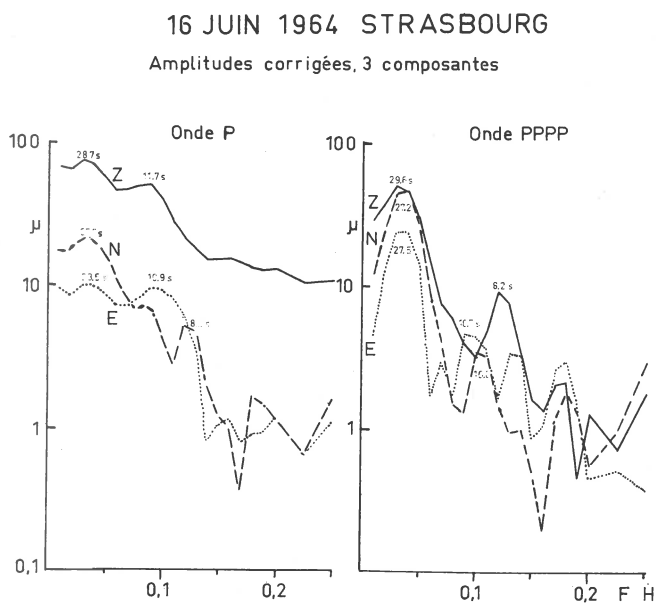

Figure 8. Analyse spectrale. Composantes horizontales et verticales des ondes P et PPPP.

L'analyse des trois composantes Z, N, E des ondes P et PPPP pour le séisme du 16 juin 1964 conduit aux résultats suivants (fig. 8).

Pour l'onde P, les spectres sont à peu près les mêmes pour la composante Z et les composantes N et E dans l'intervalle de fréquences 0,01-0,15 Hz, pour des fréquences supérieures a 0,15 Hz la composante verticale est nettement différente des composantes horizontales. Par contre pour l'onde PPPP, les 3 composantes restent semblables dans l'intervalle 0,01-0,25 Hz.

Pour les deux ondes, on trouve une superposition de deux fréquences principales, l'une de l'ordre de 0,036 Hz soit $\mathbb{T}$ = 28 secondes, l'autre pour une fréquence de l'ordre 0,1 Hz, soit pour une période de l'ordre de 10 s. Si la fréquence basse correspond bien à une composante N supérieure à la composante E et fournit un azimut en bon accord avec l'azimut réel de l'épicentre par rapport à Strasbourg soit 39°, on constate qu'aux fréquences supérieures à

environ 0,07 Hz les amplitudes sur la composante E sont systématiquement supérieures à celles notées sur la composante N, phénomène inexplicable, les constantes des deux composantes en particulier les périodes des séismographes et des galvanomètres étant pratiquement identiques. D'après l'examen direct des inscriptions, il se pourrait que le même phénomène se soit produit en d'autres stations en particulier à Stuttgart et à Addis-Abeba.

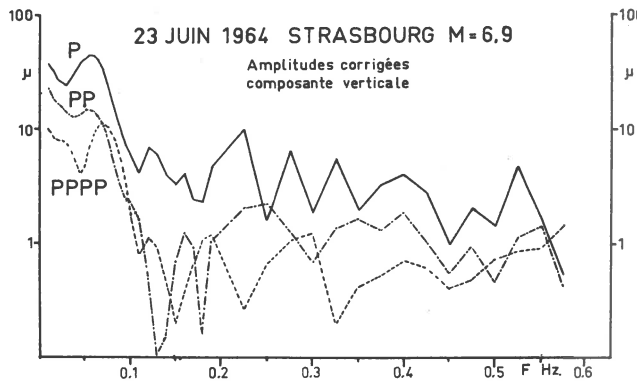

Figure 9. Analyse spectrale. Composante verticale ondes P, PP et PPPP.

Le gradient des amplitudes par rapport aux fréquences - $\partial \log A/\partial F$ - est notablement plus faible pour l'onde P que pour les ondes réfléchies PP, PPP, PPPP - figures 8 et 9. Le phénomène est absolument général et traduit l'absorption plus grande dans les parties supérieures du manteau - ondes réfléchies - que dans les couches plus profondes - ondes directes.

Périodes

Les périodes des ondes Pa ou PPPP étudiées dans ce travail sont grandes - comprises entre 15 et 30 secondes. Il y a une différence fondamentale entre ces ondes et les ondes Pa décrites par Båth et Lopez-Arroyo (1963). Pour ces auteurs la période nettement prédominante des ondes Pa est de 10 secondes avec un intervalle de périodes observées

compris entre 6 et 22 secondes. A l'heure actuelle le critère de période semble devoir permettre une distinction entre les ondes canalisées, les Pa et les ondes de type nP.

Conclusion

L'analyse d'ondes à trajet continental Eurasiatique, interprétées à l'origine comme ondes Pa telles qu'elles ont été décrites par Caloi, a montré que cette interprétation devait être abandonnée pour les séismes étudiés, au profit d'une explication en tant qu'ondes réfléchies multiples nP, en particulier en tant qu'ondes PPPP dans le domaine de distances de 8000 à 9800 kilomètres.

Bibliographie

Båth, M., (1957): Shadow Zone, Travel Times, and Energies of longitudinal seismic Waves in the Presence of an Asthenosphere Low-Velocity Layer, Trans.Amer.Geophys. Union, 38, 526-538.

Båth, M., Arroyo, A.L. (1963): Pa and Sa Waves and the Upper Mantle, Geofisica Pura e Applicata, Milano, 56, 67-92.

Caloi, P., (1954): L'Astenosfera come Canale-Guida dell' Energia Sismica, Annali di Geofisica, 7, 491-501.

Caloi, P., (1965): On the Canalization of seismic energy, Annali di Geofisica, 17, 513-522.

Dorman, J., Ewing, M., Oliver, J. (1960): Study of Shear-Velocity. Distribution in the Upper Mantle by Mantle Rayleigh Waves, B.S.S.A., 50, 87-115.

Guidroz, R.R., Baker, R.G. (1963): Channel Waves in World-Wide Collection and Evaluation of Earthquake Data. Report No.IV, Texas Instruments Inc., Dallas.

Magnitsky, V.A., Khoroshewa, V.V. (1961): The Waveguide in the Mantle of the Earth and its probable physical Nature. Annali di Geofisica, 14, 87-94.

Richter, C.F., (1958): Elementary Seismology, W.H.Freeman and Company, San Francisco.

Vanek, J. (1959): Die Amplituden von PP und SS-Wellen in der Nähe von 40° und die Struktur des äusseren Erdmantels. Annali di Geofisica 12, 2, 239-248.

Vanek, J., Stelzner, J. (1962): Amplitudenkurven der seismischen Raumwellen. Gerl.Beit.Geoph. 71, 2, 105-119.

B.Mohammadioun

STRUCTURE DU MANTEAU TERRESTRE D'APRES LES SPECTRES D'ENERGIE DES ONDES DE VOLUME LONGITUDINALES

Introduction

La plupart des résultats publiés sur l'énergie des ondes séismiques ont été déduits de mesures de périodes apparentes et d'amplitudes effectuées directement sur les séismogrammes. Une grande part d'arbitraire intervient dans ces mesures. Je me suis proposé d'obtenir des informations, d'une part, sur le phénomène à la source, d'autre part, sur les propriétés élastiques des milieux environnant le foyer ou traversés par les ondes séismiques; cela, en substituant aux mesures conventionnelles de périodes et d'amplitudes une définition précise du signal par son spectre d'énergie.

Afin d'obtenir une bonne définition du spectre d'énergie, il était indispensable de disposer de séismographes ayant une amplification suffisante dans une large bande de fréquence, ce qui a été réalisé au moyen d'un dispositif spécial comprenant un ensemble de huit séismographes verticaux dont les amplifications maximales s'échelonnaient entre 0,1 s et 10 s, et qui a fonctionné pendant quatre ans, de 1962 à 1965, au Centre de Recherches géophysiques de Garchy, sous le contrôle de M.Baltenberger.

205 spectres d'énergie ont été obtenus par transformation de Fourier au moyen d'ordinateurs électroniques.

Les séismes ont été séparés pour l'interprétation, en séismes normaux ($h < 60$ km) et en séismes profonds ($60 < h < 700$ km). Dans chaque catégorie, ils ont été classés par ordre de distance croissante.

L'effet de l'appareillage sur le signal séismique ayant été éliminé, le spectre d'énergie à la station dépend du spectre à l'origine et de l'effet du milieu traversé par l'onde au cours de la propagation.

La répartition spectrale de l'énergie à la source a été étudiée en fonction de l'énergie du séisme et en fonction de la profondeur du foyer.

Energie

Pour étudier l'effet de l'énergie du séisme, j'ai comparé le spectre des ondes P d'un séisme principal à celui d'une réplique ou d'un prémonitoire (Fig. 1). Ainsi la distance et la profondeur de foyer restent pratiquement invariables.

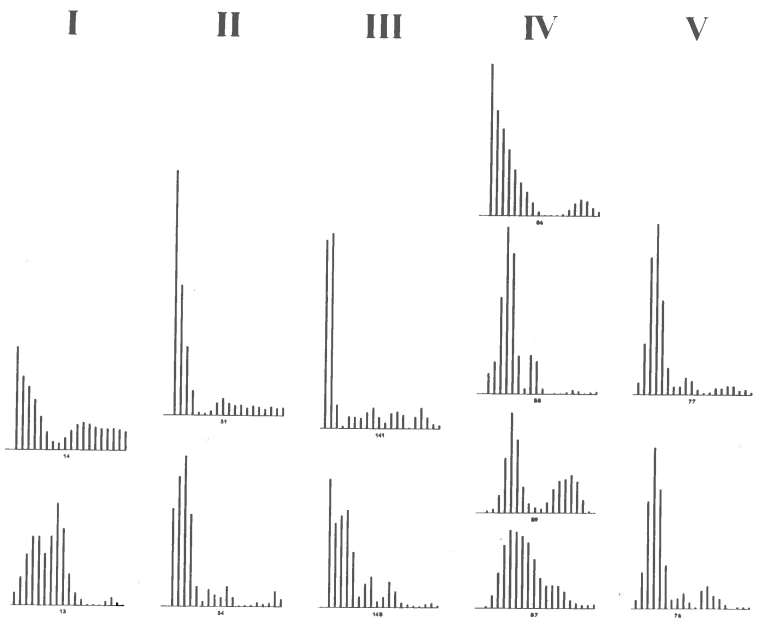

Figure 1

Le déplacement du maximum d'énergie vers les basses fréquences apparaît clairement dans le spectre d'un séisme principal d'Anatolie par rapport au prémonitoire (colonne I). Pour deux séismes d'énergie très différentes (le grand séisme d'Alaska du 28 mars 1964, de magnitude 8 1/2 et une de ses répliques de magnitude 5 1/2), le spectre du séisme principal se réduit à une étroite bande de basse fréquence (colonne II).

Le déplacement du maximum est également manifeste dans les spectres de la colonne III; mais on doit remarquer que, dans ce dernier cas, les valeurs publiées pour la magnitude n'indiquaient pas la grande différence d'énergie qui existe en réalité entre ces séismes et qui explique le changement d'aspect du spectre.

La même remarque s'applique aux quatre séismes des îles Kouriles (colonne IV): le premier de ces séismes, dont l'énergie est nettement plus grande que celle des trois autres, a seul un maximum de basse fréquence.

La répartition spectrale de l'énergie apporte donc, sur la valeur de l'énergie à la source, des données beaucoup plus précises que la magnitude.

Enfin, à titre de comparaison, on a représenté, dans la dernière colonne V, les spectres de deux séismes de faible énergie pour lesquels la distance est la même 8.850 km, ainsi que la profondeur de foyer 25-32 km. On vérifie que dans ces conditions les spectres sont bien comparables.

Structure de la croûte terrestre

Une étude détaillée a pu être faite sur quinze répliques du grand séisme du 28 mars 1964 en Alaska: les foyers de ces répliques sont répartis en deux groupes, l'un au nord au voisinage de la Baie du Prince Guillaume, l'autre au sud de l'île Kodiak.

Les profondeurs de foyer des séismes étudiés ont été comparées à la structure de la croûte terrestre, d'après les résultats obtenus par G.G.Shor, au moyen de la réfraction séismique en mer. On disposait en particulier de trois profils le long de la fosse Aléoutienne et d'autres profils au-dessus du plateau continental, des collines abyssales et de la plaine abyssale, ainsi que près du talus continental, à proximité du détroit de Dixon.

La position des foyers, ainsi que celles des profils de réfraction, ont été définies par leur distance à la ligne bathymétrique -1 km mesurée normalement aux fosses (Fig. 2). En ordonnées, sont portées, les profondeurs des foyers et celles de la discontinuité de Mohorovičić en kilomètres au-dessous du niveau de la mer.

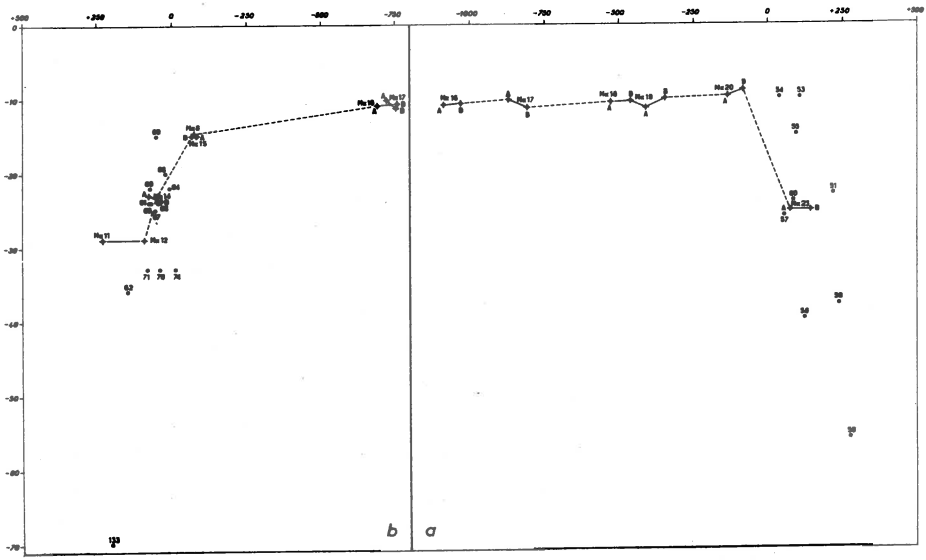

Figure 2

On constate que les foyers voisins de l'île Kodiak s'alignent dans une bande comprise entre la structure continentale et la structure océanique et plongeant sous le continent. Les autres se trouvent décalés par rapport aux précédents vers l'intérieur du continent. Ce décalage s'explique par le fait que la distance séparant la fosse Aléoutienne de la chaîne Aléoutienne, puis de la chaîne de l'Alaska augmente progressivement du sud vers le nord.

Les spectres d'énergie (fig. 3) se classent en quatre groupes correspondant, à l'intérieur de cette bande, à des alignements sensiblement parallèles:

1: Les spectres de la colonne I caractérisant les séismes dont les foyers sont situés dans la croûte continentale; ils se présentent sous forme d'une bande étroite dans les basses fréquences, avec un déplacement du maximum vers les hautes fréquences dans le séisme le moins profond.

2: Dans la colonne II, une série de six spectres doubles, avec des maximums bien séparés. L'alignement des foyers correspondants définit la limite entre la structure continentale et la structure océanique.

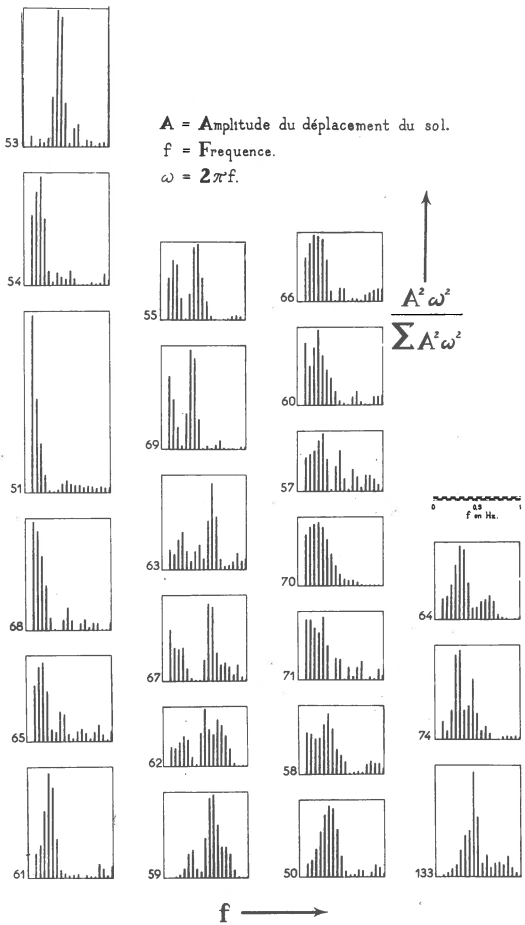

Figure 3

3 et 4: Dix spectres caractérisant les séismes du manteau supérieur: ils comportent une large bande dont le maximum se situe à des fréquences plus basses pour les séismes de la colonne III, que pour ceux de la colonne IV. On remarque le déplacement de ce maximum vers les hautes fréquences quand la profondeur augmente.

Structure du manteau

I. Spectres des séismes profonds en fonction de la profondeur

Phase P. - Le même déplacement du maximum vers les hautes fréquences est visible dans les spectres des séismes profonds issus de Méditerranée orientale, des Kouriles, du Japon et d'Amérique latine (fig. 4).

Dans la colonne I les spectres de trois séismes profonds de la Méditerranée orientale montrent le déplacement du maximum vers les hautes fréquences quand la profondeur augmente de 70 à 100 km et le décalage très net, vers les basses fréquences, du spectre relatif à un foyer situé à 160 km de profondeur.

Dans la colonne II, le foyer de l'Hindou-Kouch, situé vers 200 km, correspond également à un spectre de basse fréquence.

Les spectres des colonnes III et IV correspondant à des distances épicentrales de 9.000 ou 10.000 km, sont, dans l'ensemble, de plus basse fréquence que les précédents, ce qui résulte, comme on le verra plus loin, de l'absorption au cours de la propagation dans la partie inférieure du Manteau; mais les mêmes variations apparaissent dans ces spectres en fonction de la profondeur du foyer.

Dans les spectres des séismes des îles Kouriles, dans la colonne III, on remarque jusqu'à 101 km, le déplacement du maximum vers les hautes fréquences. A 136 km, un dédoublement du spectre, tandis qu'aux plus grandes profondeurs, 140 et 160 km, le maximum est déplacé vers les basses fréquences. Au-dessous de la couche à faible vitesse, ce maximum se trouve de nouveau dans les fréquences élevées.

Les foyers du Japon et d'Amérique latine se trouvant dans le même intervalle de distances, leurs spectres ont été réunis dans la colonne IV. On y observe notamment l'étalement progressif vers les hautes fréquences quand la profondeur augmente jusqu'à 125 km, tandis qu'à 140 km, les hautes fréquences ont disparu.

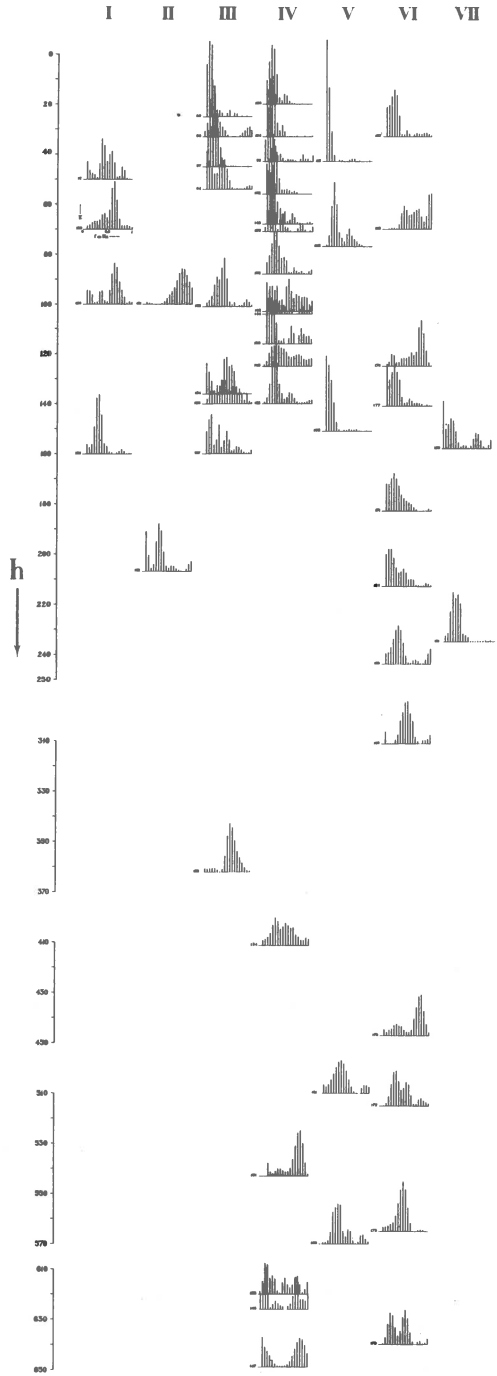

Figure 4

A grande profondeur, on observe un spectre étalé à 400 km, un déplacement du maximum vers les hautes fréquences à 550 km, puis le dédoublement des 3 derniers spectres, vers 650 km.

Phase PKIKP. - Les séismes de la zone sud-ouest du Pacifique se prêtent particulièrement bien à l'étude des spectres de la phase PKIKP en fonction de la profondeur de foyer, les distances restant comprises dans un intervalle étroit, de 16.000 à 17.200 km, alors que les profondeurs de foyer s'échelonnent entre la profondeur normale et 650 km.

Les foyers les moins profonds se groupent, à l'ouest, le long de la fosse des Nouvelles Hébrides, à l'est, le long de la fosse de Kermadec-Tonga, encadrant les foyers plus profonds des Nouvelles Hébrides et des îles Fidji.

On retrouve, dans les spectres des séismes des Nouvelles Hébrides et des Fidji (colonne VI de la fig.4) le déplacement vers les hautes fréquences jusqu'à 120 km. Les trois spectres suivants, entre 140 et 220 km sont au contraire caractérisés par une bande d'énergie de basse fréquence.

A plus grande profondeur, les foyers séismiques sont peu nombreux; les quelques spectres d'ondes PKIKP qui ont pu être étudiés montrent un déplacement du maximum d'énergie vers les hautes fréquences de 240 à 450 km, puis en sens inverse à 565 km. A une profondeur de 640 km apparaît un spectre double.

La couche à basse fréquence du Manteau supérieur s'observe également dans les séismes des îles Tonga et Kermadec, colonne VII, et dans ceux des îles Santa Cruz, colonne V. Les spectres de basses fréquences observés entre 140 et 240 km caractérisent manifestement les foyers situés dans la couche à faible vitesse.

Les résultats précédents sont réunis dans les graphiques représentant, en fonction de la profondeur du foyer, la fréquence qui correspond au maximum d'énergie de chacun des spectres (fig. 5).

On voit que la limite supérieure de la couche à faible vitesse est bien marquée dans tous les graphiques par la

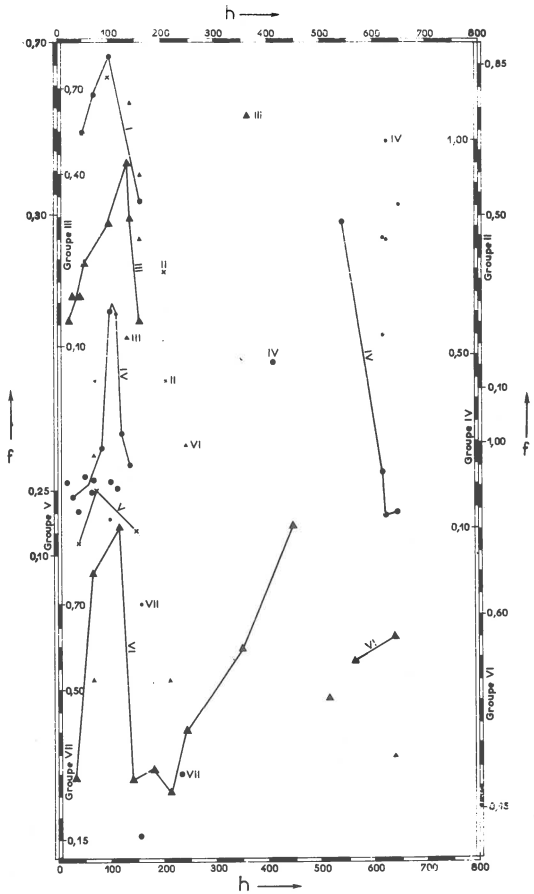

Figure 5

baisse rapide de fréquence qui permet de lui assigner une profondeur moyenne comprise entre 120 et 140 km. Sa limite inférieure n'est mise en évidence que dans le cas des séismes des Fidji, Nouvelles Hébrides, Tonga, à une profondeur comprise entre 215 et 235 km.

La deuxième couche caractérisée par des spectres de basse fréquence apparaît dans le cas des séismes de l'Amérique latine et des îles Fidji. On peut assigner à la limite supérieure de cette couche une profondeur comprise entre 540 et 620 km.

II. Spectres des séismes normaux en fonction de la distance

Phase P. - On constate d'abord que les déplacements du maximum d'énergie qui ont été mis en évidence quand la profondeur du foyer varie se retrouvent lorsqu'on considère les spectres de séismes normaux en fonction de la distance, mais le phénomène est, d'une manière générale, atténué et plus progressif (fig. 6, colonne I et II).

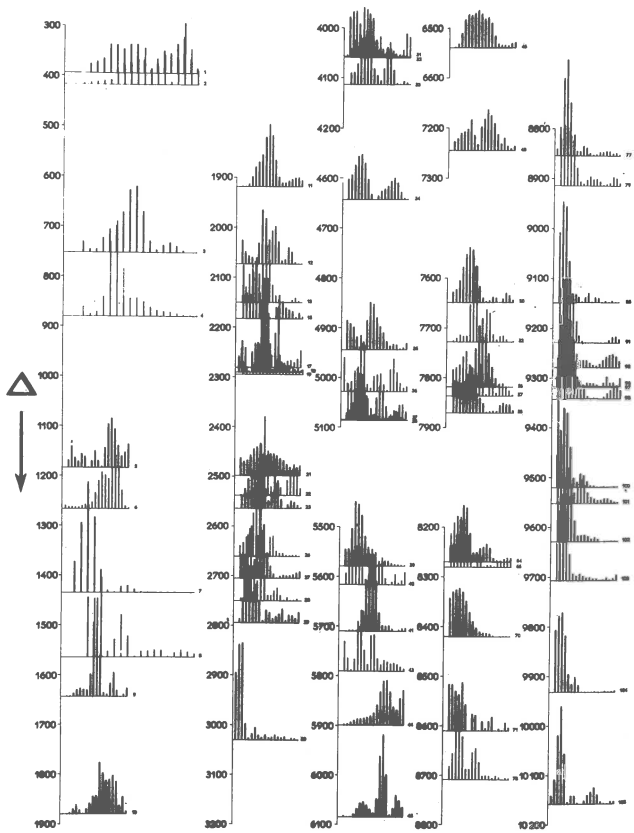

Figure 6

On obtient en outre des informations sur le Manteau inférieur:

Dans les colonnes III et IV, les seize spectres de 4.000 à 7.000 km, montrent des bandes étalées, tandis que la fréquence du maximum d'énergie se déplace graduellement vers les fréquences élevées; au-delà, l'énergie se concentre dans une bande plus étroite, en même temps que le maximum se déplace rapidement vers les basses fréquences. Entre 8.800 et 10.000 km (colonne V), les spectres présentent une bande étroite dans les basses fréquences.

Les déplacements du maximum d'énergie quand la distance augmente correspondent à la pénétration progressive de la partie inférieure de la trajectoire dans une nouvelle couche ayant des propriétés absorbantes différentes. En vue de situer les limites des couches ainsi mises en évidence, on a tracé le graphique qui montre comment varient, en fonction de la profondeur du point le plus bas de la trajectoire, la largeur des spectres et la fréquence correspondant au maximum d'énergie (fig. 7).

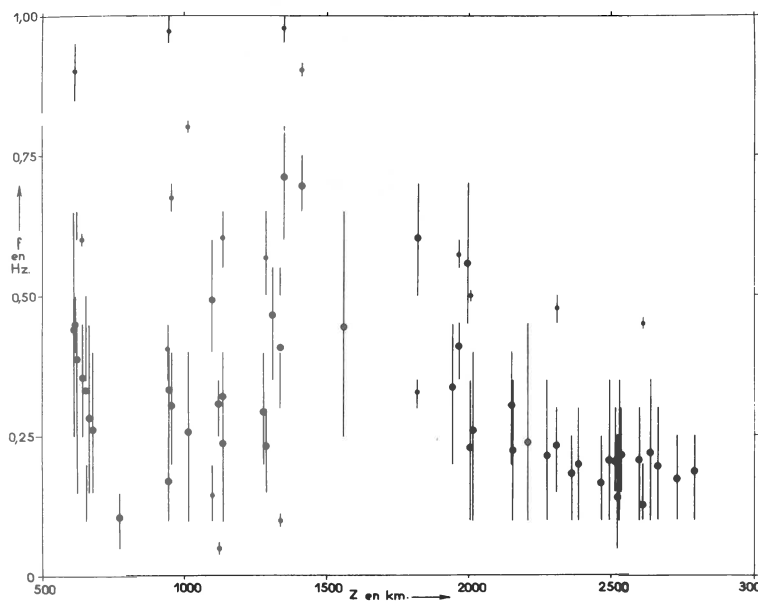

Figure 7

Les deux couches caractérisées par des spectres de basses fréquences y apparaissent dans le Manteau inférieur: la première se situe entre 650 et 950 km, d'après les déplacements en sens contraires du maximum d'énergie de part et d'autre de ces limites. La limite supérieure avait été située entre 540 et 620 km d'après les séismes profonds.

La deuxième couche se manifeste à une profondeur d'environ 2.000 km; son existence est démontrée par de nombreuses observations.

Conclusion

L'ensemble des résultats déduits des spectres d'énergie permet de représenter schématiquement la structure de la Terre (fig. 8). On a représenté schématiquement, dans la partie inférieure de la figure, le graphique des fréquences correspondant au maximum d'énergie.

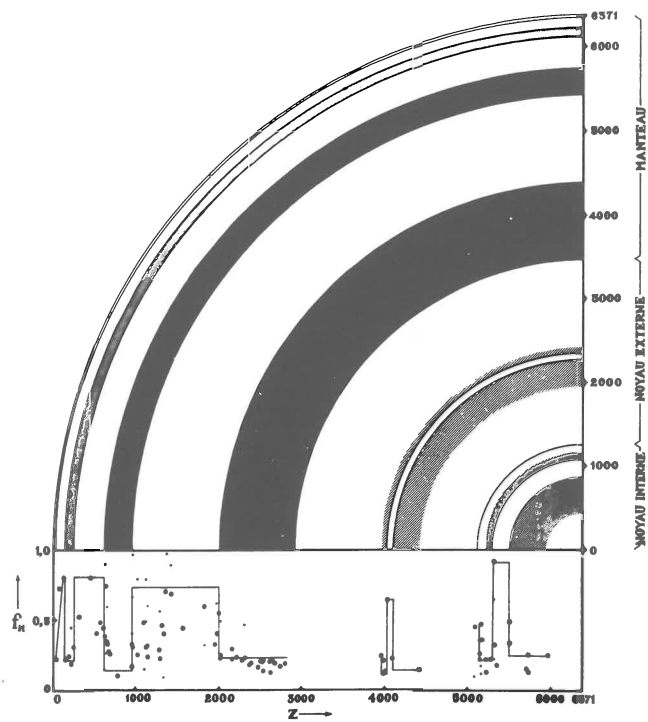

Figure 8

A partir des spectres des ondes longitudinales en fonction de la distance, un calcul simple a été tenté pour trouver les valeurs du coefficient d'atténuation γ et du facteur de qualité $Q = \frac{\omega}{2\alpha\gamma}$ (ω : pulsation; α : vitesse des ondes longitudinales) dans les trois couches de basse fréquence du Manteau M_2, M_4 et M_6.

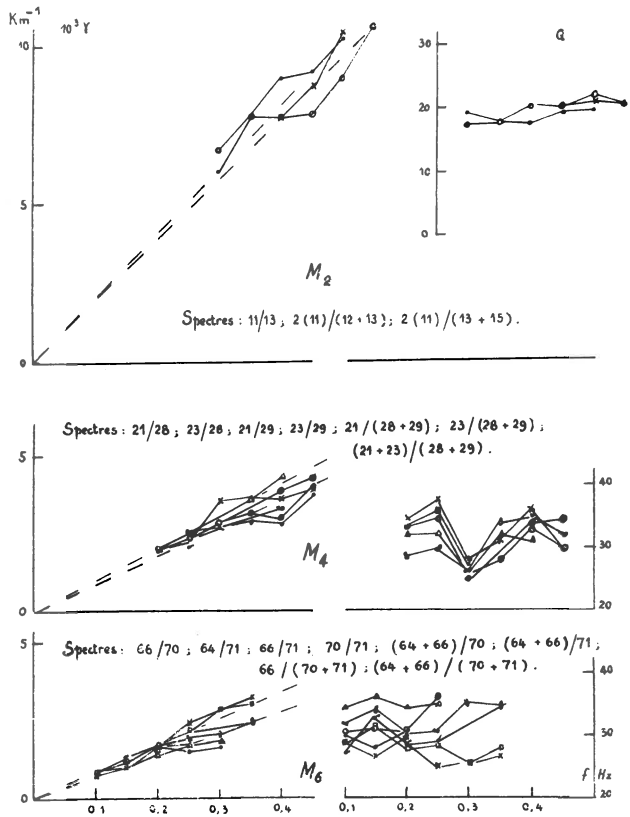

Figure 9

La figure 9 représente les valeurs de γ et de Q, en fonction de la fréquence f. On voit que la valeur de Q y est sensiblement indépendante de la fréquence dans chaque intervalle d'observations. Les valeurs moyennes sont respectivement de 20, 30 et 30, correspondant à des fréquences moyennes de 0,4, 0,3 et 0,2 Hz.

Gonzalo Payo

CRUSTAL STRUCTURE OF THE MEDITERRANEAN SEA BY SURFACE WAVES. PART I - GROUP VELOCITY

Abstract

The purpose of the paper is to obtain a first idea of the Crust-Mantle structure of the Mediterranean Regions, using only group velocity data.

Earthquakes whose seismic paths cross totally or partially the Mediterranean Sea have been used. Fortyeight earthquakes have been selected and their corresponding Rayleigh and Love group velocity dispersion curves were calculated. Most of the records belong to the Standard Seismological Stations installed in the borders of the Mediterranean Sea.

The Rayleigh and Love wave dispersion curves obtained have been classified in four different groups which show the same dispersive character. There is a correlation of such classification with the oceanic percentage and geographic region crossed by the paths, i.e., obviously, with the corresponding type of crustal structure.

Crust-Mantle theoretical models have been computed for both Rayleigh and Love waves. The dispersion curves of these models fit acceptably into an average of the data of each group. They show a remarkable difference between the Eastern and Western Mediterranean crust, which is considered as one of the main results of this investigation. The crust to the South of the Ionian and Aegean Seas shows somewhat smaller velocities and larger thicknesses, for the uppermost crustal layers, than that of the Western Mediterranean, which seems to be of a more oceanic character.

The full text has been printed in Bull.Seism.Soc.Am. vol.57, p.151-172. (1967). (Editor's note).

ESC. COPENHAGEN. 1966

B.Papazachos, N.Mandalos and M.Polatou

DISPERSION OF SURFACE WAVES RECORDED IN ATHENS

Group and phase velocities of fundamental mode Rayleigh and Love waves along paths in the southeastern Europe and Asia Minor have been computed. These data are compared with a three-layered model of the crust in this region found previously by using travel times of body waves.

The mean crustal thickness along two paths of Love waves from Austria and north Jugoslavia to Athens was found equal to 35 km. A thickness equal to 40-45 km along two paths from Ligurian Sea and Algeria to Athens was found from study of Rayleighs waves. Study of dispersion of Love waves along three paths from central, eastern and northeastern Turkey gave crustal thicknesses 35 km, 35 km and 40 km, respectively.

Group velocities have been found along thirtyfive paths from several places of the world to Athens. These data were compared with the standard Press's curves to estimate the mean crustal thickness along each path. The mean crustal thickness was correlated with the elevation along each path.

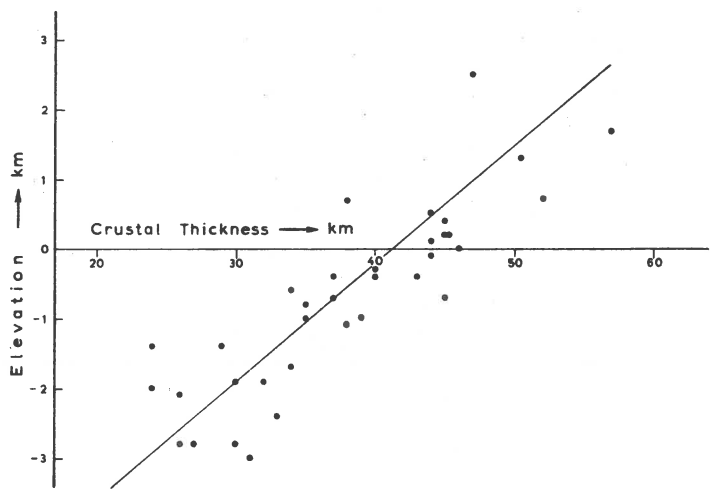

Fig. 1

The mean elevation along each path is plotted against the mean crustal thickness of the same path in Fig. 1. We see that this relation is almost linear although the scattering is large. For zero elevation the crustal thickness is a little more than 40 km. It is known however that the normal crustal thickness is about 35 km. This difference is attributed to systematic errors which shifted the curve to the right.

Assuming that the normal crustal thickness is 35 km (the crustal thickness for elevation equal to zero) the relation:

$$h = -6.0 + 0.17\,H \qquad (1)$$

was found between the mean elevation h of a large region and the mean crustal thickness H of this region. This equation is in agreement with Airy's isostatic hypothesis if the ratio of the density just below the crust to the mean crustal density is 1.20. We used formula (1) to calculate the crustal thickness for h = 2, 3, 4, 6, and -5 km. This model is shown in Fig. 2.

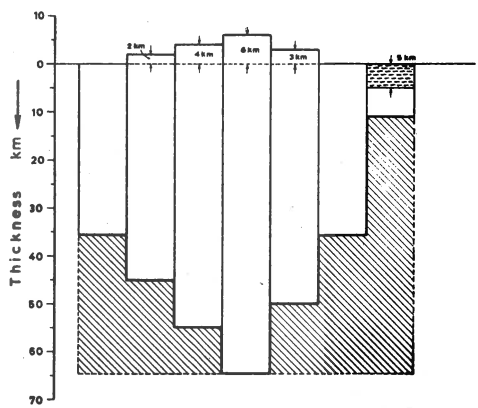

Fig. 2

I.Noponen, M.T.Porkka, S.Pirhonen and U.Luosto

THE CRUST AND MANTLE IN FINLAND

Abstract

The structure of the crust and upper mantle in Finland has been studied by utilizing results of surface wave phase and group velocity determinations and of explosion seismic refraction measurements. The dispersion curves for a set of theoretical models have been calculated by the Thomson-Haskell matrix method. The earth-stretching transformations of Anderson and Toksöz were used in the calculation of Love wave dispersion.

Introduction

The velocities of surface waves reflect the properties of the outer layers of the earth. The calculation of a corresponding layer model, however, requires auxiliary information on which the model may be based or a limitation of the number of layers and permissible ranges of velocity of body waves.

In this study the inversion of observed surface wave velocities is based on a crustal model calculated from an explosion seismic refraction study. A tentative search for the best-fitting two-layer model of the crust has also been made.

The refraction study

The refraction line AA can be seen in the insert in figure 1. The explosions were located in the Bothnian Bay, and the 7 recording stations used were all on land. Records of 49 explosions were used. After the impulses had been identified from the records, the travel time curves, which were assumed to be straight lines, were calculated by the method of least squares. Consequently, homogeneous layers with horizontal interfaces were assumed. Four different compressional wave velocities were found; the model calculated from the data is shown in table 1. The table also

includes S-wave velocities, which were derived from the P-wave velocities on the assumption that the Poisson constant is 0.250.

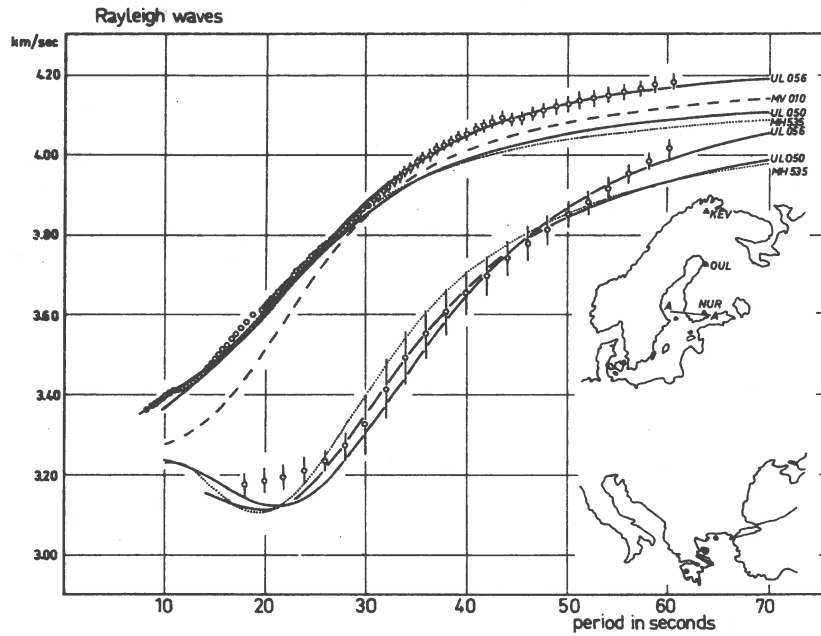

Fig. 1: The circles mark the observed Rayleigh wave velocities, vertical lines showing the mean standard deviations; the curves show dispersions of some layer models. Model MV 010 has one layer with a compressional wave velocity of 6.1 km/s, underlain by a mantle with a corresponding velocity of 8.1 km/sec. Insert shows the refraction line AA and the stations used in the surface wave velocity measurements. Epicentra in Greece of the earthquakes used are denoted by black circles.

Table 1

Crustal model UL 050 for Finland

layer	layer depth	P-wave velocity	S-wave velocity	
1	12.2 km	6.07 km/s	3.51 km/s	
2	30.2	6.51	3.76	Poisson's constant assumed to be 0.250
3	42.0	6.64	3.83	
		8.03	4.64	

Observations of the P-wave through the uppermost layer and P_n-wave both include more than 80 readings, observations of impulses connected with other layers being slightly less numerous. If we assume a crustal model consisting of only one layer, in which the compressional wave velocity is that found for the uppermost layer, and underlain by a mantle with the P_n velocity observed, the intercept times give a thickness of 37 kilometres for the crust. This is the smallest possible thickness of crust on line AA according to these data, regardless of the crustal substructure.

This refraction line is not inverted and its results are limited to south-western Finland. However, of all the models from refraction studies for which we have calculated surface wave velocities, this gives the best fit to observed dispersion in Finland. For a fuller discussion of this deep seismic sounding, see Luosto (1967).

Experimental surface wave velocities

Surface wave velocities were measured on a path across Finland from the WWSSN station Nurmijärvi (NUR) in the south to the similar station Kevo (KEV) in the north. They are shown as circles in figures 1 and 2. Greek earthquakes were used, because they were almost on the great circle through the stations and the path from Greece to Finland is entirely continental, so that lateral refractions are minimized. In the insert in figure 1, the locations of the stations NUR, OUL (Oulu), and KEV and the epicentres of the earthquakes used in the study are shown.

Rayleigh and Love wave phase velocities have been calculated by the Fourier analysis method from the digitized recordings. Group velocities have been calculated by fitting a polynomial to the arrival times of peaks and troughs of the surface wave groups and evaluating group velocities from it. Velocities between two stations are then calculated from differences of velocities observed at the stations. Thus, these two methods are based on different principles, one working in the frequency domain and the other in the time domain. Measuring the phase and group veloci-

ties separately has the usual advantages of independent measurements of an experimental function and its derivative.

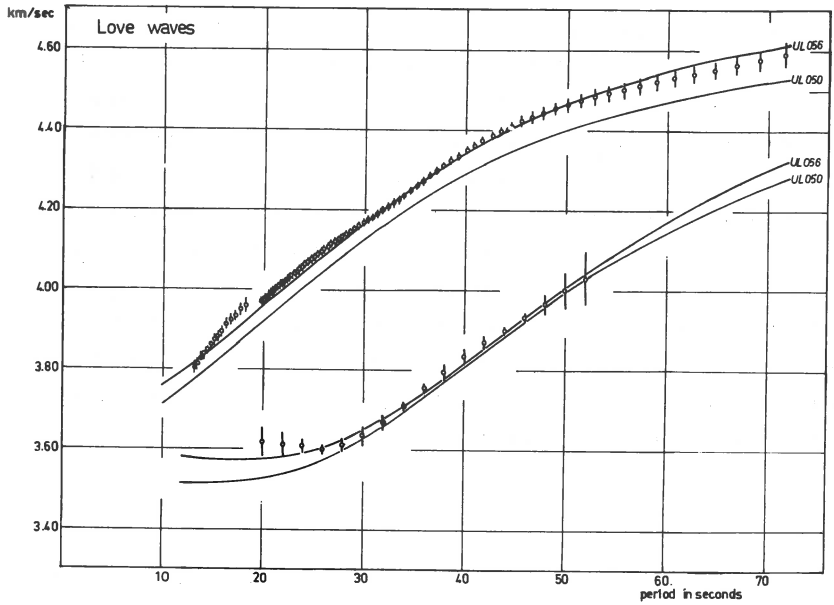

Fig. 2: Love wave velocities

For more detailed discussions of experimental determination of surface wave velocities in Finland, see Luosto (1965), Noponen (1966) and Pirhonen (1967).

Selection of a fitting layer model

Surface wave velocities of layer models have been calculated by the Thomson-Haskell matrix method. Rayleigh wave velocities have not been corrected for the earth's curvature: such a measure was considered unnecessary for these data with periods of less than 60 seconds. Curvature correction for the Love waves was calculated with Anderson and Toksöz's earth-stretching transformations (Anderson, 1965).

Before the refraction results used in this study were available, experiments were made to compare the observed surface wave velocities with combinations of several crust

and mantle layer models published for different areas, including the 33-km-thick average crustal model for Finland from early refraction and near earthquake studies (Vesanen et al., 1962). None of these gave a satisfying fit to observed data.

Experiments were also made, starting from a crustal model consisting of two 20-km-thick layers, in which the elastic parameters were varied. A suitable model could not be found simply by selecting the velocities appropriately, which also indicated that a one-layer model cannot satisfy the observed data. When the relative and absolute thicknesses of the two layers were also varied, a relatively good fit was achieved with upper and lower layer thicknesses of 10 and 26 km, respectively. The resulting model is called MH 535 and its shear velocities are shown in figure 4. In figure 1 Rayleigh wave velocities calculated from it are compared with the observed velocities.

The crustal model UL 050, which is shown in table 1, was found to give surface wave velocities rather similar to those observed. In calculating the velocities, the necessary density values of the layers were selected to be those currently accepted as most probable. Their effect on the surface wave velocities is smaller than on the body wave velocities. The calculated and observed velocities of surface waves are shown in figures 1 and 2. As can be seen, some modifications of the model were necessary to achieve a closer fit. They were based on the observed phase velocities and resulted in a better fit to the observed group velocities as well. It was found that a velocity increase in the mantle at the depth of 70 km increased the surface wave velocities by an amount sufficient to bring them within the mean standard deviation of the velocities observed in the long-period part of the spectrum.

At short periods the surface wave velocities of the model UL 050 are also too low, the deviation from the observed data being larger for Love than for Rayleigh waves. Because we did not want to change the rather accurately determined compressional wave velocities of the upper layers of the model and because a larger increase would be achieved for

Love than for Rayleigh waves, Poisson's constant was given a value smaller than 0.250, so that higher shear velocities were obtained for the upper layers. The ratios of the body wave velocities measured from near quakes in Finland suggest that Poisson's constant is, in fact, smaller than 0.250 for the upper layers (figure 3). It is interesting to note that a change of the ratio of body wave velocities in the mantle at some depth to the direction suggested by figure 3 would result in a slightly closer fit of velocities of long-period Love waves.

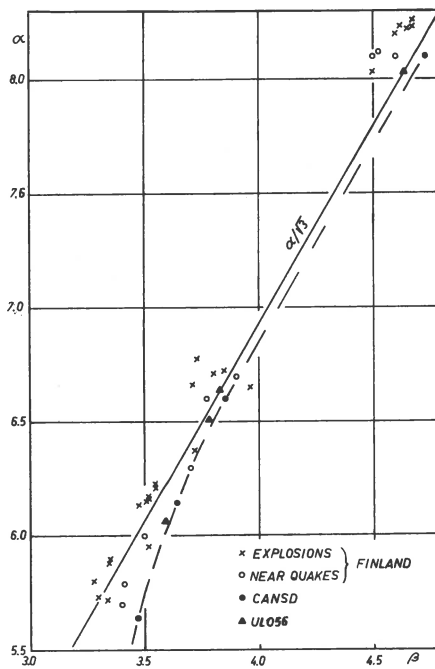

Fig. 3: Ratios of the observed P and S velocities in Finland. The line corresponds to the value 0.25 of Poisson's constant. Black circles correspond to those accepted for the model CANSD (Brune and Dorman, 1963), black triangles to those accepted in this study.

The layer model of the crust and upper mantle after these modifications is called UL 056 and is shown in figure 4 and

table 2. The surface wave velocities calculated from this model are shown in figures 1 and 2.

Table 2

Layer model UL 056 for Finland

layer	layer depth	P-wave velocity	S-wave velocity	Poisson's ratio
1	12.2 km	6.07 km/s	3.59 km/s	0.231
2	30.2	6.51	3.78	0.246
3	42.0	6.64	3.83	0.250
4	70.0	8.03	4.64	0.250
		8.30	4.79	0.250

The uppermost layer from the surface to a depth of 2 or 3 kilometres with compressional wave velocity less than 6.0 km/s (Pentillä, 1965) could not be defined with the data used in this study. However, its presence was suggested by the non-zero intercept time of the travel time line corresponding to the uppermost layer in the present study.

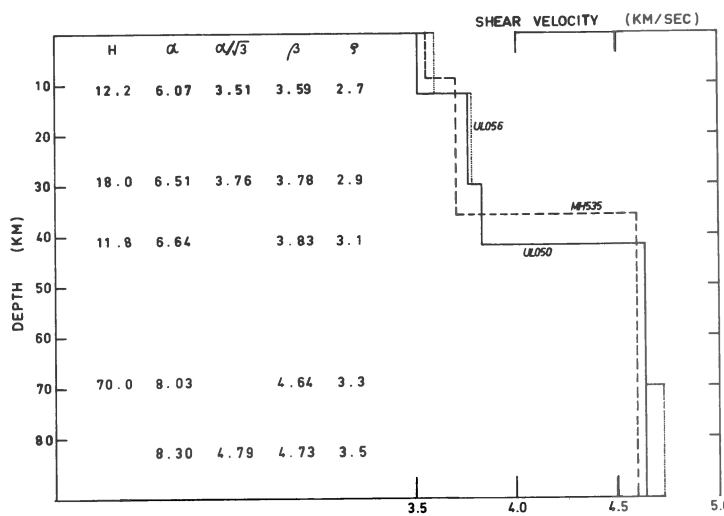

Fig. 4: Properties of the final model UL 056 (dotted line and parametres), model UL 050 from the refraction study and the two-layer model MH 535. Note the similarity between this and UL 050.

These results should not be interpreted to show the existense of a first degree discontinuity at the depth of 70 km or at any depth in the upper mantle. However, the authors believe that in the uppermost 100 kilometres of the mantle an increase of body wave velocities with depth from the value 8.03 km/sec immediately below the Moho is necessary according to these data. Even if we were to consider the velocity of 8.03 km/sec determined in the refraction study to be local, we cannot find any single velocity for the mantle which would alone give a good fit to the observed long-period surface wave data, assuming a crustal structure of this type.

Conclusions

The whole area of Finland is situated on the Baltic shield, comprising a large part of it. Hence, the results given here should apply to the shield area. The assumed uniformity of structure on shields gives significance to the surface wave dispersion results. This is further confirmed by comparing Rayleigh wave phase velocities on paths NUR - OUL in southern and OUL - KEV in northern Finland, which were found to be equal within the available period range of 10-40 seconds.

In this paper the authors present a layer model for the crust and upper mantle in Finland. It has three layers in the crust. The upper discontinuity in the crust might be associated with the Conrad discontinuity and has a depth of 12.2 kilometres, the total crust thickness being 42 km. There is evidence suggesting that Poisson's constant is smaller than 0.25 in the upper part of the crust and near the value found by Yoshiyama (1957) for Japan. In general, the body wave velocities in the crust are high, the compressional wave velocity having the average value of 6.42 km/sec.

The compressional wave velocity below the Moho is 8.03 km/sec. The mantle exhibits an increase of velocity with depth to a depth of at least 100 km. The nature of this velocity increase is uncertain, but it does have approximately the same numerical effect on the surface wave velo-

cities as an abrupt velocity increase from 8.03 to 8.30 km/sec at the depth of 70 km. It has not been necessary to include a low-velocity layer in the upper mantle in the model. If such a layer exists it must be less pronounced than in some other regions, for example in the Canadian shield model CANSD.

References

Anderson, D. (1965). Recent evidence concerning the structure and composition of the earth's mantle. Physics and Chemistry of the Earth, Vol.6, Pergamon Press, London.

Brune, J. and J.Dorman (1963). Seismic waves and earth structure in the Canadian shield. Bull.Seism.Soc.Am., 53: 167-210.

Luosto, U. (1965). Phase velocities of Rayleigh waves in southern Fennoscandia. Geophysica, Vol.9, No.2.

Luosto, U. (1967). Preliminary results of a seismic refraction study of the earth's crust in S.W.Finland. Inst. of Seism., Univ. of Helsinki, Publ.82.

Noponen, I. (1966). Surface wave phase velocities in Finland. Bull.Seism.Soc.Am., 56, No.5.

Penttilä, E. (1966). Wave velocities and earth's crust in Finland. Progress Report, Seismology and physics of the earth's interior in Finland, 1965. Compiled by M.T.Porkka. Inst. of Seismology, Univ. of Helsinki, Publ. 80.

Pirhonen, S. (1967). Group velocity of surface waves in Finland determined by curve fitting. Papers presented at the ESC Meeting, Copenhagen, 1966.

Vesanen, E., A.Kataja, U. Luosto, E. Penttilä, M.T. Porkka, J. Riihimaa, P. Saastamoinen and P.Teikari (1962). Progress Report for 1961, Seismological Laboratory of University of Helsinki. Inst.of Seism., Univ.of Helsinki, Publ.52.

Yoshiyama, R. (1957). The ratio of the velocity of P and S waves. Bull.Earthquake Res.Inst. Tokyo Univ., 35:627-640.

M.T.Porkka

SURFACE WAVE STUDIES ON THE CRUST AND UPPER MANTLE IN EURASIA

Abstract

A theoretical model is calculated for the crust and upper mantle, which agrees with Rayleigh and Love wave group velocity observations. It is concluded that rather low shear velocities are characteristic of the area investigated and that a low-velocity layer exists in the upper mantle.

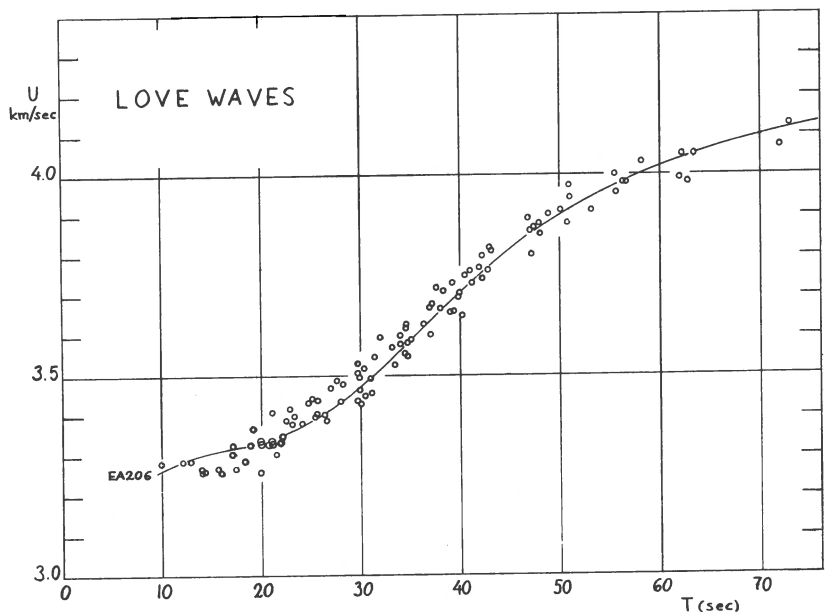

Fig. 1. Observed Love wave group velocity data compared with theoretical calculations for model EA206

Previously published experimental dispersion curves of Love waves for the paths from Hokkaido, Formosa and Altai to Southern Finland (Fig. 1) are similar enough to suggest rather similar crustal structures (Porkka, 1961). Some tests performed on new seismogram data substantiate former

results. Dispersion curves corresponding to the paths which cross the Himalayan massif are characterized by lower group velocities. These paths, however, are not used in this work.

Rayleigh wave group velocities were determined from the seismograms of Kamchatka, Kurile Islands and Japanese shocks (Fig. 2). They were recorded at Nurmijärvi with Press-Ewing type vertical seismographs.

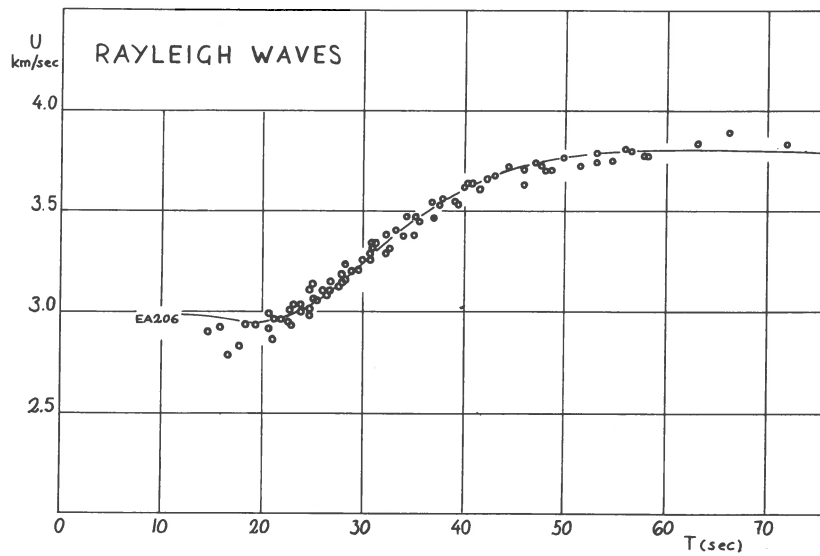

Fig. 2. Observed Rayleigh wave group velocity data compared with theoretical calculations for model EA206.

The problem of this study is to find a theoretical model which agrees with both Rayleigh and Love wave group velocity dispersion results. Only the fundamental mode waves are used in this work.

In order to find a model of satisfactory fit, theoretical curves of several models were calculated. The calculations were performed by the well-known Haskel matrix method. The effect of the earth's sphericity on the dispersion of Love waves is taken into account with the aid of the pseudo-spherical or earth-stretching method developed by Anderson (Anderson, 1965).

The parameters of the models were selected from published deep sounding and dispersion results. The crustal thickness had values of 35 km and 40 km. The best fit was shown by a 40 km model with crustal parameters corresponding to those of the Magadan-Kolima line, which is located north of the Sea of Okhotsk. The velocity distribution below the Moho was of Lehmann type.

This model was chosen as the basis for further investigations. The solid curve marked EA206 in the figures is one of its modifications. According to the calculated models, it exhibits the best agreement with observational dispersion.

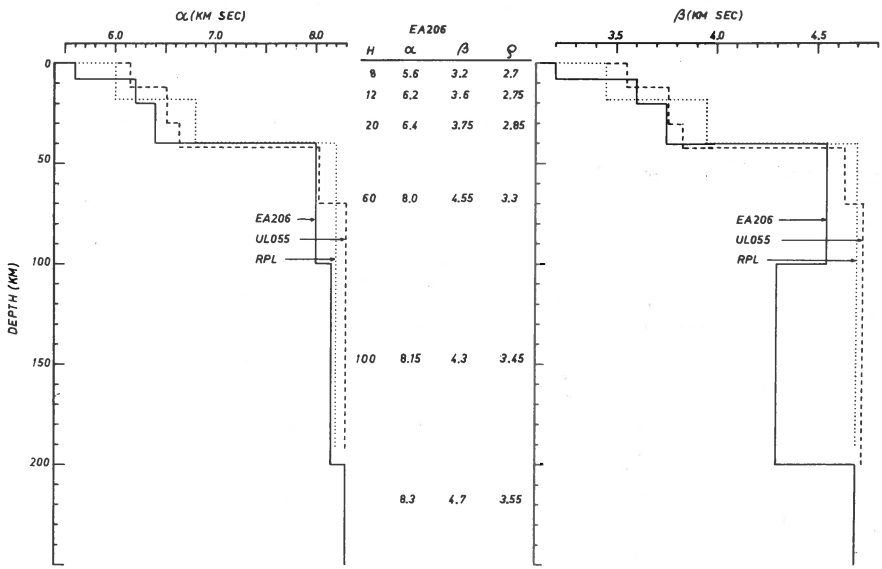

Fig. 3. Parameters of model EA206

Fig. 3 presents the parameters of model EA206. The table in the centre indicates the layer thicknesses, compressional and shear velocities and densities. The velocity distributions are also compared with two other models: UL056 and RPL. UL056 represents a structural model for Finland (Noponen et al., 1966). Model RPL was calculated with the aid of parameters representing the Russian Platform (Savarensky, 1966).

The shear velocity has the strongest effect on the dispersion. Therefore, the main attention is also directed toward its values. Compressional velocities have received less attention and densities are accepted without further consideration.

The model EA206 is characterized by rather slow velocities. The slow group velocities observed near the period of 20 sec lead to a low-velocity surface layer. In addition, the velocities in the layers just above and below the Moho are smaller than those of the models used for comparison. Without the rather strong low-velocity layer in the Upper Mantle, the velocities below the Moho would be even lower. On the other hand, if the crustal thickness increases, we can increase the seismic velocities on both sides of the Moho.

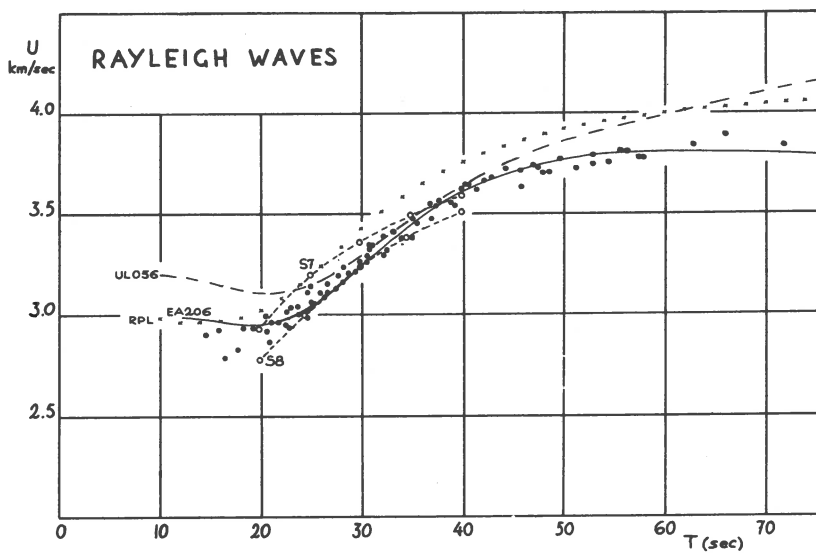

Fig. 4. Rayleigh wave dispersion curve of the model EA206 compared with some other curves; explanations in the text.

In Fig. 4. the Rayleigh wave dispersion curve of the model EA206 is compared with some other curves. The observed dispersion points are indicated by small black points. The curves denoted S7 and S8 are standard disper-

sion curves of Santo (1965). With the so-called crossing path technique, he has divided the areas investigated into regions having special dispersion characters. The paths investigated in this paper belong to his regions 7 and 8. The theoretical curve for the model of the Russian Platform is marked with crosses. The model UL056 is also shown in the same picture.

This study does not prented to claim that the accepted model EA206 is representative of the structure of the investigated area. More experimental data are needed for a more reliable solution: deep sounding results, better group velocity data, including a broader spectrum of periods, dispersion results of higher mode waves, and phase velocity results.

It is, however, possible to conclude that:

1. The investigated area is characterized by rather low shear velocities and/or rather thick crust. In a recent paper Kovach (1965) has likewise concluded that the Love wave data for the Eurasian continent indicate a low mean crustal shear velocity and/or thick crust.

2. There exixts a low-velocity layer in the upper mantle.

References

Anderson, Don L., 1965: Recent evidence concerning the structure and composition of the earth's mantle. Physics and Chemistry of the Earth, vol.6, Pergamon Press, London, pp. 1-131.

Kovach, Robert L., 1965: Seismic surface waves: Some observations and recent development. Ibid., pp.251-314.

Noponen, Ilkka, M.T.Porkka, Seppo E.Pirhonen and Urmas Luosto, 1966: Structure of the crust and upper mantle in Finland. Papers presented at the ESC Meeting, Copenhagen 1966.

Porkka, M.T., 1961: Surface wave dispersion for some Eurasian paths. II. Love waves. Geophysica 7, 151-160.

Santo, Tetsuo, 1965: Lateral variation of Rayleigh wave dispersion character. Part II: Eurasia. Pure and Appl. Geophys. 62, 67-80.

Savarensky, E.F., 1966: Oral communication.

M.J.Berry, L.Knopoff and S.Müller

THE LOW-VELOCITY LAYER IN THE UPPER MANTLE UNDER THE WESTERN MEDITERRANEAN SEA FROM PHASE VELOCITY OF RAYLEIGH WAVES

Data on the phase velocity of teleseismic Rayleigh waves have been obtained from recordings at four identical temporary long-period instruments at Alger (A), Monaco (M), Tortosa (T) and Cuglieri (C) situated around the western basin of the Mediterranean Sea (see Figure 1). These instruments were in operation from June to September, 1961.

The method of processing the data closely follows the technique developed previously for the study of the Alps in which attention is focussed on the dispersion of surface waves for events whose great circle paths lie close to one of the lines connecting two stations in the network (ref. Knopoff, Müller and Pilant, 1966). During the period of observation, seven events were observed which fit this criterion. These seven events provide some information about the structure under the basin for seven of the twelve possible lines connecting pairs of stations. The results of the data processing for the seven events are presented in the upper half of Figure 1.

Because of interference with waves traversing the adjacent continental structures, the data at periods shorter than about 35 seconds are unreliable; hence the interpretation is restricted to an investigation of the upper mantle structure in the basin in the period range from 35 to 90 seconds. The experimentally determined phase velocity curves in this range of periods are remarkably flat and show quite low phase velocity values.

A number of numerical experiments have been performed to compute phase velocity curves for certain hypothetical structures. The constraints on the structures have been taken to be (1) the crustal structure of the upper 11 km obtained by Fahlquist (1963) from explosion seismology

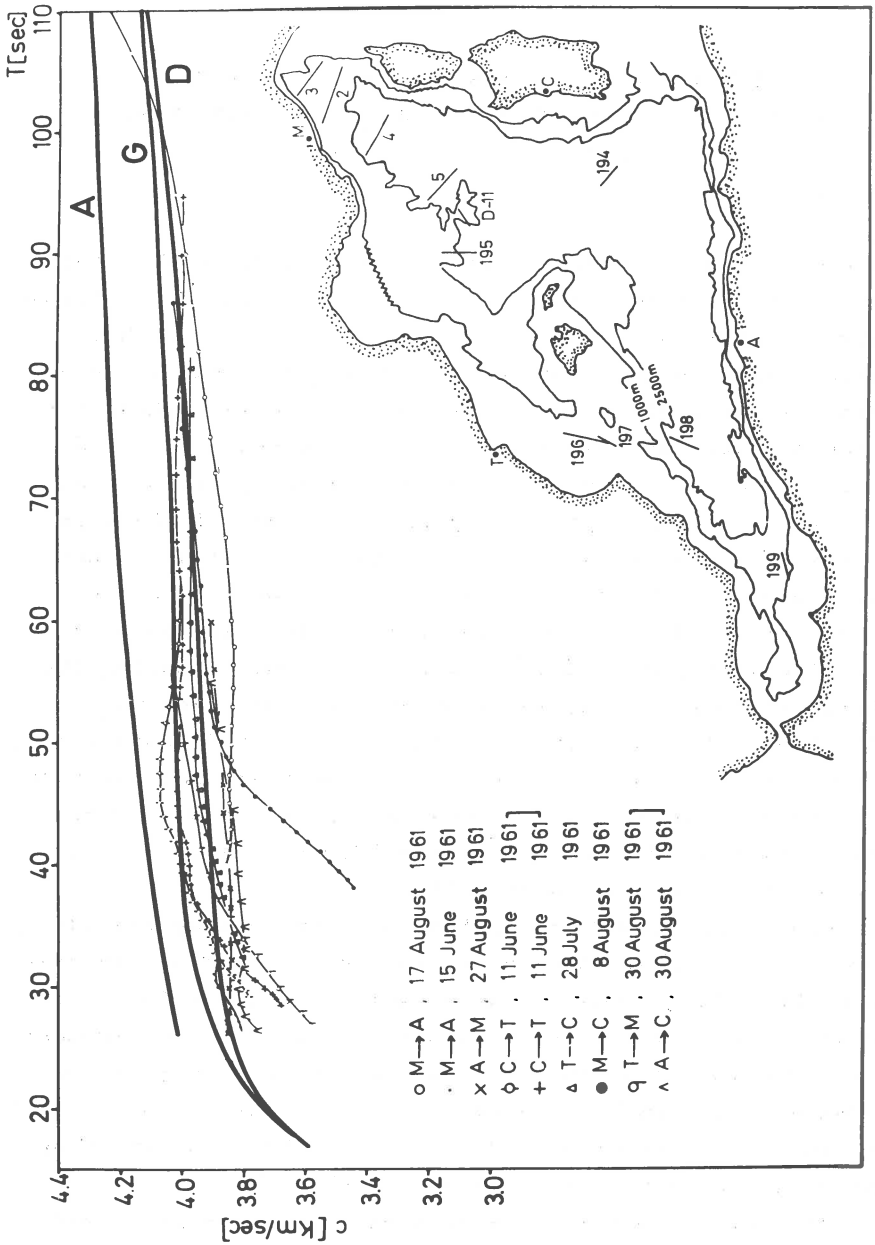
T[sec]
20
30
40
50
60
70
80
90
100
110
A
G
D
c [KM/sec]
4.4
4.2
4.0
3.8
3.6
3.4
3.2
3.0
o M→A , 17 August 1961
· M→A , 15 June 1961
x A→M , 27 August 1961
◊ C→T , 11 June 1961
+ C→T , 11 June 1961
▵ T→C , 28 July 1961
● M→C , 8 August 1961
▽ T→M , 30 August 1961
^ A→C , 30 August 1961
M
C
T
A
D-11
195
196
197
198
199
194
1000m
2500m
1
2
3
4
5

Figure 1

techniques and (2) the structure of the deeper parts of the mantle consistent with the body wave models of Lehmann (1959, 1961). In the computations the hypothetical structures have been varied to include or exclude a low-velocity channel; an additional parameter in the models was the depth to which the 7.7 km/sec P-wave velocity horizon found by Fahlquist (1963) extends.

Finally, in Figure 1 a comparison is made between the phase velocity curves of the observations and for a selection of three of the theoretical models computed. Model A contains no low-velocity layer, while models G and D have both a channel and a thick layer of relatively low P_n and S_n velocities. The result of the low phase velocity curve extending over a broad range of periods can now be interpreted. Model D fits the data best of the models investigated and the result is interpreted as being partly due to a pronounced low-velocity layer at a depth between 60 and 220 km and partly due to a relatively thick layer of material with a P-wave velocity of 7.7 km/sec at shallow depth. The S-wave velocity in the channel seems to be higher under the margins of the basin and lower in the central portion.

References

Fahlquist, D.A., "Seismic Refraction Measurements in the Western Mediterranean Sea". Ph.D. Thesis, Massachusetts Institute of Technology, 1963.

Lehmann, I., "Velocities of Longitudinal Waves in the Upper Part of the Earth's Mantle". Ann.Géophysique, 15, 93-118, 1959.

Lehmann, I., "S and the Structure of the Upper Mantle" Geophys.Journal (RAS), 4, 124-138, 1961.

Knopoff, L., Mueller, S. and W.L.Pilant, "Structure of the Crust and Upper Mantle in the Alps from the Phase Velocity of Rayleigh Waves." Bull.Seism.Soc.Amer., 56 (in press), 1966.

E.F.Savarensky, V.B.Glasko, Ja.Sh.Granit and A.B.Peshkov

VARIATIONS (PARTIAL DERIVATIVES) OF THE GROUP AND PHASE VELOCITIES OF RAYLEIGH AND LOVE WAVES BY VARIATION OF THE PARAMETERS OF A TWO-LAYERED EARTH CRUST

At present the dispersion of phase and group velocities of Rayleigh and Love surface waves for theoretical models of the Earth crust and mantle are calculated by high-speed computers.

For interpretation of observations of seismic surface waves the selection method is usually used: dispersion curves are calculated for some supposed models and are then compared with observations.

For effective selection of a model close to the real structure of the crust it is necessary to calculate the dispersions for a great number of models.

In an earlier paper (1) we calculated the dispersion curves of phase and group velocities for a number of two- and three-layered models of continental Earth crust with different thicknesses and longitudinal and transverse wave velocities.

Now we have calculated the derivatives of phase and group velocities after parameters of a two-layered Earth crust. The parameters of the Earth crust of the European part of the USSR are used. The results are presented here.

The knowledge of the derivatives makes it possible to determine the variations of phase and group velocities caused by the variation of different parameters of the model: the velocities of longitudinal (a_k) and transverse (b_k) waves in the layers of the Earth crust and mantle, thicknesses (h_k) and densities (ρ_k) of the layers. This method makes it possible to decrease the number of theoretical dispersion curves, which is necessary in practice.

The dependence of the derivatives of velocities after the medium parameters on the period makes it possible to estimate the degree of the influence of the variations of

the different Earth crust parameters on the dispersion. The accurate definition of the real Earth crust parameters by the parameters of the close model with the help of derivatives was made in the works (2), (3).

Our previous programme 1 was used for the calculations added by a special block giving automatic calculation of the derivatives of phase and group velocities depending on period T for n-layered models.

The derivatives may be calculated by any given parameters of the medium: $\frac{\partial c}{\partial a_k}$, $\frac{\partial c}{\partial b_k}$, $\frac{\partial c}{\partial \rho_k}$, $\frac{\partial c}{\partial h_k}$ depending on period T and at dimensionless parameters. $\frac{\partial c/b_{n+1}}{\partial a_k/b_{n+1}}$; $\frac{\partial c/b_{n+1}}{\partial b_k/b_{n+1}}$; $\frac{\partial c/b_{n+1}}{\partial \rho_k/\rho_{n+1}}$; $\frac{\partial c/b_{n+1}}{\partial h_k/H}$ depending on dimensionless period $\rho = \frac{Tb_{n+1}}{H}$

Here b_{n+1} is the transverse wave velocity in semispace in km/sec., H the thickness of the crust in km, T the period in sec.

For calculation of the derivatives a numeral differentiation method is used.

The formulas were selected (4) to give the maximum possible accuracy. For evaluation of the error the calculation results were compared at two close systems of calculation data. It appears that the maximum error of the results, given in this work is the following. For the derivatives of phase velocity: one unit in the third figure. For the group velocity derivatives: five units in the third figure.

The results of the calculations are presented by the graphs of the velocity-derivatives for a two-layered model of the Earth crust at variation of the different model parameters: the thicknesses of the layers, the velocities of longitudinal and transverse waves in them, the medium densities. The model parameters are given in Table 1 (model No.200) (1).

On fig. 1a,b the graphs of derivatives are presented of phase (c/b_3) and group (u/b_3) velocities of Rayleigh waves after all the medium parameters depending on the dimension-

less $\rho = \frac{Tb_3}{H}$ where b_3 = the velocity of transverse waves in semispace. The same is given on Fig. 2a,b for Love waves.

Table 1

Model Parameters 200, 202, 220, 105

Models No.	h_1/H	$\frac{a_1}{b_3}$	$\frac{b_1}{b_3}$	$\frac{\rho_1}{\rho_3}$	$\frac{a_2}{b_3}$	$\frac{b_2}{b_3}$	$\frac{\rho_2}{\rho_3}$
200	0,428	1,278	0,735	0,818	1,446	0,840	0,878
202	0,428	1,361	0,787	0,818	1,446	0,840	0,878
220	0,428	1,278	0,735	0,818	1,531	0,894	0,878
105	0,500	1,278	0,735	0,818	1,446	0,840	0,878

These curves make it possible to increase the possibilities for the interpretation of observations.

The comparison of curves 1,2 in accordance with curves 3,4 on Fig. 1a,b shows, that in the area $\rho < 4,5$ the influence of the variation of transverse velocities on phase and group velocity dispersion is more considerable that that of the variations of longitudinal velocities at any equal conditions.

For a small value of ρ the influence of parameter b_1/b_3 predominates, then the influence of parameters b_1/b_3 and b_2/b_3 becomes approximately the same. At further increase of ρ the influence of the parameter b_2/b_3 predominates.

From the comparison of curves 1,2 on Fig. 1a,b with curves 1,2 on Fig. 2a,b it is seen that the dependence of phase and group velocities upon transverse wave variations in the crust layers for Love waves is more considerable than for Rayleigh ones.

For $\rho > 4,5$ the influence upon dispersion of all parameters is less.

The curves 5,6 on Fig. 1a,b show the dependence of dispersion on density changes, curve 7 the dependence of dispersion on the density variation of the first layer of the crust. Each of these parameters influences greatly the dispersion only in extremum intervals ρ.

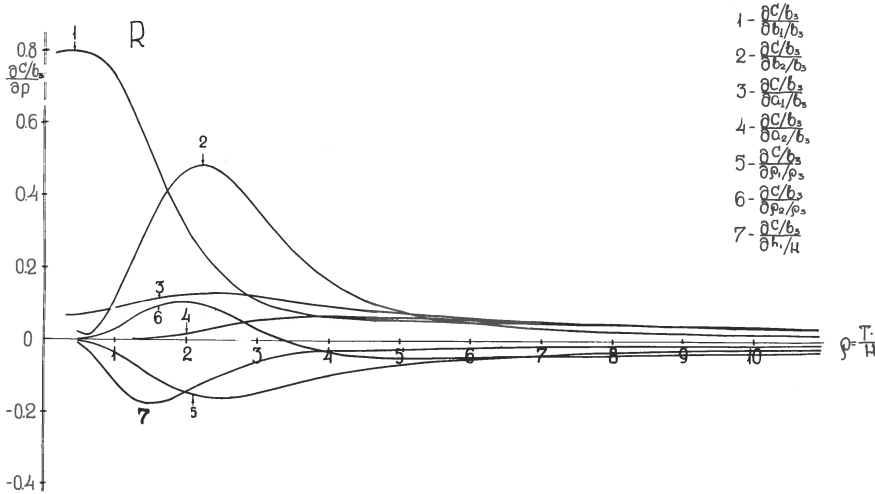

Fig. 1a

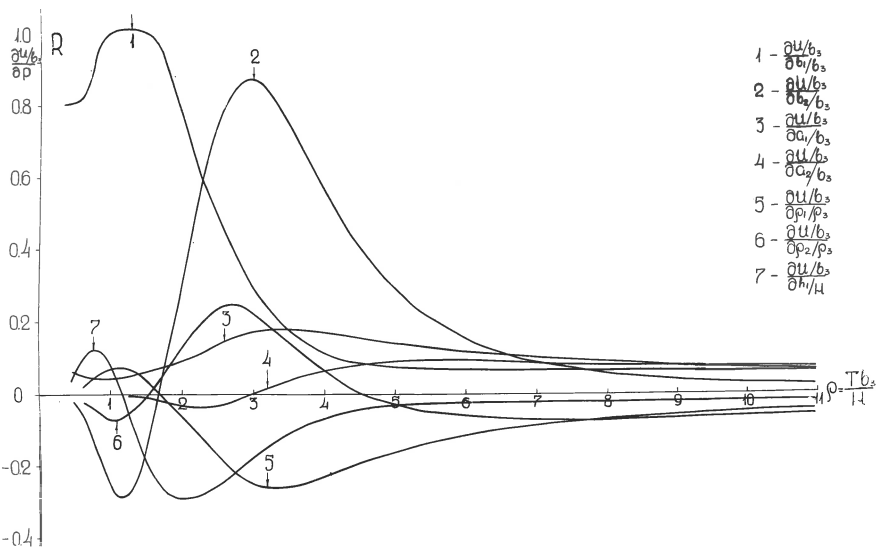

Fig. 1b

Fig. 1. Partial derivatives of Rayleigh wave velocities with respect to parameters.

a) Phase velocity.

b) Group velocity.

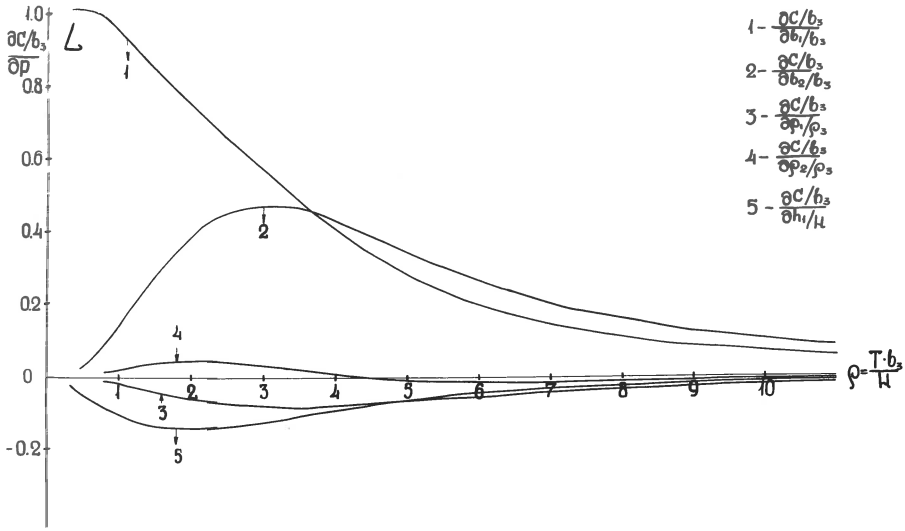

Fig. 2a

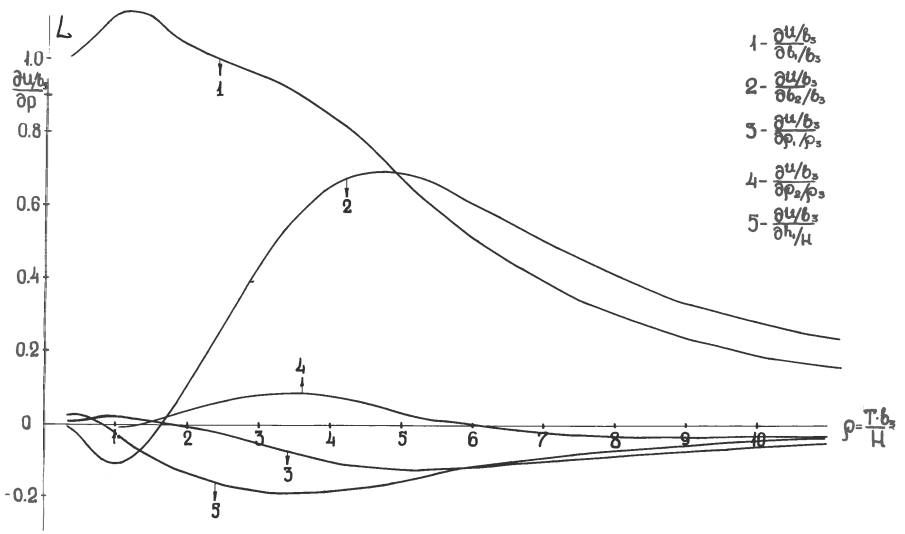

Fig. 2b

Fig. 2. Partial derivatives of Love wave velocities with respect to parameters.

a) Phase velocity.

b) Group velocity.

The practical use of the partial derivatives is the following:

Taking a_k, b_k, ρ_k, h_k as independent variables, it is possible to express the increase of phase velocity caused by parameter-variations by the formula (2):

$$\Delta c = \sum_m \frac{\partial (c/b_3)}{\partial p_m} \Delta p_m \qquad (1)$$

Here p_m is one of the medium parameters and Δp_m its variation. The sum in formula (1) is taken over all the variable parameters of the model a_k, b_k, ρ_k, h_k, $(k = 1,2)$. Variations of group velocity may be calculated in the same way.

Taking into account the variations of velocities, obtained by formulas (1), it is possible to construct dispersion curves for near-by-parameter models.

For instance, we calculated the phase and group velocities for modificated models differing from the initial model (model 200) by some parameters of the medium. The model 202 differed in parameters a_1 and b_1, the model 220 in parameters a_2 and b_2; the model 105 has a difference from the model 200 in the thickness of the first layer.

Table 2

Phase and group velocities for Love and Rayleigh waves. Models 200, 202, 220, 105

	Model 200		Model 202		Model 220		Model 105	
$\rho = \frac{Tb_3}{H}$	$\frac{c}{b_3}$	$\frac{u}{b_3}$	$\frac{c}{b_3}$	$\frac{u}{b_3}$	$\frac{c}{b_3}$	$\frac{u}{b_3}$	$\frac{c}{b_3}$	$\frac{u}{b_3}$
				Rayleigh wave				
9,4	0,8883	0,8675	0,8936	0,8773	0,8930	0,8756	0,8872	0,8659
4,7	0,8629	0,8014	0,8723	0,8180	0,8731	0,8261	0,8613	0,7980
3,13	0,8213	0,7007	0,8359	0,7291	0,8418	0,7450	0,817	0,6873
2,19	0,7670	0,6448	0,7900	0,6871	0,7941	0,6688	0,7571	0,6254
1,25	0,7059	0,6339	0,7452	0,6989	0,7175	0,6221	0,6958	0,6377
				Love wave				
9,4	0,9790	0,9395	0,9829	0,9510	0,9847	0,9556	0,9776	0,9355
4,7	0,9250	0,8189	0,9405	0,8554	0,9435	0,8551	0,9197	0,8069
3,13	0,8709	0,7529	0,8978	0,8003	0,8953	0,7788	0,8624	0,7403
2,19	0,8267	0,7309	0,8619	0,7817	0,8480	0,7389	0,8171	0,7215
1,25	0,7805	0,7242	0,8249	0,7810	0,7905	0,7185	0,7726	0,7210

Table 3

Partial derivatives of phase and group velocities with respect to physical parameters of model 200

$\rho = \frac{Tb_3}{H}$	$\frac{\partial c}{\partial b_1}$	$\frac{\partial c}{\partial b_2}$	$\frac{\partial c}{\partial a_1}$	$\frac{\partial c}{\partial a_2}$	$\frac{\partial (c/b_3)}{\partial (\rho_1/\rho_3)}$	$\frac{\partial (c/b_3)}{\partial (\rho_2/\rho_3)}$	$\frac{\partial (c/b_3)}{\partial (h_1/H)}$
			Rayleigh wave				
9,4	0,0399	0,0196	0,0381	0,0435	-0,0260	-0,0359	-0,0157
4,7	0,0563	0,0984	0,0802	0,0656	-0,0734	-0,0452	-0,0216
3,13	0,100	0,328	0,119	0,0586	-0,140	0,0190	-0,0511
2,19	0,259	0,486	0,129	0,0259	-0,154	0,100	-0,127
1,25	0,627	0,221	0,101	0,0020	-0,0680	0,0620	-0,164
			Love wave				
9,4	0,0768	0,116	-	-	-0,0258	-0,0154	-0,0181
4,7	0,311	0,367	-	-	-0,0724	-0,0055	-0,0729
3,13	0,545	0,468	-	-	-0,0813	0,0283	-0,121
2,19	0,715	0,410	-	-	-0,0642	0,0416	-0,140
1,25	0,899	0,210	-	-	-0,0317	0,0278	-0,124

$\rho = \frac{Tb_3}{H}$	$\frac{\partial u}{\partial b_1}$	$\frac{\partial u}{\partial b_2}$	$\frac{\partial u}{\partial a_1}$	$\frac{\partial u}{\partial a_2}$	$\frac{\partial (u/b_3)}{\partial (\rho_1/\rho_3)}$	$\frac{\partial (u/b_3)}{\partial (\rho_2/\rho_3)}$	$\frac{\partial (u/b_3)}{\partial (h_1/H)}$
			Rayleigh wave				
9,4	0,0650	0,0352	0,0785	0,0768	-0,0552	-0,0673	-0,0235
4,7	0,0845	0,375	0,152	0,0807	-0,184	-0,0020	-0,0393
3,13	0,279	0,860	0,177	0,0082	-0,250	-0,218	-0,162
2,19	0,669	0,457	0,108	-0,0359	-0,0930	0,170	-0,260
1,25	1,093	-0,263	0,0566	-0,0074	0,0692	-0,0562	-0,0463
			Love wave				
9,4	0,226	0,322	-	-	-0,0695	-0,0307	-0,0535
4,7	0,730	0,692	-	-	-0,120	0,0494	-0,168
3,13	0,947	0,474	-	-	-0,0625	0,0818	-0,188
2,19	1,019	0,169	-	-	-0,153	0,0440	-0,152
1,25	1,122	-	-	-	0,0108	-0,004	-0,0635

The parameters of models 202, 220, 105 together with the parameters of the model 200 are presented in Table 1. The values of the derivatives of phase and group velocities for the model 200 are given in Table 3. Variations of phase (Δ^c/b_3) and group (Δ^u/b_3) velocities for the modificated models were calculated by derivatives by formula (1) and are given in Table 4. For evaluation of the obtained results they are compared with accurate values of differences Δ^{*c}/b_3 and Δ^{*u}/b_3 between the velocities for the models 202, 220, 105 and corresponding velocities for

model 200. The accurate values of velocities for these models are given in Table 2. In Table 4 together with the values Δ^c/b_3 and Δ^u/b_3 (see above) the differences $\Delta^c/b_3 - \Delta^{*c}/b_3$, $\Delta^u/b_3 - \Delta^{*u}/b_3$ are also presented. There is a good agreement between the increases, determined by the derivatives, and the differences. At the variation of parameters on 6-8% these differences are not equal to each other. They differ on 0,0005 - 0,003.

At present many dispersion-curves exist, calculated for different models of the Earth, but as the practice shows it is not enough. Calculation of theoretical curves every-time, corresponding to a concrete model of the crust of the region in question meets with considerable difficulties of technical character. It is possible to exclude these difficulties by use of the tables of partial derivatives mentioned above.

As an example we'll show how theoretical curves for the Russian platform can be transformed into curves for the region of the Middle Asia, in particular for the profile of Andijan-Frunze. In this area phase velocities of Rayleigh surface waves for the following five earthquakes were observed: 23/XI-1955 06h 29m 23s; 18/VIII-57 21 h 42 m 30 s; 17/IX-60 07 h 52 m 51 s; 17/IX-60 08 h 05 m 29 s; 16/III-63 08 h 44 m 49 s.

Let us take the data for the model of the layered crust from the work of V.I.Ulomov (5). We have:

$a_1 = 5,7$ km/sec ; $\rho_1 = 2,65$ g/cm^3 ;

$a_2 = 6,4$ km/sec ; $\rho_2 = 2,85$ g/cm^3 ; $h_1/H = 0,46$

$a_3 = 7,9$ km/sec ; $\rho_3 = 3,25$ g/cm^3 ;

The velocities of transverse waves are taken to be equal to

$$a_i/\sqrt{3}$$

The model 200 for the Russian platform has the following parameters:

Table 4

The phase and group velocity differences between the modified models 202, 220, 105 and the original model 200

	Rayleigh waves					Love waves		
$\rho = \frac{Tb_3}{H}$	$\Delta\frac{c}{b_3}(\frac{b_1}{b_3})$	$\Delta\frac{c}{b_3}(\frac{a_1}{b_3})$	$\Delta\frac{c}{b_3}$	$\Delta^*\frac{c}{b_3}$	$\Delta\frac{c}{b_3}-\Delta^*\frac{c}{b_3}$	$\Delta\frac{c}{b_3}(\frac{b_1}{b_3})$	$\Delta^*\frac{c}{b_3}$	$\Delta\frac{c}{b_3}-\Delta^*\frac{c}{b_3}$
				Model 202				
9,4	0,0021	0,0032	0,0053	0,0053	0,0000	0,0040	0,0040	0,0000
4,7	0,0029	0,0067	0,0096	0,0094	0,0002	0,0162	0,0155	0,0007
3,13	0,0052	0,0099	0,0151	0,0146	0,0005	0,0283	0,0269	0,0014
2,19	0,0133	0,0107	0,0140	0,0230	0,001	0,0372	0,0352	0,002
1,25	0,0326	0,0084	0,0410	0,0393	0,0007	0,0468	0,0444	0,0024
				Model 220				
9,4	0,0011	0,0036	0,0047	0,0047	0,0000	0,0063	0,0058	0,0005
4,7	0,0053	0,0055	0,0108	0,0102	0,0006	0,0198	0,0185	0,0013
3,13	0,0178	0,0049	0,0227	0,0205	0,0022	0,0253	0,0244	0,0009
2,19	0,0262	0,0022	0,0284	0,0271	0,0013	0,0221	0,0214	0,0007
1,25	0,0119	0,0017	0,0121	0,0116	0,0005	0,0113	0,0100	0,0013
$\rho = \frac{Tb_3}{H}$	$\Delta\frac{u}{b_3}(\frac{b_1}{b_3})$	$\Delta\frac{u}{b_3}(\frac{a_1}{b_3})$	$\Delta\frac{u}{b_3}$	$\Delta^*\frac{u}{b_3}$	$\Delta\frac{u}{b_3}-\Delta^*\frac{u}{b_3}$	$\Delta\frac{u}{b_3}(\frac{b_1}{b_3})$	$\Delta^*\frac{u}{b_3}(\frac{b_1}{b_3})$	$\Delta\frac{u}{b_3}-\Delta^*\frac{u}{b_3}$
				Model 202				
9,4	0,0034	0,0066	0,0100	0,0098	0,0002	0,0118	0,0115	0,0003
4,7	0,0043	0,0127	0,0170	0,0166	0,0004	0,0380	0,0365	0,0015
3,13	0,0145	0,0147	0,0292	0,0284	0,0008	0,0492	0,0474	0,0018
2,19	0,0348	0,0090	0,0438	0,0423	0,0015	0,0529	0,0508	0,0021
1,25	0,0568	0,0046	0,0614	0,0620	-0,0006	0,0583	0,0568	0,0015
				Model 220				
9,4	0,0019	0,0064	0,0083	0,0081	0,0002	0,0174	0,0161	0,0013
4,7	0,0201	0,0068	0,0269	0,0247	0,0022	0,0374	0,0362	0,0012
3,13	0,0463	0,0007	0,047	0,0443	0,0027	0,0256	0,0259	-0,0003
2,19	0,0247	-0,0030	0,0217	0,0240	-0,0023	0,0091	0,008	0,0011
1,25	-0,0142	-0,0006	-0,0148	-0,0148	0,0000	-0,0049	-0,0051	0,0002

a_1 = 6,0 km/sec ; b_1 = 3,45 km/sec ; ρ_1 = 2,7 g/cm^3 ;

a_2 = 6,8 km/sec ; b_2 = 3,95 km/sec ; ρ_2 = 2,9 g/cm^3 ; h_1/H=0,428

a_3 = 8,1 km/sec ; b_3 = 4,70 km/sec ; ρ_3 = 3,3 g/cm^3 ;

The theoretical curves are given in dimensionless parameters. Therefore the values for the Middle Asia must be given in that way also:

		Model 105				
$\rho = \frac{Tb_3}{H}$	$\Delta\frac{c}{b_3}(\frac{h_1}{H})$	$\Delta^*\frac{c}{b_3}(\frac{h_1}{H})$	$\Delta\frac{c}{b_3} - \Delta^*\frac{c}{b_3}$	$\Delta\frac{u}{b_3}(\frac{h_1}{H})$	$\Delta^*\frac{u}{b_3}(\frac{h_1}{H})$	$\Delta\frac{u}{b_3} - \Delta^*\frac{u}{b_3}$
			Rayleigh waves			
9,4	-0,0011	-0,0011	0,0	-0,0017	-0,0016	-0,0001
4,7	-0,0016	-0,0016	0,0	-0,0027	-0,0034	0,0007
3,13	-0,0037	-0,0043	0,0006	-0,0117	-0,0134	0,0017
2,19	-0,0091	-0,0099	0,0008	-0,0202	-0,0194	0,0008
			Love waves			
9,4	-0,0013	-0,0014	0,0001	-0,0038	-0,0040	0,0002
4,7	-0,0052	-0,0053	0,0001	-0,0121	-0,0120	-0,0001
3,13	-0,0087	-0,0085	-0,0002	-0,0135	-0,0126	-0,0009
2,19	-0,0102	-0,0096	-0,0006	-0,0109	-0,0094	-0,0015

Using the tables of derivatives we calculate the corrections to the model 200. They are shown in Table 5.

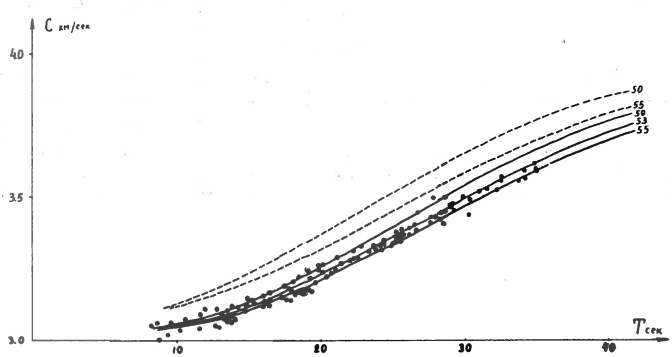

Fig. 3. Phase dispersion data over the path Andijan-Frunze. The continuous lines are theoretical curves for a model of the Central Asia crust

Table 5

ρ	c/b_3 model 200	$\frac{\partial c/b_3}{\partial b_1/b_3}\cdot\Delta\frac{b_1}{b_3}$	$\frac{\partial c/b_3}{\partial b_2/b_3}\cdot\Delta\frac{b_2}{b_3}$	$\frac{\partial c/b_3}{\partial a_1/b_2}\cdot\Delta\frac{a_1}{b_3}$	$\frac{\partial c/b_3}{\partial a_1/b_3}\cdot\Delta\frac{a_1}{b_3}$	$\frac{\partial c/b_3}{\partial \rho_1/\rho_3}\cdot\Delta\frac{\rho_1}{\rho_3}$	$\frac{\partial c/b_3}{\partial h_1/H}\cdot\Delta\frac{h_1}{H}$	c/b_3 corr.
0,8	0,683	-0,0101	-0,0014	-0,0023	0,00	0,00	-0,0022	0,667
1,0	0,692	-0,0095	-0,0033	-0,0026	0,00	0,0001	-0,0033	0,673
1,2	0,705	-0,0085	-0,0059	-0,0028	-0,0001	0,0002	-0,0050	0,680
1,4	0,715	-0,0073	-0,0087	-0,0030	-0,0002	0,0002	-0,0053	0,690
1,6	0,728	-0,0061	-0,0111	-0,0032	-0,0003	0,0003	-0,0056	0,701
1,8	0,741	-0,0050	-0,0128	-0,0035	-0,0006	0,0003	-0,0056	0,713
2,0	0,754	-0,0041	-0,0139	-0,0035	-0,0009	0,0004	-0,0053	0,726
2,2	0,763	-0,0033	-0,0146	-0,0036	-0,0012	0,0004	-0,0040	0,742
2,4	0,781	-0,0027	-0,0141	-0,0036	-0,0016	0,0004	-0,0034	0,755
2,6	0,793	-0,0022	-0,0134	-0,0036	-0,0019	0,0004	-0,0028	0,768
2,8	0,804	-0,0018	-0,0122	-0,0035	-0,0023	0,0004	-0,0023	0,782
3,0	0,815	-0,0015	-0,0108	-0,0034	-0,0025	0,0004	-0,0019	0,795
3,4	0,831	-0,0011	-0,0081	-0,0033	-0,0029	0,0004	-0,0013	0,814
3,8	0,845	-0,0009	-0,0059	-0,0028	-0,0031	0,0003	-0,0010	0,831
4,2	0,854	-0,0008	-0,0043	-0,0025	-0,0031	0,0002	-0,0008	0,842
4,6	0,861	-0,0007	-0,0032	-0,0023	-0,0030	0,0002	-0,0007	0,851
5,0	0,866	-0,0007	-0,0025	-0,0021	-0,0030	0,0002	-0,0007	0,857

Now let us consider dimensional values. For this purpose it is necessary to introduce b_3 = 4,565 km/sec and H = 50, 53, 55 km. On Fig. 3 these three curves are shown by continuous lines. It is seen quite clearly that the curve for H = 53 km best fits the experimental data. The position of the theoretical curves without the introduction of corresponding corrections is shown by dotted lines.

As another example we will mention the Pamiro-Alaiskaya zone. We'll be interested in the crust thickness within the triangle Horog-Garm-Obigarm, where we have observed dispersion curves of phase velocities of Rayleigh waves for three earthquakes. (26/VII-62 08 h 14 m 45 s, 18/IX-62 00 h 29 m 09 s, 28/III-63 00 h 15 m 49 s.)

The Deep Seismic Sounding data give the following values of the parameters:

$$a_1 = 5{,}5 \text{ km/sec}; \qquad \rho_1 = 2{,}65 \text{ g/cm}^3;$$
$$a_2 = 6{,}4 \text{ km/sec}; \qquad \rho_2 = 2{,}85 \text{ g/cm}^3; \quad h_1/H \geqq 0{,}5$$
$$a_3 = 8{,}1 \text{ km/sec}; \qquad \rho_3 = 3{,}25 \text{ g/cm}^3;$$

The velocities of transverse waves are taken to be equal to $a_i/\sqrt{3}$.

The profiles of the Deep Seismic Sounding cover the regions mainly to the north of the above mentioned triangle. Extrapolating the DSS data and using V.I.Ulomov's data (5) we can consider the average thickness of the crust on this place to be 60-65 km. Using the partial derivatives we'll determine the crust thickness by phase velocities of surface waves. As before we'll use undimensional parameters and calculate the differences from the corresponding values for the model 200. Fig. 4 shows constructed dispersion curves for the thicknesses 60, 65, 70 km.

By dotted lines the position of the theoretical curves without the introduction of corresponding corrections is shown.

At the result it is seen, that the crust thickness according to phase velocities of Rayleigh waves is equal to about 65 km.

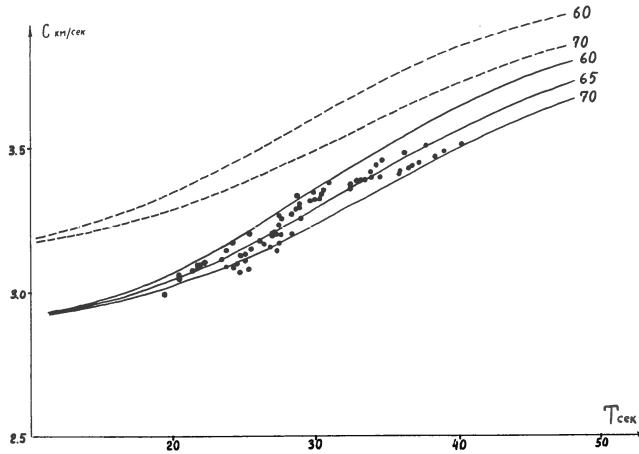

Fig. 4. Rayleigh wave phase dispersion data over the triangle Horog-Garm-Obigarm. The continous lines are the theoretical curves corresponding to an earth model given by DSS. The dotted lines are the original curves.

References

1. E.F.Savarensky, V.B.Glasko, J.Sch.Granit: Dispersionnyje krivyje voln Releja i Ljava primenitjeljno k dvuch i trechslojnoj kontinentaljnoj zemnoj kore. Izv. AN SSSR, ser.Fizika Zemlji, nr.4, 1965.

2. Fakenchi H. and J.Dorman, M.Saito: Partial derivatives of surface wave phase velocity with respect to physical parameter changes within the earth. J.Geophys. Res.69, No.16, 1964.

3. Dorman J. and M.Ewing: Numerical inversion of surface wave dispersion data and uppermantle structure in the New York-Pennsylvania area. J.Geophys.Res. 67, 5227-5241, 1962.

4. I.S.Berezin i N.P.Zhidkov: Metody vytjislenij. t. I,M., Fizmatgiz, 1960.

5. V.I.Ulomov: O resuljtatach issljedovanija glubinnogo strojenija zemnoj kory v Srednej Azii po dannym sejsmologii. Izv. AN SSSR, ser.geofiz., nr. 10, 1962.

6. I.P.Kosminskaja, G.G.Michota, J.V.Tulina: Strojenije zemnoj kory v Pamiro-Alajskoj zone po dannym glubinnogo sejsmitjeskogo zondirovanija. Izv. AN SSSR, ser.geofiz., nr.10, 1958.

D.I.Sikharoulidze

A STUDY OF REFLECTED SURFACE WAVES

The study of reflected surface seismic waves has given us a chance to reveal some peculiarities of the dispersion of group and phase velocities.

Building up and growth conditions of the surface waves in different layers of the earth crust (1-3) are ascertained. Experimental studies of the overtones of the surface waves gave us a chance to recognize the inhomogeneity in the crustal structures under the grounds of the Caspian and Black seas. In particular, it's recognized that the crustal structures under the grounds of those seas differ from the continental and oceanic structures by absence of the granite layer under the central parts of the seas and by the presence of a very thick sedimentary complex. Theoretical studies and different model experiments showed, that in case of uneven and wedge-shaped disappearance of layers and when the surface waves grow under existing conditions, a reflection effect could be expected.

Mainly these studies and also some other reasons have brought us to the conclusion that the reflected surface waves could have appeared in the Caucasus. In order to identify the reflected surface waves, the records of the earthquakes, registered by some Caucasian seismic stations, have been studied. Treatment and analysis of the data have given us an opportunity to identify waves on the records, which resemble reflected Rayleigh- and Love-waves. Reflected surface waves are recognized during the Caucasian, Iranian and Turkish earthquakes, when the wave growth races, moving from the seismic focus to the seismic station, do not traverse the Caspian and Black seas (Fig. 1, 2). The epicentral distances, when the reflected surface waves are to be observed, do not exceed 2000 kilometres.

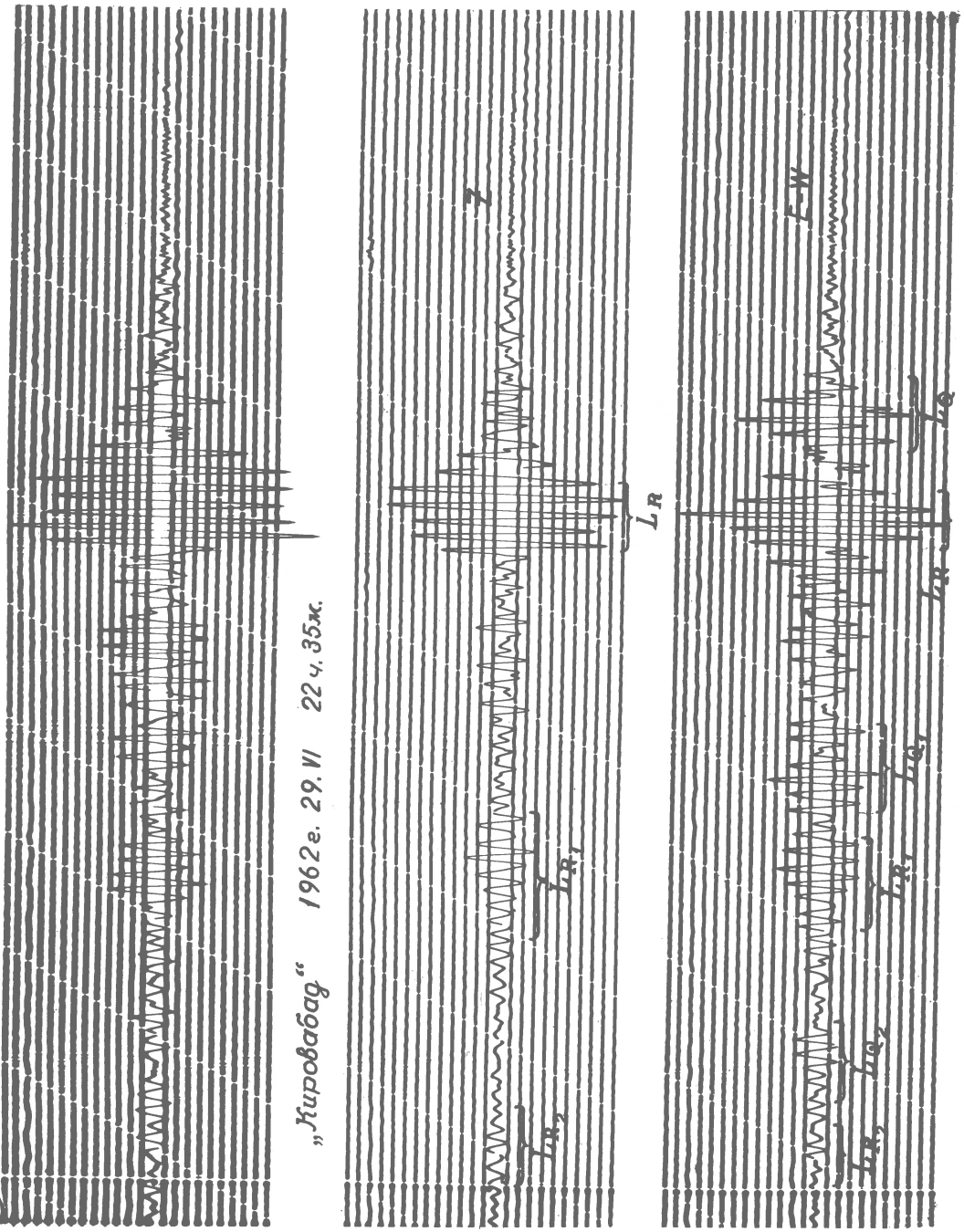

Fig. 1

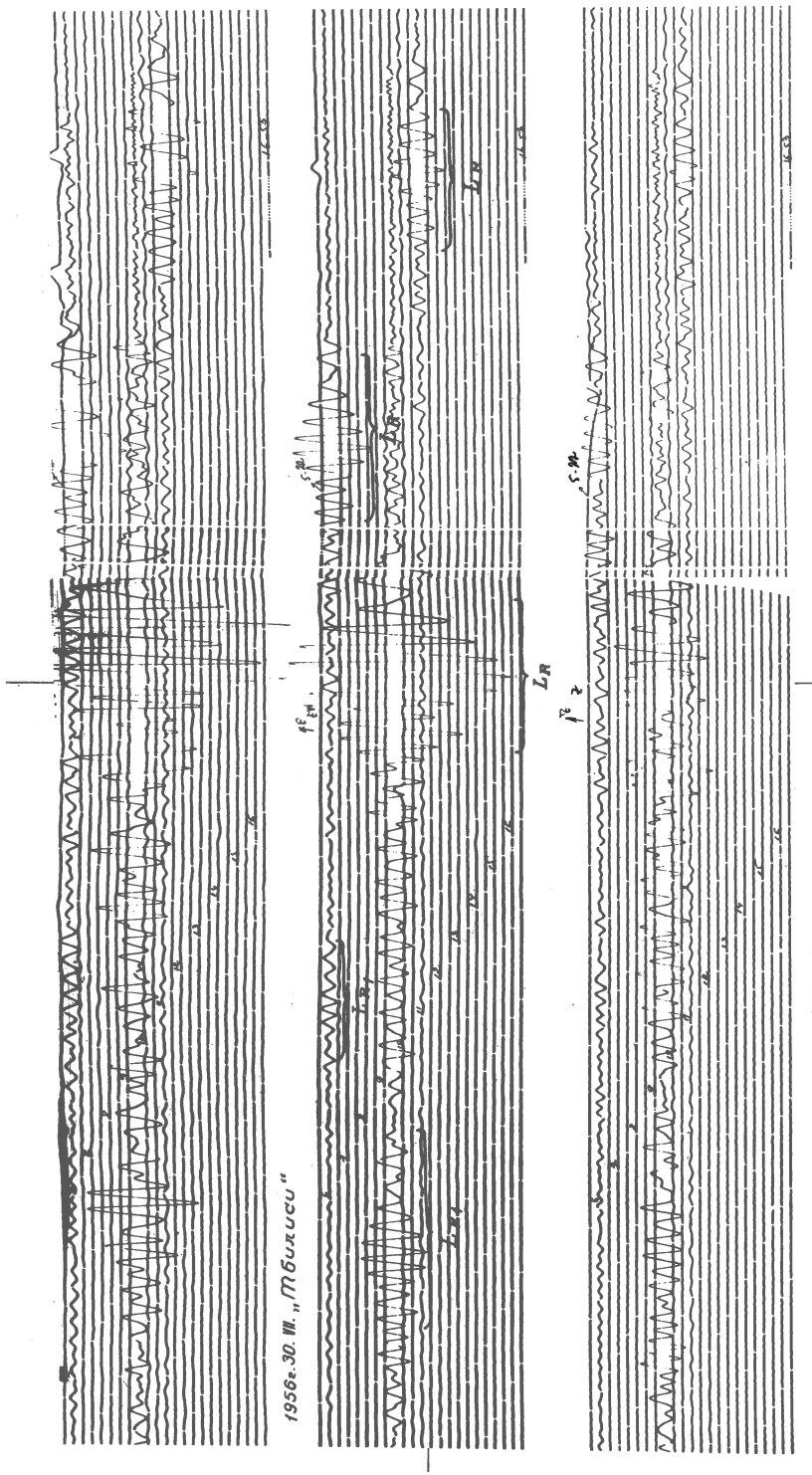

Fig. 2

The range of the periods of the straightforward surface seismic waves, observed at a distance from 400 to 2000 km., is being changed within the limits of 8-30 seconds.

The main tone of the surface waves observed at distances of 300-400 kms. is being formed in sedimentary layers of the crust (1). The surface waves formed in thinner layers of the sedimentary complex are observed at epicentral distances from 50 to 150 kms., the period range of which varies within the limits of 1-7 seconds. The composition of the sedimentary complex layers in the Caucasus varies widely depending upon the country. That is why each of the layers cannot be stretched for a long distance. Accordingly, the surface waves formed in the layers of the sedimentary complex, when the subsequent vanishing of layers takes place, would be partially reflected in the opposite direction and refracted.

In many cases, this effect has been observed in the Caucasus. From the studied earthquakes, it comes out, that the time interval between the straight lines of the waves L_Q and L_R varies depending on the epicentral distance. That is why, at the rather short epicentral distances, the difference in particular moments of their appearance on the records of the horizontal components of the seismographs, in some cases, drives us up to a certain difficulty in their tracing, whereas the period of the reflected waves L_Q and L_R is increasing, and their elucidation on the records becomes comparatively open. Some of the studied earthquakes are characterized by the multiple reflections of Love- and Rayleigh waves, but sometimes, only direct and reflected Love waves or direct and reflected Rayleigh waves can be observed.

The main responses which prove the existence of reflected Love- and Rayleigh waves are the following:

1. Reflected Love waves are held to be the waves which could be registered only by horizontal components of the seismographs. Particle motion in them is polarized in the horizontal plane perpendicularly to the waves' propagation. The reflected waves L_R could be watched on the horizontal components only after the appearance of the reflected L_Q

waves. The time interval between the moments of the L_Q and L_R waves is increasing when the multiple of reflections of the surface waves is increasing too.

2. Reflected Rayleigh waves could be registered by all components of the seismographs, especially by the vertical component. Particle motion of the reflected wave L_R is polarized in a vertical plane and has its horizontal and vertical travel components along the propagation. The particle motion, generally, is turned over elliptically.

3. In both types of the reflected L_Q and L_R waves, the way of recording of the straightforward surface waves is the same.

4. Direction towards the reflecting surface could be estimated by the reflected surface waves.

5. The higher the multiple order of the reflected waves is, the slighter is their revealing on the records. However, the way of recording, especially in Airy's phase, is preserved.

6. Dispersion features of the phase and group velocities in straightforward and reflected waves are identical. In order to elucidate that the observed surface waves are formed in the upper layers of the crust, the experimental dispersion peculiarities of the group velocities of both types of the surface waves have been studied. The granite layer can be continuously traced along the observed lines, but in some places the absence of the sedimentary complex could be noticed. In order to interpret the experimental dispersion of the group velocities of the surface waves, there have been gleaned some models, which could better represent the structure of the upper layers of the crust. Good agreement of the experimental data with the theoretical curves are got in case of monolayer modelling of the upper part of the crust, when the transversal velocities are V_1 = 3,0 km/sec., V_2 = 4,0 km/sec. The mean thickness of the granite layer including the sedimentary complex along the observed lines is 22 $\pm$ 2 km. (Fig. 3, 4). A study of the theoretical dispersion curves of the group velocities, plotted with monolayer or double-layer modelling of the upper part of the crust and with the experimental

velocity dispersion, brings us to the following: Oscillation in the Airy phase, for the observed territories, propagates with a constant group velocity - for Love waves it is U = 2,9 km/sec., for Rayleigh waves U = 2,7 km/sec. Value of the Airy phase periods for these types of the surface waves varies within the limits of T = 8 - 11 sec.

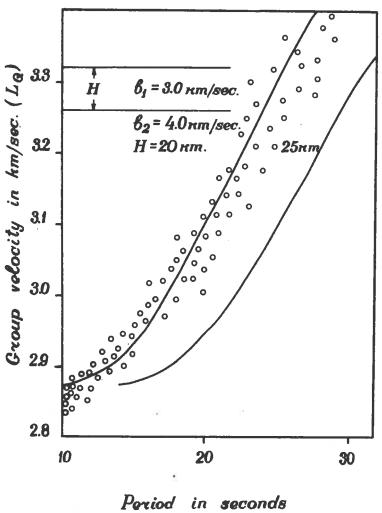

Fig. 3

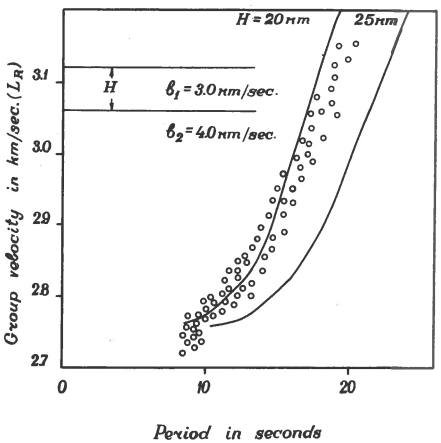

Fig. 4

When the epicentral distances are short and when the surface waves are formed in the sedimentary complex of the crust, the group velocity in the Airy phase decreases and is on an average for L_Q and L_R waves 2,6 km/sec. and 2,4 km/sec. respectively. Corresponding periods are varying within the limits of 2-6 seconds. For the reflected surface determination, the following method is used: we determine the travelling time of the reflected surface wave, particularly, it's better to use the travelling time of the reflected Airy phase. Knowing the appropriate group velocity, got on the basis of the reasonings mentioned above, we can find the travelling length of the reflected wave. Having got this length, we can draw up an ellipse, with the seismic station and the epicenter of the earth-

quake as its focuses. Angular points of the possible reflected waves would be plotted on the elliptic arc. That is why, it is impossible to do a sum unequivocally. The reflecting surface could be plotted in the presence of the surface waves reflections of different earthquakes, registered by one or several seismic stations. After having been calculating the travelling time of the reflected wave, family of the ellipses could have been plotted. A point of each ellipse would correspond to the reflecting surface. Studied reflections of the L_Q and L_R waves belong to the first and the second group of the surface waves. By means of the reflection of the first group waves, we determine changes in the structure of the sedimentary complex; by means of the reflection of the second group - in the granite layer.

Treatment and analysis of the single and multiple reflected L_Q and L_R waves lead us to the fact, that the reflecting surfaces are based under the grounds of the Caspian and Black seas. In some cases, reflections of the L_Q and L_R waves could be observed starting from the southern slope of the eastern part of the Caucasus mountains.

Starting from the eastern part of the Javakheti range, reflections of the first wave groups could be observed during the earthquakes in the middle part of the Caucasus

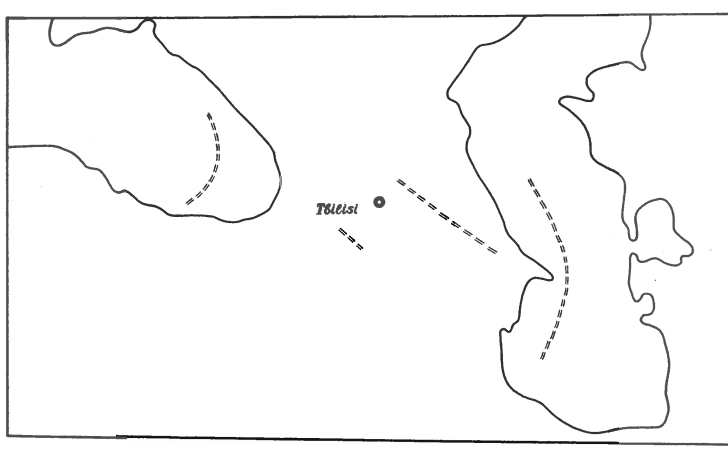

Fig. 5

mountains. Dotted lines on fig. 5 show the places of the L_Q and L_R waves origination.

In my opinion, occurrence of the reflecting surfaces under the grounds of the Caspian and Black seas could be explained by absence of a granite layer under the grounds. Reflections along the southern slope of the eastern part of the Caucasus mountains could be explained by the existence of an abyssal fault between the mountain and the depressed part of the region. Reflections from the eastern part of the Javakheti range show the absence of the sedimentary complex in that region.

Literature

1. D.I.Sikharoulidze: "Study of Love wave dispersion during the close earthquakes". - USSR Academy of Sciences, series geoph. N-4, 1959.

2. D.S.Sikharoulidze: "Nature of the L_g and R_g waves and study of the crust structure". Geoph.Inst. GSSR Academy of Sciences, vol.XXII, 1963.

3. D.S.Sikharoulidze, N.P.Toutberidze: "About the group surface seismic waves, formed in different strata of the crust". Geoph.Inst.GSSR Academy of Sciences, vol. XXII, 1965.

O.E.Starovoit, E.F.Savarensky and S.A.Fedorof

DISPERSION OF THE LONG-PERIOD SURFACE WAVES AND STRUCTURE OF THE EARTH'S MANTLE

The dispersion of surface Rayleigh and Love waves is widely used to study the structure of the Earth's crust and mantle. The dispersion of group and phase velocities of long-period surface waves ($T > 100$ sec.) depend, principally, on the distribution in the mantle of the body wave velocity and density. This dependence is determined from the comparison of observed and theoretical dispersion.

In the last years phase and group velocity for the long-period Rayleigh and Love waves have been determined in the period range 50-400 sec. by means of the seismograms and inclinograms of the four greatest earthquakes, recorded on the seismic stations "Moscow", "Pulkovo", "Simferopol", "Ashkhabad" etc. [1-3].

The epicentres, origin time and other information regarding these earthquakes are given in Table 1.

Table 1

List of earthquakes

No.	Region of earthquake	Date	Origin time	Epicentre		M
				φ	λ	
1	Chile	May 22,1960	19-11-20	38°0 S	73°0 W	8.5
2	Kuril Islands	Okt 13,1963	05-17-52	44°6 N	149°7 E	8.0
3	Alaska	March 28,1964	03-36-12	60°9 N	147°8 W	8.6
4	Aleutian Islands	Feb 4,1965	05-01-20	51°2 N	178°6 E	8.5

The values of the phase and group velocity of the Love waves have been obtained for the periods 80-390 sec as a result of processing of the inclinogram from the Chilean earthquake (station "Ashkhabad") and the seismograms of

the stations "Pulkovo", "Mundaring" etc. (Chile and Kuril Islands earthquakes). The inclinogram of the Chilean earthquake with the G-waves (U ≅ const. on T = 100-300 sec) multiple running around the Earth, is shown in Figure 1.

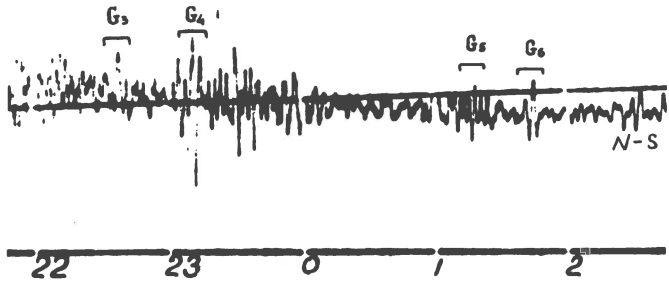

Fig. 1. The long-period Love waves several times circling the Earth (G_3-G_6), recorded by fotoelectric inclinometer by Ostrovsky from the Chilean earthquake of 1960 (component N-S, station "Ashkhabad"). The values in the lower part of the figure indicate the time.

Parts of a seismogram with G_4 and G_6 waves, recorded on a long-period Kirnos seismograph in Pulkovo, are shown in Figure 2 a.

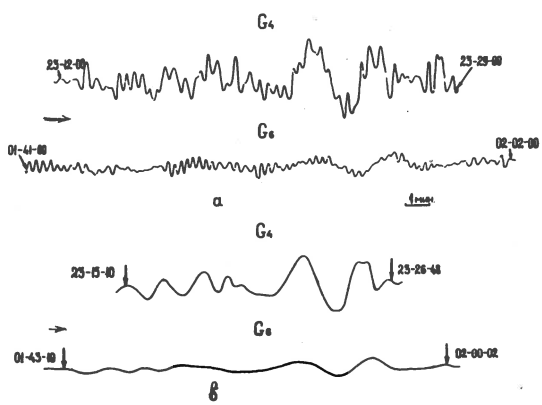

Fig. 2. Unfiltered (a) and digital low-pass filtered (b) waves G_4 and G_6 from the Chilean earthquake of 1960 recorded at Pulkovo by horizontal long-period Kirnos seismographs. The arrows designate the parts of the record subjected to spectral analysis.

Two successive passages of the same wave in the same direction are used for determining the phase velocities of G-waves. The phase velocities have been determined by spectral analysis. The waves were subject to digital filtering before the spectral analysis (fig. 2 b).

The group velocities of Love waves were computed from the phase velocities.

The values of the phase and group velocities of Love waves for periods 80-390 sec. are shown in Figure 3. The slight dependence of period for the group velocity of the G-waves is clearly seen.

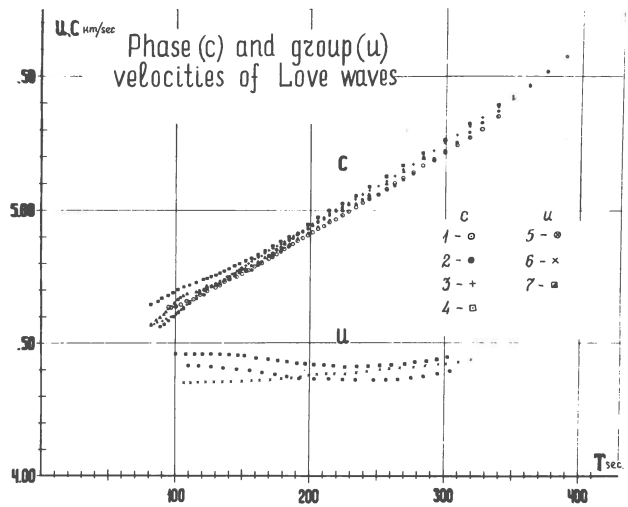

Fig. 3. Phase (C) and group (U) velocities of Love waves over great circle paths: Chile-"Pulkovo" (1,5); Chile-"Ashkhabad" (2,3,6); Kuril Islands-"Mundaring" (4,7).

The phase and group velocities of Rayleigh waves were determined earlier from the earthquakes 1,2 and 3 (Table 1) [1-3].

The Rayleigh waves $R_3 - R_7$ recorded from the Aleutian earthquake by the seismic station "Moscow" (long-period vertical seismograph) are shown in Fig. 4. The phase velocities were determined from waves R_5 and R_7, and R_3 and

R_5, by means of the phase spectra and direct measurements from the record. The differences between the values do not exceed 0.25 per cent. The group velocities were computed by usual technique [4].

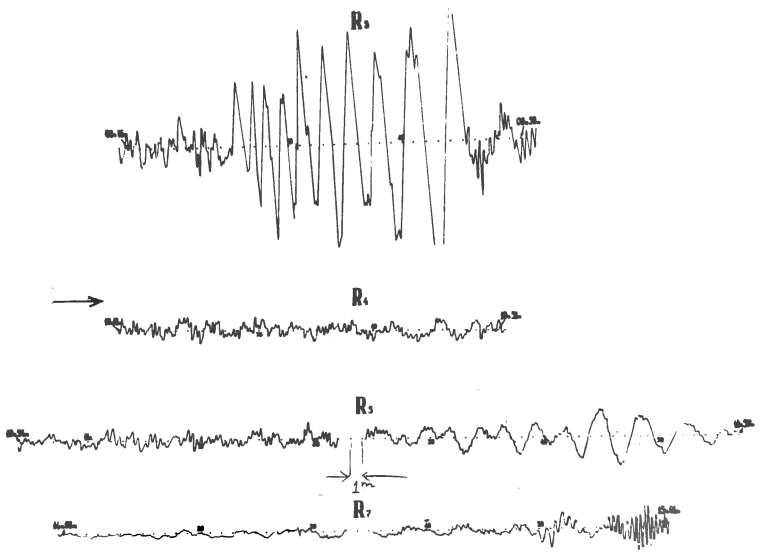

Fig. 4. Parts of seismogram with record of Rayleigh waves $R_3 - R_7$ of Aleutian earthquake (February 4, 1965) recorded by long-period vertical seismographs at station "Moscow". The points are minute-marks.

The values of the phase (C) and group (U) velocities of Rayleigh waves for the periods 50-400 sec from the four earthquakes (Table 1) are shown in Fig. 5. The group velocities in the field of anomalous dispersion ($T < 225$ sec) were determined with a mean square error $\sigma = \pm 0.04$ km/sec; in the field of normal dispersion ($T > 225$ sec) with a mean square error $\sigma = \pm 0.09$ km/sec. The phase velocities were determined with $\sigma = \pm 0.015$ km/sec.

The theoretical curves computed for the model Gutenberg - Bullen "A" give the better agreement with the experimental data of Rayleigh waves as indicated before [2,3]. The experimental phase velocities are smaller than the theoretical phase velocities in the period range 200-350 sec.

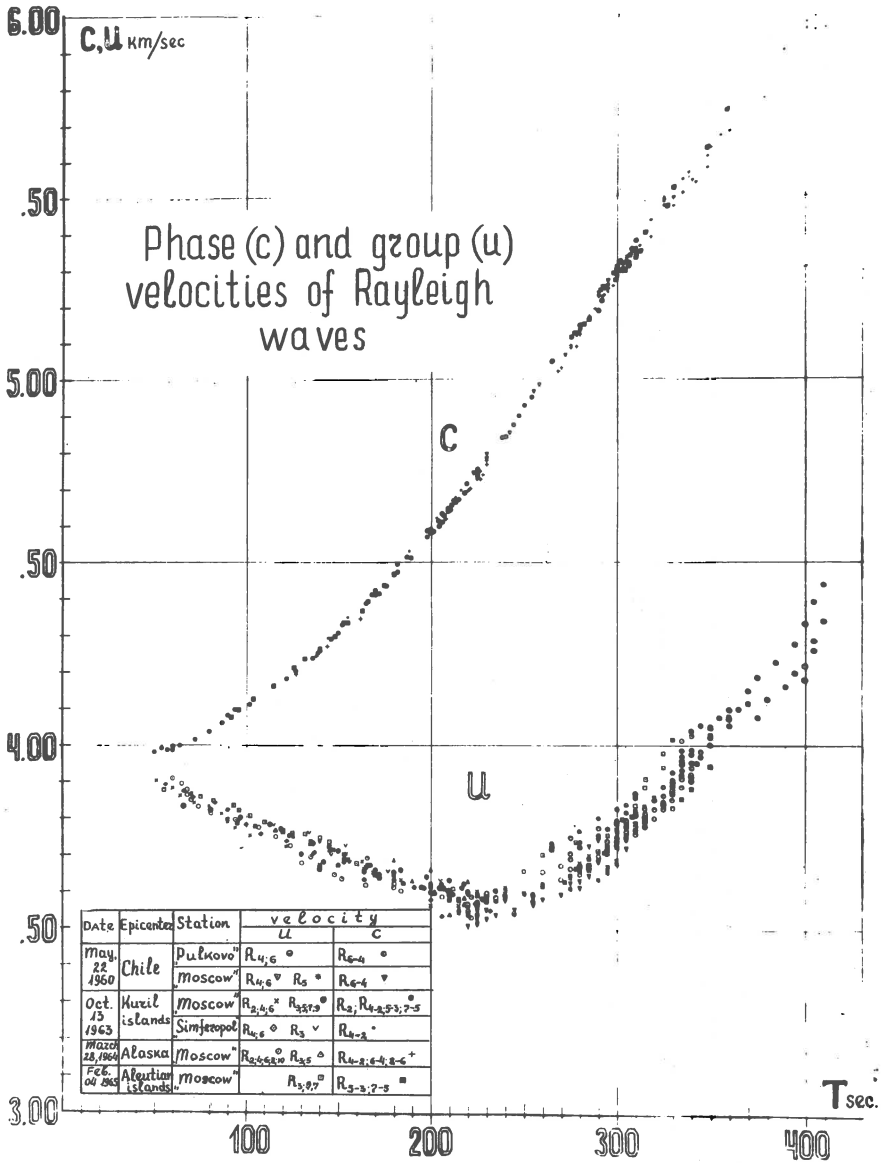

Fig. 5. Phase and group velocities of Rayleigh waves circling the Earth several times.

The differences between the observed (C_H) and theoretical (C_T) values of the phase velocities are shown in Fig.6.

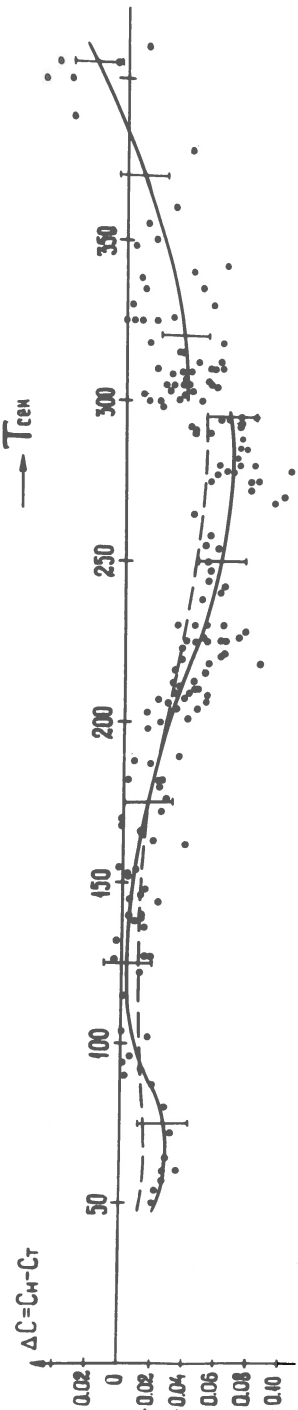

Fig. 6. The difference between the observed (C_H) and theoretical (C_T) values of the phase velocities of Rayleigh waves. The solid circles indicate the experimental dates, the solid curve the average experimental result. The vertical lines show the mean square error. The dashed curve shows the difference between the theoretical curve [5] and the curve computed by the authors after modification of Gutenberg's velocity distribution.

The solid line is the average experimental curve. The vertical lines show the mean square error.

The theoretical phase velocities of Rayleigh waves have been given by [5] (for $T < 300$ sec) and [6] (for $T > 300$ sec). This explains the rupture at the period 300 sec.

The difference $C_H - C_T$ is larger than the mean square error of the experimental data in the region of periods 190 sec to 350 sec (Fig. 6).

The observed data show that a slight modification of the model Gutenberg - Bullen "A" is necessary. The analysis of the partial derivatives of phase velocity with respect to physical parameter changes within the layers [5] has shown that the variations of the shear wave velocities have the largest influence on the phase velocity.

The best agreement with observed data have been obtained if the shear wave velocity decreases in average 0.06-0.09 km/sec in the range of depth 350 to 900 km. The shear wave velocity decreased 0.12-0.14 km/sec in the range of depth 450 to 500 km.

The theoretical curve was re-computed by means of the partial derivatives [5] after introduction of these changes. The dashed line (Fig. 6) corresponds to the difference between the old and the new theoretical curves.

The estimation of the influence of the variation of the shear wave velocity in the crust on the phase velocity for the periods 190 to 350 sec is interesting. If the shear wave velocity is changed 0.1 km/sec. in the depth 0 to 38 km, then the phase velocity at $T = 200$ sec. is changed 0.05 per cent; at $T = 295$ sec - 0.03 per cent; and at $T = 125$ sec - 0.1 per cent.

We must change the distribution of the shear wave velocity in such a way that the phase velocity does hardly change for the periods 100 to 150 sec. This may be obtained by changing the velocity in the Earth only on depths more than 350-400 km.

Note, that the velocity decrease found at the depth 350 to 900 km. is in agreement with the new distribution of velocity, which has been given by Gutenberg in 1959 [7] in the same range of depth.

The modification of Gutenberg's velocity is not the only explanation of the difference between observed and theoretical values of phase velocity. This interpretation have been realised without change of the distribution density (model Bullen "A") and the longitudinal wave velocity (the old model Gutenberg).

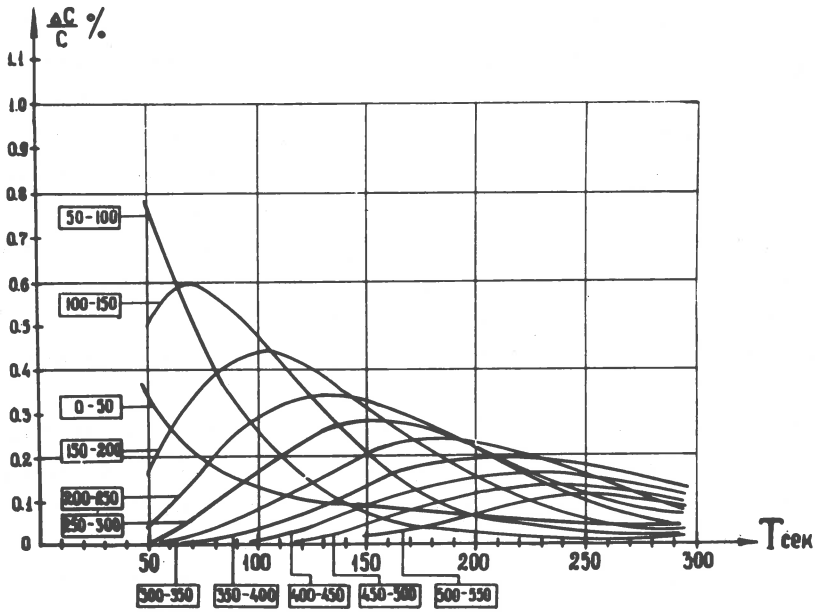

Fig. 7. Family of curves showing change of phase velocity of Rayleigh waves ($\Delta C/C$ in per cent) for periods 50-300 sec. produced by variation of the shear wave velocity of 0.1 km/sec. in layers of thickness 50 km. The framed values show the depth of layers.

The influence of the variation of the shear wave velocity at the various depths have been analysed in the process of the interpretation. This analysis can have general significance and some of the results are shown in Fig. 7. Let the variation of the shear wave velocity be 0.1 km/sec. The values $\frac{\Delta C}{C}$ in per cent at the various periods as produced by this change are shown in Fig. 7. Each curve corresponds to a 0.1 km/sec velocity variation within the layer thickness 50 km. The framed figures show the

depth. This family of curves shows for example, that at $T > 150$ sec. $\frac{\Delta C}{C}$ is more dependent of the variation of the shear wave velocity in the crust than of variation in layers on the depth 50 to 100 km.

A similar family of curves has been computed for Love waves. The analysis shows, that when the shear wave velocity is changed 0.1 km/sec. in the crust, the influence on the phase velocity of periods 150 to 220 sec. is the same as if the change in the shear wave velocity was made on the depth 100 to 150 km.

Literature

1. E.F.Savarensky, I.I.Popov, A.P.Lazareva: Nabljudenija dlinnoperiodnych voln Tjilijskogo zemletrjasenija 1960 g. Izv. AN SSSR, ser.geofizitjeskaja, nr.8, 1961.

2. E.F.Savarensky, O.E.Starovojt, S.A.Fedorov: Dlinnoperiodnyje volny Releja Aljaskinskogo zemletrjasenija 28 marta 1964. Izv. AN SSSR, ser.geofizitjeskaja, nr.12, 1964.

3. O.E.Starovojt: Fazovyje i gruppovyje skorosti dlinnoperiodnych voln Releja. Izv. AN SSSR, ser. Fizika Zemlji, nr.11, 1965.

4. E.F.Savarensky: Ob opredelenii gruppovoj i fazovoj skorosti iz nabljudenij. Izv. AN SSSR, ser. geofizitjeskaja, nr.11, 1959.

5. Takeuchi, Dorman, J., Saito, M.: Partial derivatives of surface wave phase velocity with respect to physical parameter changes within the Earth. Journal Geoph.Res. v.69, nr.16, 1964.

6. Z.Alterman, H.Jarosch, H.L.Pekeris: Rasprostranenije relejevskich voln v Zemlje. Sb.Perev. "Sobstvennyje kolebanija Zemlji", M., 1964.

7. B.Gutenberg: Astenosfernyj sloj ponzhennoj skorosti. Sb.Perev. "Verchnjaja mantija Zemlji", M., 1964.

B.N.Schechkov

SEISMIC SURFACE WAVES AND TECTONICS OF EURASIA

During some years the writer analysed the dispersion of velocities for surface waves for traces, crossing almost all regions of Eurasia [1-10].

Both group and phase velocities of the fundamental mode of Love and Rayleigh waves with periods 10-60 sec were determined at distances of 200-8000 km. The records of surface waves were analysed for more than 500 earthquakes, which were situated inside the continent or on its borders.

In this note we have considered the use of group velocity dispersion for a large number of traces, intersecting some tectonic blocks. The aim of the study is to obtain the local dispersion in these blocks and data about the crustal structure.

We used the idea of Santo [11-12] about determination of the boundaries between areas from observed surface wave dispersion. The writer of this article determined beforehand the boundaries of blocks, homogeneous in a tectonic sense [13], and calculated the corresponding dispersion curves.

Let us shortly consider this method. If the surface waves intersect two blocks 1 and 2 with different crustal structure, the resulting group velocity may be obtained from the following simple equation:

$$\frac{\Delta_1}{V_1} + \frac{\Delta_2}{V_2} = \frac{\Delta}{V} = t(T) \qquad (1)$$

where V_1 and V_2 are the group velocities corresponding to blocks 1 and 2. If we have some blocks (n) and a large number of traces (m), then one can make up a system of linear equations for each period T_o of the surface waves:

$$\frac{\Delta_{11}}{V_1} + \frac{\Delta_{21}}{V_2} + \cdots + \frac{\Delta_{n1}}{V_n} = t_1(T_o)$$

$$\cdots\cdots\cdots\cdots\cdots\cdots\cdots\cdots \qquad (2)$$

$$\frac{\Delta_{1m}}{V_1} + \frac{\Delta_{2m}}{V_2} + \cdots + \frac{\Delta_{nm}}{V_n} = t_m(T_o)$$

This is correct in the case where the character if dispersion is the same along each trace in each block. Practically this condition is fulfilled, because the tectonic blocks are chosen according to approximately identical crustal structure inside the blocks. In equation (2), for example, Δ_{21}, is the length of the part of the trace with epicentre 1, which corresponds to block 2; V_2 is the group velocity of the surface waves in block 2; $t_1(T_o)$ is the travel time of the surface waves with period T_o for trace 1. From these equations one can calculate $V_1 \cdots V_n$ for a given period by means of the least square method. And the same can be made for other periods.

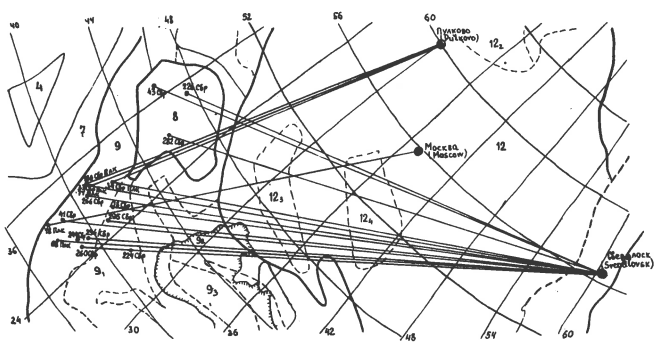

Fig. 1. The epicentres, seismic stations and traces of surface waves for case A_2. 8) Hungarian basin, 9) the Balkans, 12) the Russian platform.

Let us consider two examples to illustrate the application of the given method for Eurasia. Fig. 1 shows the traces of surface waves, intersecting 3 large blocks: The Balkans, the Hungarian basin (8) and the Russian platform (12) (case A_2). The dispersion of the group velocity of Love

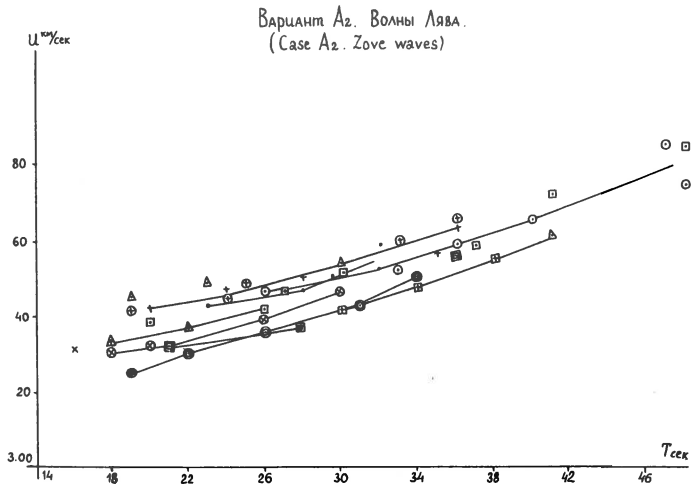

Fig. 2. The group velocities for Love waves for all traces used in the case A_2 (the different signs correspond to different traces).

waves for these traces is shown on Fig. 2. On Fig. 3 the calculated velocities for the three blocks are shown. The velocities are calculated for T = 20, 25, 30 and 35 sec. Table 1 gives the initial data for the calculation of dispersion for T = 30 sec.

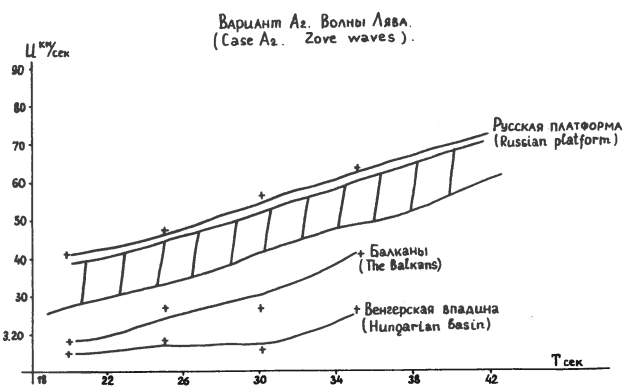

Fig. 3. Group velocities for three blocks (8, 9, 12 see Fig. 1), calculated by means of the least squares method. Shading is velocities for all traces crossing the Russian platform.

Table 1

No.of earth-quakes	Δ_8 km	Δ_9 km	Δ_{12} km	t sec
224 Svr	0	752	2276	885
260 Svr	0	1075	2293	961
294 Svr	0	989	2333	950
244 Svr	0	1059	2333	961
68 Plk	230	969	1302	748
33 Svr	0	859	2525	988
22 Svr	0	993	2351	957
18 Svr	0	729	2470	923
41 Svr	0	1167	2351	1008
34 Svr	0	742	2495	934
43 Svr	494	124	2566	912
48 Msk	0	1144	1222	693
34 Plk	363	444	1269	607
74 Plk	543	418	1242	649
180 Svr	0	859	2525	985
33 Plk	543	418	1242	646
265 Svr	0	902	2487	960
282 Svr	347	77	2546	839
295 Svr	0	849	2351	910

Svr: Sverdlovsk, Plk: Pulkovo, Msk: Moscow.
Calculated group velocities: $V_8 = 3.27$; $V_9 = 3.41$; $V_{12} = 3.63$ km/sec. The mean square deviation of t: 11.6 sec.

From Fig.3 one can see, that the velocities for the Russian platform are considerably higher than velocities for the Balkans. This means, that the crust on the platform is thinner than on the Balkans. It is impossible to understand the small values of velocity for the Hungarian basin, that contradict the modern geophysical data. Great errors might have occurred due to insufficient data for the block (Fig. 1 and Table 1 show, that this block is intersected only by six short parts of traces). These small values of group velocities could also be explained, if the average velocity

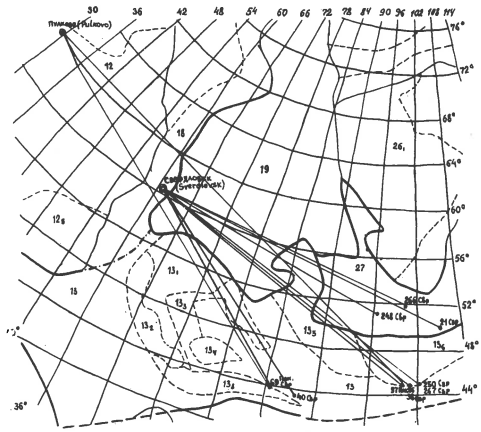

Fig. 4. The epicentres, seismic stations and traces of surface waves for case P_3. 12) Russian platform, 19) West-Siberian depression, 27) Pribaikal area, 13) Kazachstan, Mongolia.

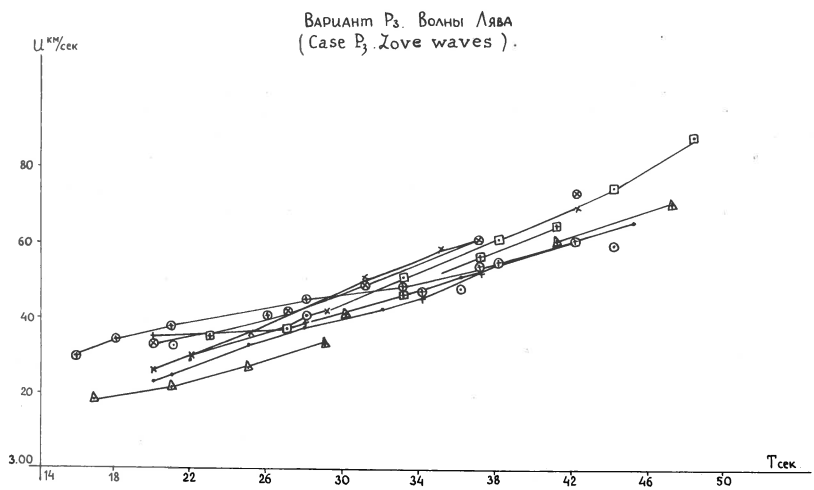

Fig. 5. Group velocities for Love waves for all traces used in the case P_3 (the different signs correspond to different traces).

of shear waves in the crust and mantle for the Hungarian basin were equal, about 3.1 and 4.2 km/sec for the thickness of 25 km for the crust [14, fig. 33, 47]. But this

is unlikely. As an explanation to this fact it is necessary to add additional data. On Fig. 6 are compared the group velocities for the Russian platform, calculated in case A_2, in case P_6 (which is obtained from case A_2 after removing traces crossing the Hungarian basin) and in case P_3 (the traces and the dispersion for this case are shown on Fig. 4, 5).

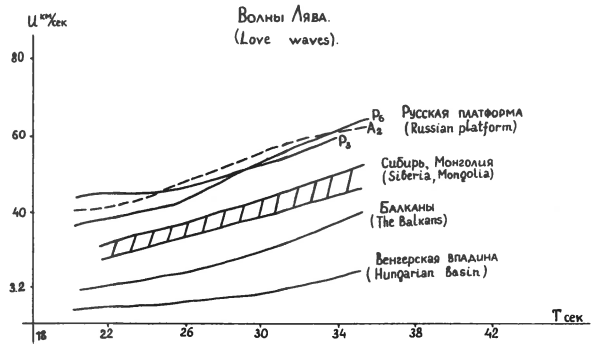

Fig. 6. Comparison between calculated group velocities for blocks considered in cases A_2, P_6 and P_3. The velocity for the Russian platform, calculated in these cases, agree. The velocities for the West-Siberia depression, the Pribaikal area and Kazachstan, Mongolia are almost the same. 1) Russian platform, 2) Siberia, Mongolia, 3) the Balkans, 4) The Hungarian basin.

From Fig. 6 one can see that the velocities for the Russian platform, obtained by use of different cases of combination traces, agree well enough. Below on the graph are shown the velocities for Kazachstan and Mongolia (13), the West-Siberia depression (19), the Pribaikal area (27), and the Balkans and Hungarian basin. This method of calculation of group velocities will be applied for the whole Eurasia.

Bibliography

1. E.F.Savarensky, O.N.Solovjeva, B.N.Schetjkov: O nabljudenijach voln Ljava na moskovskoj sejsmitjeskoj stantsij i strojenije zemnoj kory. Izv., AN SSSR, ser.geofiz, 1959, nr.5.

2. B.N.Schetjkov: Strojenije zemnoj kory v Evrazii po dispersii poverchnostnych voln. Izv., AN SSSR, ser.geofiz, 1961, nr.5.

3. E.F.Savarensky, B.N.Schetjkov: Strojenije zemnoj kory Sibiri i Daljnego Vostoka po dispersii poverchnostnych voln. Izv., AN SSSR, ser.geofiz., 1961, nr.5.

4. B.N.Schetjkov, O.N.Solovjeva: O gruppovych skorostjach relejevskich voln dlja smeschannogo puti kontinent-okean. Izv., AN SSSR, ser.geofiz., 1961, nr.8.

5. B.N.Schetjkov, O.I.Jurkevitj: Opredelenije tolstjiny zemnoj kory na Ukrainskom kristallitjeskom massive po dispersii poverchnostnych voln. Geofizitjeskij sbornik, 1962, nr. 1(3), s.75-78.

6. Schechkov, B.N.: Crustal structure of the Eurasia from dispersion surface seismic waves. Abstr.Papers, Intern.Ass.Seism. and Phys. Earth's Inter., Berkeley, USA, 1963, B-61.

7. V.B.Glasko, E.F.Savarensky, B.N.Schetjkov: Dannyje o fazovych i gruppovych skorostjach poverchnostnych sejsmitjeskich voln. Izv., AN SSSR, ser.geofiz., 1963, nr.10.

8. B.N.Schetjkov: Dispersija poverchnostnych sejsmitjeskich voln i strojenije zemnoj kory Evrazii. Izv., AN SSSR, ser.geofiz., 1964, nr.3.

9. Schechkov, B.N.: The use of surface seismic waves for the determination of crustal structure in Eurasia. Veröffentlich. d. Inst. für Bodendynamik und Erdbebenforschung in Jena, 1964, heft 77, s. 177-183.

10. E.F.Savarensky, B.N.Schetjkov: O vyjavlenii variatsij tolstjiny zemnoj kory gruppovym skorostjam sejsmitjeskich voln. Izv., AN SSSR, Fizika Zemlji, 1965, II, s.63-66.

11. Santo, T.A.: Division of the south-western Pacific area into several regions in each of which Rayleigh waves have the same dispersion characters. Bull.Earth. Res.Inst., Univ.Tokyo, 1961, v.39, pt.4, p.603-630.

12. Santo, T.A.: Division of the Pacific area into seven regions in each of which Rayleigh waves have the same group velocities. Bull.Earth.Res.Inst., 1963, v.41,4, p.719-732.

13. Tektonitjeskaja karta Evrazii pod redaktsijej A.L. Janschina, M., "Nauka", 1966.

14. Jamaguchi, R., Kizawa, T.: Surface waves and layered structures. Bull.Earth.Res.Inst., 1961, v.39, p.669-809.

S.E.Pirhonen

GROUP VELOCITY OF SURFACE WAVES IN FINLAND DETERMINED BY CURVE FITTING

Abstract

The group velocities of Rayleigh and Love waves between the Finnish stations NUR and KEV have been computed. A polynomial of the fourth degree has been fitted to the travel times of surface waves determined by the "peak and trough" method. By differentiation of this polynomial the group velocity dispersion curve has been computed. From the fitted polynomials of different stations placed on about the same great circle as the epicentre, the group velocities between these stations have been determined.

The group velocities of surface seismic waves are generally determined by the graphical method, the arrival times of the peaks and troughs of surface waves being plotted as a function of their ordinal number. The plotted points are fitted by the free-hand method to a continuous curve, from which the arrival time of a certain period is obtained by graphical differentiation. In this study the curve fitting is made by the method of least squares. In this way the subjective influences of the graphical method can be eliminated and all calculations can be performed with a digital computer.

The fitting was made in coordinates where the ordinal number was on the abscissa and the origin was selected in such a way that the numerical solution of the normal equation of the method of least squares did not lose accuracy in computation. In some trials it has been proved that the polynomial of the fourth degree gives a reliable approximation of the travel time curve of surface waves in the normally observed period interval 18-60 sec. However, if the observed points are too irregular or too few, the polynomial fitting tends to lead to distorted results.

Good data for testing the fitting method have been obtained from the surface waves of Greek earthquakes registered at the standard stations Nurmijärvi and Kevo. Because the epicentres and these stations lie on about the same great circle of the Earth, the same differential procedure which Savarensky and Schechkov (1965) have used can be applied to group velocities. It is possible to compute by numerical iteration the travel time of period T to both stations. Then the group velocity is

$$U(T) = \frac{\Delta_2 - \Delta_1}{t_2(T) - t_1(T)} ,$$

where Δ and t mean epicentral distance and travel time respectively and indices 1 and 2 the stations NUR and KEV respectively.

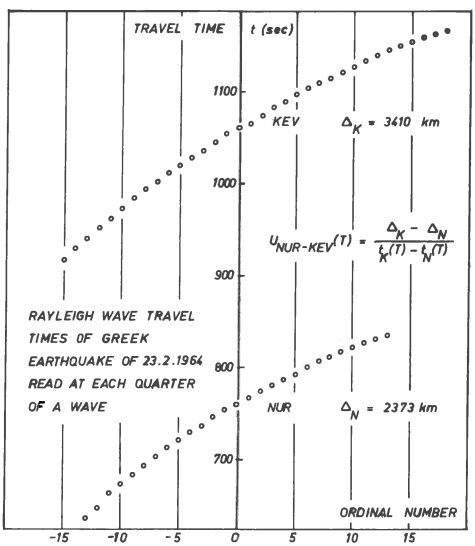

Fig. 1

Figures 1 and 2 present graphically the data and results of a good example of differential group velocity determination. The origin of the ordinal number has been removed to the middle of the data points. The standard deviations of the fitted polynomials of the fourth degree were 0.80 sec at NUR and 0.82 sec at KEV. The travel times of different

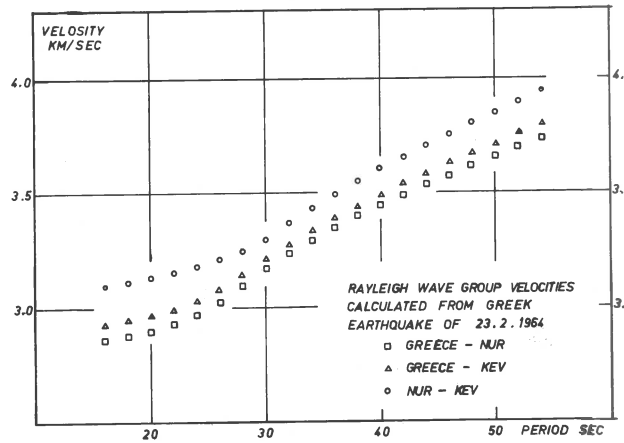

Fig. 2

whole periods to NUR and KEV have been sought by iteration from the derivatives of the polynomials. After this it is easy to calculate group velocities on the paths Greece-NUR, Greece-KEV and NUR-KEV. These dispersion curves are presented in Fig. 2.

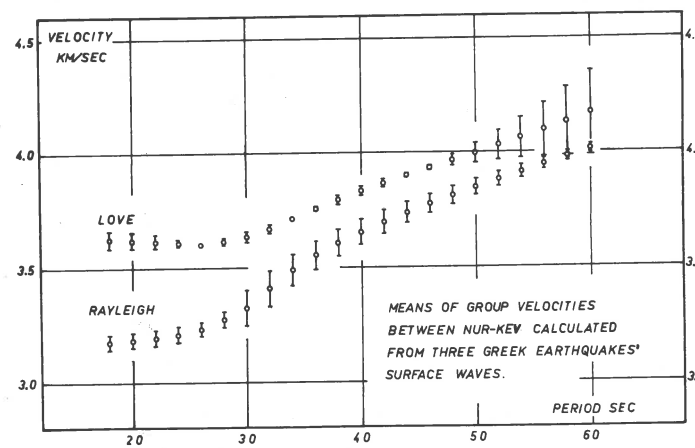

Fig. 3

This fitting method also has the advantage that one can compute the mean of group velocity dispersion curves. It has been possible to select three good Rayleigh and Love wave trains from Greece to NUR and KEV. The group velocities between NUR and KEV are computed and the means taken. The results and standard deviations of the means are pre-

sented in Fig. 3. It is seen that the deviations fluctuate with the period, which is partly due to the polynomial fitting. Because the data points do not extend outside the period interval 18-60 sec, the fluctuation reflects the boundary effects in fitting.

This same data has been used by Noponen (1966) in the determination of phase velocities between NUR and KEV. It is interesting to compare the group velocities obtained with the phase velocity results. The theoretical dispersion curves were calculated for a layer model UL056 in Finland. This model gives the compatible dispersion curves with the observed phase velocities of Rayleigh and Love waves (Noponen et al., 1966, Fig. 2 and 3). The respective theoretical group velocities agree reasonably well with the observed group velocities, which shows that the polynomial fitting method gives reliable results at least with the data used here. The discrepancy in periods under 25 sec between theoretical and observed group velocities in both Rayleigh and Love waves is remarkable. This is partly caused by the boundary effect of the fitting method, but perhaps we must also revise the earth crust model. It should be noticed that the derivative of the phase velocity curve is critical in these periods. The meaning of the discrepancy must be left for interpretation in future studies.

References

Noponen, Ilkka (1966): Surface Wave Phase Velocities in Finland. Bull.Seism.Soc.Am. 56, 1093-1104.

Noponen, I., M.T.Porkka, S.E.Pirhonen and U.Luosto (1967): The crust and mantle in Finland. Papers presented at the 9. Assembly of the ESC.

Savarensky, E.F. and B.N.Schechkov (1965): On the Determination of Variations of Thickness from the Group Velocities of Seismic Waves. Izv.Acad.Sci. USSR, Physics of Solid Earth, 11, 751-753 (English edition).

Yvonne Beaufils

EXPERIENCE DU LAC BLANC

En 1964, sous la présidence du Professeur Cloos, la "Sous-Commission des Explosions Alpines" a organisé une série de tirs de 0,2 à 10 tonnes dans un lac des Alpes Suisses: le Lac Blanc, situé à environ 140 km S-E de Bâle à une altitude de 2 300 m.

Ces tirs se sont déroulés entre le 29 Juin et le 9 Juillet.

13 équipes appartenant au Laboratoire de Physique de l' Ecole Normale Supérieure et au Commissariat à l' Energie Atomique ont participé aux expériences sur un profil en direction des Vosges: 5 équipes ont été réparties sur le territoire suisse, couvrant une distance de 110 km, en 17 points d'enregistrement; en France, 8 équipes ont parcouru un profil long de 145 km, obtenant des enregistrements en 29 points.

La station la plus éloignée du point de tir se situe à l'Est de Nancy, soit à une distance de 293 km.

Appareillage

Un appareillage homogène a été utilisé.

La chaîne d'enregistrement comprend: un séismographe miniature et son amplificateur, mis au point au Laboratoire de Physique de l' Ecole Normale Supérieure, un enregistreur 2 voies à moteur synchrone de tension 110 ou 220 volts. Pour l'autonomie de l'ensemble, un convertisseur alimenté par une batterie de 6 ou 12 volts est utilisé.

La seconde des voies de l'enregistreur, permet l'inscription des signaux horaires émis en quasi permanence par la station radio de Nauen. Par mesure de précaution, en cas de silence dans l'emission Radio, un topeur relié à un chronostat de précision, assure une base de temps.

La gamme de vitesse du dérouleur de papier est étendue: 7 vitesses sont possibles par combinaison de couples de pignons - lors des expériences, la vitesse de 25 mm/sec. a été utilisée.

L'ensemble de l'appareillage pèse approximativement 50 kg; il tient facilement dans une malle ou à l'arrière d'une voiture.

Amplification

L'amplification de la chaîne séismo, amplificateur et enregistreur, est de $1 \cdot 10^6$ à 1 Hertz, son maximum se trouve à 6 Hertz où le gain atteint $4{,}5 \cdot 10^6$. Pour des tirs de 200 kg, des équipes se trouvant à des stations, où le bruit de fond était très faible, ont pu utiliser la plus grande amplification - de beaux enregistrements ont été obtenus à des distances de l'ordre de 200 km.

Les coordonnées des stations ont été relevées sur des cartes 1/20 000e, les distances calculées à l'aide d'une machine électronique M.Dassault.

L'altitude de certaines stations principalement en Suisse étant élevée une correction a été appliquée afin de réduire les temps d'arrivée à l'altitude zéro.

Position des stations

Les 2 premières stations situées respectivement à 16 et 33 km, se trouvent sur le massif de l' Aar. Des difficultés dues au relief du terrain n'ont pas permis de suivre le projet initial, lequel avait prévu des stations espacées seulement de 5 en 5 km. A ces deux emplacements, les séismos reposent directement sur le granite qui affleure largement le massif.

La station suivante n'a pu être installée qu'au point 55 km, toujours en raison des difficultés d'accès, elle se trouve dans les Préalpes Suisses.

Ensuite, les distances entre les stations sont plus régulières, elles varient de 5 à 7 km sur tout le parcours.

Onde Pg

A partir du point d'enregistrement 55 km, l'hodochrone de l'onde Pg commence à montrer des anomalies de temps d'arrivée, causées par la structure sous-jacente; ce retard de temps dans la propagation s'accentue à partir du plateau Suisse, entre 67 et 112 km, où plusieurs kilomètres d'épaisseur de molasse donnent un retard d'arrivée de l'onde Pg allant jusqu'à 1,3 seconde, ceci à 78 km du point d'explosion.

Avec le Jura, ces retards se réduisent; à partir de la latitude de Bâle et jusqu'aux dernières stations, l'hodochrone de l'onde Pg est défini par une droite passant par l'origine et les points représentatifs des stations de 16 et 33 km.

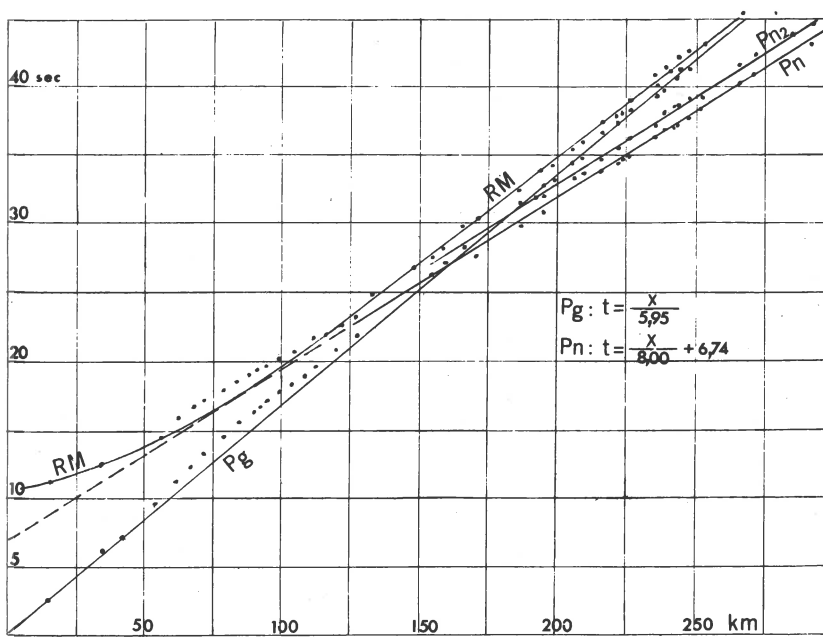

Figure 1. Hodochrone.

L'équation de cette droite est:

$$Pg = \frac{\Delta}{5,95}$$

Onde Pn

L'onde Pn arrive en tête d'enregistrement à partir de 150 km, cependant, son amplitude ne devient nette que dans la partie Nord du massif Vosgien - c'est du reste dans cette région que des tirs de 200 kg ont été enregistrés, comme il a été indiqué précédemment. La droite définissant la vitesse moyenne de l'onde Pn est de 8,02 km/sec. avec un intercept de l'axe des temps de 6,74 secondes.

Onde Pn_2

Une arrivée d'onde que l'on peut retrouver sur presque tous les enregistrements à partir de 150 km se produit 1,3 seconde après l'arrivée de Pn. Cette onde a été considérée comme une réflexion se produisant près de la source; en effet, à 4 km Sud-Est du Lac Blanc, se trouve un massif gneissique d'étendue considérable qui forme le noyau de la nappe d'Antigorio - Monte-Leone.

On peut imaginer l'arrivée d'un front d'ondes émis par le tir, sur une paroi verticale de ce massif, d'où la réflexion de l'onde qui suit alors la Pn avec cet écart de temps de 1,3 seconde.

Mohorovičić

Le schéma représentatif de la profondeur du Moho sous le profil a été étudié - d'une part par les temps d'arrivée de l'onde réfléchie de vitesse 5,95 km/sec., ceci entre 15 et 120 km de point de réflexion, c'est-à-dire à des stations se trouvant entre 16 et 240 km du point de tir - d'autre part à l'aide du temps de propagation de l'onde réfractée.

Onde Réfléchie

Dans un premier calcul de la profondeur du Moho, on a admis pour chaque temps d'arrivée, une réflexion sur un miroir horizontal. Connaissant, la distance, la vitesse et le temps de propagation, le niveau du Moho a été calculé par l'équation:

$$h = \frac{1}{2} \sqrt{v^2 \cdot t^2 - \Delta^2}$$

Ayant observé un pendage assez important entre les Préalpes et le plateau Suisse. et craignant de ne pas obtenir par la méthode employée précédemment une image réelle de la forme du Moho un second calcul a été fait en prenant les temps de propagation par couple de stations et faisant varier le pendage de façon à retrouver les temps observés. Les résultats par ce mode de calcul sont très peu différents de ceux obtenus précédemment, l'on observe simplement un léger décalage horizontal en direction du point de tir.

Onde Réfractés

La propagation des ondes réfractées a également été étudiée. La connaissance de la vitesse moyenne de propagation, déterminée expérimentalement, permet de voir de légères différences entre le temps moyen et le temps réellement observé. Ces différences sont attribuées à des différences d'épaisseur de la croûte, d'où l'on calcule très simplement le profil résultant du Moho.

Conclusion

Les résultats obtenus, aussi bien à l'aide des ondes réfléchies que par les ondes réfractées, sont représentés sur le graphique montrant la coupe de la croûte terrestre entre le Lac Blanc et Nancy.

Entre 8 et 50 km, le Moho aurait une profondeur de l'ordre de 35 km, on trouve ensuite un pendage ascendant de 22%, ce qui conduit à une distance d'une centaine de kilomètres du point de tir, c'est-à-dire près de la limite du plateau Suisse et du Jura où l'on trouve une profondeur de l'ordre de 24 km.

Ensuite l'on observe de légères fluctuations avec un maximum de profondeur de 28 km au début du massif des Vosges - puis une remontée assez brusque nous fait à nouveau trouver 24 km. Enfin un enfoncement nous donne, jusqu'aux dernières observations, un Moho de l'ordre de 26 km. Cette profondeur, dans les Vosges variant de 24 à 26 km a été confirmée par des tirs de 100 à 200 kg de dynamite déposée dans des forages autour de nos 3 stations des Vosges, en vue de les tester.

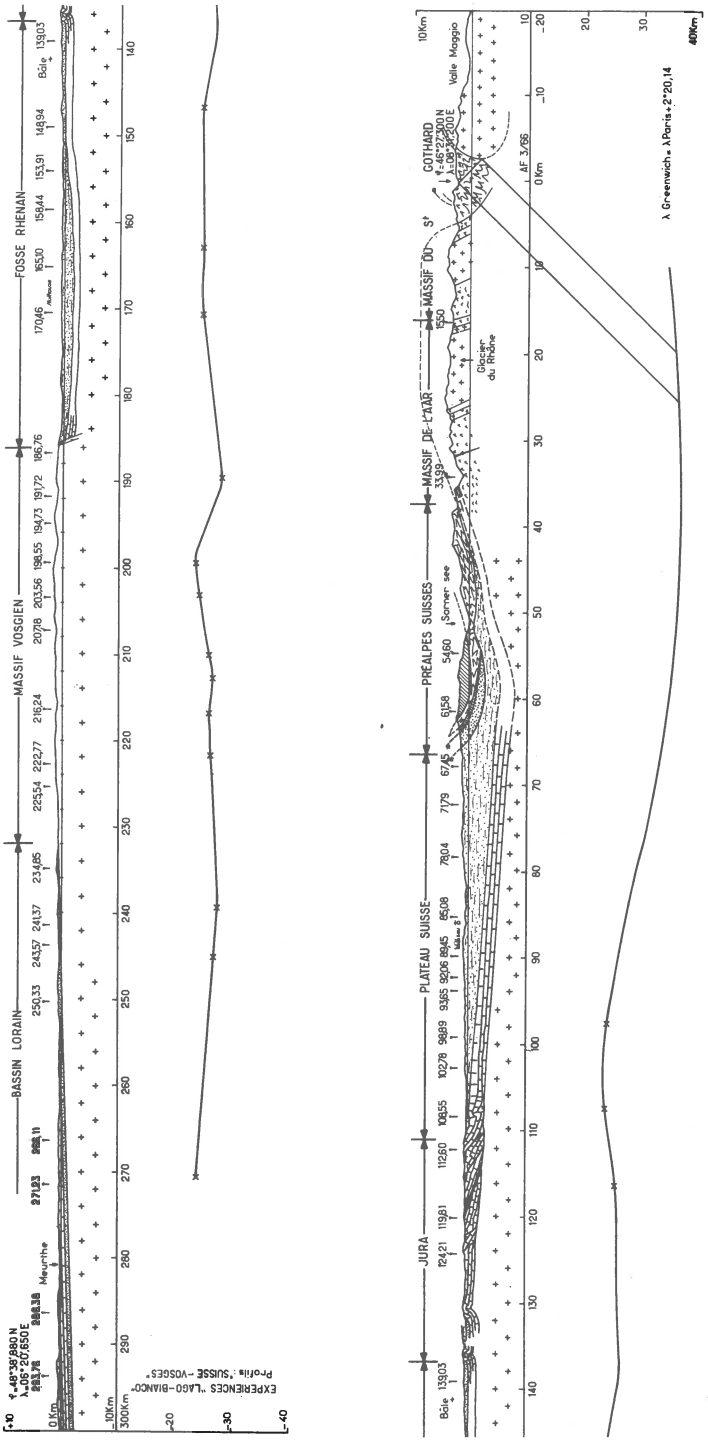

Figure 2. Coupe géologique du profil à fractionner pour obtenir les réductions voulues.

Nous avons profité de ces expériences pour former des profils d'une dizaine de stations échelonnées, entre 15 et 150 km des points de tir, les résultats nous ont permis de déterminer avec certitude la profondeur du Moho dans cette région.

Hans-Jürgen Dürbaum, Jürgen Fritsch and Heinz Nickel

DEEP SEISMIC SOUNDING IN THE EASTERN PART OF THE RHENISH MASSIF

In the iron-ore province of the Siegerland in the eastern part of the Rhenish massif, various geophysical methods have been employed to obtain more exact ideas about the source of the ores, and thus additional means to find new iron ore lodes worth to be exploited. In the last period of these investigations, also the reflection seismograph has been introduced. The survey remained, with respect to its original task, practically without result because of the lack of reflected energy from within the uppermost few kms, but quite unexpectedly at that time (1958), relatively late seismic events with reflection times between 5 and 10 s were observed on part of the seismograms [1]. With longitudinal wave velocities between 5 and 6 km/s in the uppermost 5 kms, the seismic information could come from depths of reflecting horizons between 12 and 30 kms. The Siegerland was one of the first places where such late nearly-vertically reflected events had been observed and where, due to the lack of good reflections from shallow depths, doubt about the character of these events were less than in other places. - From 1963 to 1965 the Bundesanstalt für Bodenforschung with the help of the Forschungsgemeinschaft Seismik e.V. tried to utilize these possibilities to find out possible relations between shallow tectonics known from surface and subsurface geologic studies, and deep tectonics. In order to resolve deep tectonics it had to be tried to obtain practically continuous information from reflecting horizons at great depths. It is quite evident that - with exceptions certainly - optimum recording conditions would be necessary to achieve that aim. - During this survey also special investigations have been carried out to obtain some additional material about the character

of the late seismic events. In the following the experiences and results of this survey are briefly reviewed.

The area of the survey is mountainous and cut to pieces by many meandering river valleys without any well-preferred trend - these valleys being highly industrialized and inhabited. On the highlands the Devonian slates and greywacke are only covered by a layer of a few meters of weathered material so that recording conditions here were excellent if there would not be so many high voltage powerlines. Continuous profiling would be mandatory to solve the tectonic problems; the need for optimum recording conditions limits the investigations to a certain part of the highlands if the expenses should not be prohibitive. It has been tried to obtain comparable results as by continuous profiling narrowing the gaps by a suitable arrangement of shotpoints and recording locations and applying correlation techniques to the data after digitization. Noise analyzing, in advance checking possible recording positions for disturbing electric "noise" and the use of active 50 cps filters should further have helped to improve the data. - Charges were between 60 and 120 kg, distributed in 3 holes at a depth of 20 m, within unweathered rock. Recording amplifiers were ETL M5; 11 traces with 50 m between take-outs; 8 geophones per trace at 5 m distances; no mixing. - In the major part of the area under survey records of good quality with events between 5 and 10 s were obtained. Where the chance existed to record a continuous profile of several kms length under optimum conditions, generally satisfying continuous results are to be reported. Possible explanations of the varying quality of the records as e.g. by focussing effects will be discussed in a later publication in detail. But it is to be stated here that focussing effects are not at all the only cause that these near-vertical reflections could be recorded.

Fig. 1 displays the section between 5 and 7 s of 4 seismograms from this area. They reveal a band of several more or less high amplitude seismic events over this portion of the seismograms. Fig. 2 shows the respective position of

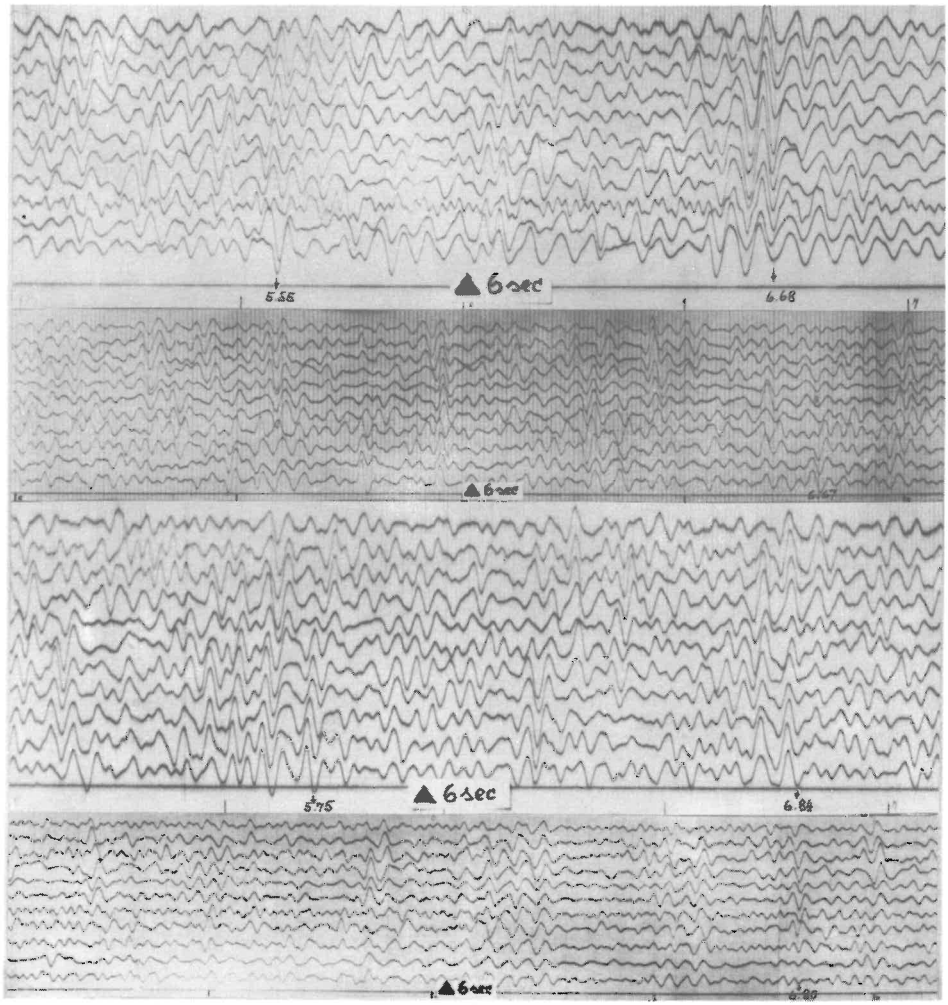

Fig. 1

the reflecting elements under the assumption of the reflectors being horizontal. Fig. 3 presents the results of a statistical analysis of the seismic events of the recorded 82 seismograms. Nearly 60% were recorded up to a time of 12 s, one third longer than 14 s. The reflection band between 5 and 7 s is clearly recognized in the statistical curve. A closer look at Fig. 1 will make evident that a correlation between these seismograms should be pos-

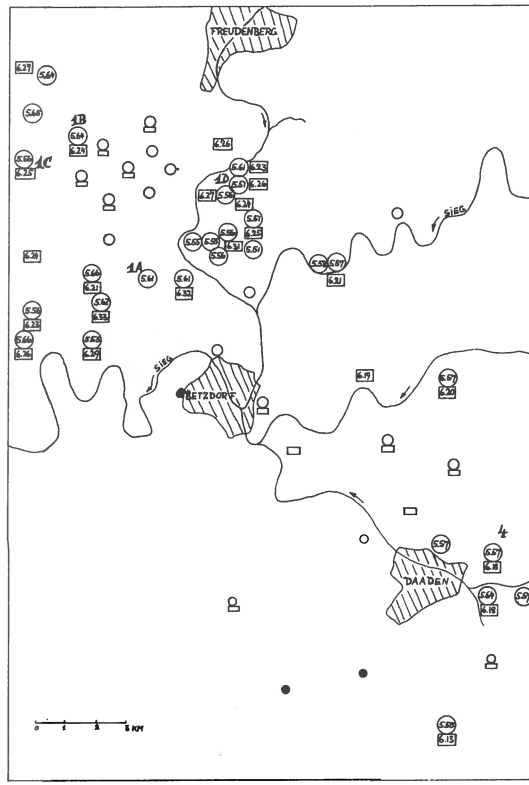
FREUDENBERG
SIEG
SIEG
BETZDORF
DAADEN
1A
1B
1C
1D
4
0 1 2 3 KM

Fig. 2

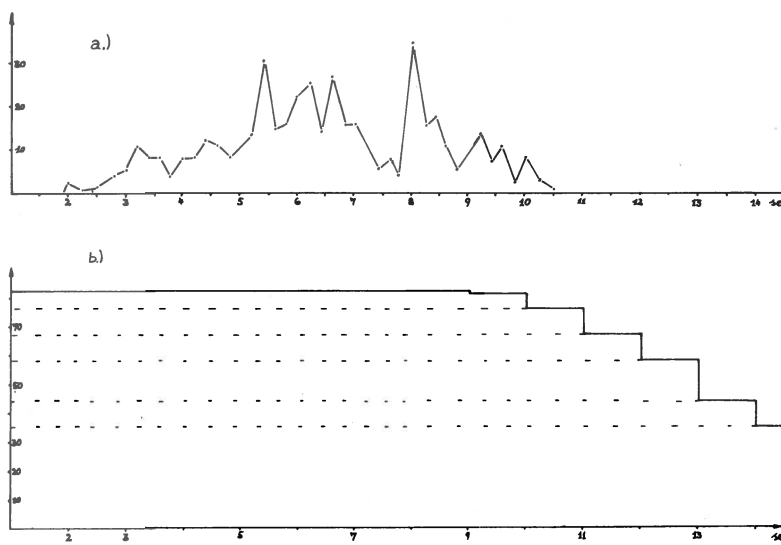
a.)
b.)
sec

Fig. 3

sible. Not all the events are of the same quality on the seismograms, but it appears to us that the comparison of the ensemble supports our correlation. Fig. 2 gives the results of a correlation of this band of reflections over the area under survey. Reliable reflections in this time-interval have been recorded where reflecting elements have been marked by circles or rectangles. Where arrival times have been filled in into these circles or triangles resp., a specific reflection of the 5-7 s band was clearly recognizable. Arrival times have been approximately corrected for topography. Black circles stand for locations where reliable deep reflections have been recorded, but not within the 5-7 s time interval.

There is another reflection band observed in the statistical curve around 8.2 s, but this is very pronounced and narrow contrary to the broad several peak reflection band between 5 and 7 s.

The possibility of these high amplitude reflections to be multiples has been excluded due to the result of the following experiment: Several seismograms were recorded at the same position without automatic gain control with increasing charges. These seismograms consist of two parts: the first one because of overloading of the amplifiers is useless; in the second portion amplitudes which differ by a factor 2-3, may be compared because of the piecewise linearity of the amplification curve of the amplifiers. Using the various records the events between 1.5 and 10 s could be compared. The amplitudes of the 8.5-reflection and of a few reflections of the 5-7 s band were greater than the amplitudes of all other reflections with arrival times greater than 2 s. - Also experiments of azimuthal recording after Gamburzew and Galperin have been carried out. Six geophone groups were placed at azimuths 0, 60, 120, 180, 240 and 300 degrees with respect to the direction towards the shotpoint on a circle of 1.5 m diameter and with an inclination of 45° with respect to the vertical. Longitudinal waves with their direction of propagation inside the cone which is set up by the geophones are characterized by all the traces being in phase. Linearly

polarized transverse waves would subdivide the cone into two parts which are of opposite phase. The azimuthal seismogram reproduced as Fig. 4 shows that the 8.6 s-reflection is a strong longitudinal event. The other events are not so good to be studied on this one.

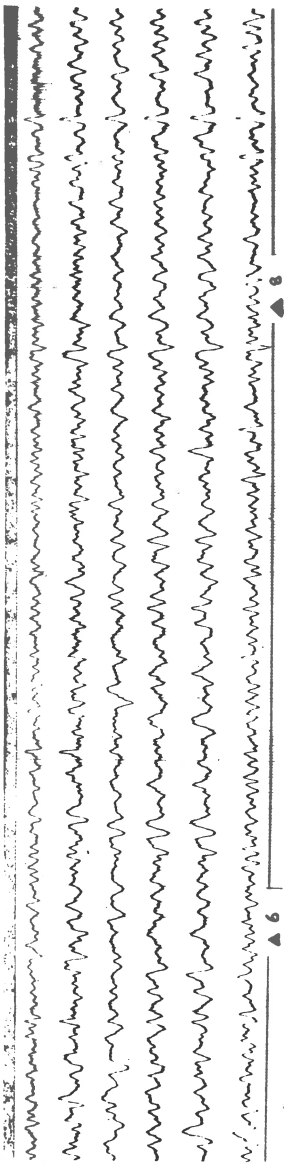

Fig. 4

Summarizing, the following statements can be made:

1. Longitudinal primary reflections with 2way-times of 8-8.6 s have been recorded at many positions in the surveyed area. The depth of the reflector should be greater than 25 kms. - 2. A sequence of events with travel-times between 5 and 7 s has been observed which could be correlated over the entire area of our investigation because of the characteristic series of the time intervals. Amplitudes and frequency range (10-20 cps) are about the same as those for the 8 s-reflection. - 3. Although a high percentage of our records were observed beyond 10 and even 14 s, later reflections ($T \geqq 9$ s) are recognized only on a very low percentage of the seismograms. - 4. A comparison of the depths of the reflecting zones with the depths of the Conrad and Mohorovičić discontinuity in the central part of Germany, and also a comparison with the statistical curves after Dohr [2;3] suggest that the narrow reflection band at about 8 s should correspond with the Moho and the broader reflection band (5-7 s) with the Conrad. This correlation would mean that the structure of the Moho is close to that of a simple discontinuity. For an explanation of amplitudes and frequencies of the seismic energy returning from below the sedimentary section of the crust, several authors, e.g. [4], have proposed a lamellar structure of a zone above the Moho, that is a sequence of alternating beds of seismically different behaviour. Such a more complicated structure would be proposed by the 5-7 s broad band of several distinct reflections as the structure of the "Conrad" zone.

Literature

[1] R.Reichenbach, G.Schmidt, Geophys.Prosp. vol.7, no.3 (1959).

[2] G.Dohr, Z.f.Geophys. 25 (1959).

[3] H.J.Liebscher, Z.f.Geophys. 28 (1962).

[4] R.Meissner, Geophys.Prosp. vol.14, no.1 (1966).

G.D.Panasenko

THE PROSPECTS OF TILTMETRIC INVESTIGATIONS IN FENNOSCANDIA

The study of the abyssal structure of the earth crust and its mantle is not at all sufficient without the detailed investigation of the processes occuring there. They are revealed in particular in the earthquakes and slower earth crust movements. These may be reasonably considered as one of the means to estimate and evaluate the probable sources of recent tectonical phenomena and, consequently, as one of the possible instruments of cognition the moving forces of the tectonic history of our planet.

This namely is one of the most important reasons for rising interest to the study of modern movements of the earth crust and for striving to obtain the absolute quantitative notions concerning the rates and directions of these movements. Against the background of total increase of the investigations and development of all methods the proportion of instrumental and especially geodetic methods is ever growing. However, all the traditional methods - geologic-geomorphological, geodetic etc. - in virtue of their specificity provide only averaged information about the character of the movement. The interval of averaging depends mainly upon the peculiarities of the method itself and partly upon the mode of its utilization. Eventually we obtain only the discrete pictures - snapshots, and by comparing them by their ultimate results we make an attempt to divine what could have happened and how it had happened during the period between two consecutive photographs.

Undoubtedly that using even this method, after the expiry of certain period (in my opinion exceeding too far the bounds of one generation life) the mankind would manage to accumulate sufficient series of such snapshots and accordingly to constitute the certain concept about the main features of development of the earth crust movements

in time. But it is hardly reasonable to wait for several generations for obtaining the possibility to conceive the modern earth crust movements in dynamics of their evolution. Moreover, by such approach there would appear a probability of missing some very important features of these movements distinguishing by relatively short-time development. All this suggests that the decrease of discretion in study of modern movements of the earth crust, the transition to examining their continuity in time, becomes the matter of urgent necessity.

At present geophysics has to its disposal a number of technical facilities favouring the continuous registration of relative inclination, horizontal and vertical modern movements of the upper earth crust levels within a wide range of sensibility. These are the different modifications of horizontal pendulums, rod extensometers, liquid level-variometers and others.

In practical geophysical investigations the horizontal pendulums, tiltmeters, are the most widely adopted. The tiltmeter station may be established nearly everywhere and at relatively small expenses. For this purpose it is only necessary to have small isothermal (better underground) premises and a resistant basement of bedrocks, preferably of rocky ones. More unfrequently extensometers and level-variometers are used; for establishment rather extended horizontal excavations are needed, passing through resistant bedrocks and being wholly isothermal. Special construction of such excavations is very expensive and adjusting of already existing ones is not always possible (and, besides, they may not exist everywhere).

The observations carried out with a help of these instruments are assigned for the purposes which are far from studying the tectonical movements of the earth crust. But there is no important fundamental obstacles of technical and methodical character (unless of material one) to use them for the purpose of continuous registration of slow movements of the earth crust. Their prospects are proved by certain tiltmeter-, extensometer-, and level-variometer examinations.

Such examinations are being carried out as yet only at single sometimes randomly chosen points of the earth crust. As a rule, the registration is accomplished either by one set of tiltmeters or by extensometer or level-variometer along the direction or, rather unfrequently, by any combination of these instruments.

Practically it is impossible to compare the observation data of single stations though located not far apart from one another. Sometimes a sufficient overlapping of series of observations is lacking, sometimes there is a sharp difference in apparatus used and in the methodics of observations, in the adjustment requirements and maintenance of the instruments, and so on.

There is an obvious necessity of organizing such observations on the surface by means of the network of stations equipped by uniform apparatus and carrying out their observations according to the single procedure. Undoubtedly, for this purposes the proper districts should be selected. They have to meet the requirements that the modern earth crust movements would reveal intensively enough on chosen territory and that their common features would have been studied by the other methods; that the geological conditions would allow the installation of equipment satisfying the higher demands; that the level of economical and scientific development in that country would conform with such investigations.

In this respect Fennoscandia is one of the most prospecting districts in the world. The modern movements of the earth crust are there intensive enough and on the whole are thoroughly studied by different methods; the closeness of the rocky bedrocks to the surface and the relatively small amount of daily temperature variations are considered to be favourable factors from the viewpoint of the possibility of placing the instruments in conditions close to the ideal and at relatively small expences. The level of development of geophysical researches in Scandinavian countries, the broad network of geophysical observatories, particularly the seismic stations, form a proper basis for the development of tiltmeter investigations for studying

the connection of tilts with the modern movements of the earth crust and with seismic manifestations in Fennoscandia. The experience of level-variometric observations carried out by Egedal and Fjeldstad (1934) in Bergen (1) and tiltmetric observations at station "Apatity" having been run since 1959 (2) prove that realization of the international experiment cited below would be a success, i.e. the science would get uniform informations concerning the dynamics of modern earth crust movements both in the particular regions of Fennoscandia and on the whole.

The essence of the proposal includes the following: on the territory of Fennoscandia a network of tiltmetric stations provided by uniform apparatus and working according the single technique is to be created. These stations are to be equipped with instruments capable of registration the tilts with sensibility not less than 0".1-0".01. In the USSR the tiltmeters H-VI with sensibility not less than 0".1, and tiltmeters NFm with sensibility up to 0".001 are broadly used. The procedure of observations carried out by these instruments is mastered properly enough.

Probably it is worth-while to accomplish the organization of the network of tiltmeter stations in two stages. Firstly, for installation of tiltmeters the existing stations should be used. It is easier from economical and practical viewpoints. Many of the seismic stations probably have premises suitable for installation of tiltmeters, and its maintenance may be well performed by the service personnel. It is believed that the first stage might be easily accomplished by 1969-1970.

At the second stage it is suggested to increase uniformly the amount of tiltmeter stations so that the distance between the nearest ones would be approximately 150-200 km. The speciel construction of new stations in this case seems unavoidable.

It stands to reason that all the tiltmeter stations are to be connected with lines of repeated levelling.

It is not excluded that in some places conditions may exist favouring the organization of tiltmeter observations

along a profile or even along orthogonal profiles (the distance between observation points being about 2-3 km). It is highly desirable to make use of such possibilities. There is no need to prove that observation materials of such "bunches" of stations would be of great interest.

Undoubtedly, the complex observations - profile tiltmetric, extensometric and level-variometric, carried out at special underground observatories - are also of great interest. The first such observatory is being erected in the USSR on the Kola Peninsula. The erection of such observatories is rather difficult and expensive. It is desirable, however, in the interest of science, to have in different regions of Fennoscandia several (5-6) such observatories which in the suggested project would play the role of the basic points.

All the expenses for their construction would undoubtedly be justified by the unique observation material.

It is probably worth while to organize a subcommission of the ESC to examine the tilts of the earth surface in Fennoscandia. This SC would be responsible for working out the common principles of organization and accomplishing the tiltmetric observations, for correlation and coordination of the research plans.

References

1. Egedal J. and Fjeldstad J.E., Observations of tidal motion of the Earth's crust made at the Geophysical Institute Bergen. Geophys.publikasjoner, v.XI, no.14, Oslo, 1937.

2. Panasenko G.D., Naklonomernie nabludenija na kolskom poluostrove "Nauka", M-L., 1965.

H.Berckhemer and K.H.Jacob

SYNTHETIC SEISMIC PULSES FROM PROPAGATING FAULTS

Berichte des Instituts für Meteorologie und Geophysik der Universität Frankfurt/Main Nr.7 (1965)

Abstract

A simple numerical method is presented to calculate the displacement pulses of bodywaves radiated from extending fault planes in a homogenious medium. Beginning with some analytic expressions for point sources seismic pulses for extending sources are obtained as a superposition of the displacements from delayed point sources. The variability of the focus model includes: The final focus shape, final focus size, geometry of fracture propagation, fracture velocity and its variation with focus expansion and the type of force system. Certain statistical properties of the focal models are discussed.

A computer is described which serves for the numerical calculations of the displacement pulses radiated in different directions as well as for further treatments such as spectral analysis, convolution with seismograph response, calculation of seismic energy density. Results are plotted for various focus models. Finally conclusions are drawn from calculated examples to gain criteria for the determination of focal parameters from real earthquake pulses.

ESC. COPENHAGEN. 1966

Agustin Udias, S.J.

THE FOCAL MECHANISM OF EARTHQUAKES IN THE SOUTHERN COAST OF THE IBERIAN PENINSULA

Abstract

A group of earthquakes in the southern coast of the Iberian peninsula from 1962 to 1964 are studied in order to determine the characteristics of the regional stresses. The largest of these earthquakes which occurred in March 15, 1964, of Magnitude 7.1, has been used in the determination of the focal mechanism in a joined analysis of P and S wave data. For this analysis a new computer program has been designed for optimizing a solution based on the polarization angle of S and the sign of the first arrival of P. The principal axes of stresses derived from this solution are related to the strike of the Guadalquivir fault confirming the presumption of a SW continuation of this fault. The analysis of the smaller earthquakes does not support the view of a homogeneous mechanism for all earthquakes in the region.

The full text will appear in TECTONOPHYSICS.

Nezihi Canitez and S.Balamir Üçer

ON THE MECHANISM OF THE EARTHQUAKES IN AND NEAR ANATOLIA DURING THE PERIOD FROM 1939 TO 1965

The Mechanism of 70 earthquakes among those which occurred in and near Turkey during the period from 1936 to 1965, are studied mainly on the basis of the first motion of P waves as a first part of this investigation. For this purpose a computer program coded by A.J.Wickens in S.P.S. is applied for the determination of nodal planes of earthquakes using a digital computer IBM. 1620. And the relations between the features of the distribution of the foci of the earthquakes, the directions of the maximum pressure and tension as the causes of the earthquakes and the null vector and so on, were investigated statistically. The second part of this study will depend on S waves data of WWSSS. (This study is a part of Research project Nr. MAG-78 supported by Scientific and Technical Research Council of Turkey.)

The full text will appear in TECTONOPHYSICS.

K.Hinz, S.Plaumann und A.Stein

GEOPHYSIKALISCHE UNTERSUCHUNGEN IM RAUM DES RINGKJÖBING-FÜNEN-HOCHS

Einführung

Im Mai 1964 wurde auf Initiative und unter Leitung des Dänischen Geodätischen Instituts von der dänischen Marine im Lillebelt eine Serie von Sprengungen mit Ladungen von 250 bis 3 000 kg für seismische Tiefensondierungen abgetan. Die Sprengungen wurden vom Geodätischen Institut und vom Institut für Physik des Erdkörpers, Hamburg, auf einem NNW-Profil durch Jütland registriert. Vier Messtrupps der Bundesanstalt für Bodenforschung und des Niedersächsischen Landesamtes für Bodenforschung, Hannover, registrierten diese Sprengserie auf einem ca. 130 km langen Profil, das vom Lillebelt bis an die Nordseeküste in die Nähe von Husum verlief (Abb.1). Die Deutsche Forschungsgemeinschaft ermöglichte die Registrierungen.

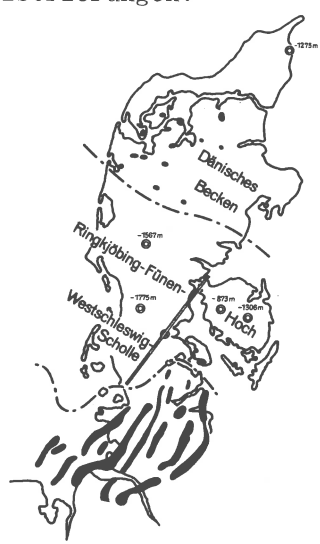

Abb. 1

Geologische Verhältnisse

Das refraktionsseismisch vermessene Profil verläuft vom Dänischen Becken mit seinen mächtigen jungpaläozoischen, mesozoischen und känozoischen Sedimenten nach SSW über das Ringkjöbing-Fünen-Hoch, in das Gebiet der Westschleswig-Scholle. Das Ringkjöbing-Fünen-Hoch, das das Dänische Becken vom Norddeutschen Senkungsraum trennt, ist durch positive gravimetrische und magnetische Anomalien ausgezeichnet. In seinem Zentrum fehlen Paläozoikum und Jura. Das kristalline Grundgebirge, vorwiegend unter triassischer Bedeckung, ist mehrfach erbohrt worden. Die Westschleswig-Scholle, Teil des Norddeutschen Senkungsraumes, zeichnet sich durch ruhige Lagerungsverhältnisse der etwa 4 000 m mächtigen Schichtfolge Tertiär bis einschliesslich Zechstein aus.

Zum Schwerefeld

In den Schwerekarten der geophysikalischen Reichsaufnahme und der Schwerekarte von Saxov findet man eine breite Zone relativ hoher Schwerewerte, die von Mecklenburg bis Jütland verläuft und im südlichen Jütland sich mit dem geologisch bekannten Ringkjöbing-Fünen-Hoch deckt. Wo dieses Hoch von der seismischen Messlinie überquert wird, liegt ein Schweremaximum mit + 38 mgal bei Aabenraa und Haderslev. Von Süden her nimmt die Schwere in einer etwa 15 bis 20 km breiten Zone unmittelbar nördlich der deutsch-dänischen Grenze zu, wobei horizontale Gradienten von 3 bis 4 mgal/km vorkommen.

Seismische Auswertung

Zunächst wurde ein geologisches Modell unter Berücksichtigung aller zugänglichen Bohrungen und aller zugänglichen reflexions-seismischen Unterlagen entworfen. Als Basis der Sedimente wurden metamorphe Schiefer und Gneise vermutet mit einer angenommenen Geschwindigkeit von 6.0 km/s. Für das Tertiär wurde für die spätere Berechnung eine Geschwindigkeit von 1,8 km/s, für die Kreide eine Geschwindigkeit von 3,4 km/s gewählt. Dem Muschelkalk und dem Bundsandstein wurde eine Geschwindigkeit von 4 km/s zugeordnet, dem Sechstein und dem salinaren Rotliegenden ein Wert von

4,6 km/sec. Für die präpermischen Sedimente erschien ein Geschwindigkeitswert von 4,8 km/s zutreffend. Für den nördlichen Profilabschnitt im Bereich des Ringkjöbing-Fünen-Hochs konnten Dänische Bohrergebnisse herangezogen werden. In einigen Bohrungen ist das kristalline Grundgebirge in Tiefen von etwa 1,5 km unter triassischer Bedeckung erbohrt worden.

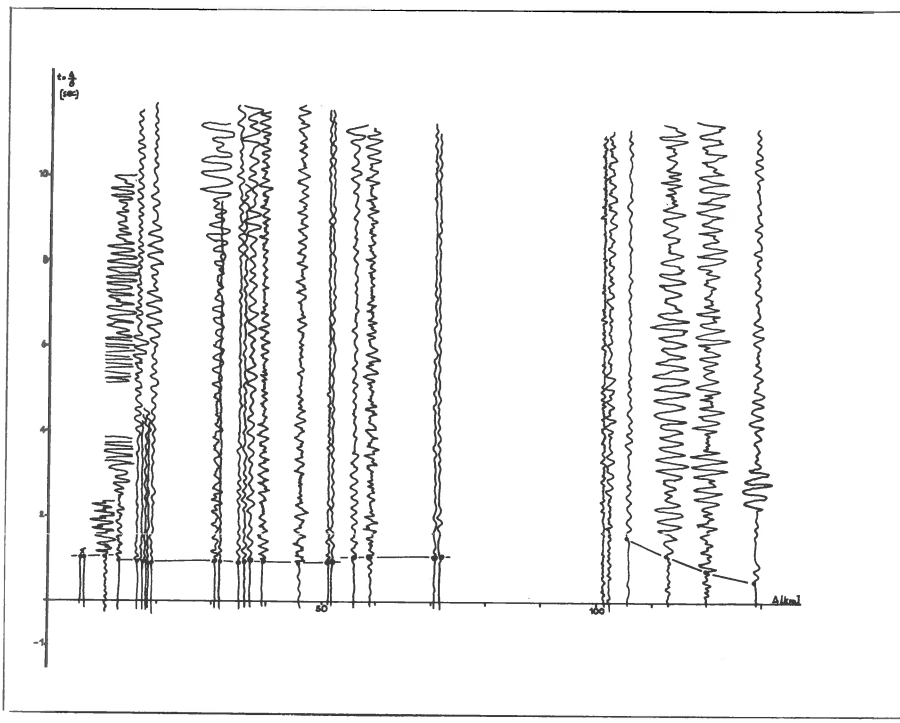

Abb. 2

Repräsentative Spuren aller Seismogramme sind in Abbildung 2 dargestellt worden. Bis zu einer Schusspunktentfernung von 70 km wurden eindeutige Ersteinsätze beobachtet. Einsätze von der Conrad-Diskontinuität konnten nicht nachgewiesen werden. Dagegen wurden in den letzten Seismogrammen des Profils spätere Einsätze registriert, die als Moho-Einsätze gedeutet werden. Die scheinbare Geschwindigkeit beträgt 8,2 km/s.

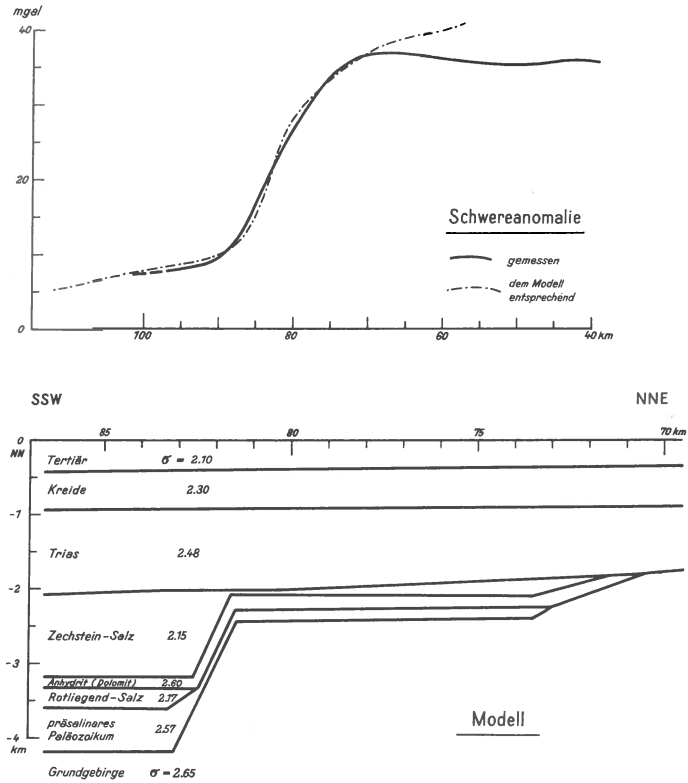

Südrand des Ringkjöbing-Fünen-Hochs.

Schematisiertes Modell (mit Dichteangaben) und Schwereanomalien

Abb. 3

Zur Ermittlung der Kristallintiefe aus den Laufzeiten wurde ein Rechenprogramm für die IBM 1620 aufgestellt. Nach Eingabe der bekannten Mächtigkeiten und Geschwindigkeiten des Deckgebirges sowie der angenommenen Geschwindigkeit von 6,0 km/s für das kristalline Grundgebirge wird der Beitrag der bekannten Deckschichten zur intercept time berechnet. Aus der Rest-intercept-time lässt sich dann die Mächtigkeit der dem Kristallin direkt aufliegenden Schicht bestimmen.

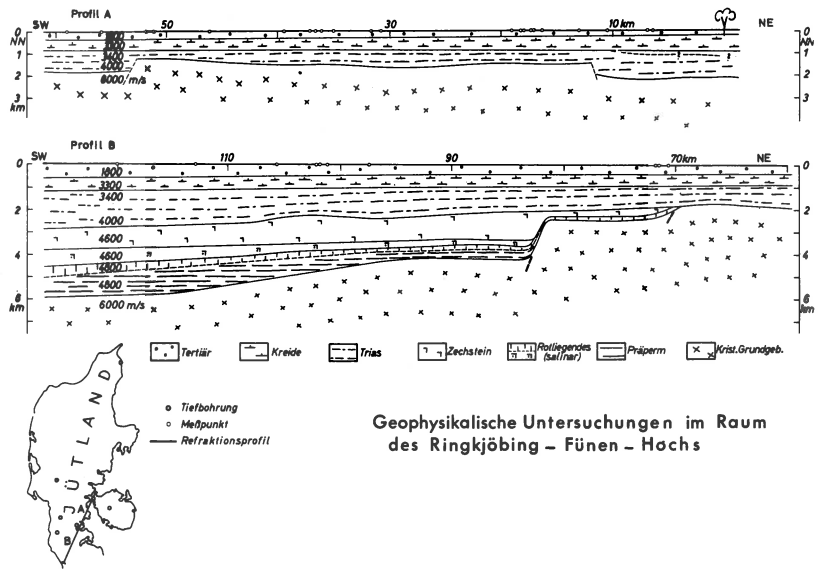

Abb. 4

Das Relief des Grundgebirges im Bereich des Ringkjöbing-Fünen-Hochs, wie es sich nach der seismischen Auswertung ergab, ist in Abbildung 4 dargestellt.

Die beiden Störungen innerhalb des Hochs sind in ihrer Existenz als relativ sicher zu bezeichnen. Die in Abbildung 2 angedeuteten Einsätze mit der Scheingeschwindigkeit 8,2 km/s wurden für eine Tiefenabschätzung der Moho benutzt. Unter Berücksichtigung der seismischen Verhältnisse im Deckgebirge ergibt sich, dass die Moho-Diskontinuität in einer Tiefe von etwa 25 km liegt, wenn man noch annimmt, dass sie im refraktionsseismisch vermessenen Bereich horizontal verläuft.

Gravimetrische Betrachtung

Da die Genauigkeit der seismischen Auswertungsergebnisse im südlichen Teil des Profils entsprechend der erheblich geringeren Qualität der Seismogramme ungenügend war, wurde versucht, für diesen Teil mit Hilfe der Gravimetrie Aussagen über den Verlauf des kristallinen Grundgebirges zu gewinnen. Ausgehend von den bekannten Tatsachen werden

dabei in der üblichen Weise verschiedene plausible Modelle entworfen und solange variiert, bis eine hinreichende Übereinstimmung zwischen Modell-anomalie und wirklichem Schwereverlauf erzielt wurde. Die dabei benutzten Dichten (siehe Abbildung 3) beruhen teilweise auf Dichtebestimmungen an Kernen aus in der Nähe des Bearbeitungsgebietes im norddeutschen Raum gelegenen Tiefbohrungen, teilweise auf Annahmen. Die unterschiedliche fazielle Ausbildung entsprechender Schichten in den deutschen und dänischen Bohrungen wurde berücksichtigt. Der Wert 2,57 gcm^{-3} für das ungefaltete präsalinare Paläozoikum wurde in Analogie zu bekannten Gebieten, wie z.B. dem Saarland, gewählt. Als relativ unsicher muss die Dichteannahme für das Grundgebirge gelten; hier konnte nur ein Mittelwert für die Gesteine angesetzt werden, die man erwarten darf.

Der starke horizontale Schweregradient bei km 80 (Abbildung 3) des Profiles verlangt eine starke horizontale Dichteänderung. Die Möglichkeit, fazielle Änderungen und entsprechende Dichtegradienten innerhalb einiger Formationen anzunehmen, wurde diskutiert. Mit entsprechenden Modellen konnten die starken Schweregradienten jedoch nicht erreicht werden. Man wird zwangsläufig zur Annahme sehr steil verlaufender Dichtegrenzen etwa bei km 82 bis 83 geführt, d.h. zur Annahme einer Flexur oder Verwerfung. Die Mächtigkeit des Zechsteins muss dabei nördlich der Verwerfung als sehr stark reduziert angenommen werden. Die Abbildung 3 repräsentiert die gegenwärtig als am besten angesehene Modellvorstellung, die den Hauptzügen der beobachteten Anomalie (Bereich km 70 bis 90) gerecht wird. Die Berechnung der Modellanomalien erfolgte auf der IBM 1620 mit einem Programm, das nach einer Veröffenlichung von Talwani u.a. entwickelt wurde.

Zusammenfassung

Eine mit Bohrergebnissen kombinierte seismisch-gravimetrische Auswertung zeigt, dass das kristalline Grundgebirge im Ringkjöbing-Fünen-Hoch, durch welches das dänische und das nordwestdeutsche Becken getrennt werden, in Tiefen zwischen 1,2 und 2 km liegt und im NE wie im SW durch Störungen

gegliedert ist. Die Störung im SW, die den Übergang zur Westschleswig-Platte bildet, erreicht nahezu 2 km. Das Rotliegende und die präpermischen Sedimente beissen hier mit einiger Wahrscheinlichkeit aus, während der Zechstein eine starke Mächtigkeitsreduktion erfährt, die auf intensive Bewegungen während der Zechsteinzeit hinweist. Die Grenze zwischen Erdkruste und Erdmantel liegt im Untersuchungsgebiet in ungefähr 25 km Tiefe.

Literaturverzeichnis

de Bruyn, J.W.: Isogam maps of Europe and North Africa. - Geophysical Prospecting III, 1 (1955), S.1.

Closs, H. u.Schleusener, A.: Schwerekarte von Zentraleuropa nach Grave.

Gregersen, A. u. Sorgenfrei, Th.: Efterforskningsarbejdet i Danmarks dybere undergrund. - Medd. Dansk geol. Foren., 12, 1, 141-151, 1951.

Hecht, F., Helms, v.H. u. Kehrer, W.: Reflection-seismic exploration of Schleswig-Holstein, Germany, and its geological interpretation by well data. World Petroleum Congress, Rom 1956.

Hinz, K.: Zur Geologie der südl. Nordsee nach reflexionsseismischen Untersuchungen. Dissertation, Bergakademie Clausthal, 1964.

Hirschleber, H., Hjelme, J. u.Sellevoll, M.: A Refraction Profile through the Northern Jutland. - Geodætisk Institut, Meddelelse No.41, København, 1966.

N.L.f.B.: Schwerekarten 1:200 000 der geophysikalischen Reichsaufnahme 1935-1944, hier insbesondere die Karte Schleswig b 2.

Reich, H.: Geophysikalische Karte von Nordwestdeutschland, 1:500 000, 1948 (Magnetik I, Gravimetrie II, Seismik III), Berlin, 1948.

Saxov, S.: Some gravity measurements in Sønderjylland. Geodætisk Instituts Skrifter 3. Række Bind XXXVI S. 5-59, 1965.

Sorgenfrei, Th.: Deep tests in Denmark 1935-1959. Dånmarks Geologiske Undersøgelse III.Række, Nr.36, 1964.

Talwani, M., Worzel, J.L. u. Landismann, M.: Rapid gravity computations for two-dimensional bodies with application to the Mendocino submarine fracture zone. - Journal of Geoph. Res. 64 (1959), S.49.

Weber, H.: Der Geologische Bau des Untergrundes von Schleswig-Holstein und seine Erdöllagerstätten; Übersichtskarten zur Geologie von Schleswig-Holstein. Herausgegeben vom Geologischen Landesamt Schleswig-Holstein, Kiel, 1957.

H.B.Hirschleber

REFLEXIONSSEISMISCHE BEOBACHTUNGEN AUF FÜNEN BEI SPRENGUNGEN IM KLEINEN BELT

Publ. Nr.6 der "Working Group on the Skagerrak Project"

Im Jahre 1964 sind im Kleinen Belt 17 Sprengungen mit Ladungen zwischen 250 und 3000 kg für Refraktionsbeobachtungen in Jütland, Skagerrak und Südnorwegen gezündet worden (1). Diese Sprengungen sind auch mit einer Reflexionsstation des Institutes für die Physik des Erdkörpers der Universität Hamburg auf Fünen registriert worden. Für den Entfernungsbereich von 2 bis 18 km konnten neben sehr guten Refraktionseinsätzen zahlreiche Reflexionen sowohl aus dem unterkritischen als auch aus dem überkritischen Bereich beobachtet werden. Die vorläufige Auswertung der Messergebnisse hat folgende Geschwindigkeiten für die einzelnen Schichten ergeben, die mit Hilfe der beiden Tiefbohrungen Horsens 1 und Glamsbjerg 1 geologischen Formationen zugeordnet werden konnten:

1.9 - 2.2 km/s (Quartär/Tertiär)
2.6 - 2.9 km/s (Kreide)
4.0 - 4.1 km/s (Trias/Jura)
5.7 - 6.1 km/s (Kristallin)

Die Mächtigkeit der Sedimente im Messgebiet schwankt zwischen 1.5 und 2 km.

Mehrfachreflexionen an den verschiedenen Sedimenthorizonten, vor allem aber an der sehr ausgeprägten Kristallinoberkante, erschweren die Interpretation sämtlicher Einsätze in den Seismogrammen, geben aber gelegentlich auch zusätzliche Informationen. Dies gilt insbesondere für die tieferen Horizonte. Eine Anhäufung von Reflexionen in den Bereichen von 6.8 bis 8.1 s und von 9.5 bis 10.2 s lassen auf das Vorhandensein von Diskontinuitäten im tieferen Untergrund schliessen. Je nach Geschwindigkeitsmodell erhält man für die Tiefenlagen der Diskontinuitäten 20-24 km und 29-32 km. Reflexionen von einer "Conrad-Diskontinuität"

in einer Tiefe von weniger als 10 km - wie in Jütland gefunden (1) - konnten bei der ersten Auswertung nicht entdeckt werden. Sicher ist das Vorhandensein von Reflexionen mit einer grösseren Laufzeit als 12 s, deren Deutung noch aussteht. Eine ausführliche Darstellung der endgültigen Auswertung der Messergebnisse wird zu einem späteren Zeitpunkt in der "Zeitschrift für Geophysik" erfolgen.

Der dänischen Marine sei gedankt für den Sprengstoff und die Durchführung der Sprengungen, dem Geodätischen Institut Kopenhagen für die Hilfe bei der Anlage der Messungen, der Deutsvhen Forschungsgemeinschaft und der NATO für die finanzielle Unterstützung der Arbeiten. Herrn Prof.Dr. Menzel danke ich für die Beratung bei der Auswertung der Ergebnisse, Herrn Dipl.-Geophys. Kaminski für die Durchführung der Messungen, den Herren Bol, Kind und Wiemann für die Hilfe bei der Auswertung.

Bisherige Publikationen der "Working Group on the Skagerrak Project"

1. Hirschleber, H., J.Hjelme u. M.Sellevoll: A Refraction Profile through the Northern Jutland. Geod.Inst.Medd. No.41, Kopenhagen, 1966.

2. Hirschleber, H.B. u. H.Menzel: Das Amplituden-Ladungsgesetz für Sprengungen im Kleinen Belt. Zeitschrift für Geophysik, Sonderband 1966.

3. Andersen, O.B.: Surface-Ship Gravity Measurements in the Skagerrak 1965-66. Geod.Inst.Medd. No.42, Kopenhagen, 1966.

4. Kloster, K. u. M.A.Sellevoll: Refraksjonsseismiske undersøkelser på Jaeren (With English Summary). Universitetet i Bergen, Jordskjelvstasjonen, 1965.

5. Behrens, J. u. W.Weigel: Bemerkungen zu Blubberbeobachtungen bei sprengseismischen Messungen auf See. Zeitschrift für Geophysik, 1966 (in Druck).

H.Hirschleber, J.Hjelme and M.Sellevoll

A REFRACTION PROFILE THROUGH THE NORTHERN JUTLAND

A working group on the Skagerrak Project has been set up by the University of Bergen, the Royal Danish Geodetic Institute, and the University of Hamburg.

The Skagerrak Project also comprises seismic investigations. The profiles in the sea have been extended into Norway to the north and into Jutland, Denmark to the south. This part of the work shall be reported here (Fig. 1).

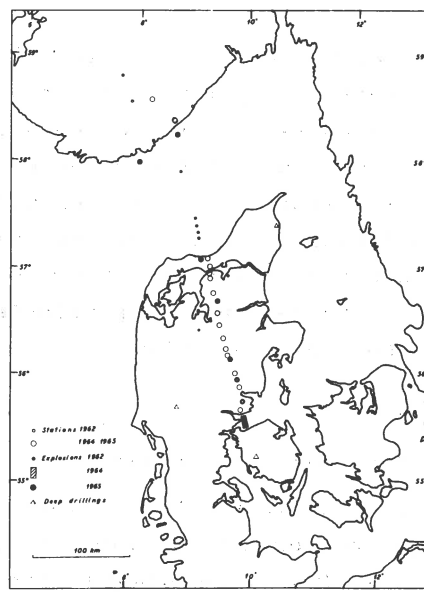

Fig. 1. Explosion- and shotpoints

Charges of 1000-3000 kg TNT have been fired at the seabottom in the Skagerrak and in the entrance of the Little Belt. In the Skagerrak the explosions were made near the Norwegian coast and at four different places in the Jammerbugt of Jutland. In the Little Belt several smaller explo-

sions were distributed in the shooting area. Thus the picture given by the travel-time-curves is a little more complicated than in case of only one shot-point in each end of a profile.

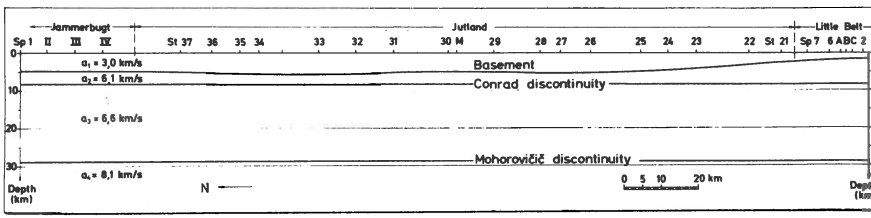

Fig. 2. A model with variation only in the sedimentary cover.

A four layer model has been made (Fig. 2). The top layer is the sediments. Only few observations refer to this layer. The thickness of the sediments is about 1.7 km near Little Belt and the thickness increases towards north. Below the sediments a velocity of 6.1 km/sec has been found. This "granitic layer" extends down to a depth of about 8 km, where a velocity of 6.6 km/sec is found. The fourth layer is the Mantle with a velocity of 8.1 km/sec. The thickness of the crust is 29 km.

The complete paper has been published as follows:

Hirschleber,H., J.Hjelme and M.Sellevoll: A Refraction Profile through the Northern Jutland. - Geodætisk Instituts Meddelelse No.41, Copenhagen 1966 (Paper No.1 of the Working Group on the Skagerrak Project).

W.Sponheuer

A NEW SEISMICITY MAP OF THE GDR FOR 1900-1960, COMPILED BY THE THEORETICAL METHOD BY ULLMANN AND MAAZ

According to Ullmann and Maaz the distribution density for the epicentre of the i^{th} earthquake in a point Z on the surface of the earth is written

$$p_i(Z) = \frac{p_i(Z_i)}{\cos^4 \frac{\Delta}{2R}} \exp\left[-\left(\frac{2R}{a_i} \tan \frac{\Delta}{2R}\right)^2\right] . \qquad (1)$$

R = radius of the earth,

Δ = epicentral distance,

Z_i = fixed point representing the epicentre of the i^{th} earthquake with maximum probability.

The seismicity in point Z for the epicentre of the i^{th} earthquake with the energy Z is defined:

$$S_i(Z) = E_i p_i(Z) .$$

If the number of the earthquakes is n, the seismicity for point Z in the given time-interval is

$$S(Z) = \sum_{i=1}^{n} S_i(Z) .$$

In the first equation we can practically regard $\cos^4 \frac{\Delta}{2R} \approx 1$, if Δ is not to great, and $\tan \frac{\Delta}{2R} \approx \frac{\Delta}{2R}$. Hence equation (1) reads

$$p_i(Z) = p_i(Z_i) \exp\left[-\left(\frac{\Delta}{a_i}\right)^2\right]$$

and

$$S_i(Z) = E_i p_i(Z_i) \exp\left[-\left(\frac{\Delta}{a_i}\right)^2\right] .$$

$S_i(Z)$ means the energy per unit area at the point Z in consequence of the distribution of E_i caused by $p_i(Z)$.

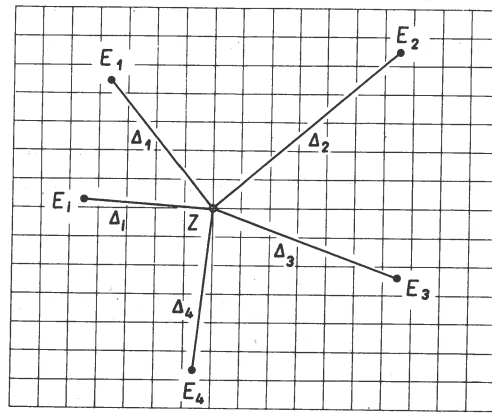

Fig. 1. Computation of the seismicity in a point Z caused by the epicentres in different distances.

It is therefore possible to compute the seismicity at each point of a network covering the examinated region, which is produced by one or any epicentres (s. Fig. 1). By changing the value a_i it is possible to choose the distribution density in a suitable manner. In practice a_i should be chosen so, as to correspond with the propagating of earthquake energy.

In the region of the GDR mainly macroseismic data are available. It was supposed that in the average the intensity of earthquakes decreases by 3 degrees at an epicentral distance of 50 km, the acceleration decreases to $\frac{1}{10}$ with the majority of scales. As the acceleration of the ground movement (sinusoidal) is proportional to the amplitude, the energy, however, proportional to the square of the amplitude, it follows, that the energy drops to be one hundred times smaller than the epicentral energy at a distance of 50 km.

For example

$$\frac{p_i(Z)}{p_i(Z_i)} = \exp[-(\frac{50}{a_i})^2] = 0{,}01 ,$$

$$a_i = 23{,}3 .$$

For the seismicity map of the GDR a_i was taken to be 25 for the epicentres included there and for the average value of focal depth ξ = 10 km. It was stated that the energy sum of each epicentre of the weak shocks of earthquake swarms is too small to come into consideration for computing seismicity. Therefore it was not necessary to take into account the smaller focal depth of those shocks. But there are some distant epicentres in the South-Western-Germany, which have a great radius of perceptibility, for example the earthquakes of 1911 and 1943. For the earthquake of 1911 the intensity decreased by 3 degrees at a distance of about Δ = 300 km with a_i being 140. The influence of this earthquake upon the region of the GDR was mainly observed in its western part. For the earthquakes of 1943 in the same region Δ = 160 km and a_i = 75. The influence of these quakes are negligible. For instance at an epicentral distance of 300 km

$$\frac{p_i(Z)}{p_i(Z_i)} = \exp[-(\frac{300}{75})^2] = e^{-16} .$$

The seismicity map of the GDR (s. Fig. 2) shows the epicentres (about 70) with $E \geqq 10^{17}$ erg, which served for computation of the isolines of energy. The distance between the points of the network is 0,25 degree for geographic longitude and latitude. The distance of the points was subdivided when necessary. As it was to be expected, the highest seismicity is experienced in the region of the Vogtland and caused by earthquake swarms. The form of the inner isoline is due to the Rhenian direction, which is an important tectonic element in Middle-Germany. The small maximum of seismicity in the North-Western part is caused by some earthquakes, which may be traced back to mining in that region. This map is of preliminary character. If

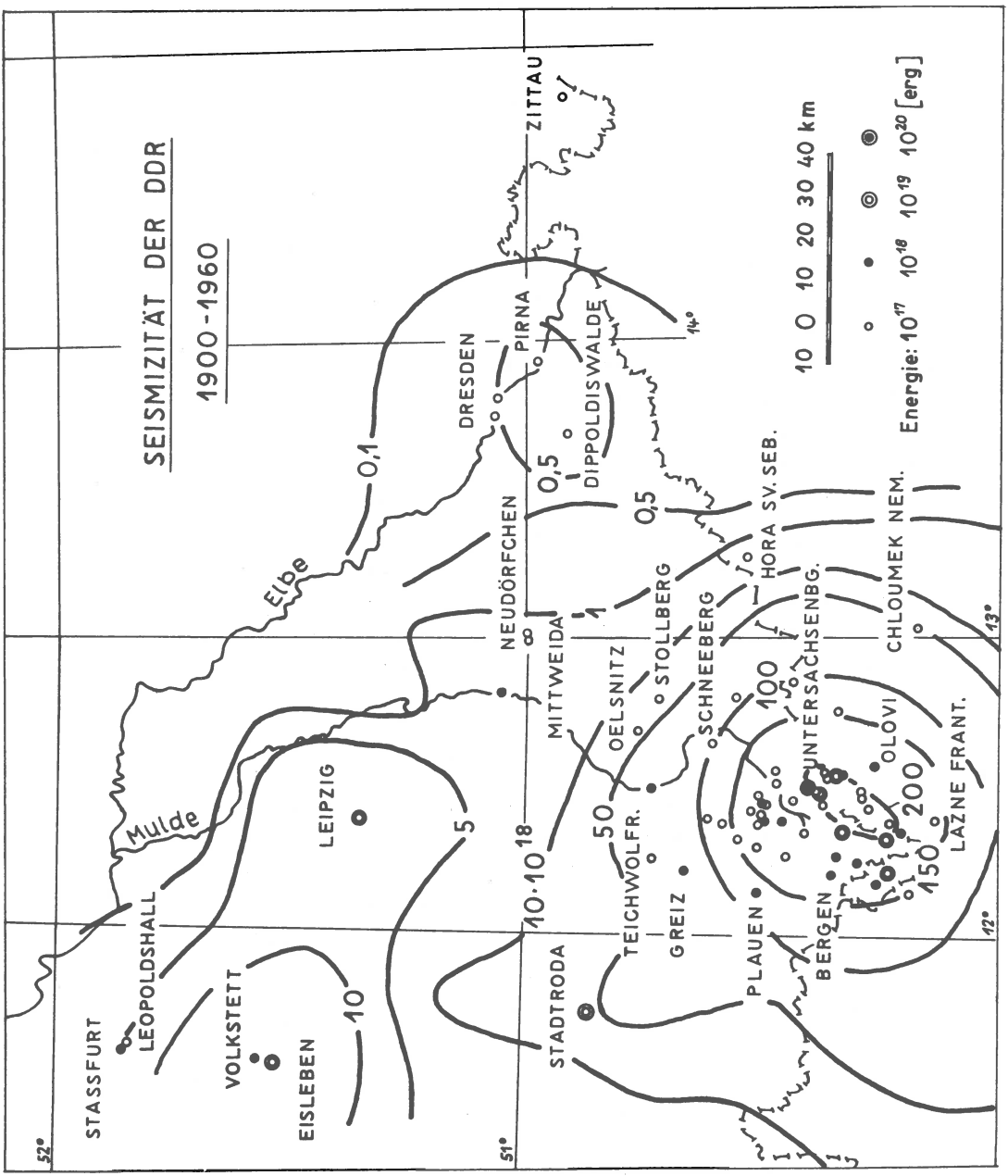

Fig. 2. A seismicity map of the GDR for 1900-1960.

all the parameters of each earthquake can be taken into consideration the map will doubtless disclose more details.

Literature

[1] Sponheuer, W.: Untersuchung zur Seismizität von Deutschland. Veröff.d.Inst.f.Bodendynamik und Erdbebenforschung in Jena d.Ak.d.Wiss. zu Berlin, Heft 72, Akademie-Verlag Berlin, 1962, s.23-52.

[2] Sponheuer, W.: Katalog der Erdbeben Deutschlands 1900-1960. (Manuskript).

[3] Sponheuer, W.: Seismizität des Gebiets der DDR und ihre Beziehung zur Tektonik. Petermanns Geographische Mitteilungen, 1965, II.Quartalsheft, s.156-158.

[4] Ullmann, W. and R.Maaz: A New Method for Computation of Seismicity. Pure and Applied Geophysics, Basel, 63 (1966/I), 15-22.

[5] Sponheuer, W.: Die Seismizität des Gebiets der DDR. Vortrag, gehalten auf der CSE-Tagung 1964 in Budapest (im Druck).

Slawomir Gibowicz

LA SEISMICITE DE LA HAUTE SILESIE DE 1950 A 1960

Dans ce travail on a élaboré 120 secousses choisies de la région d'Haute Silésie, qui ont été enregistrées dans la période 1950-1960. Les épicentres ont été déterminés à l'aide de différences de temps d'arrivée des ondes P et S. Les matériaux nombreux d'observation ont permis d'admettre que la vélocité des "ondes" S-P préserve une valeur constante dans l'intervalle examiné des distances épicentrales de 2 à 80 km.

Dans 76 des cas les secousses ont été liées avec des coups des toits dans les mines du charbon connues, et dans 9 des cas des observations macroséismiques ont été ajoutées sans coups des toits, il en est ainsi que dans 85 cas les épicentres calculés d'après des données séismiques ont pu être comparés avec les données macroséismiques.

Les secousses dont il fut tenu compte dans l'élaboration de la carte de séismicité avaient la magnitude de 2,6 à 4,2. La carte de séismicité de la Haute Silésie (Fig. 1) a été exécuté à l'échelle de 1:100 000.

En tenant compte de la relation, qui a été déterminée autrefois, entre l'énergie et la magnitude pour la région de la Haute Silésie ($\log E = 9{,}2 + 1{,}9\ M$) on a déterminé l'énergie des secousses étudiées. Cette énergie avait la grandeur de 10^{14} à 10^{17} ergs.

L'étude présente aussi la relation qui détermine la récurrence des secousses en Haute Silésie, élaborée pour la période de 1955 - 1959, dans laquelle on a enregistrée 402 des secousses avec la magnitude $M \geqq 2{,}3$. Cette relation pour la magnitude $M = 2{,}3 - 3{,}7$ s'exprime comme suit:

$\log N = 1{,}05 - 0{,}92\ M$ pour $\delta M = 0{,}3$

$\log N = 0{,}56 - 0{,}93\ M$ pour $\delta M = 0{,}1$

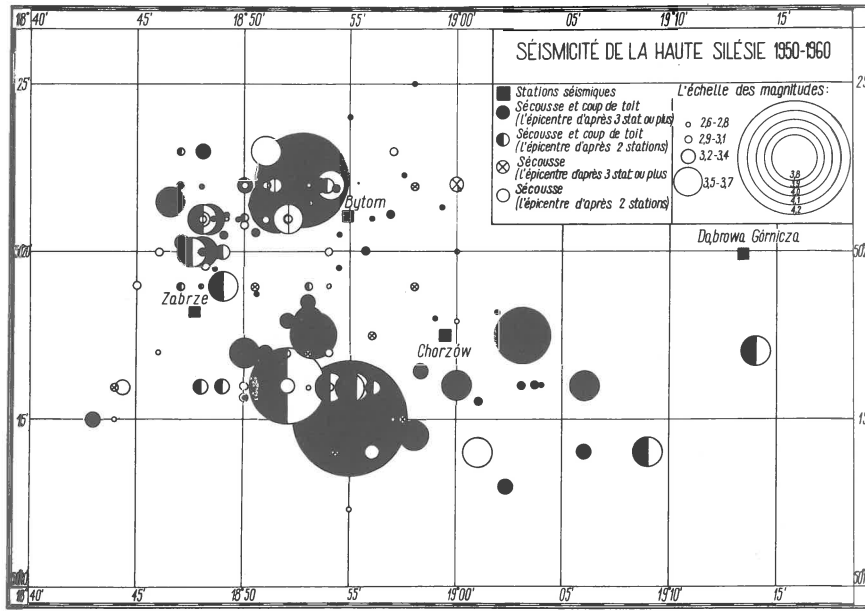

Figure 1

Cettes formules pour les secousses avec la magnitude $M > 3,7$ ne sont pas valables. Les secousses les plus grands apparoissent beaucoup plus rarement.

Une analyse même approximatif de la carte de séismicité indique, que deux directions privilégiés existent en Haute Silésie, au long des quelles se groupent les épicentres. Ce sont la direction SW-NE dans la région de Zabrze-Bytom, et la direction E-W dans la région centrale de la Haute Silésie.

La carte présentée ici est la première approximatif à ce problème, dont la solution précise sera possible en s'appuyant sur des matériaux d'enregistrement plus nombreux et plus modernes.

Au commencement de 1965 l'Institut de Géophysique a commencé des études nouvelles des phénomènes séismiques en Haute Silésie. Dans la mine du charbon "Miechowice" on a installé une station séismique complexe. Les séismographes ont été situés dans un profil verticale sur les quatre horizons:

première horizon - surface, deuxième - sur le profond 320 m, troisième - 720 m et quatrième - 850 m.

La registration dans une cave sur la surface est continue tout le jour avec une vitesse de déroulement 40 cm/min.

Types des séismographes qui sont installés dans cette station, ce sont les séismographes SU-59 de court période avec la registration galvanométrique. Sensibilités maximales sont différents dans quatres horizons: de 1000 à surface à 8000 sur le profond 850 m.

Chaque jour on se registre 20-30 des sécoisses locaux d'intensivité différent. Les matériaux sont maintenant élaborés.

Yu.V.Riznichenko

GEOPHYSICAL PRINCIPLES OF EVALUATION OF THE SEISMIC DANGER

From an engineering and economical point of view the seismic danger of any territory depends not only on a maximum intensity I_{max} of the ground vibrations possible, but also on an average frequency B_I of occurrence of destructive shocks of a given intensity I expected. A modern system of seismic zoning, especially that one which is under elaboration for Europe, must undoubtedly take into account this consideration.

At present on a basis of detailed, mostly instrumental statistical studies of earthquakes we usually know much enough about the distribution of earthquakes in their foci, beneath our feet. But our knowledge about their effects on the earth's surface is left behind. It is a right time to bring both sides of the problem into a due concordance.

The following procedure can be suggested [1-3].

The focal seismicity is supposed to be presented in terms of a long time average frequency N of occurrence of earthquakes of various seismic energies $E = 10^K$ or magnitudes M ($0 < E \leqq E_{max}$, $-\infty < K \leqq K_{max}$, $-\infty < M \leqq M_{max}$). For each spatial element of the focal region a frequency-energy or a frequency-magnitude relation

$$N = N(E) \quad \text{or} \quad N = N(M) \tag{1}$$

must be known. They can usually be taken in a form of a log-linear dependance (Fig. 1).

Practically a frequency-energy (or magnitude) relation (Fig. 1) is established from observations for the whole region under study or for a few large parts of it, if statistics allows. The value γ of the slope of the line on Fig. 1 may be taken as a constant.

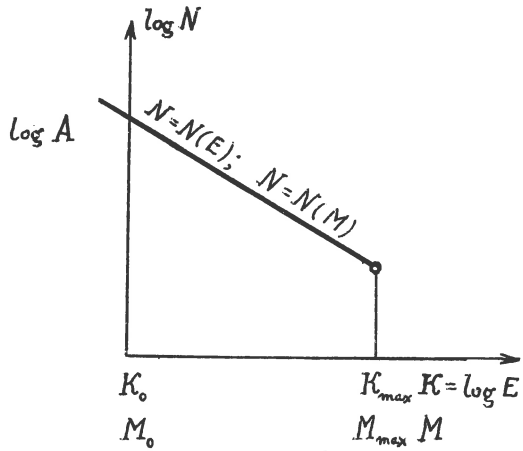

Fig. 1. Frequency-magnitude relation, representation of the focal seismicity. A) seismic activity; $\gamma_K = -d \log N/dK$ (or $\gamma_M = -d \log N/dM$) - the slope of the graph; $E_{max} = 10^{K_{max}}$ (or M_{max}) - energy (or magnitude) of the maximum earthquake possible.

The seismic activity A, which varies substantially from spot to spot, must be given by a contour seismic activity map (see e.g. [4,5]).

For the same reason the maximum possible magnitude K_{max} or M_{max} has also to be mapped in any way. The simplest - but perhaps not the best - way consists in dividing the region into several presumably homogeneous "seismo-tectonic zones", in each of which the maximum magnitude is supposed to be constant and equal to the maximum magnitude observed in any spot of it. Other possibilities have been discussed in [5-9]. Surely, the best solution of the problem will be based on a combination of seismic, geodetic, geological and may be some other data (e.g. thermal), but in order to get practical results already now, any preliminary rough approximation may be applied.

Now we have to go over from the focal, underground seismicity to its effects on the surface (Fig. 2). These effects must be expressed in terms of an average frequency B of occurrence of vibrations of any intensity I (Fig. 3)

$$B = B(I) . \qquad (2)$$

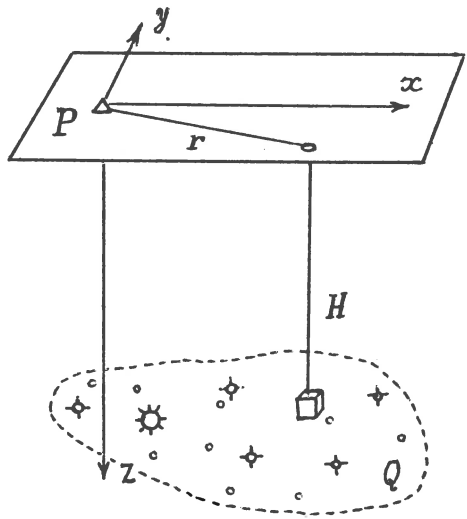

Fig. 2. The problem of quantitative determination of seismic danger is similar to that of the potential theory. Q) Region of seismic sources; P) Point of observation; r) epicentral distance; H) focal depth.

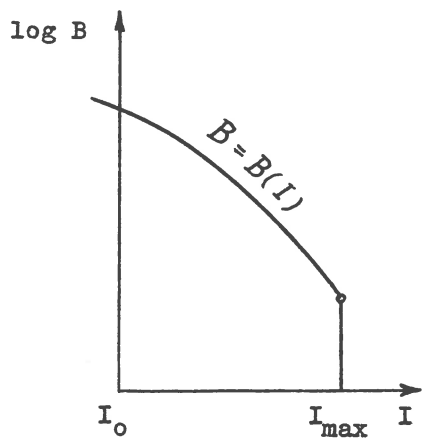

Fig. 3. Frequency-intensity relation, representation of the amount of seismic danger in any point P. $B_I = B(I)$ - average frequency of occurrence of ground vibrations of a given intensity I.

The problem is similar to that of the potential theory: the sources in a certain spatial region Q are given; a summary effect of all of them in any point P has to be determined. An algorithm how to do it has been described and both theoretical and practical examples of calculations given in [1,3], so that we will not go into further detailes here. We must only point out that the main task of such calculations consists in considering that a weak nearby earthquake may produce an effect of the same intensity I at the point P as a strong, but more distant earthquake. Hence, the frequencies of occurrence of those earthquakes, which give the same effect I at the point of observation P must be summarized.

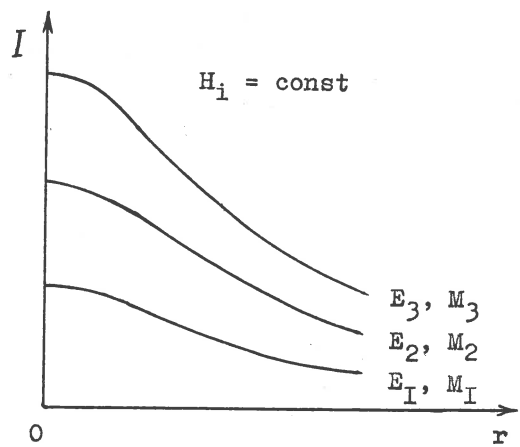

Fig. 4. Intensity-distance relation for a given magnitude K = log E (or M) and focal depth H of earthquakes. It is needed for calculations of seismic danger in terms of B (Fig. 3).

For this purpose additional information must be available, namely, we must know the intensity-distance relations I(r) (Fig. 4) for any energy E or magnitude M and a given focal depth H. Dependance of I upon azimuth can also be taken into account. If the foci are distributed within a considerable depth interval, calculations have to be carried out layer by layer, and the results on B summarized.

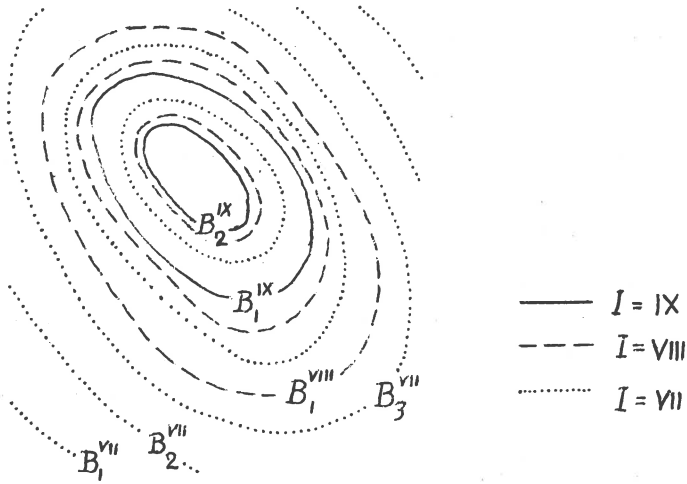

Fig. 5. A seismic danger map. Contour lines - frequencies B_I^I of occurrence of shocks of a given intensity I. It has to reflect long-term average values.

Thus the amount of seismic danger at any given spot P on the earth's surface is given by a frequency-intensity relation B(I) (Fig. 3). In order to get knowledge about the seismic danger of a territory, we must calculate such relations for all the points of it - practically, for a certain two-dimensional grid of points. The final result may be presented as a set of contour maps, each of them giving the value of frequency of occurrence of vibrations of a given intensity I, for instance, maps for intensities IX, VIII and VII (Fig. 5).

The principle of calculations of the seismic danger will not be changed if instead of "intensities" some other, more physical and up-to-date values will be used, such as maximum accelerations of the ground particles or any other parametres adopted in anti-seismic engineering.

References

1. Riznichenko Yu.V. From the focal activity of earthquakes to their effect at the ground surface (in Russian). Izvestiya Acad.Sci. USSR, Fizika Zemli, No.II, 1-12,1965.

2. Riznichenko Yu.V. Problems of physics of earthquakes (in Russian). Izvestiya Acad.Sci. USSR, Fizika Zemli, No.2, 3-24, 1966.

3. Riznichenko Yu.V. Calculations of the frequency of occurrence of shocks at the earth's surface, which are due to earthquakes in a surrounding region (in Russian). Izvestiya Acad.Sci. USSR, Fizika Zemli, No.5, 16-32, 1966.

4. Riznichenko Yu.V. On quantitative determination and mapping of seismic activity. Annali di Geofisica, Roma, 12, No.2, 227-237, 1959.

5. Gorbunova I.V., Riznichenko Yu.V. An essay of mapping the seismic activity using a summation method (in Russian). Izvestiya Acad.Sci. USSR, Fizika Zemli, No.7, 22-29, 1965.

6. Riznichenko Yu.V. On possibilities to calculate the maximum possible earthquakes (in Russian). Trudi Instituta Fiziki Zemli Acad.Sci. USSR, No.25, 5-15, 1962.

7. Riznichenko, Yu.V. On a relation between the energy of the maximum earthquakes and the seismic activity (in Russian). Dokladi Acad.Sci. USSR, v.157, No.6, 1352-1354, 1964.

8. Riznichenko Yu.V. On seismic flow of the earth's masses (in Russian). In a book: Dinamika zemnoy kori, "Nauka", 56-63, Moscow, 1965.

9. Riznichenko Yu.V. Earthquakes as a display of the earth's crust and mantle flow. Proceedings of the European Seismological Commission, Copenhagen, 1966.

B.Papazachos, N.Delibasis, N.Liapis,
G.Moumoulidis and G.Purcaru

AFTERSHOCK SEQUENCES OF SOME LARGE EARTHQUAKES IN THE REGION OF GREECE

The foreshock and mainly the aftershock sequences of all (43 cases) the normal earthquakes (focal depth smaller than about 70 km) of magnitude $M \geqq 6$, occurred in the region of and near Greece from 1926 to 1964, are investigated in this paper. The region is bordered by the 34° N and 42° N parallels and 19° E and 29° E meridians.

The time and magnitude distribution of the aftershocks, the deformation characteristics and some properties of the material in the space domain of the several aftershock sequences are investigated.

In studying the deformation characteristics of the aftershock sequences of these earthquakes the known phases, compressional and "shear", were observed in almost all cases, when the focal depth is between about 15 and 55 km. In about thirty per cent of the cases a third phase was noticed. The most part of the energy in this phase is released by the so called major "late aftershocks" which occur from about one month up to some months after the main shock. There is evidence that the aftershock region of the large "late aftershocks" is close to the aftershock region of the main shock but it is not entirely included in it. The mean relaxation time for the "shear phase" was found equal to 2.0 days. This gives a coefficient of viscosity equal to 10^{17} gr/sec-cm in a depth of about 40 km. The deformation characteristics of the aftershocks of the large earthquake (M = 7 1/4), August 12, 1953 in the Ionian islands region are depicted in Figure 1. The three phases are clearly shown.

The largest aftershock of the shear phase which is usually the largest of all the aftershocks of the sequence occurs between a few minutes up to fourteen days after the

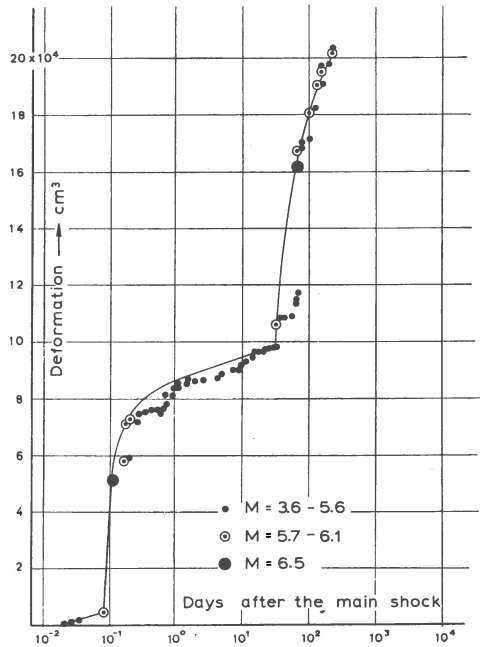

Fig. 1

main shock and its magnitude, M_1, can be roughly predicted by using the formula:

$$M_1 = 1.07 + 0.71\ M, \qquad 5\ 3/4 < M \qquad (1)$$

where M is the magnitude of the main shock. The magnitude of the largest aftershock is plotted against the magnitude of the main shock in Figure 2. For more accurate prediction, knowledge of the depth of the focus is necessary. For constant magnitude of the main shock the magnitude of the largest aftershock has large value in a depth of about 15 km and gradually decreases up to a depth of about 42 km where it increases abruptly and then it decreases gradually up to a depth of about 70 km. For depths smaller than 15 km or larger than 70 km the magnitude of the largest aftershock is small. The magnitude of the major "late aftershock" is usually of the same order as the magnitude of the largest aftershock of the sequence but it can be smaller or larger than that. Formula 1 holds only for M > 5 3/4.

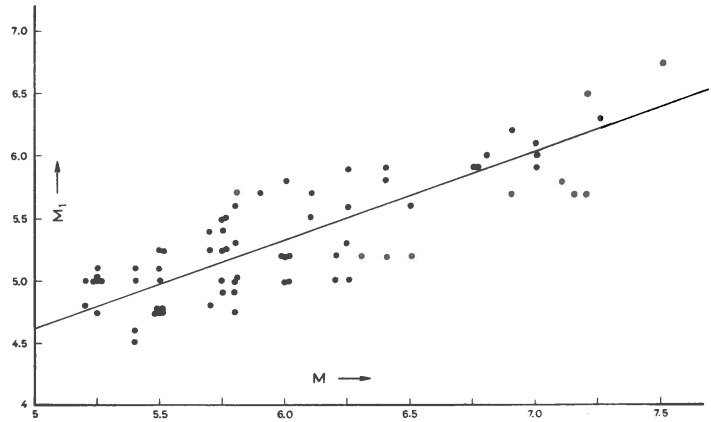

Fig. 2

For M < 5 3/4 this formula gives only an estimation of the largest possible expected aftershock.

The formula $N = N_o\,(M,h)t^{-0.4}$, $t < t_1$ describes roughly the time distribution of the aftershocks with $M \geqq 4$ when the magnitude and focal depth of the main shock is such that a considerable number of large aftershocks occur. N is the number of aftershocks (with $M \geqq 4$) which occur after t - 1 days after the main shock. N_o is the total number of aftershocks with $M \geqq 4$, which depends on the magnitude and focal depth of the main shock. The N_o increases with magnitude. For constant magnitude, the N_o is large in a depth of about 15 km and it decreases up to the Mohorovičić discontinuity. From the Mohorovičić discontinuity up to 70 km the rate of decrease of N_o is larger. Below the depth of about 70 km and above the depth of about 15 km the number of aftershocks with $M \geqq 4$ is very small. The t_1 varies between a few days and a few months.

A decrease of the constant b' of the cumulative frequency function of the magnitude with depth was observed. This is interpreted as an increase of the homogeneity of the material with depth. A horizontal variation of the b' was also noticed. The calculated values of the constant b' are

plotted against focal depths in Figure 3. This relation can be very roughly expressed by

$$b' = 1.26 - 0.0135\ h, \qquad 15\ \text{km} < h < 70\ \text{km}$$

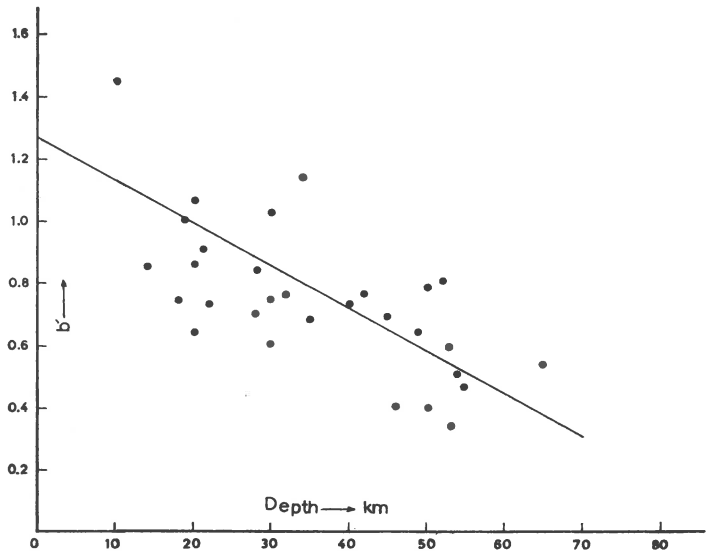

Fig. 3

There are some indications that for h < 15 km the b' increases much. The main shocks were preceded by one or more foreshocks in 16 cases. This means that 37% of the shallow earthquakes are preceded by one or more foreshocks of magnitude M > 3.5. The earthquakes which have foreshocks do not originate from certain regions but their epicentres are distributed all over the area considered. Data for studying the cumulative distribution of the magnitudes of the foreshocks were available in three cases only. It was found that in all three cases the constant b' of the foreshocks is smaller than that of the aftershocks of the same sequence. The mean value of this difference is approximately 0.2.

It can be generally concluded that: Studies on foreshock and aftershock sequences can give information about

some properties of the material (homogeneity, viscosity etc) and the distribution of stress in the aftershock region. Combination of observational, experimental and theoretical work on problems related with foreshock and aftershock sequences could turn out to be one of the powerful methods for studying the anatomy and physiology of the crust and uppermost part of the mantle and may contribute to the problem of earthquake prediction.

S.I.Subbotin

PROBLEM OF CAUSES OF TECTONIC MOVEMENTS

The Earth's crust, its structural manifestations and mineral deposits associated with them are the result of the processes occurring in the upper mantle of the Earth at the depths of the first hundreds of kilometers. Regularities of distribution of structural forms and accumulations of mineral raw materials are subordinated to the processes in the upper mantle which is the source of the crustal substance and energy for the tectonic movements. In this connection cognition of these regularities is impossible without investigations of the upper mantle.

The problem of causes of the tectonic movements which is one of the cardinal problems of modern geotectonics must be treated in several aspects: geological, physical, physico-chemical, geophysical, astronomical, or more exactly cosmophysical.

Geological aspect. In the Earth's crust there exist various structural forms: depressions, uplifts, dislocations, blocks, folded structures, magmatic bodies and smaller, subordinated structural forms and mineral deposits. During the last decades it has been determined that exploration and prospecting for mineral deposits are associated with the necessity of studying deeper and deeper crustal levels where the largest field mineral deposits are distributed. Investigation of the interrelations between different structures, their link zones and relationships between the surface and abyssal forms is necessary for the clarification of causes of the tectonic movements.

Physical and physico-chemical aspect. Various substances, rocks including, vary smoothly in their volume with smooth variations of temperature and pressure. There exist, however, critical thermodynamic conditions (temperature and pressure) under which on the background of smooth variations a sharp discontinuous change of the substance volume

occurs - its reduction with the increased pressure and expansion with pressure decrease. It has been stated both theoretically and experimentally that the discontinuous changes of volume are associated with the phase, polymorphous and electronic transitions of the substance. Thus, volume is a monotonous function of pressure and temperature, disturbed by discontinuities at critical values of P and T.

Known are phase transitions solid ⇆ liquid ⇆ gas; transition from one mineral association to another (for instance, eclogite ⇆ basalt and olivine + water = serpentine + thermal energy); polymorphous transitions associated with changes in structure of the crystal lattice from the less compact atomic texture to a closer one and vice versa; electronic transitions caused by transfer, with the help of the increasing pressure, of the external electrons on the internal orbits with reduction of the atomic radius; volume variations of the substance owing to thermal expansion or contraction; of a certain significance are the changes in the crustal and mantle material occurring because of the radioactive decay; finally, existence of other processes can be assumed whose essence has not been revealed by science yet. Investigations of these and other processes form physical and physico-chemical aspect of the problem.

Geophysical aspect. It is known that with the increasing depth continuous, regular elevations of temperature and pressure are observed. However, in connection with the inhomogeneities of composition and state of the crustal and mantle substance inhomogeneities of thermodynamic conditions are also found in them. The Gutenberg seismic channel appears, irregular thermoelastic stresses, additional geodynamic stresses and other irregular phenomena. Their investigation forms the geophysical aspect of causes of the tectonic movements.

Astrophysical or cosmophysical aspect. The Earth is a rotatory system. Its rotation rate around the axis is not constant and these variations together with the inhomogeneous composition and state of the substance cause additio-

nal geodynamic stresses, the distribution of which is subordinated to the regularities of distribution of the inhomogeneities, mainly in the upper mantle. These additional stresses adding to or subtracting from the existing general stresses bring the pressure up to critical levels in areas where normal pressures were close to critical ones. It is such areas where polymorphous, phase, electronic transitions occur and chemical reorganization of the substance with the discontinuous variations of volume takes place which is the cause of subsidence or uplifting of the overlying crustal sections. Investigations of origination of the additional stresses caused in the Earth by its rotation rate irregularities form the astrophysical aspect of the problem.

Analysis and data generalization carried out by a number of researchers (Bernal, Jeffreys, Goranson, Gutenberg, Arkhangelski, Shatski, Magnitski, Lustich, Bridgeman, Lowering, Ringwood, Uffen, Ramsey, Byeloussov, Bullen, Kropotkin, Lyubimova and many others) allowed us to work out a general scheme and ways of studying the causes of tectonic movements and mechanism of formation of the most principal crustal elements.

Main statements of the scheme are these:

The Earth's mantle and especially its upper part characterized by mobility and nonstability of the substance state is the arena and source of energy for movements of the upper mantle and crustal material of which the Earth's crust has been formed as well as all kinds of mineral deposits.

The Earth's upper mantle is characterized by inhomogeneities of its substance composition and especially physical, mainly, thermodynamic conditions. Inhomogeneities are distributed both in vertical and horizontal directions and are manifested as variations of density, magnetization, electric, and elastic properties of substance, pressure, temperature, mineralogical, lithological, petrographic, and chemical peculiarities, changes of type of the crystal lattice, state of aggregation of the substance etc.

The mantle substance is subject to high pressure and sufficiently high temperatures, in other words it is under definite thermodynamic and thermoelastic stresses. In a number of the mantle regions its substance is under thermodynamic conditions close to the critical level at which phase, polymorphous and electronic transitions of the substance or its chemical reorganization may occur.

Under such conditions for the initiation of the reorganization necessary and sufficient is a slight change in the level of pressure or temperature or both parameters simultaneously, that is thermodynamic and thermoelastic stresses. This change takes place owing to the additional pressure or its partial reduction which occurs in certain zones of the mantle due to the irregularities of the Earth's rotation, or some internal processes in the lower levels of the mantle, or in connection with certain variations of the Earth's shape caused by the mass transfer on its surface or at depth.

With the inhomogeneities the processes of polymorphous, phase and electronic transitions and chemical rearrangement of the substance encompass different areas of the upper mantle. In some places where additional stresses arise the regions of the mantle substance contraction appear with the reduction of the volume, and in the zones of stress relaxation the regions of the substance expansion with volume increase.

The processes of contraction and expansion of the mantle substance are the cause of formation of crustal depressions and uplifts, respectively. Zone where these processes occur is the Earth's upper mantle whose thickness is described by the depths of 100 to 500-700 km, in other words it is the mobile region where medium and deep seismic centers appear and in the upper part of which the "softened" zone of the mantle substance exists known as the Gutenberg "seismic channel".

On the boundaries of the contraction and expansion zones deep fractures appear. They are generated at the depths of the first hundreds of kilometers, and developing upwards they disrupt the subcrustal part of the mantle and

the crust. As the upper mantle substance is at temperatures of hundreds and first thousands of degrees centigrade and under pressures of tens and first hundreds of thousands atmospheres - fractures cannot be looked upon as discontinuities of the solid material layers with the yawning cavities and splits. We associate with the term "deep fracture" the idea of combination of three main elements of such a structure:

1. Zone on the horizontal margin of the region where the transition occurs from the contracted or expanded mantle substance to its stable state, or the region of transition from one contraction or expansion regime to another;

2. Zone of stresses and shearing arising over the preceeding zone and caused by the relatively vertical transfer of the masses on both sides of the fracture;

3. Zone of crustal fracturing situated over the zone of stresses and shearing.

The depths of zones of the substance transformation processes caused by the changes of pressure and thermal conditions are different in the regions of formation of the platform depressions and uplifts on one side and geosynclinal zones and folded mountainous structures - on the other. In the platform zones the processes of the substance volume variations at the expense of the polymorphous phase and electronic transitions occur probably in one active belt and at a smaller rate, while during formation of the geosynclinal downwarps they take place at least in two active belts: 1) the lower, responsible for the formation of the general depression during the initial stage and also of the folded structure in the stage of general uplifting during the concluding phase of development of the geosynclinal region; and 2) in the upper belt, responsible for the formation of the intrageosynclines, intrageoanticlines, separate depressions and uplifts among the mountainous structures of a given area. The rate of these processes in the geosynclinal zones several times exceeds their rate on the platforms. If on the platforms the period of formation of depressions is determined by hundreds

of millions years, in the geosynclines it is only tens of millions years.

Magmatism in the light of the theory of causes of the tectonic movements is closely related to the same processes that underlie the tectonic movements. Moreover, the manifestitations of magmatism - melting of the mantle substance, its accumulation, motion inside the mantle, overtravel into the Earth's crust and eruption on its surface - are the immediate consequences of the processes which result in the formation of principal geostructural units of the Earth's crust. At the initial stage of formation of the depressions the substance contraction leads to the downward displacement of its strata contained between the crust and the contraction zone. During this period the Earth's crust, possessing considerable stability, was maintained in the form of an arch, lagging behind the upper mantle regions in their movements downwards. Owing to this in the subcrustal part of this zone, in connection with the manifestations of the stability and rigidity forces, the pressure reduction occurs resulting in the reduction of the heat capacity, increase of the temperature level, decrease of the melting point, which are the causes of origination of the melting center, giving rise to the magmatic activity.

That is how we picture the principal statements of the theory of causes of the tectonic movements and the mechanism of formation of the main tectonic units of the Earth's crust.

A.P.Sinitsyn

THE INSTABILITY EFFECT OF SURFACE WAVES IN ELASTIC MEDIA

Abstract

The conditions of beatings arising by seismic wave propagation in elastic layers were investigated. The wave equations were worked out by using the continuity conditions on the layer boundary. The influence of gravity forces was investigated. The correlation between the wave length and layer thickness was determined this correlation giving rise to the instability effect.

Statement of the problem

The rise of beating by propagation of seismic waves was investigated experimentally by Savarensky [1], Medvedev [2], and Knopoff [3]. The solution for a two layered medium was given in [4]. The instability effect was investigated by the author when the surface wave was propagated under the rigid structure [5, 6]. In this report the method will be applied to solve a more complicated case when the seismic wave propagates on the boundary of an elastic layer. The vertical component of surface waves is analysed in detail. On this component the great influence is affected by the gravity field. On the horizontal boundary of the layer the gravity field will be directed perpendicular to it. The vertical component of travelling surface waves will change the stress distribution on the layer caused by the gravity field. The monochromatic wave magnifies the stress of the gravity field on that half wave where the compression stresses arise. On the second half wave there are tension stresses and the gravity field stresses are diminished. If the tension stresses in the wave exceed the gravity field compression stresses breaking of the contact on the layer boundary may occur. On this part of the boundary the next half waves will be propagated with magni-

fied amplitudes, which correspond to the free layer boundary. Now the instability effect and the characteristic beatings arise.

Method of solution

In this problem it is possible to take out the gravity forces on the boundary of the layer. The stationary monochromatic plane wave for a fixed time moment can be described by the equations:

$$v_i = V_i \cos \frac{2\pi x}{L} \tag{1}$$

$$(\sigma_{yy})_i = [\sigma_i + \rho_i g V_i] \cos \frac{2\pi x}{L} \tag{2}$$

in which v_i is the vertical component of the seismic wave, L the length of the wave, ρ_i the layer density, g the gravity acceleration, σ_i the vertical compression stress on the layer boundary, and V_i the amplitude of the vertical displacement.

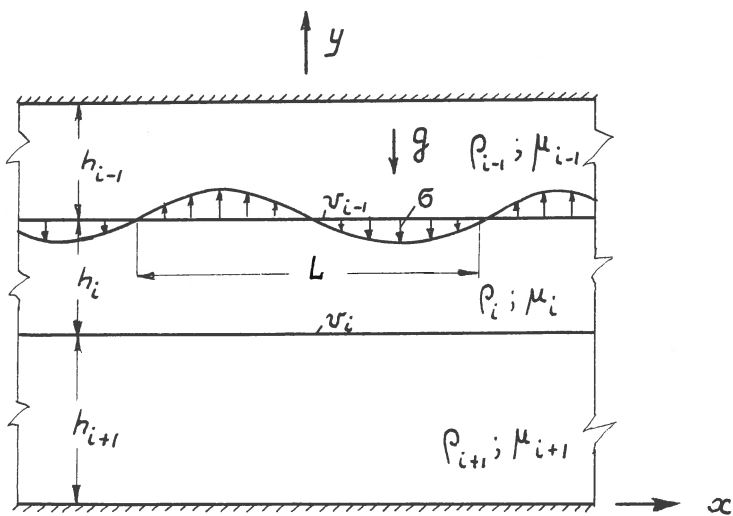

Fig. 1. The scheme of elastic layer.

The continuity conditions of the upper and lower boundary of the layer are:

$$(\sigma_{yy})^{1}_{i-1} = (\sigma_{yy})_i \qquad (3)$$

where $(\sigma_{yy})^{1}_{i-1}$ is the stresses on the lower boundary of the (i-1) layer, and $(\sigma_{yy})_i$ is the stresses on the upper boundary of the i-layer. Substituting the value of σ from equation (2) into equation (3) we obtain:

$$\sigma^{1}_{i-1} + \rho_{i-1}\, g\, V_{i-1} = \sigma_i + \rho_i\, g\, V_{i-1} . \qquad (4)$$

This equation may be written in the more generalized form:

$$\sigma_i = \sigma^{1}_{i-1} + (\rho_{i-1} - \rho_i)\, g\, V_{i-1} \qquad (5)$$

From equation (5) it is clear, that the correlation between the densities of the layers influences the result. If the density of the lower layer is greater than on the lower boundary of the upper layer the stresses increase. When the density of the lower layer is less ($\rho_i < \rho_{i-1}$) than the density of the upper layer the gravity field will unload the layer and the instability effect arises.

Twolayered systems

Let us consider a system consisting of two layers. The first (upper) layer has an upper boundary free of stresses, i.e. $\sigma_1 = 0$. The lower layer is situated on a rigid foundation. The vertical displacement of the lower boundary of this second layer is equal to zero, i.e. $V_3 = 0$. The displacements at the layer boundary will be expressed by stresses in matrix form as following:

$$\begin{vmatrix} \sigma_1 \\ \\ \sigma_2 \end{vmatrix} = \frac{2\pi\mu_1}{L} \begin{vmatrix} A, & B \\ \\ -B, & -A \end{vmatrix} \cdot \begin{vmatrix} V_1 \\ \\ V_2 \end{vmatrix} \qquad (6)$$

where μ_1 is the shear modulus.

The coefficients A and B were calculated by the following formulas:

$$A = 2\left[\frac{sh^2\gamma_i}{sh2\gamma_i + 2\gamma_i} + \frac{ch^2\gamma_i}{sh2\gamma_i - 2\gamma_i}\right] \tag{7}$$

$$B = 2\left[\frac{sh^2\gamma_i}{sh2\gamma_i + 2\gamma_i} - \frac{ch^2\gamma_i}{sh2\gamma_i - 2\gamma_i}\right] \tag{8}$$

in which

$$\gamma_i = \frac{\pi h_i}{L} \tag{9}$$

By substituting the value σ_i from formula (6) into formula (5) and taking into account (7), (8) and (9) we obtain:

$$\frac{2\pi\mu_1}{L}(A_1V_1 + B_1V_2) + \rho_1 g V_1 = 0 \tag{10}$$

$$\frac{2\pi\mu_2}{L}(A_2V_2 + B_2V_3) = \frac{2\pi\mu_1}{L}(-B_1V_1 - A_1V_2) + (\rho_1 - \rho_2) g V_2 .$$

To determine the instability equation we shall put the determinant of the equation system (10) equal to zero:

$$a_{11}a_{22} - a_{12}a_{21} = 0 \tag{11}$$

The quantities in equation (10) are:

$$a_{11} = \left[A_1 + \frac{L}{2\pi h_2}\left(1 + \frac{\rho_2}{\rho_1}\right)\beta\right]; \qquad a_{12} = a_{21} = B_1$$

$$a_{22} = \left[A_1 + \frac{\mu_2}{\mu_1} A_2 - \frac{L}{2\pi h_2}\beta\right]. \tag{12}$$

where

$$\beta = \frac{(\rho_1 - \rho_2) g h_2}{\mu_1} . \tag{13}$$

The equation (11) for determination of the parameter β is quadratic.

The positive root of this equation is correlated to the amplitudes increasing with time by an exponential law and is typical for the instability effect.

Discussion of results

The stability equation (11) can be extended in the following way:

$$\beta^2 + p\beta - q = 0 \qquad (14)$$

where p and q are functions of wave length and of the correlation between thicknesses and densities of the layers. We obtain the value of the parameter β by which the beatings arise by solving the equation (14) and by taking into account the real and positive root of this equation.

$$\beta = -\frac{1}{2}p + \sqrt{\frac{1}{4}p^2 + q} \qquad (15)$$

The dependence of β of the length of the seismic wave by different layer thicknesses and by constant value of density changes is shown in Fig. 2.

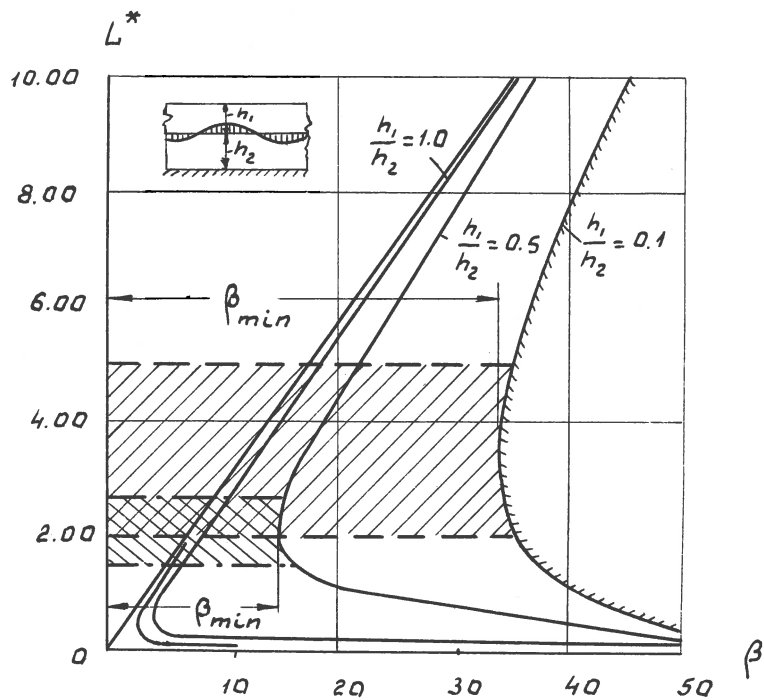

Fig. 2. The instability regions.

The wave length is taken in dimensionless form:

$$L^* = \frac{\pi h_2}{L} \quad .$$

To each value of the thickness-ratio h_1/h_2 a curve corresponds, which divide the coordinate plane into two parts. To the left of β_{min} on each curve are situated the values β by which the wave of any length does not cause the beatings. For each value $\beta > \beta_{min}$ there are two waves by which the beatings arise, the one is a short wave, the other is a long wave. The instability area due to long waves has a small correlation to the layer thicknesses when $h_1/h_2 > 1$, that is why the beatings can be observed more often by long waves. The beatings arise by one certain value of the parameter β when the wave is short. In this case their observation is more difficult. When the thickness of the upper layer is smaller than that of the lower layer there is an interval on the curves with almost constant values of β. By this value of β the instability arises for a whole region of wave length values. The width of this region increases when the thickness of the upper layer decreases. For example: if $h_1/h_2 = 0.10$ the width of instability region is from $L^* = 2$ to $L^* = 5$ of dimensionless wave length. This conclusion indicates that a thin upper layer can be easily put into the instability conditions by the vertical component of a seismic wave travelling under the footing of this layer.

Conclusion

The simplified investigations carried out show that the gravity forces exert a great influence on the arising of the instability effect. For a twolayered medium with small thickness of the upper layer the instability arises in a wide range of wave length. The investigations in this field must be continued, and the obtained theoretical conclusions checked by experiments.

Literature

1. Savarensky, E.F. and Kirnos, D.P. The Elements of Seismology and Seismometry. Gos.Techniko-Theoreticheskoe Publishing house II ed. Moscow, 1955. Germ.ed. 1960.

2. Medvedev, S.W. Engineering Seismology. Stroyisdat 1962, Moscow. English edition 1965.

3. Knopoff, L. and others. "The structure of superior Earth Mantle in Alpes Region". Report on Budapest meeting of E.S.C. 1964.

4. Biot, M.A. and Ode, H. Theory of Gravity Instability with Variable Overburden and Compaction. Geophysics vol.XXX, no.2, April 1965, pp.213-227.

5. Sinitsyn, A.P. On the Cause of Beating Arising by Structure Vibrations. Scientific Work of Earth Physic Institute No.22 (189) 1962, Moscow.

6. Sinitsyn, A.P. Über das Zusammenwirken zwischen seismischen Wellen und dem Bauwerk. Deutsche Akad. d. Wissenschaften. Veröffentlichungen des Inst. für Bodendynamik Heft 77, Berlin, 1964.

L.P.Vinnik

STRUCTURE OF MICROSEISMS

Introduction

The development of the multichannel recording methods in seismology gave an impetus and opened possibilities of the investigation of the structure of microseisms on a scale which was impossible a few years ago. In order to design optimal multichannel systems for the extraction of seismic signals from ambient noise, the knowledge of the noise spectral density which depends on frequency and wave numbers is required (1). At the same time the threedimensional spectral density contains a considerable information which is especially important for seismologists studying the nature of microseisms. The spectral density of microseisms in turn cannot be obtained without multichannel systems. If it were possible to use sufficiently large and dense seismograph grids for the analysis, it would not be more complicated than the common spectral analysis; but the seismograph arrays actually available are not good for the purpose and the problem therefore should be solved otherwise: one should take a certain model of the field and evaulate its parameters following the observations or assume a certain hypothesis and test its agreement with the observation data.

The method and the results of the analysis of microseism structure made for some regions of the USSR are presented here. Microseisms in the frequency range of 0.5-2 cps were recorded by 3 arrays located in quiet regions of Middle Asia and Kazakhstan. Microseisms in the frequency range 0.17-0.25 cps (4-6 second periods) were recorded by 2 arrays, one of them (No.1) being located in Kazakhstan and the other (No.2) - in the Moscow region. The array No.1 consisted of vertical and horizontal seismographs located as shown on the diagram on Figure 1. Records obtained

as ordinary seismograms were digitized and processed on a high speed computer.

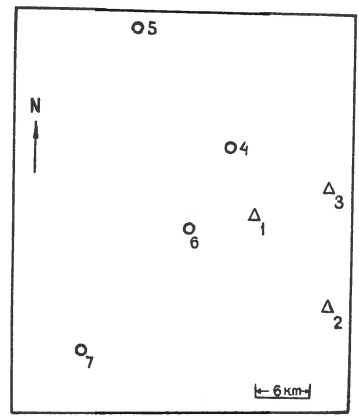

Fig. 1. Diagram of seismograph location of array No.1; O - vertical seismograph, △ - three-component set.

Analysis

Estimates of the auto-correlation function, the spectral density of each seismograph record, the cross-correlation function, and the cross-spectral density of each pair of records were computed by means of a method similar to that described in (2). The subsequent analysis was performed by a set of methods the main of which is the summing up of the records of homonymous motion components with time shifts linearly depending on seismograph Cartesian coordinates in the plane. Actually mean squares were determined for each array tuning instead of instantaneous values. This method is equivalent to one of the correlation analysis methods. The mean square of the array output can be represented as the sum of a constant term and a variable one depending on the array tuning. The variable term can be derived from the cross-correlation functions and represented as the function of apparent velocities V and propagation azimuths α of the waves to which the array is tuned. The variable which is referred to as Q (V,α) is set on a correlation diagram. The diagram construction allows to map the (V,α)-plane into the

plane of wave numbers. The diagram is drawn in Cartesian coordinates (W-E, S-N); the value of Q (V,α) is related to the end of the radius-vector forming the angle α with the axis (W-E) and having modulus ν/V, ν being the prevailing frequency of the process. This way of diagram drawing makes its interpretation easier.

A model of the field should be taken prior to the interpretation of the diagram. It is supposed that the field consists of waves and of an "irregular" component the spectral density of which does not depend on wave numbers; apparent velocities, propagation azimuths, intensities of each wave, and intensity of the irregular component should be evaluated.

The array directivity diagram shifts along the plane of wave numbers as the array tuning is changed and the components of the field with some wave numbers are passed through while the rest are extinguished (1). The main difficulties encountered in the interpretation of the correlation diagram are due to the side pass-areas of the array directivity diagram. The case of one wave and of an irregular component is the most simple one. The necessary manifestation of this case is the similarity of relieves of the correlation diagram and of the directivity diagram provided the main pass-area of the directivity diagram and the main rise of the correlation diagram are placed together. This sign may be regarded sufficient in many cases in the sense that the probability of such similiraty in case of a few waves is sufficiently small. In complicated cases it is necessary to test the possibility of obtaining every rise of the correlation diagram as a side rise relative to another rise or as the sum of a few side rises. The rise is regarded the main one if it cannot be thus obtained. Our experience proves that an effective use of the method is possible in the cases of 2-3 waves with nearly equal energy.

The tuning of the arrays of horizontal seismographs to the wave with a certain azimuth of propagation can be accompanied by the rotation of the seismograph axes in the same direction or in the perpendicular one, and correlation

diagrams $Q_{SV}(V,\alpha)$ and $Q_{SH}(V,\alpha)$ which facilitate discrimination between SV and SH modes can be made up.

Correlation diagrams of the third type $Q_{\pi/2}(V,\alpha)$ and $Q_o(V,\alpha)$ describe the coherence of the vertical and horizontal motion components at the array outputs and facilitate discrimination between the elliptically and linearly polarized waves; for the linearly polarized wave, $Q_{\pi/2}(V,\alpha) \approx 0$; for the elliptically polarized one, with the vertical axis of the ellipse, $Q_o(V,\alpha) \approx 0$, $Q_{\pi/2}(V,\alpha) \neq 0$.

The methods described above deliver little information on the weakest waves included in the irregular component although, according to our data, it holds more than a half of full process energy. Therefore these methods are complemented by the integral method of analysis which is not based on the division of the field into different wave components. The principle of the integral method can be described as follows. Nearly all of the seismograph grids used in our observations include isosceles rectangular triangles. For each of such triangles 3 cross-spectral estimates were obtained, their real parts being devided by the spectral density. The average of 3 normalized estimates referred to as K was computed for each triangle. The observational values of K are compared with the values obtained for a certain model imitated on a high speed computer. The imitated field consists of 15 weak waves and 2 comparatively strong ones; the energy portions of both parts are the same. All the waves have equal velocities and similar spectrum shapes; their azimuths of propagation are random numbers distributed evenly between 0 and 2π. A standard corridor is constructed in which the values of K obtained from the modelling fall with nearly 90% probability. The standard corridor of $K(\zeta)$ and the curve of

$$K_o(\zeta) = \frac{2J_o(2\pi\zeta) + J_o(2\sqrt{2}\pi\zeta)}{3}$$

are drawn on Figure 2; J_o is the Bessel function of the first kind of zero order, $\zeta = f\Delta/V$, f - frequency in cps, Δ - triangle cathetus length. To analyse the observational data one may either fix Δ and V and compare standard and

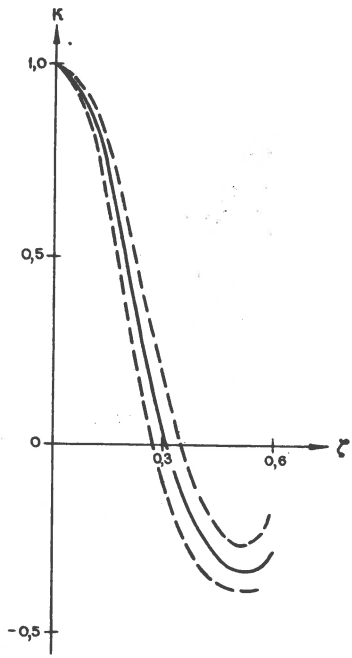

Fig. 2. Standard corridor of $K(\zeta)$ (dotted lines) and curve of $K_o(\zeta)$.

observational curves of K(f) or fix V and f and compare curves of $K(\Delta)$. If the values of K obtained from the observations do not fall into the corridor, it is considered the manifestation of the velocity difference between the observed field and the model.

Examples of the analysis

As an illustration of the integral method, observational curves of K(f) for one of the triangles are shown on Figure 3; for the standard corridor the phase velocity of the fundamental Rayleigh mode is taken. The figure shows that the curves lie above the corridor; it indicates the presence of waves with much higher apparent velocities than that taken for the corridor. If it is assumed that the field consists of Rayleigh waves and of waves with much higher apparent velocities (20-40 km/sec), the coherence

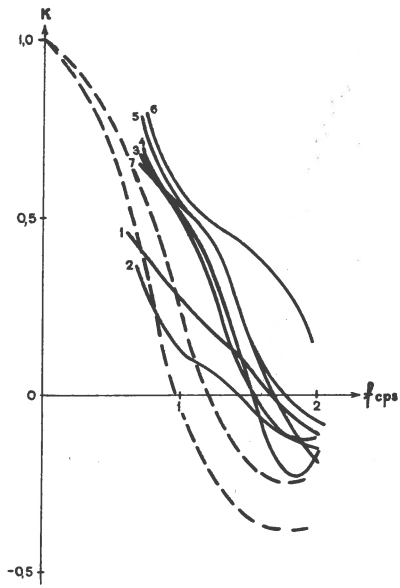

Fig. 3. Curves of K(f) for Δ = 1 km (continuous lines) and standard corridor for fundamental Rayleigh mode (dotted lines).

loss of the high-velocity component for the frequency where the coherence of Rayleigh waves diminished to 0, is negligibly small; the value of K for this frequency may be considered the evaluation of the energy portion of high-velocity waves. (In the case concerned, this portion is approximately 0.6 or 60% of full process energy for 1 cps.) If one assumes that the prevailing velocity of high-velocity waves is not 20-40 km/sec but 5-10 km/sec, the previous value (60%) should be increased.

The use of the correlation diagrams is illustrated by the data of the array No.1 (4-6 second microseisms, Kazakhstan). In Figure 4 the correlation diagram $Q(V, \alpha)$ of the vertical component of a seismogram obtained in October 1961 is shown; the coordinate axes coincide with the (W-E) and (S-N) directions; the same axes are the axes of wave numbers for operation with a directivity diagram; apparent velocities are set down on the vertical axis as scale; the band 3-4 km/sec within which the phase velocity of the

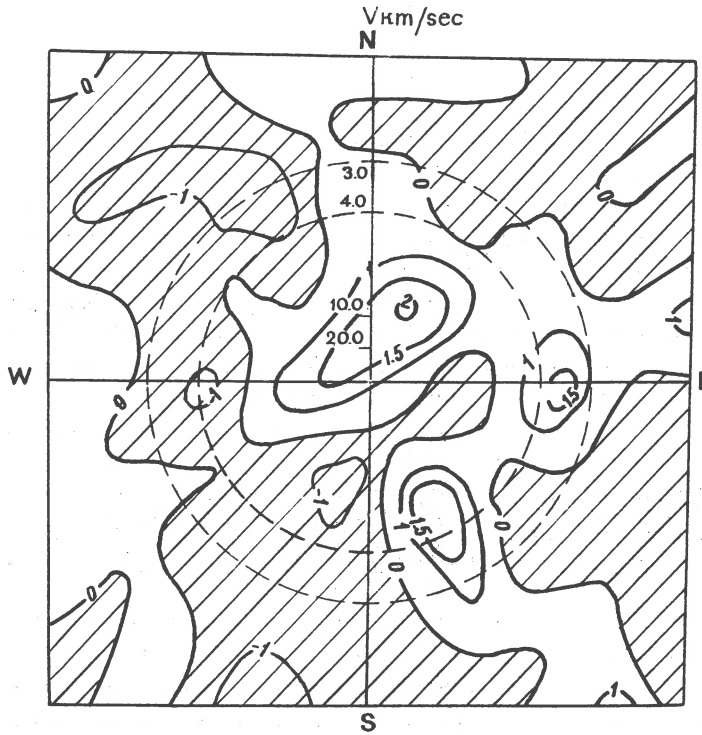

Fig. 4. Correlation diagram $Q(V,\alpha)$ of vertical component of seismogram 31/10-61, array No.1.

fundamental Rayleigh mode lies is marked by dotted lines; points of equal values of Q are connected by lines; the negative value area is hatched. There are 3 rises on the diagram; using the directivity diagram (Figure 5) it is easy to find out that they correspond to 3 different waves with the parameters: $V_1 \approx 10$ km/sec, $\alpha_1 \approx 70°$; $V_2 \approx 3{,}5$ km/sec, $\alpha_2 \approx 0°$; $V_3 \approx 4$ km/sec, $\alpha_3 \approx 300°$. The energy portion of each wave is approximately 10% of the full process energy; the presence of a high-velocity wave can be established independently by means of the integral method. On the diagram of the (S-N)-component (Figure 6a) there are a few rises but only one of them, at the right part of the diagram, gives a velocity value which is physically possible (3.7 km/sec). The relief of the diagram coincides

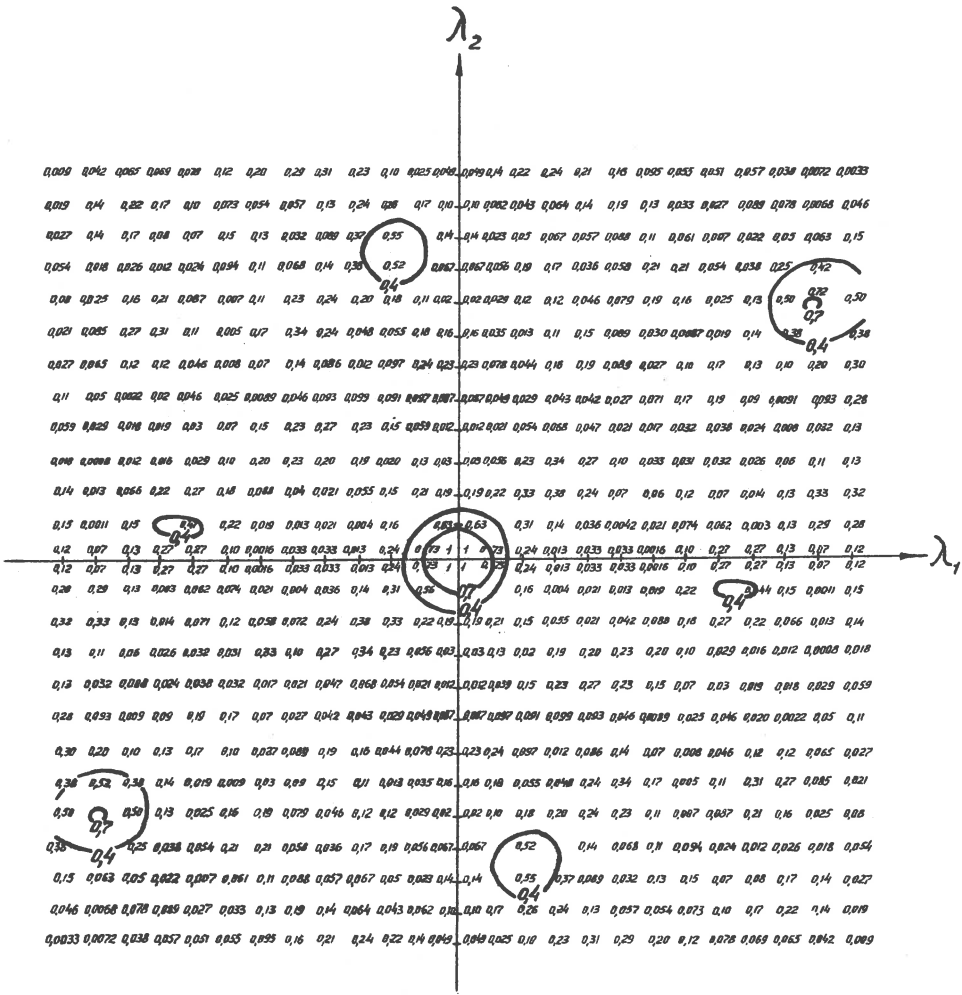

Fig. 5. Directivity diagram of array No.1 (vertical seismographs).

with that of the directivity diagram (Figure 7), as it should be in the case of one wave. The diagram of the (W-E)-component is of similar character. The type of this wave is determined by means of the diagrams $Q_{SV}(V,\alpha)$ and $Q_{SH}(V,\alpha)$ (Figure 9). There is a rise on the diagram $Q_{SH}(V,\alpha)$ corresponding to shear SH or Love wave, its energy portion being close to 35%, $V \approx 4$ km/sec, $\alpha \approx 340°$. At the same point of the diagram $Q_{SV}(V)$ there is a small rise

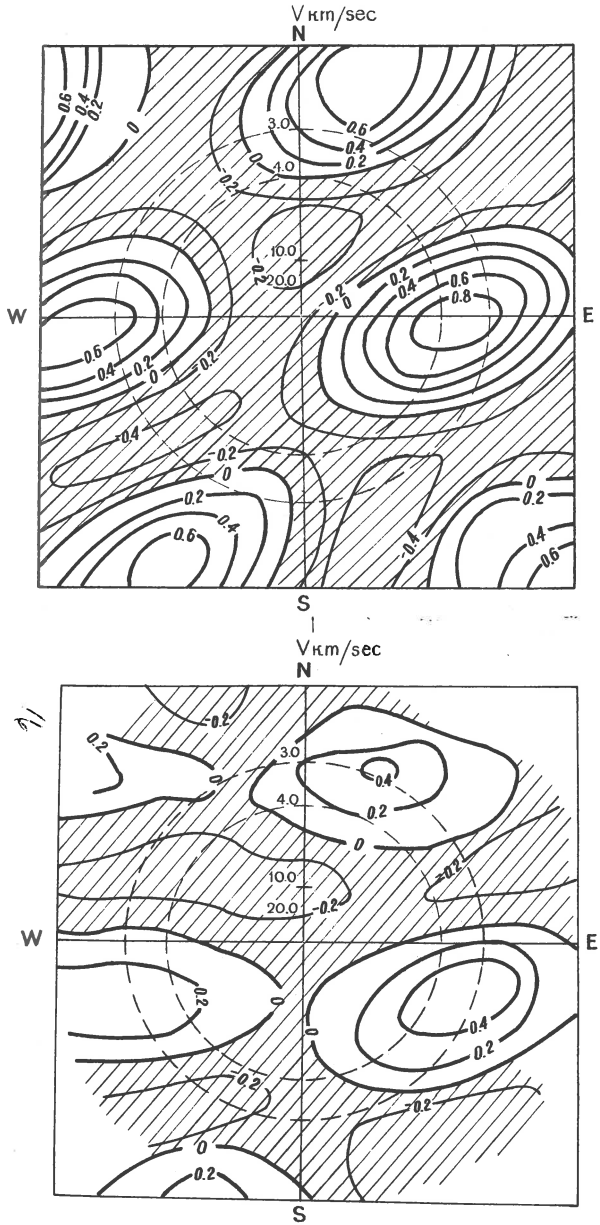

Fig. 6. Correlation diagrams of seismogram 31/10-61, array No.1: a) $Q_{S-N}(V,\alpha)$, b) $Q_{W-E}(V,\alpha)$.

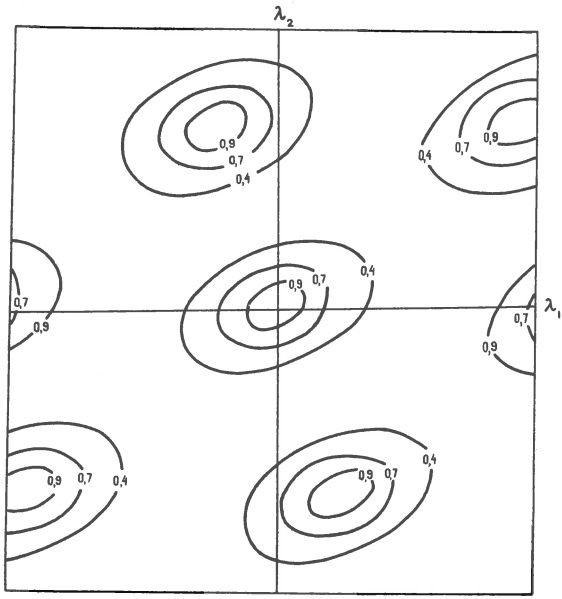

Fig. 7. Directivity diagram of array No.1 (horizontal seismographs).

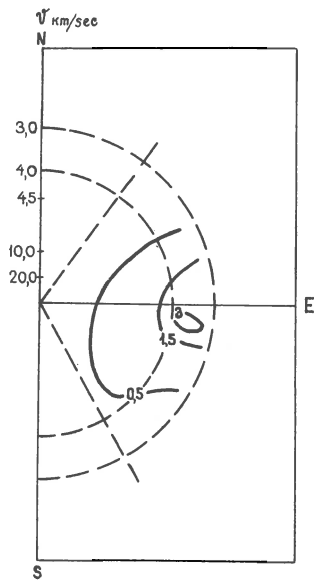

Fig. 8. Correlation diagram $Q_{\pi/2}(V,\alpha)$ of seismogram 31/10-61, array No.1.

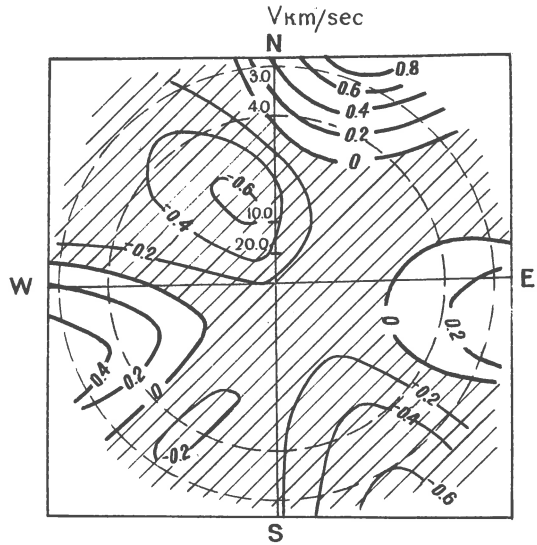

a

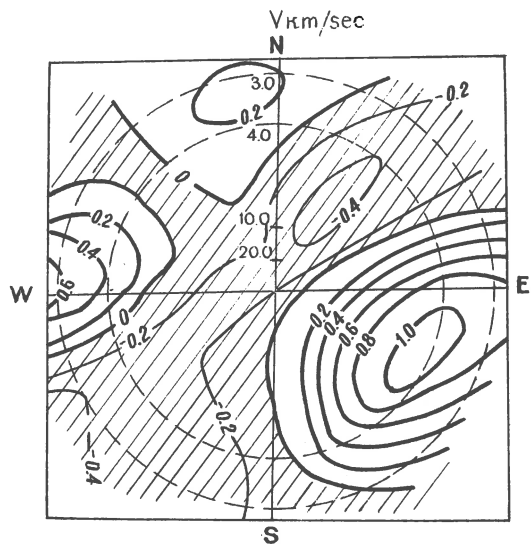

b

Fig. 9. Correlation diagrams of seismogram 31/10-61, array No.1: a) $Q_{SV}(V,\alpha)$, b) $Q_{SH}(V,\alpha)$.

which may be investigated by means of the diagrams $Q_{\pi/2}(V,\alpha)$ (Figure 8) and $Q_o(V,\alpha)$. $Q_o(V,\alpha) \approx 0$ for the point concerned

and on the diagram $Q_{\pi/2}(V,\alpha)$ there is a rise which corresponds with the elliptically polarized wave with $V \approx 3,5$ km/sec. Using all the diagrams, it is possible to identify the waves detected in the vertical component. The wave with $V \approx 10$ km/sec produces purely vertical motion; hence it is a P-wave. The velocity and the polarization of the wave with $V \approx 3.5$ km/sec are those of the fundamental Rayleigh mode. The wave with $V \approx 3.7$ km/sec produces purely vertical motion and is similar to a shear SV wave with an angle of incidence close to $\pi/2$, but it is more likely according to (3) that it is one of the higher Rayleigh modes or a mixture of a few higher modes.

Main results

When interpreting the observations made by the array No.1 (4.6 second microseisms, Kazakhstan) the presence was established of P waves with an apparent velocity of 10-20 km/sec and an energy portion of 10-35% of the full process energy. Waves with velocities of 3.5-4 km/sec were also detected sometimes, but the energy of the P wave is, as a rule, the highest among the waves detected in the vertical component. In the vertical component waves with velocities of 3.5-4 km/sec are represented by the fundamental Rayleigh mode and by waves with certain signs of shear SV modes; we prefer to identify them with the higher Rayleigh modes. In the horizontal component waves with the signs of shear SH wave or, what is more likely, Love waves prevail. The total energy portion of all detected waves is, as a rule, less than 50% of full process energy; the irregular component holds the rest. It is difficult to ascertain any regularity in the azimuths of wave propagation; they change in different seismograms. There are significant differences (of the order of dozens of degrees) between the propagation azimuths of different waves in the same seismogram.

When analysing high frequency microseisms in the same seismo-geological region (Kazakhstan, Middle Asia) the following conclusion is drawn. In the vicinity of 1 cps waves with apparent velocity much higher of the velocity

of Rayleigh wave often prevail; the energy portion of the high-velocity component is close to 60% or more in the 0.5-1 cps frequency band; there are waves with apparent velocity close to 20 km/sec or higher among the high-velocity waves; in the frequency band 0,5-2 cps either the energy portion of the high-velocity component decreases as frequency rises, or prevailing velocity decreases, or both phenomena take place. We believe these waves to be, at least partly, the high frequency components of P waves detected in 4-6 second microseisms. There is the same steady correlation of wave energy and of the energy of the irregular component as for 4-6 second microseisms.

When analysing the vertical component of 4-6 second microseisms recorded by the array No.2 (Moscow region), high-velocity waves were not detected; there is a strong irregular component together with the Rayleigh wave with phase velocity of 2.9-3.3 km/sec, its source being in the North Atlantic direction. The deviation of phase velocity estimates is mostly due to the variations of the actual velocity rather than to the measurement errors.

The microseismic amplitudes on the records of the array No.2 located comparatively close to the Atlantic are a few times higher than those recorded by the other arrays placed in the middle of a continent. Apparently the amplitude decrease in the middle of a continent is caused mainly by the surface wave attenuation resulted also in the prevalence of P waves. This phenomenon seems paradoxical, but it becomes more clear if it is taken into account that a short-period surface wave propagates mainly in the upper, highly heterogeneous part of the Earth's crust, where effects of scattering are of great importance. At the same time the greater part of a teleseismic P wave path lies in a comparatively homogeneous medium; the comparatively low absorption in the deeper mantle is of importance too.

We believe that the P wave source is the same as for other wave components of microseisms: motion of great water masses. Otherwise it would be difficult to explain the independence of P wave energy portion on microseisms amplitude fluctuations. Large dimensions of the microseism

sources may result in the energy focalizing of P waves propagating approximately down-ward, and it may be the additional factor that maintains relatively high amplitudes of P waves on great epicentral distances.

The presence of P waves in ambient noise is an unfavourable factor for P wave-signal detection; it may limit the effectiveness of certain signal detection arrangements such as seismograph arrays or deep well seismographs.

Some of the problems discussed above are considered in detail in the following papers: (1, 4, 5, 6).

References

1. Vinnik, L.P. "Prostranstvenno-vremennaja filtratzia seismicheskogo signala." Izvestija Akademii Nauk SSSR, serija geofhiz, 6, 1963.

2. Blackman, R.B., Tukey, J.W. The measurement of power spectra from the point of view of communication engineering. Bell System Techn.J., v.37, No.1, 2, 1958.

3. Kovach, R.L. and Anderson, D.L. Higher mode surface waves and their bearing on the structure of the Earth's mantle. Bull. Seism.Soc.Amer., v.54, No.1, 1964.

4. Vinnik, L.P., Deniskov, A.S., Konkov, G.D. "Structura microseism v oblasti 1 gtz." Fizica Zemli, in press.

5. Vinnik, L.P. "Structura 4-6 secundnich microseism." Dokladi Akademii Nauk SSSR, 162, 5, 1965.

6. Vinnik, L.P. "Structura 4-6 secundnich microseism." Fizica Zemli, in press.

E.F.Savarensky, T.A.Proskurjakova and E.V.Voronina

ON MICROSEISM PHASE VELOCITIES AND THE DIRECTIONS TO THE EXCITATION SOURCE

Introduction

The method of dispersion of group and phase velocities of surface waves for studying the structure of the Earth crust and upper mantle has been widely used lately as well in the USSR as abroad. In this field the works are dedicated to the use of long-period surface waves of Rayleigh and Love in order to study the deeper layers of the Earth.

In this paper an attempt has been made to obtain information about the utmost upper layers of the Earth crust using the dispersion of microseism phase velocities in the interval of periods from 3 to 8 sec.

The method and the material used

In the USSR the observations of microseisms at the tripartite microseism stations Pulkovo (P) and Simpheropol (S) have been carried out. These stations were described in full detail in the works published earlier, and here we shall give only a few data. The vertical seismographs were installed in the vertices of a triangle with sides from 600 to 1500 m. The magnification of each set reached its maximum value 15-20 thousands at the period 5,5 sec. The recording speed was increased to 15-20 mm/sec., which made it possible to carry out the calculation of the phase shift with an error less than 0,03 sec. The seismographs at both stations were identical. From the material of observations four cases with the intensity slightly above average were chosen: 28/1-61, 13/1-62, 18/1-62, 12/2-62.

In each of these cases trains of recording with the duration from 1 to 3 min., were chosen. By means of a special machine the ordinates of recording with the interval of 0,5 sec. were measured. The calculation of amplitude and phase spectra was made by means of the computer.

Microseism phase velocities were determined for each station by phase spectra. For this purpose the usual method allowing carrying out of the determination of phase velocity and the direction to the source of the microseisms was used (2). (Fig. 1).

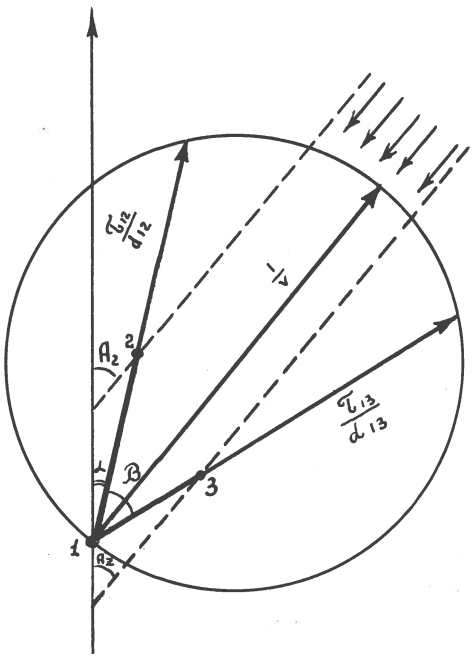

Fig. 1. The scheme of determining the directions to the microseism source and phase velocity.

The results obtained

In Fig. 2 amplitude spectra for Simpheropol are given as an example. The illustrated curves are given by taking into account the frequency characteristics of the seismographs. It appeared that the amplitudes at P are much higher that at S, the amplitude maximum at P being 5-6 sec., at S 6-7 sec. The width of the maximum of the spectrum at the rise equal to 1/2 is 1,5-2 sec. The amplitude in the spectrum maximum is about 4-5 times more than the amplitude of the basic microseism background (on the left T = 4 sec., on the right T = 8 sec.).

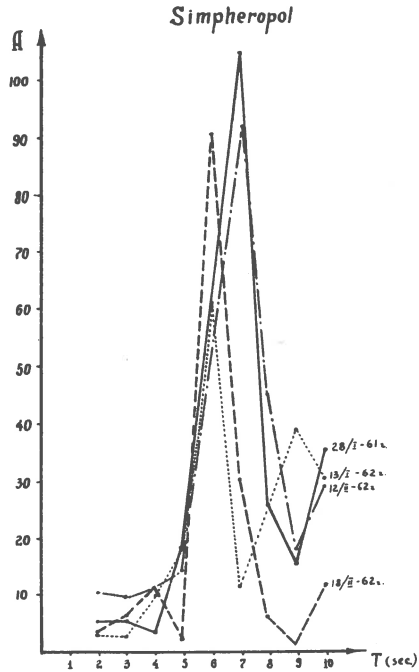

Fig. 2. Amplitude spectra in Simferopol.

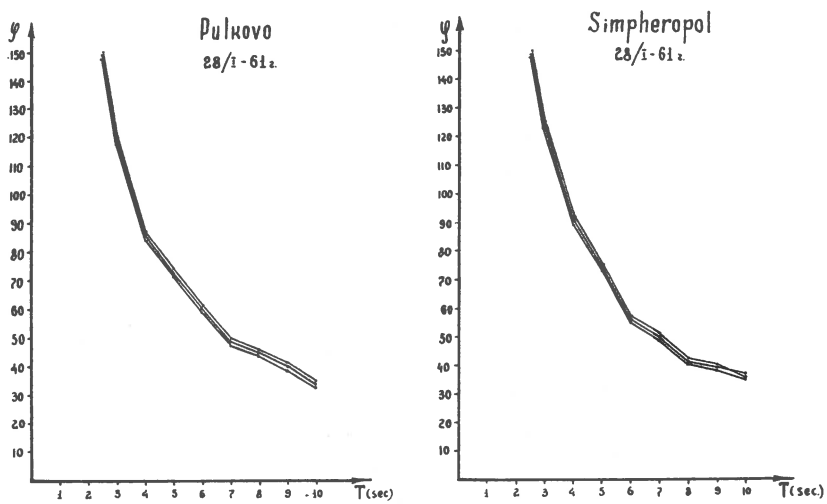

Fig. 3. Phase spectra in Pulkovo and Simferopol.

The calculated phase spectra (Fig. 3) allowed determination of the phase velocities and of the direction to the source of the microseism excitation. Let us analyse the microseism excitation sources obtained.

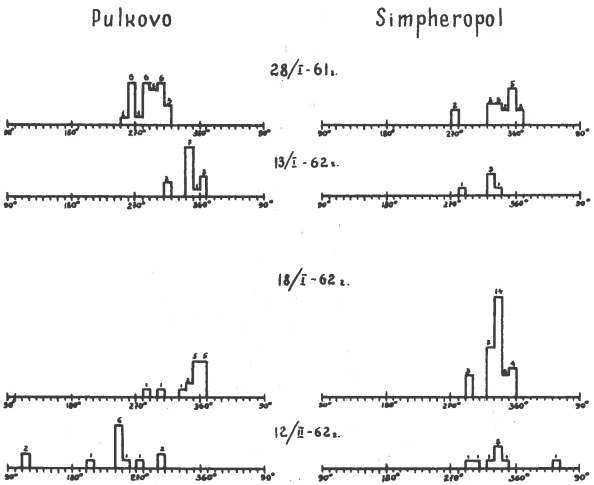

Fig. 4. The obtained azimuth directions for Pulkovo and Simferopol.

1. 28/1-61. As it is seen from Fig. 4, the excited region in P is determined by the sector 280-310°. In S the azimuth directions fill the sector 320-360°. The region of intersection of these vectors may be in the same place as the cold front of the rear (back) part of the cyclone. It should be emphasized that the meteorological situation over the Atlantic is very complex and the microseism excitation may be affected by other cyclones occurring over the Atlantic (Fig. 5a).

2. 13/1-62. There were only few azimuth determinations especially in S. P-azimuth-sector 340-360° points to the cold front in the North of Scandinavia (Fig. 5b).

3. 18/1-62. There are a little more azimuth determinations of observation in this case. In S the direction sector is 320-360° and points to the cold front acting in the North of Scandinavia. The sector of azimuth directions

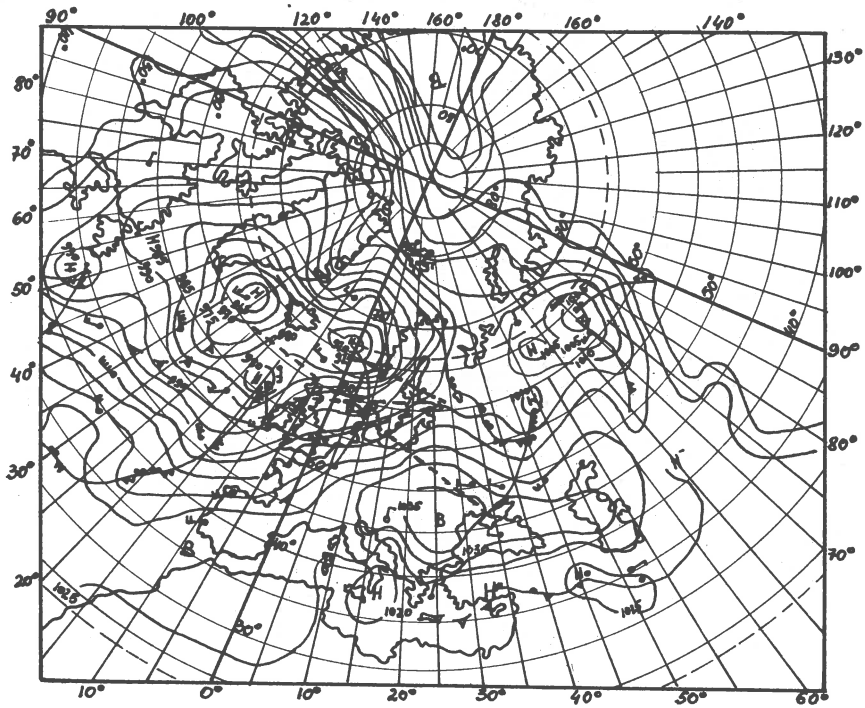

Fig. 5a. Synoptic map, dated 28/1-61.

in P - 340-10° - also points to the region of cold fronts (Fig. 5c).

4. 12/2-62. This case has the least number of azimuth determinations, therefore we may mention only the azimuth in P, which points to the cold front in the Norwegian Sea from a cyclone near the Scandinavian shores (Fig. 5d). All the determinations of azimuth directions to the microseism source were made having in mind the curvature of the earth.

Generally speaking, from the cases discussed it is possible to say that the results of the determination of the microseism excitation sources do not contradict the results of investigations obtained by us earlier [1]. Let us turn to the results obtained from the phase velocity determina-

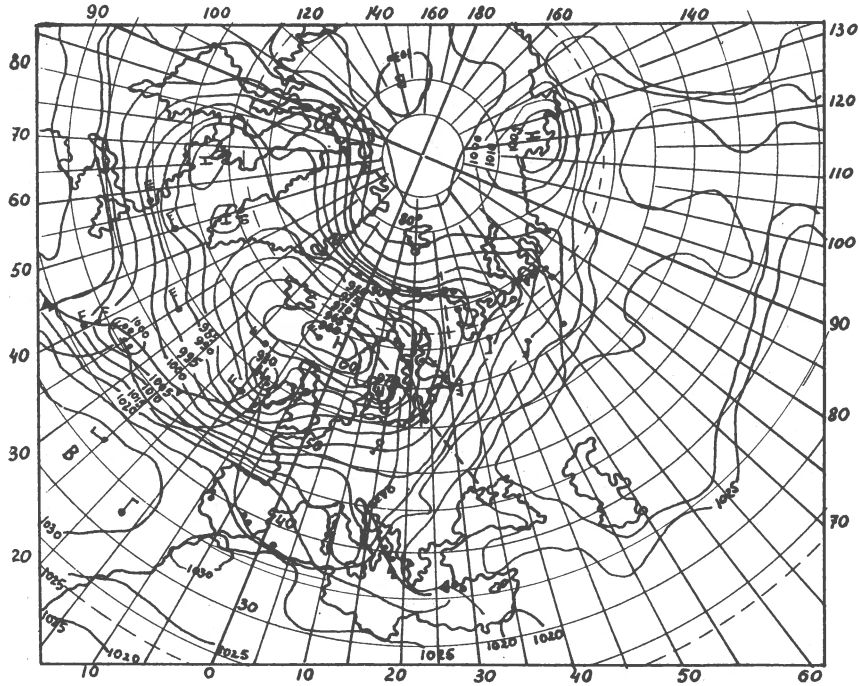

Fig. 5b. Synoptic map, dated 12/1-62.

tions. In Fig. 6 a dispersion curve of phase velocities is given for P. The big scattering can be explained by the fact that "not-pure" groups of microseisms were analysed but the regions of recording with irregular configuration, e.g., the regions of interfering waves. It explains a rather complex synoptic situation. A region is marked (singled out) in the figure (we have shown it by the dotted line), where the velocities have quite real meanings and an obvious tendency of growth with the increase of the period. So we thought it possible to try to determine the average curve for phase velocities in the interval of periods from 3 to 7 sec. This curve is shown by the bold dotted line. The vertical segments designate the mean arithmetic error of calculating each dot of the curve.

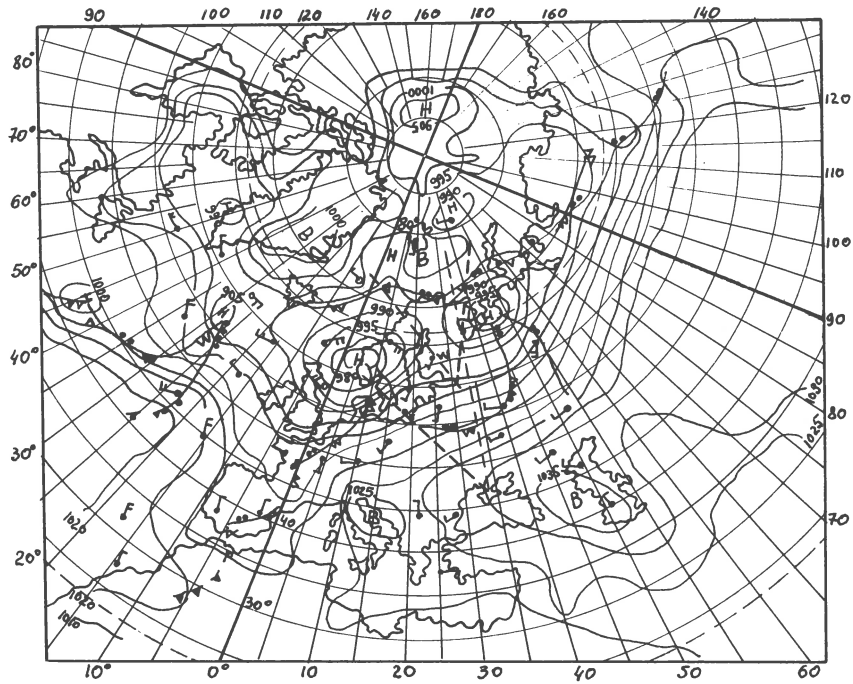

Fig. 5c. Synoptic map, dated 18/1-62.

For the P-region several theoretical dispersion curves were calculated, which corresponded to the different models of the earth crust structure. The model of the earth crust of this region was approximately determined from the data of the earth crust in the adjoining regions. The curves for two models are shown in the figure by thin continuous lines, the first (the general tone) and the second modes of model 1 and the first mode of model 2. The first mode of model 2 and the second mode of model 1 are beyond the limits of errors of the determination of the mean curve, and it agrees best of all with the first mode of model 1. Model 1 is a three-layer model of the earth crust with a thickness of 38 km. (The layer of sediments: H = 1 km, vP = 2 km/sec. The granitic layer: H = 12.5 km, vP = 5.7 km/sec. The basaltic layer: H = 24.5 km, vP = 7.0 km/sec.

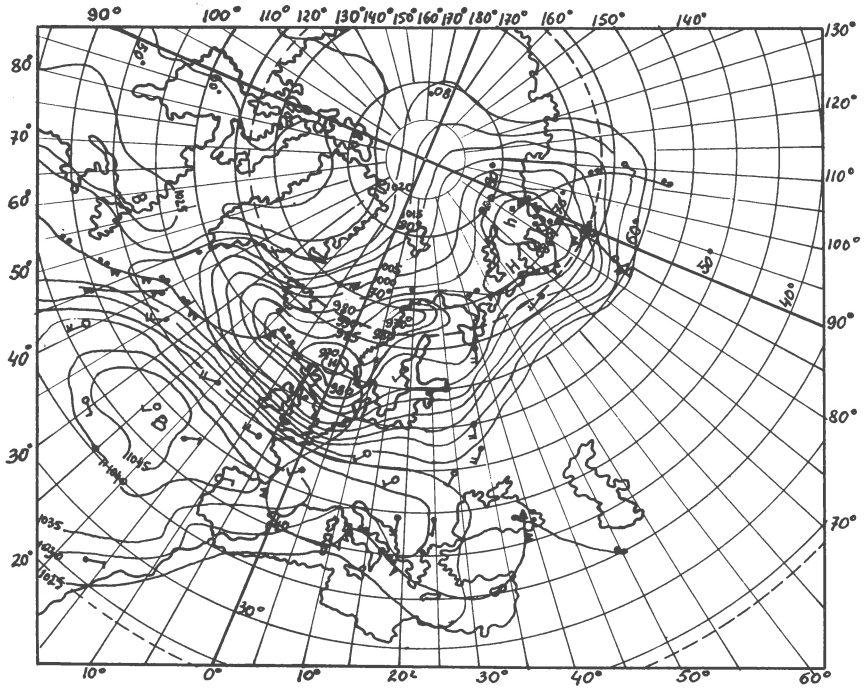

Fig. 5d. Synoptic map, dated 12/2-62

The P-velocity under Moho: 8.1 km/sec.) The velocity of the transverse wave for the first layer was determined from the relation $\frac{a}{b} = 3$; for the rest of the layers from the relation $\frac{a}{b} = 1.73$.

A few dispersion curves of phase velocities for three and four layer models were calculated for the S-region. The model of the earth crust of the given region was approximately determined from the data obtained in the works of DSP (Deep Seismic Sounding) of the Ukrainian Academy of Sciences. In the figure (Fig. 7) are given the dispersion curves only for three models, the most closely spaced to the average curve; while analysing curves for other models it can be pointed out that the increase of the total thickness of the crust results in rising of the curve, for example, the curve calculated for the model of the earth crust of about

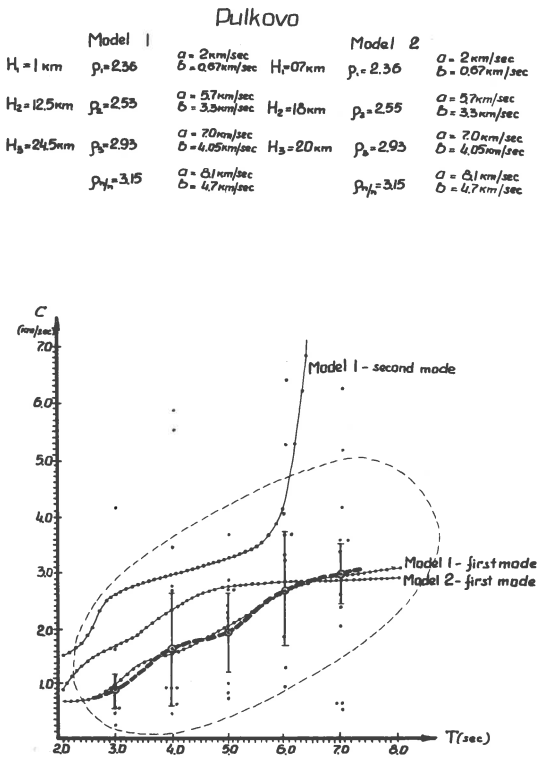

Fig. 6. Dispersion curve of phase velocities for Pulkovo.

38 km passes close to the upper boundary of errors.

It is the four layer model (Fig. 7) of the earth crust of a total thickness of 35.5 km that agrees best of all with the average curve: The not so hard sediments: H = 500 m, vP = 3 km/sec. The denser sediments: H = 3 km, vP = 4.5 km/sec. The granitic layer: H = 14 km, vP = 5.5 km/sec. The basaltic layer: H = 18 km, vP = 6.5 km/sec. The velocity of the S-wave for the first layer was determined from the relation $\frac{a}{b} = 2.5$; for the rest of the layers - from the relation $\frac{a}{b} = 1.73$.

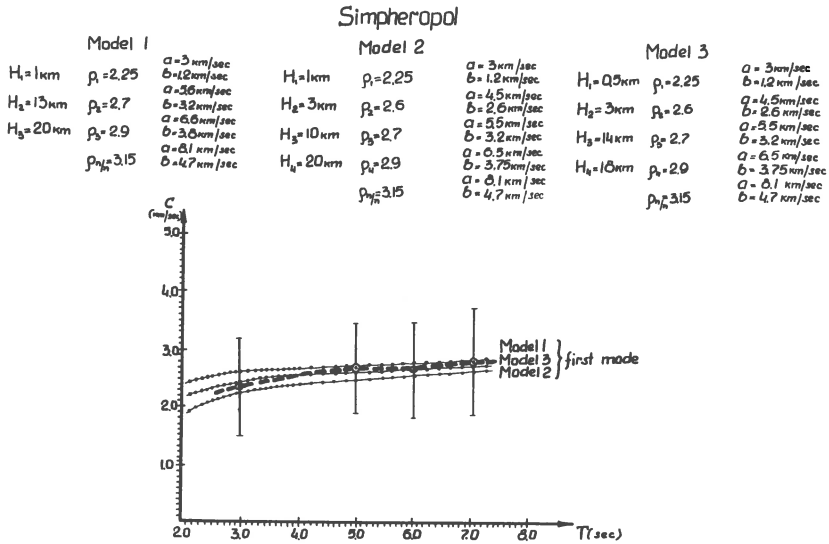

Fig. 7. Dispersion curve of phase velocities for Simferopol.

Summary

1. The observations of microseisms at tripartite microseism Soviet stations with properly identified instruments can be used for the determination of phase velocity curves and the structure of the earth crust, particularly its upper layers.

2. Microseisms of the storm origin in the interval of the periods 3-7 sec from their wave structure are the general tone (the first mode of Rayleigh waves).

Literature

1. Proskuryakova, T.A. Some results on microseism observations in Pulkovo and Yalta. Seismic investigations. Collections of papers, No.4, 1960.

2. Savarensky, E.F. and Kirnos, D.P. Elements of seismology and seismometry. Moscow, 1955. (German edition 1960).

A.Zátopek

UTILIZATION OF MICROSEISMS FOR STRUCTURAL STUDY OF THE EARTH'S CRUST

Introduction

The propagation of microseisms in the Earth's crust is dependent as well on the mechanism at their source as on the effects of geology and tectonics between the source and the recording station. For the European microseisms in a period range from 3 to 10 seconds, which we are considering here, the effects of tectonic structure have been ascertained and studied by many authors. The purpose of my present contribution is to give some sort of synthesis including the results of a long term comparative study of the European microseisms in Prague.

Structural effects in records of the European microseisms

Some four decades ago, Gutenberg [1] published for the first time a map (Fig. 1) representing a correspondence between the origin areas of the Atlantic microseisms and the parts of the European continent, where those are mainly observed. Microseisms, produced in regions situated west and northwest of the Bay of Biscay, are predominantly observed on the Pyrenean Peninsula, in France, partially also in England and in the western part of Central Europe. Microseisms originated in the neighbourhood of the English Channel and the coast of British Isles are observed chiefly in a zone which proceeds from Northern France towards the South-East, but does not include the Bohemian Massif and the Alps. Microseisms coming from the northeastern part of the Atlantic are observed mainly in a band covering, roughly speaking, the central part of Europe from the north to south and south-east, but also microseisms produces in other regions may be recorded in this area. The microseisms originating along the coast of Scandinavia and the adjacent northern coast of Russia propagate with a very

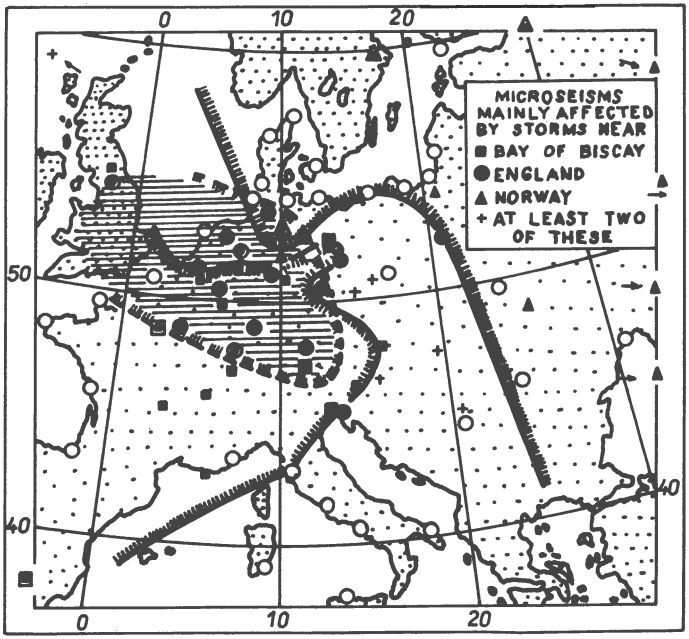

Fig. 1. Areas with relatively large microseisms in Europe for three different locations of storm centres, after B.Gutenberg [1].

little loss of energy through Scandinavia and the Russian platform far into Central Asia, but not so well in the southern and southwestern directions. Simultaneously, it was stated by Båth for Scandinavia, and by some Soviet seismologists for the Russian platform that the propagation of microseisms, originating far off shore on the open Atlantic, is poor through the substratum layers of the ocean bottom eastwards to the continent. These anomalies must be ascribed to the geological structure and were confirmed many times (cf. e.g. Båth [2], Bonchkovsky [3], Monakhov [4], Savarensky [5], Zátopek [6] and others).

In examining the relations between microseisms and the structure of Central Europe, G.Schneider [7] located the source areas of microseisms, as observed in Stuttgart, i.e. in the southwestern part of Central Europe, and found their distribution along the whole Atlantic coast of Europe, as represented on Fig. 2. Similar conditions (with slightly

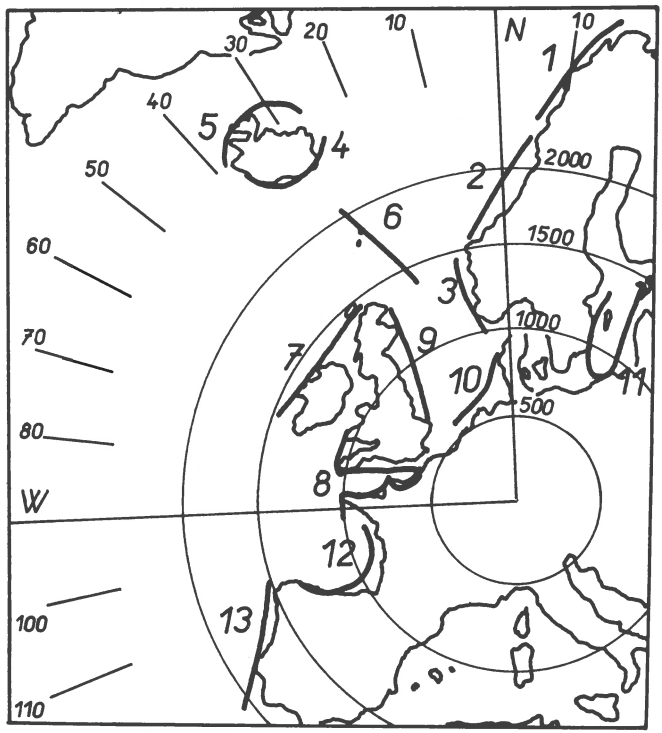

Fig. 2. Origin areas of microseisms in Europe, after G.Schneider [7].

different amplitude ratios) seem to be dominating also in Strasbourg. On a basis of the Airy phase diagrams G.Schneider estimated the thickness of the Earth's crust in North Germany to some 27 km, and in South Germany to 34 km, respectively, in a good agreement with the results of deep seismic soundings.

As a result of his statistical investigation of directions of approach of microseisms to the station of Hamburg, K.Strobach [8] obtained a distribution given on Fig. 3, where the area of the Norwegian coast appears to be the most important zone producing microseisms, as recorded in Hamburg. Similarly, the northern directions prevailed for Copenhagen, according to the statistics by Jensen.

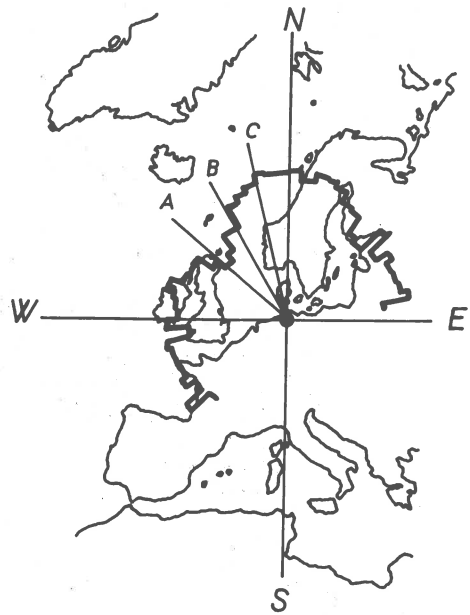

Fig. 3. Direction of approach of microseisms to the seismic station of Hamburg according to the statistics by K.Strobach [8].

For the central part of Europe, represented by Prague, [9, 10], where the shortperiodic vibrations, typical for coastal microseisms, are filtered out, the correlation between the cyclonic activity in the North Atlantic frontal zone and the amplitudes of microseisms gave a location of the sources of Atlantic microseisms as shown on Fig.s 4 and 5. The region situated west and southwest of Iceland appears to be the most important for the generation of microseisms as observed in this part of Europe, while the respective regions situated off the western and northwestern Scandinavian shore and that of the Baltic Sea are of a secondary importance. The effects of meteorologic disturbances acting in the region of the Bay of Biscay, as well as of those passing near the English Channel or on the North Sea, which provoke strong microseisms in West Europe, are very small, if any, in this region. Further it was stated, that the amplitudes of microseisms, as recorded in Praha, are several

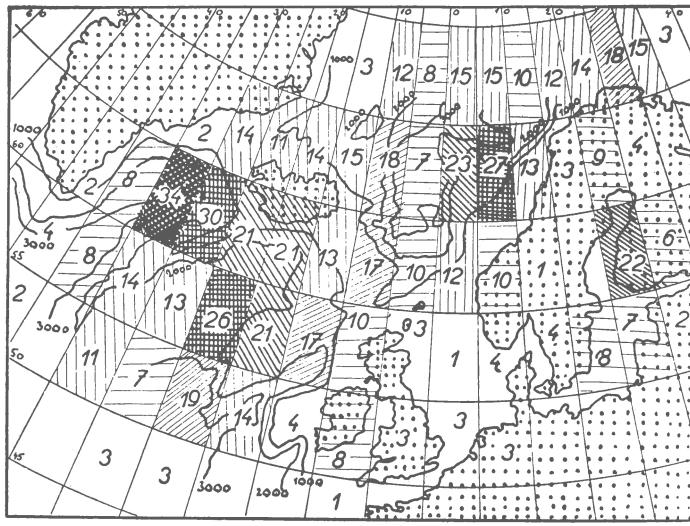

Fig. 4. Correlation between the position of cyclonic centres and the simultaneous amplitudes of microseisms in Praha for 1948/49 and 1956/57, expressed by frequency numbers according to [6].

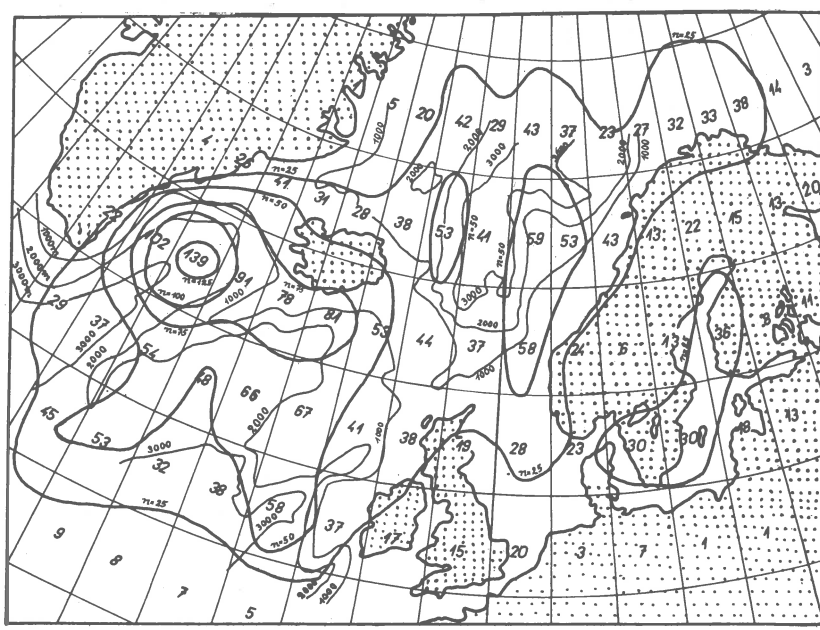

Fig. 5. Isolines of frequency numbers for Praha superimposed for the periods of microseismic activity 1948/49 - 1959/60. See [6].

times smaller than those of e.g. Stuttgart, Strasbourg and Warsaw, and considerably lower than in Halle or in Potsdam, being, on the contrary, well comparable with the amplitudes of Jena. A similar behaviour was stated also when comparing the amplitudes of earthquakes. As Praque and Jena are situated on the same great structure unit, the former inside the Bohemian (or Czech) Massif, the latter on its continuation in Saxony and Thüringen, this elevated attenuation must be due to the regional geologic and tectonic conditions. Obviously the same reasons are responsible for the fact that even the strongest Atlantic meteorological disturbances, when situated west of the meridian of 45° W and south of the parallel of 50° N, do not cause any reliably observable influence on the microseismic activity. However, microseisms appear immediately when a strongly pronounced barometric low proceeding eastwards passes over the border zone just mentioned.

The propagation of microseisms originating in the Mediterranean region is strongly limited to the North, as no perceptible microseisms appear in Praque which would correspond to the meteorological disturbances in the Mediterranean region, in spite of their often considerable influence on the synoptic situation in Central Europe. Probably this is due to geological conditions. Maybe similar statements would fit also to Stuttgart and Hamburg.

Although the microseismic activity in Europe as a whole is determined by the Atlantic system of circulation, (what is demonstrated by Fig. 6 showing clearly the decrease of amplitudes southwards), strong microseisms due to the Mediterranean circulation are observed in South Europe. A number of authors (e.g. D´Henry [11], Caloi [12], Morelli [13], Rizhikova [14] and some Russian authors) discovered various types of microseisms connected with atmospheric disturbances in the Black Sea and Mediterranean areas.

For demonstration I would like to present several typical examples. The figures 7-12 illustrate qualitatively characteristic cases of the simultaneous microseismic activity in various regions of Europe, where the influence of geology can also be estimated.

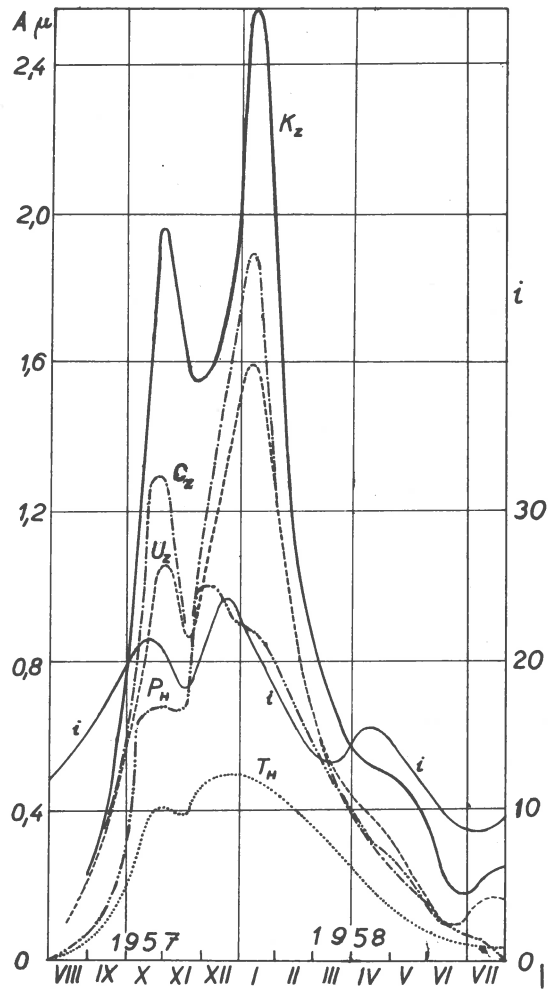

Fig. 6. Decrease of adjusted amplitudes of European microseisms from N to S: K_Z = Kiruna Z, U_Z = Uppsala Z, C_Z = Copenhagen Z, P_H = Praha horiz., T_H = Trieste horiz. Curve i = meteorological index i, roughly proportional to the W-component of geostrophic wind in 500 mb level.

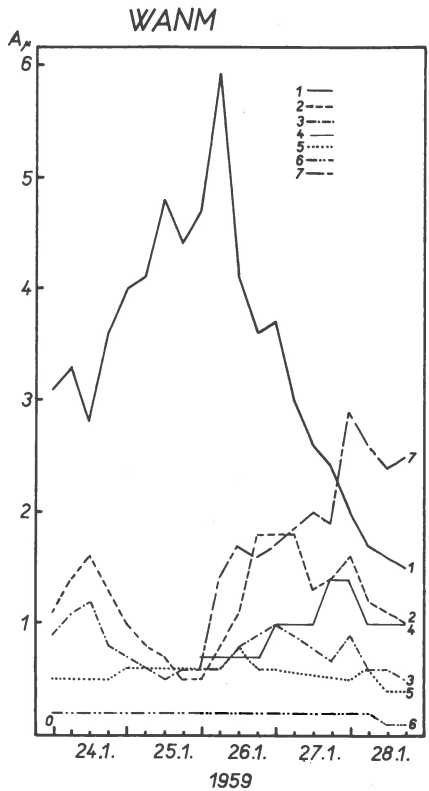

Fig. 7. Different course of amplitudes in connection with various synoptic situations for some European seismic stations: 1 = Toledo (horiz.), 2 = Warsaw (Z), 3 = Copenhagen (Z), 4 = Belgrade (horiz.), 5 = Praha (horiz.), 6 = Trieste (E), Athens (E). For explanation see the text.

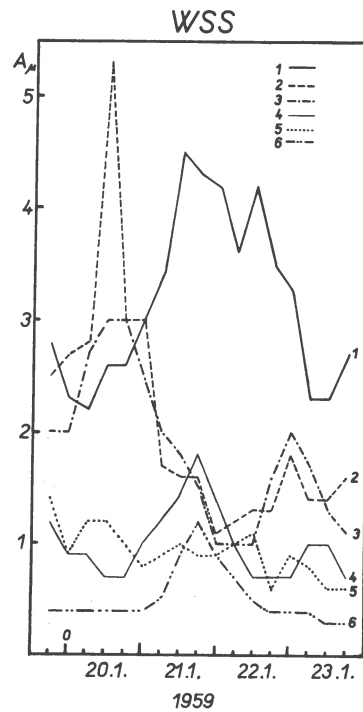

Fig. 8. Symbols: see Fig. 7. For explanation see the text.

Fig. 7: A storm at Toledo, caused by a disturbance west of the Bay of Biscay, not recorded at other stations; cyclonic activity in East Mediterranean causes an amplitude increase in Athens, Belgrade and Trieste.

Fig. 8: A cyclone over the West Atlantic, minor disturbances over the Baltic Sea and North Scandinavia (see Warsaw, Copenhagen, Prague); activity in the Mediterranean (see Toledo, Belgrade, Trieste).

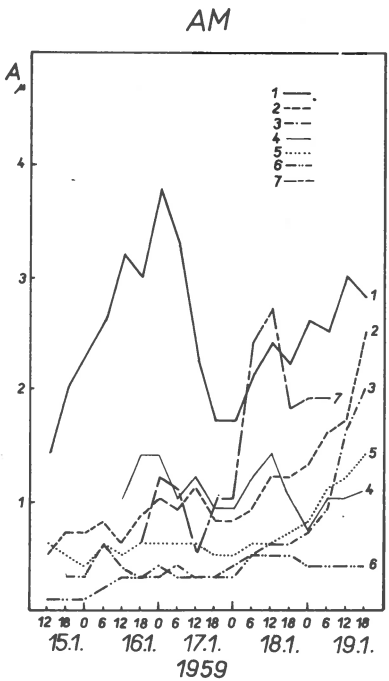

Fig. 9. See Fig. 7 and the text.

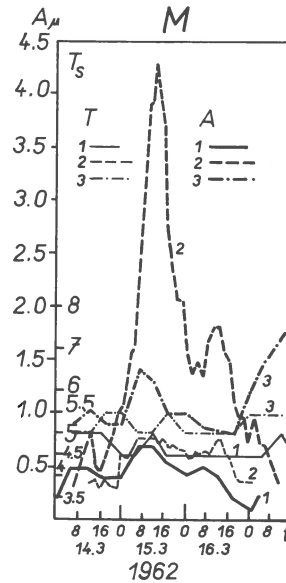

Fig. 10. Variation of amplitudes A and periods T in Praha (1), Sofia (2) and Warsaw (3). For explanation see the text.

Fig. 9: A low proceeding from Atlantic eastwards (Toledo and other stations); a low in the Mediterranean (see Trieste, Belgrade, Athens).

Fig. 10: A low over the Ionian Sea (strong microseisms Sofia, weak Prague and Warsaw).

Fig. 11: Atlantic regime visible in Warsaw, Prague and Sofia; depressions along the western coast of Europe, core of a cyclone NW of Norway.

Fig. 12: Disturbance on the Ionian Sea (Sofia), another in the Barents Sea (Warsaw), small amplitudes in Prague.

In order to explain the rapid and irregular variations of microseismic amplitudes and cases of a microseismic

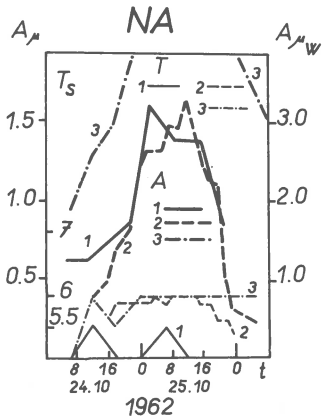

Fig. 11. See Fig. 10 and the text.

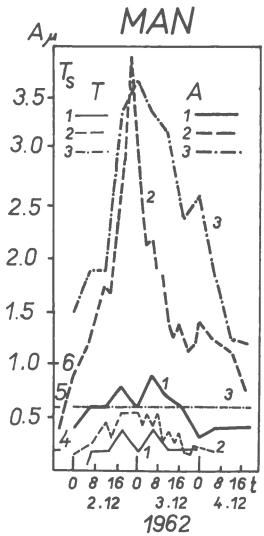

Fig. 12. See Fig. 10 and the text.

"shadow" of which some examples were just given and mentioned several times before in this contribution, one often speaks of so called "microseismic barriers" and "barrier effects". These may be physically interpreted either as effects of discontinuities in the Earth's crust or as waveguide-effects (channel effects) or a combination of both.

Examples: As already mentioned, Båth [17] interpreted the low ability of oceanic structures to transmit the energy of microseisms from the region of Iceland to the continental block of Scandinavia and the Russian platform as a barrier effect, being caused by a fault passing along the western coast of Norway. Caloi assumed a barrier in the narrows of Messina, another is assumed in the western part of the Mediterranean.

It seems also that the systematic appearance of higher amplitudes of Atlantic microseisms in Rome which are, as stated by Morelli, about twice as strong as those in Trieste, could be ascribed to a barrier effect of the Alps

(shadow by mountain roots and effect of longitudinal deep faults along the Apennines).

Rothé [15] considers the possibility of a barrier effect of the British Isles, which appears as a decrease of microseismic energy, transmitted from a source north of the British Isles, to the territory of France. One could expect further barrier effects connected with deep faults of the Bohemian Massif and of the Saxony-Thüringen system. That would explain the low amplitudes of Atlantic microseisms, as observed in Prague and Jena. The absence of a clearly observable effect of the Mediterranean microseisms in Prague could be connected with some barrier effects of the substrata of the Alps and the Carpathians as stated also from observations of seismic waves (e.g. Båth [16]).

These indications speak of a need for a more comprehensive study. However, if we take into consideration the complexity of factors involved, we see that, for many reasons, the existing observational basis does not ensure the reliability of results which would be able to make Gutenberg's map more accurate. The main obstacle is to be seen in the heterogeneity of instruments and methods of evaluation of amplitudes in consequence of insufficient knowledge of the real values of dynamical magnification. The lack of a permanent homogeneity of operation of the individual stations is a seriously disturbing factor, too.

Conclusion

The utilization of microseisms for the crustal structure study in Europe appears very promising provided that reliable and homogeneous data of an appropriate network of stations with standardized instruments are at disposal for a complex comparative analysis as well of individual microseismic storms as of the long term microseismic activity. As a considerable progress has been reached in standardizing seismic equipment in many European stations last years, the time is ripe to repeat the ancient investigations of Professor Gutenberg by use of up-to-date instruments and methods. This research should be included into the programme

of the E.S.C. The results just quoted may be seen as an encouraging preparatory step in this direction.

References

[1] B.Gutenberg, Die seismische Bodenunruhe, 1924, Berlin.

[2] M.Båth, The Distribution of Microseismic Energy with Special Reference to Scandinavia, Arkiv för Geofysik, 1 (1951) 359.

[3] V.F.Bonchkovsky, Microseisms and their Causes (in Russian, Summary in English), Publ.Seism.Inst.As.Sc. USSR, No. 120, Moscow-Leningrad, 1946.

[4] F.I.Monakhov, Usloviya obrazovaniya i rasprostraneniya severo-atlanticheskikh mikroseysm, Seysmol. i glaciolog. issled. v period MGG, No.2, Izd. AN SSSR (1959) 39, Moscow.

[5] E.F.Savarensky, T.A.Proskuryakova, V.S.Cirel-Sprincson, O svyazi mezhdu mikroseysmicheskimi kolebaniyami i polozheniyem ciklonov nad okeanami, Meteorol. i gidrologiya, No.6, 1955, Moscow.

[6] A.Zátopek, Sur la nature et l'origine des microséismes européens, Studia geoph. et geod., 5 (1961) 51.

[7] G.Schneider, Zusammenhänge zwischen mikroseismischer Bodenunruhe in Stuttgart und Aufbau der Erdkruste in Mitteleuropa, Dissertation, Techn. Hochschule Stuttgart, 1958.

[8] K.Strobach, Ein Beitrag zum Problem der Entstehung und der Wellennatur der mikroseismischen Bodenunruhe (Habilitationsschrift), Hamburger Geophysikalische Einzelschriften, H.5, 1962, Hamburg.

[9] A.Zátopek, Long-Period Microseisms Generated in Eastern Part of Atlantic Frontal Zone, Studia geoph. et geod., 8, (1964) 127.

[10] A.Zátopek, Les microséismes de Praha, Publ. BCIS, Série A, Travaux Scientifiques, 19, 183, 1954, Strasbourg.

[11] G.D'Henry, Sulla natura fisica dei microsismi, Annali di Geofisica, 3 (1950) 87.

[12] P.Caloi, Sull' origine dei microsismi con particulare riguardo all' alto Adriatico, Annali di Geofisica, 4 (1951) 525.

[13] G.D'Henry, C.Morelli, Sulle cause dei microsismi, Annali di Geofisica 2 (1949) 281.

[14] S.Rizhikova, Vorkhu mikroseizmite, registrirani v Sofiya, i vrozkata im hidrometeorologichnite usloviya, Bulletin de l' Inst. de l'Ac. Bulgare des Sciences, 7 (1965) 101.

[15] J.P.Rothé, Etude des mouvements microséismiques, Pontificiae Academiae Scientiarum Scripta Varia, 12 (1952) 19, Rome.

[16] M.Båth, Seismic Channel Waves, New Observations and Discussions, Gerlands Beiträge z.Geophys., 68 (1959) 360.

[17] M.Båth, The Problem of Microseismic Barriers with Special Reference to Scandinavia, Geol.Fören.Förhandl., 74 (1952) 427.

Henry Jensen

DIRECTION OF APPROACH OF MICROSEISMS AT SOME NORTHERN STATIONS

The sketch-map presented shows some results concerning the statistical behaviour of the direction of approach of the 3-8 sec. microseisms at some stations around the North Atlantic and the Norwegian Sea, viz. Godhavn, Ivigtut Scoresbysund, Nord, Barentsburg, Copenhagen, Viborg and Murmansk - marked on the map by their initial letters.

For every one of the stations the smallest angle in which 50 per cent of all measured directions are included is shown. In most cases the material covers one full year but not the same year for all stations.

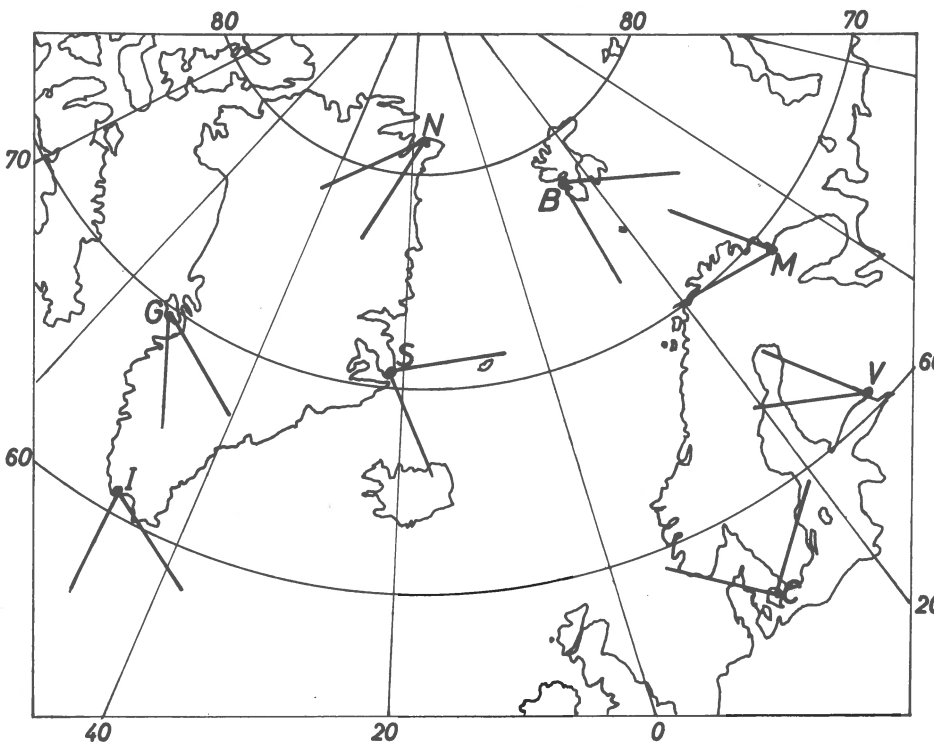

For the Russian stations the directions have been extracted from the IGY bulletins of the tripartite stations docketed at the World Data Centers. The results for the Danish stations - obtained by the method of the empty halfplane - have been published in detail in the series Geodætisk Instituts Meddelelser.

To a certain extent the illustration will be misleading if more than one direction prevails. Another drawback is that the width of the angle depends on the instrumental response at the station in question. However, when a detailed study is not intended, but only a rough outline of the big-scale conditions, some conclusions may be drawn from the map.

N seems to be in discordance with the three other Greenland stations (G, I, and S). This could be caused by a refraction phenomenon in the shelf area off the south-eastern coast of Greenland. Perhaps some direction determinations on the central part of the ice cap (e.g. at Camp Inge Lehmann) might elucidate the problem.

Another striking feature is that the stations N and B in spite of their small geographical distance seem to belong to two different noise-systems.

P.Bernard

EQUIPEMENT MICROSEISMIQUE DE L'OBSERVATOIRE DU PARC SAINT-MAUR

Abstract

Owing to increasing industrial disturbance, the seismological work in Parc St.Maur was recently specialized in microseisms of meteorological origin, the best seismograph for them, 12 seconds Galitzin, being completely insensitive to man-made vibrations. A new recording apparatus has therefore been set for this seismograph (which belongs to the Observatory since 1912): a "spot follower" (patent Sefram) mounted on a seismic drum recording at 30 mm per minute on a daily sheet 90 × 30 cm.

Moreover the mechanical force applied to the ink-pen is sufficient to act an integrating device giving one impulse for each millimeter of spotmotion in any direction. These impulses are summed up by an electronic circuit and recorded in an analog graph showing the variation of mean microseismic amplitude.

L'intérêt des microséismes proprement dits (ceux de 3 à 9 sec. de période) pour la météorologie a été signalé à maintes reprises. Ils sont capables de détecter les dépressions cycloniques en mer à une grande distance et de renseigner sur l'évolution de leur intensité. Cependant la mise en pratique de cette utilisation n'a pas abouti du fait que les observations ne peuvent être fournies aux météorologistes qu'avec le délai de 24 heures au moins nécessaire au développement des inscriptions photographiques.

Depuis le 1er janvier 1966 la station séismologique du Parc Saint Maur, trop perturbée pour l'enregistrement des ondes séismiques en courte période, a été spécialisée dans les microséismes, revenant ainsi à sa vocation première d'observatoire météorologique.

On a donc cherché à obtenir des inscriptions immédiatement visibles avec une sensibilité plus grande que celle des anciens séismographes Wiechert à noir de fumée. Pour cela,

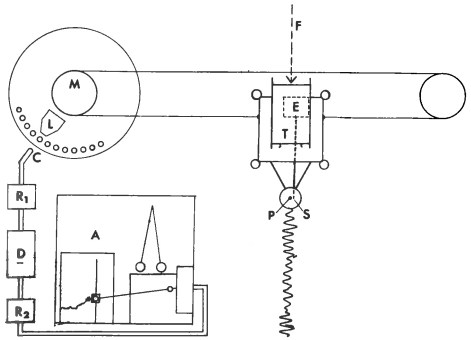

Fig. 1. Schéma du dispositif d'enregistrement Richard-Sefram.

F - faisceau lumineux provenant du miroir du galvanomètre. T - Cellules différentielles. M - poulie motrice du suiveur de spot. P - plume d'inscription permanente. S - plume signal commandée par l'électroaimant E (marques de minute de durée 2 secondes). L - lampe de l'intégrateur. C - cellule photoélectrique de l'intégrateur. R_1, R_2 - relais. D - diviseur électronique. A - anémo-cinémographe enregistreur.

le séismographe vertical Galitzine, parfaitement approprié à l'étude des microséismes par sa période de 12 secondes qui lui donne un maximum d'amplification vers 7 secondes, et par son insensibilité totale aux vibrations industrielles, a été doté d'un enregistreur (1) associant à la forme classique du cylindre de séismographe inscrivant en hélice, un suiveur de spot Sefram qui comporte des cellules photoélectriques différentielles (en T sur la fig. 1) montées sur un chariot mobile. Les cellules, par l'intermédiaire d'un amplificateur, commandent un moteur qui déplace le chariot sur des rails parallèles aux génératrices du cylindre à chaque mouvement du spot renvoyé par le miroir du galvanomètre sur les cellules. A mesure que le cylindre se déplace longitudinalement, le chariot se maintient de lui-même à la position d'équilibre du galvanomètre. Il porte une plume à encre P reportant tous les mouvement du spot sur la feuille de papier et, à 2 mm. de la première, une seconde plume signal S, commandée par un électroaimant E,

et inscrivant les minutes à côté du trait principal. Les deux plumes sont alimentées d'encres de couleurs différentes, par des flacons de plastique contenant la consommation d'une semaine ou plus.

Pour l'exactitude du repère horaire, un réglage permet d'amener les deux plumes exactement sur la même génératrice du cylindre: il est facile de s'en assurer, après avoir arrêté la rotation du cylindre et excité l'électro-aimant du signal, en déplaçant à la main l'enscripteur sur le papier: les deux traits doivent se superposer exactement, sinon on agit sur la position des plumes.

En vue d'obtenir une caractérisation statistique de l'amplitude de l'agitation, nous avons, G.Unal et moi, ajouté des dispositifs complémentaires sur cet appareil: un disque monté sur l'axe du moteur intercepte la lumière tombant sur une cellule photoélectrique et chaque impulsion de celle-ci actionne un relais. Comme la poulie entraînant le câble d'acier du chariot, montée sur la même axe, a exactement 10 mm. de rayon, un tour complet déplace le chariot de 62,8 ^{mm}. Le disque porte donc à sa périphérie 63 trous et le passage de chacun devant la cellule correspond à 1^{mm} de déplacement de la plume.

Les impulsions obtenues sont envoyées sur un diviseur électronique à transistors, dont l'alimentation peut être, au choix, à piles, à accumulateurs, ou à courant continu basse tension transformé du secteur alternatif. Ce diviseur conserve 1 impulsion sur 4 ou 8 suivant la saison (faible ou forte agitation) et, par l'intermédiaire d'un deuxième relais, elles actionnent un enregistreur qui est actuellement un anémocinémographe Richard.

Dans ce dernier appareil, chaque impulsion fait monter la plume d'une quantité d'ailleurs réglable, en même temps que la rotation d'un pendule conique la fait redescendre d'une façon continue avec une vitesse proportionnelle à la hauteur de la plume, de sorte que cette dernière prend une position d'équilibre plus ou moins élevée suivant la fréquence des impulsions, et les variations d'intensité de l'agitation microséismique sont traduites d'une façon analogique (fig. 2).

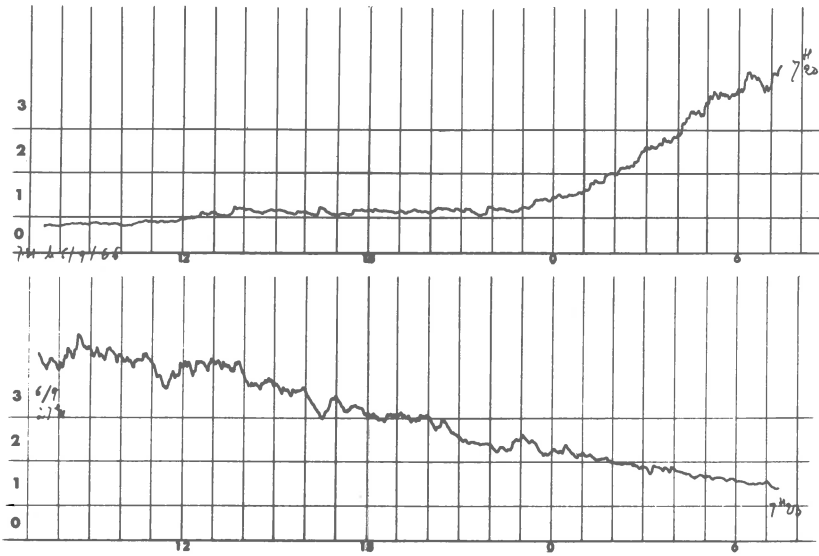

Fig. 2. - Enregistrement sur deux jours successifs d'une tempête microséismique au Parc Saint Maur. Le journal microséismique est obtenu en recouvrant chaque enregistrement d'une grille horaire où sont indiqués les "niveaux" d'agitation 0, 1, 2, 3 utilisés depuis plus de 50 ans à la caractérisation des microséismes de cette station.

La façon dont est réglé l'appareil a une grande importance pour l'aspect de la courbe: avec une constante de temps trop petite (grande vitesse de descente de la plume) la courbe est agitée au point d'être inutilisable. Pour avoir une courbe suffisamment fine l'appareil en service a été doté d'un engrenage augmentant cette constante de temps dans le rapport 10 (retour à la moitié de la hauteur initiale en 17 minutes). Corrélativement, la sensibilité aux impulsions, c'est-à-dire l'amplitude de montée par impulsion, peut aussi être diminuée dans le rapport de 1 à 5 ou 8. Le réglage qui convient est celui qui ne fait monter la plume en haut de la feuille que pour des tempêtes microséismiques exceptionnelles ou pour de forts tremblements de terre, qui s'inscrivent sur notre intégrateur par des crochets aisément reconnaissables.

Il est évident que la réponse de l'appareil est inversement proportionnelle à la période des microséismes puisqu'à amplitude égale une onde de 4 secondes de période par exemple donnera dans le même temps un nombre d'impulsions double de celui fourni par une onde de 8 secondes. Pour la détection qualitative des tempêtes, ce n'est pas un inconvénient, les microséismes de période 3 ou 4 secondes ayant des amplitudes moins fortes que les ondes à plus grande période tout en ayant, par leur origine fréquente sur la Manche ou la Méditerranée, une importance parfois plus grande pour les applications météorologiques. Pour un calcul quantitatif des amplitudes, la connaissance de la période moyenne est nécessaire et on peut la déterminer directement sur le séismogramme, mais le matériel décrit ici est capable d'en fournir une mesure automatique actuellement en cours de mise au point.

L'emploi de ces procédés d'enregistrement est particulièrement envisagé pour la prévision de la houle. On sait en effet que les variations de l'agitation microséismique précèdent celles de la houle arrivant sur les côtes d'un temps variable qui dépend de la distance des dépressions cycloniques à la côte considérée (2). Au Maroc on peut compter dans le cas général sur un avertissement de 1 à 2 jours en avance des aggravations de la houle, et de même pour ses améliorations une fois le maximum dépassé, ce qui apparaît sur le graphique. Même pour des côtes plus proches, le secours des microséismes ne serait pas inutile. Nous avons cherché d'abord à résoudre les questions de commodité d'appareillage qui pourront se poser.

Bibliographie

1. Bernard, P.: Nouveau type d'enregistreur à inscription visible. Cah.Océanogr. 16, no.8, p.619-22 (1964).

2. Bernard, P.: Relation entre la houle sur la côte du Maroc et l'agitation microséismique en Europe Occidentale. C.R.Ac.Sc., 205, p.163-5 (1937).

Recherches sur l'agitation microséismiques. Congrès de l'Association française pour l'avancement des sciences Paris 1945, t. II, p.282-5.

H.Korhonen

SPECTRAL ANALYSIS OF MICROSEISMS AT OULU

Abstract

Power spectra calculated on a digital computer were used in an analysis of different types of microseisms with a frequency range of 0.1-0.3 Hz recorded at the Oulu seismograph station. The results were compared with simultaneous spectra of microseisms at some neighboring stations as well as with sea wave spectra on the Norwegian coast. The spectrum type was found to vary according to different effects generating and transforming microseisms.

In this study a spectral analysis of microseisms was made, using ordinary recordings of Press-Ewing type LP-Z seismographs. At first, samples from selected seismograms were enlarged and digitalized at intervals of one second. Then their power spectra were calculated by means of the "Elliot 803" computer. The program was based on the description of Southworth [7]. It calculates the power spectrum as a Fourier transform of the autocorrelation function. The rough spectral density estimates were finally smoothed by the method of Hamming. After taking into account the instrumental response, the so-called displacement spectra [3, 4] were obtained and drawn for the frequency range of 100-300 mcps.

The suitable record length was found by comparing spectra from samples of various durations. The spectra from 3- and 6-minute samples did not differ remarkably when a resolution of 25 mcps was used [1].

As one might expect, the spectra formed in this way from various kinds of microseisms differ from each other both in energy level and in the distribution of energy density. In Fig. 1 we can see five spectra from microseisms at Oulu taken every sixth hour during the microseismic storm of November 29 to 30, 1965. As can be seen, the max. peak is moving toward the lower frequencies with increasing storm and vice versa. The spectra naturally give a more detailed

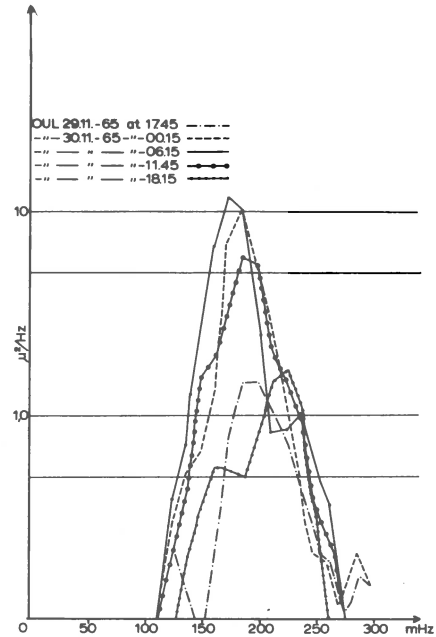

Fig. 1. Spectra from the microseismic storm 29.-30.11-65

picture of the development of the storm than the conventional max. amplitude and period measurements. Comparison of the spectra from different microseismic storms enables us to draw some conclusions about the connections of the spectrum types with the possible sources of microseisms.

Thus, for instance, cyclones over the North-Atlantic ocean seem to appear in connection with a relatively clear max. peak in the low-frequency part of the microseismic spectrum at Oulu (Fig. 2a). When, on the other hand, the coastal effect is assumed to be dominant in generating microseisms [2], the spectrum, especially the high-frequency part of it, seems to be broad and flat (Fig. 3).

Now we can see how the spectrum changes when a cyclone is approaching the Norwegian coast. On December 17, 1965, the centre of a low of 970 mb is lying to the west of Iceland at a distance of 1800 km from the Norwegian coast. On the next day it is over the Norwegian sea, only 600 km from

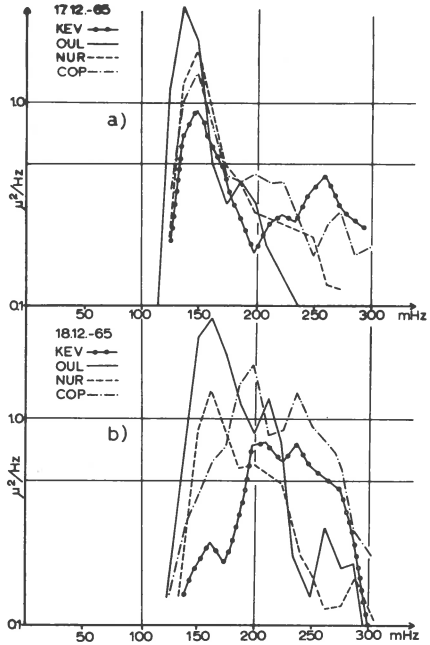

Fig. 2. Simultaneous spectra from Kevo, Oulu, Nurmijärvi and Copenhagen seismograph stations.

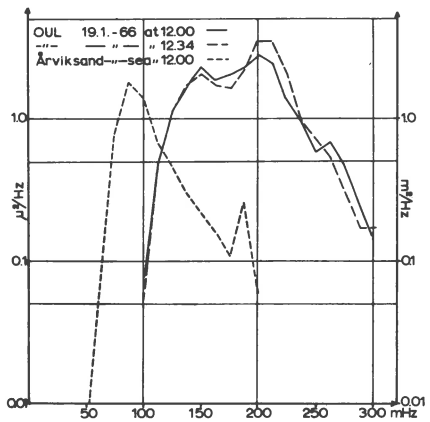

Fig. 3. Simultaneous spectra of microseisms at Oulu and of sea waves at Årviksand.

from the coast. However, there are no strong winds blowing toward the coast. A direction analysis of microseisms made from the seismograms of the Nurmijärvi station by the method of Jensen [5] shows that the direction of approach is from the northwest on these days. The simultaneous spectra (Fig. 2a) from Kevo, Oulu, Nurmijärvi and Copenhagen have their max. peaks between 125-175 mcps on December 17. According to the similarity of the spectra in Fig. 2a, the microseisms at these stations might have the same source. On the next day the high frequency part of the spectrum is increasing and the max. peaks have moved toward higher frequencies (Fig. 2b). There is also more heterogeneity in the microseismic spectra at different stations. In the simultaneous spectra from the station Kap Tobin in Greenland near Scoresbysund there is on these days a slight re-

spective displacement of the max. peak in the opposite direction, but these microseisms do not necessarily have the same source.

Finally, we consider the spectra of microseisms at Oulu and the sea waves at Årviksand in Norway near Tromsø on January 17, 1966. This day belongs to a longer microseismic storm period. The centre of the low is over the Barents sea and the winds are blowing nearly orthogonally toward the Norwegian coast. The sea wave recorder at Årviksand reports a max. wave height of 3.5 meters with a respective period of 12 seconds. The sea wave spectrum was calculated by the method described above for microseisms and drawn for the frequency range of 50-200 mcps. As one would expect from the theory of Longuet-Higgins [6], the frequency of the max. peak in the spectrum of microseisms is twice that in the simultaneous sea wave spectrum (Fig.3). The maximum in the microseismic spectrum is much broader, however, showing a weak triplet structure. Although the stationarity test of microseisms shows that the peak with highest frequency is no longer present in the spectrum taken half an hour later, the other properties of the spectrum, especially its width, have remained stable. In these weather conditions the direction of approach of microseisms is not generally from the Barents sea but from the Norwegian coast near the Lofoten Islands. So one may think that the random character of this spectrum is due to the oscillations of different Caledonian mountain blocks agitated by surf and perhaps partly directly by wind, too.

Acknowledgment is tendered to Dr. E.Hjortenberg, Geodetic Institute, Copenhagen, and to Dr. M.T.Porkka, Seismological Institute, Helsinki, for the seismogram material, as well as to Prof. A.Brandtzaeg, Technical High School, Trondheim, for the sea wave record obtained for this study. The author is also grateful to the Computer Centre of Oulu University for calculating the spectra.

References

[1] Blackman, R.B. and Tukey, J.W.: The measurement of power spectra. New York 1958.

[2] Båth, M.: An investigation of the Uppsala microseisms. Uppsala 1949.

[3] Haubrich et al.: Comparative spectra of microseisms and swell; Bull.Seismol.Soc.Amer. 53: 27-37, 1963.

[4] Hinde, B.J. and Gaunt, D.J.: Some new technique for recording and analysing microseisms; Proc.Roy.Soc. A, 290: 297-317, 1966.

[5] Jensen, H.: A procedure for the determination of the direction of approach of microseismic waves; Geod.Inst. no.36, København, 1958.

[6] Longuet-Higgins, M.S.: A theory of the origin of microseisms. Phil.Trans. A, 243: 1-35, 1950.

[7] Southworth, R.W.: Autocorrelation and spectral analysis; Mathematical methods for digital computers edited by Ralston A. and Wilf, H.S., pp.213-215.

R.Parks

SPECTRAL ANALYSIS OF SHORT-PERIOD NOISE

Spectral analysis has been applied to tape-recordings of background noise in the band 0.1 to 40.0 Hz by speeding up the tape 60 times on playback so that the signals can be handled by a normal audio-frequency spectrum analyser.

The diagram shows comparative analysis of noise for four temporary stations, for the morning of 22nd Sept. 1965. Details of the world weather situation for that time have not been investigated, but the noise was typical of the preceeding month and showed no significant short-term changes (i.e. over an interval of 4 hours).

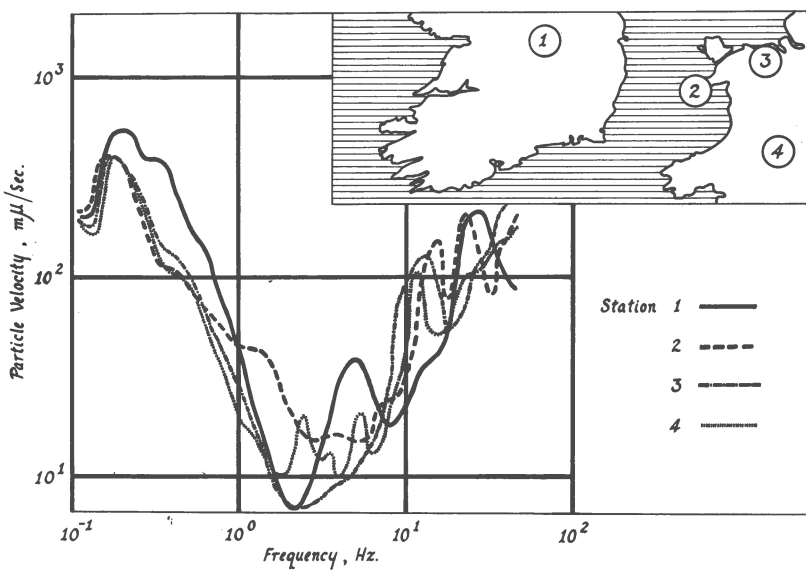

The differences in noise (of presumably microseismic origin) at individual stations show some correlation with the proximity to major bodies of water which could contribute to microseism activity; the dominant frequency of microseisms is related to the extent of the body of water in which they are developed.

Station 1, nearest the Atlantic, is the most active in the band 0.15-1.0 Hz, typical of oceanic microseisms.

Station 2, on a headland in the Irish Sea, shows greater activity around 2 Hz, more typical of a small shallow sea.

Stations 3 and 4, more remote from the Atlantic and the Irish Sea, are both quieter in the microseismic range.

Note that the range in level between the quietest and noisiest sites is no more than a factor of 2.

Erik Hjortenberg

ANNUAL VARIATION OF SHORT PERIOD MICROSEISMS

It is an established fact that 3-8 second period microseisms have an annual variation with a maximum in winter and a minimum in summer. The annual variation of the microseisms of shorter period is less known, since very few publications deal with this problem. Basham and Whitham (1966) investigated 0.5 to 1.5 second period microseisms at eight Canadian seismic stations during 1962 and found a marked variation at all stations, but this variation was not consistent from one station to another. The summer levels were generally lower than the winter levels. At the Arctic stations Resolute and Mould Bay the largest monthly means occurred in September.

The present study deals with the annual variation of the microseisms in Scoresbysund, Greenland, as deduced from the routine readings of microseisms made on the short period Grenet records. These routine readings were made by measuring typical maximum values of the microseisms during a 20 minute interval. The readings were made at 0, 6, 12 and 18 hours GMT during July 1952 to June 1957. The paper speed was 30 mm per minute, and hence periods shorter than 1 second were not reported. The peak of the magnification curve was around 1 second.

The procedure used was to divide the readings into three groups according to their period and within each group to select the largest amplitude readings that occurred during one month. The results are shown on the Figure. Each square represents one monthly maximum value of microseism readings. When the number of squares for a given month is less than 5 it indicates that readings in that particular period range were not available during all of the five years. The amplitude readings given on the figure are peak to peak trace amplitudes; they may be converted to approximate peak to peak ground amplitude by applying the following

factors: 1/7000 at 1.25 seconds, 1/2000 at 2 seconds, 1/120 at 5 seconds.

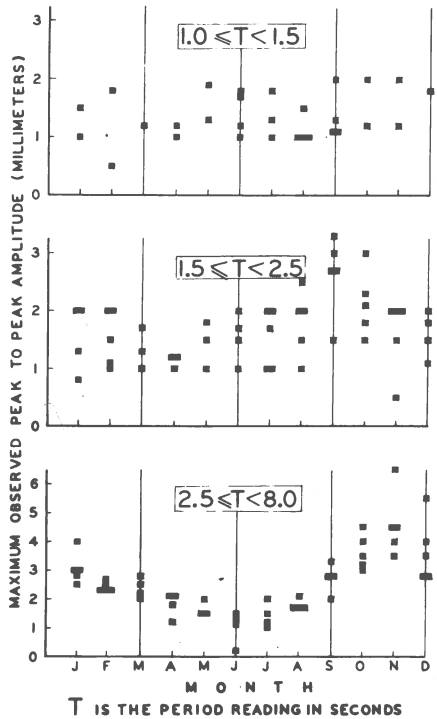

Each square represents a monthly maximum reading among the six-hourly readings of microseisms at the short-period instrument Grenet at Scoresbysund, Greenland, during July 1952 - June 1957. The readings were divided in three groups according to their period.

The reason for choosing the procedure of plotting maxima is that these are likely to represent the maximum level of the corresponding microseisms. Microseismic storms of different period ranges appeared to occur independent of each other, so whenever a maximum value of microseisms within one period range occurred it is not likely that the observer would choose to read a different period. If mean values had been formed of the amplitudes of the available readings within any of the specified period ranges, these mean values would have a strong bias as compared to a mean value

representing all the microseisms within that range and its value would be dependent on the criteria used by the observer to choose among different types of simultaneously occurring microseisms.

The following conclusions about microseisms in Scoresbysund may be deduced from the figure:

1. The annual variation of 1.0-1.4 second period microseisms is too small to show up in the present study.

2. Microseisms with periods of 1.5 to 2.4 seconds tend to increase their amplitude somewhat during September - October as compared to the level during the rest of the year.

3. Microseisms with periods of 2.5 to 8 seconds have the wellknown annual variation with a maximum in November - December.

The generation of the 1-8 second period microseisms can be assumed to be governed to a large extent by wave interaction in water, and it will hence be dependent on the winds and on the extent of the ice cover. These two factors appear to have different relative importance for the different period ranges.

Microseisms of periods 2.5 to 8 seconds have an annual variation that appears to be related to the annual variation of the wind. They suffer less attenuation than microseisms of shorter periods, and can travel for distances much longer that the few hundred kilometers, that is the extent of the ice cover near Scoresbysund.

Microseisms of periods shorter than 2.5 seconds have a much smaller annual variation. This may be due to a combination of the opposite effects of the increase of the ice cover and of the increase of the winds during winter in the source areas for such microseisms. The small increase of the 1.5-2.4 second period microseisms during September and October may indicate that in the source areas for these microseisms the increase of the ice cover generally lags a couple of months behind the increase of the autumn winds.

Reference

Basham, P.W. and Whitham, K.: Microseismic noise on Canadian seismograph records in 1962 and station capabilities. Publications of the Dominion Observatory, v.32,no.4, 1966.

L.Grinda

QUELQUES DONNEES NOUVELLES DU PROBLEME DES MICROSEISMES

L'étude des microséismes commencée il y a un demi-siècle, avance lentement car, si des corrélations entre l'apparition et l'évolution des ondes microséismiques d'une part, et l'existence de dépressions atmosphériques, les caractéristiques des houles engendrées par ces dépressions, la nature géologique des terrains traversés par les ondes au cours de leur propagation, d'autre part, ont été bien établies, la génèse de toutes les causes de production de microséismes et le mécanisme de leur action sont encore du domaine de l'hypothèse.

Nous croyons apporter une contribution utile à cette étude, en soumettant à l'examen de la C.S.E., trois informations concernant:

la nature des ondes microséismiques.
la vérification expérimentale des ondes de pression au fond de la mer.
les effets de la turbulence atmosphérique.

I - Nature des ondes microséismiques

La plupart des auteurs ont affirmé que les ondes microséismiques étaient un mélange d'ondes R et d'ondes Q. Personne ne conteste que ce soit effectivement le phénomène principal, et M.Jensen a utilisé avec beaucoup de succès cette notion dans ses déterminations d'approche des microséismes. Cependant quelques séismologues, et pour ne citer que les plus connus, Ewing, Press, Rocard, avaient émis l'idée que l'existence d'ondes longitudinales n'était pas à rejeter a priori.

Cette idée s'est révélée juste puisque nos collègues de l'U.R.S.S. ont identifié en plein continent asiatique des

ondes longitudinales dont ils ont mesuré la vitesse. M. Vinnik a donné de très bons exemples de ces mesures.

Ce point me paraît important car il explique à mon sens certains faits d'observation. En particulier ceux que j'observe depuis dix ans à Monaco, où en été, la Méditerranée étant calme, à l'échelle synoptique, la brise solaire souffle tous les jours durant deux ou trois heures. Cette brise fait naître des vagues, dans une bande étroite très près de la côte, et j'observe quelques minutes après des microséismes de 1,5 à 2 secondes de période. Il était difficile de croire à la qualité d'ondes superficielles de ces microséismes dont la source est à quelques centaines de mètres de l'observatoire.

Comment ces ondes longitudinales peuvent-elles naître sous le fond de la mer? Le Professeur Rocard et son assistant Hiéblot ont étudié ce problème dans un article des Annales de Géophysique, (1959, T15, Fas.4). Ils font remarquer que, si des ondes de pression en phase s'exercent sur le fond de la mer, sur une immense étendue, les ondes longitudinales engendrées par ces ondes de pression se propageraient dans une direction normale au fond de la mer. Pour qu'il y ait propagation oblique il faut que le diagramme de rayonnement comporte des lobes latéraux ce qui ne peut se produire que si l'aire génératrice a une largeur faible par rapport à la longueur d'onde des ondes séismiques engendrées. Ces conditions restreignent donc l'énergie propagée par les ondes longitudinales, celle qui est transmise au fond de la mer, sur une bande relativement étroite; circonstance réalisée au passage d'un front froid d'une dépression atmosphérique. MM. Rocard et Hiéblot ont calculé cette énergie et ont montré qu'elle était suffisante pour que ces ondes longitudinales atteignent de grandes distances.

Ce mécanisme qui s'ajoute aux autres, très classiques, ne préjuge pas le processus de formation des ondes de pression au fond de la mer.

Il a une conséquence qu'il faut signaler. Les ondes longitudinales ayant des périodes plus courtes que les ondes de Rayleigh, ne devraient pas les perturber, sauf si ces dernières ont des périodes relativement faibles. Dans

ce cas, il y aurait superposition et ces deux types d'ondes se propageant dans le même plan, l'élément directionnel stable de la méthode de Jensen, se trouverait renforcé. Dans un certain intervalle de temps, la distribution des ondes de Love, ayant un caractère aléatoire, la moyenne des composantes horizontales auraient donc bien la direction de l'origine. La différence de vitesse entre les ondes R et P entraînerait un décalage négligeable, dans le cas où les ondes R auraient des périodes faibles. Cependant les ondes longitudinales, ne seraient pas soumises aux réfractions latérales observées dans le cas des ondes de Rayleigh en fonction de la structure de la croûte terrestre et elles ne subiraient pas l'effet des barrières microséismiques.

II - Vérification expérimentale des ondes de pression sous la mer

La théorie de Longuet-Higgins qui a rencontré une très large approbation de la part des séismologues, semble expliquer la cause principale des microséismes à savoir, l'existence d'ondes de pression au fond de la mer, engendrées par une houle stationnaire de fréquence moitié. On ne pense jamais assez au fait que l'existence de ce genre d'ondes de pression est la conséquence d'un pur calcul, fait en 1944 par le Docteur Miche. Aucune vérification expérimentale n'a encore été faite de ces ondes de pression. Les travaux sur les microséismes auraient une base plus solide, si elle était acquise. Les océanographes qui sont intéressés par ce problème, pour d'autres raisons, experiment le même voeu.

Au Congrès d'Océanographie de Moscou, en juin dernier, je me suis entretenu de cette question avec le Professeur Munk et l'Ingénieur en chef Peluchon, qui ont utilisé l'un l'appareil Erdely en France et l'autre, l'appareil Snodgrass aux U.S.A. Ils sont depuis longtemps soucieux de mesurer ces ondes de pression au fond de la mer, aussi bien celles qui permettent de déterminer la hauteur en mer profonde des marées, que celles qui pourraient être la cause des microséismes. Voici ce qui a été décidé pendant ce congrès;

Ces deux types d'appareils qui sont en cours de révision, en vue d'augmenter leur sensibilité et la rapidité des réponses, seront essayés dès que possible. Le Docteur Munk a même invité des océanographes aux essais qui seront faits en février 1967 en Californie. Si ces essais sont concluants, les résultats en seront présentés au Congrès de l'U.G.G.I. en 1967. Ils apporteront sans doute une réponse à une question très controversée. Est-ce que des houles de grande longueur d'onde engendrent des ondes de pression sous le fond de la mer, de même fréquence qu'elles? Dans la zone intermédiaire entre les ondes de surface et les ondes longues, la pression hydrostatique peut prendre le pas sur les phénomènes dynamiques et suivre les variations de niveau des ondes marines.

III - Effets de la turbulence atmosphérique

Un certain nombre de problèmes se posent quand on veut déterminer l'aire de génération des microséismes, dans l'hypothèse que nous croyons tous exacte de la relation directe entre la mer du vent et les microséismes.

- Les microséismes naissent-ils immédiatement après l'apparition du vent?

- La mer du vent se creuse-t-elle assez rapidement pour justifier l'amplitude croissante des microséismes dès leur arrivée à une station?

- Est-ce que la prépondérance observée de l'action des fonds froids d'une dépression s'explique par les connaissances que nous avons de la houle ?

Il n'y a pas encore longtemps que les océanographes ont pu fournir une réponse affirmative à ces questions. C'est en étudiant depuis dix ans les effets de la turbulence de l'air que Miles, Philips, et Longuet-Higgins, ont éclairci tous ces problèmes au terme de très nombreux travaux théoriques, dont les références sont données ci-après.

Bien que ces travaux n'aboutissent pas toujours aux mêmes conclusions, on peut dire, sans les trahir, qu'ils reconnaissent tous:

- l'apparition d'un phénomène de résonance entre les fluctuations de pressions dues à la turbulence de l'air et les vagues formées.

- la grande rapidité de la formation des vagues quand le vent commence à souffler.

- l'accélération des phénomènes précédents dans le secteur froid des dépressions, secteur où la turbulence de l'air est maximum.

Enfin je suis heureux de faire savoir que l'Observatoire Séismologique de Monaco a actuellement trois séismographes du type Ewing-Press, pour l'étude des microséismes de longues périodes. Les séismographes L.P. de la station d'Isola à 60 km de Monaco, serviront également à cette étude. Je pense que les microséismes de longues périodes, bien que représentant une énergie faible par rapport à celle de la bande des 6 à 10 secondes, peuvent donner une image plus pure d'une aire dépressionnaire, parce que dépouillée des effets des phénomènes secondaires. Il reste à le prouver!

Bibliographie

Longuet-Higgins (1962): The directional spectrum of ocean waves and processes of wave generation (Proc.Roy.Soc. A, Vol.265, pp.286-315).

Miles (1957): On the generation of surface waves by shear flows. (Journ.Fluid Mech, 3, p.185).

(1959, a et b): On the generation of surface waves by shear flows, parts 2, 3 (Journ.Fluid Mech. 6,4 p. 568 et 583).

(1960): On the generation of surface waves by turbulent shear flows (Journ.Fluid Mech. 7,3, p.469).

(1962 a): Transient gravity wave response to an oscillating pressure (Journ.Fluid Mech. 13,1, p.145).

(1962 b): On the generation of surface waves by shear flows, part 4 (Journ.Fluid Mech. 13,3, p.433).

Philips (1957): On the generation of waves by turbulent wind (Journ.Fluid Mech. 2, p.417).

Philips (1958): The equilibrium range in the spectrum of wind-generated waves (Journ.Fluid Mech. 4, p.426).

(1960): On the dynamics of unsteady gravity waves of finite amplitude (Journ.Fluid Mech. 9, p.193),

(1962): Recent developments in the theory of wave generation by wind (Symp. on fundamental problems in turbulence, Marseille, sept. 1961, Journ. of Geoph. Research 67,8).

Pour l'ensemble des questions concernant la houle, H.Lacombe - Cours d'Océanographie physique 1965 (Gauthier-Villars, Paris).

Vlastislav Červený und Jaromír Janský

ÜBER EINIGE DYNAMISCHE EIGENSCHAFTEN DER TAUCHWELLE

Die Dynamik einiger seismischen Wellen, wie ihre Amplitudenkurven, Spektren usw., hängt wesentlich von der Existenz des Geschwindigkeitsgradienten in dem zubeobachtenden Medium ab. In diesem Beitrag diskutieren wir den Einfluss des schwachen positiven Gradienten unter der Moho-Diskontinuität auf die Dynamik der Tauchwelle.

Haben wir eine einfache einschichtige homogene Erdkruste mit der Tiefe der Moho-Diskontinuität gleich 30 km und Geschwindigkeiten der Longitudinalwellen 6,4 km/sec in der Erdkruste und 8,0 km/sec unter der Moho-Diskontinuität. Weiter werden wir voraussetzen, dass $\rho_1 = \rho_2$ - weil die Ergebnisse nicht wesentlich von ρ abhängen, und dass $v_P/v_S = \sqrt{3}$, wobei ρ_1 bzw. ρ_2 die Dichte oben bzw. unter der Moho-Diskontinuität, v_P bzw. v_S die Geschwindigkeiten der Longitudinal - bzw. der Transversalwellen sind. Wenn die Geschwindigkeit unter der Moho-Diskontinuität mit der Tiefe konstant bleibt, breitet sich längs der Moho-Diskontinuität die Kopfwelle, die Eigenschaften welcher schon gut theoretisch bekannt sind. In dem Fall, dass die Geschwindigkeit unter der Moho-Diskontinuität mit der Tiefe zunimmt (wir nehmen hier eine lineare Zunahme, das heisst einen konstanten Gradienten), breitet sich längs der Moho-Diskontinuität eine komplizierte Interferenz-Tauchwelle (Abb. 1). Die Kinematik dieser Interferenz-Tauchwelle ist, in dem Fall des schwachen Gradienten, sehr nahe der Kinematik der Kopfwelle. Die Dynamik unterscheidet sich aber ganz von der Dynamik der Kopfwelle.

Man kann die Strahlenmethode der geometrischen Seismik im Falle eines schwachen Gradienten für das Studium der dynamischen Eigenschaften der Tauchwelle nur für grosse Herdentfernungen benutzen. Für die Entfernungen, die uns aus dem Standpunkt des Studiums der Erdkruste interessieren, liefert die Strahlenmethode oft Ergebnisse, die mit grossen

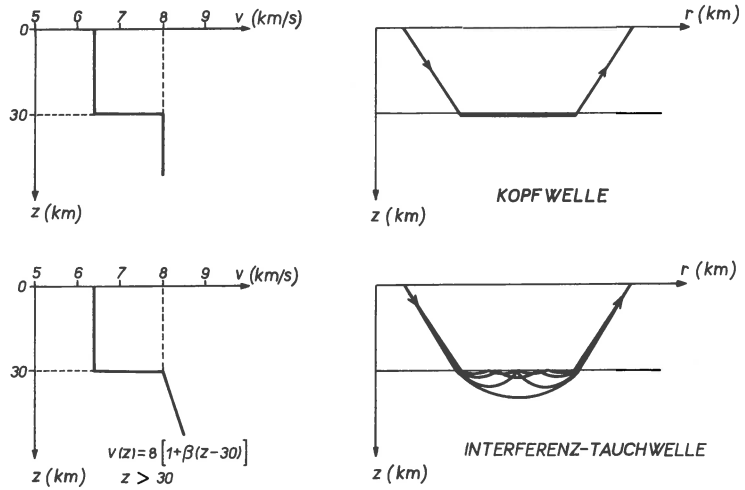

Abb. 1

Fehlern belastet sind. Mit einer Analyse der Interferenz-Tauchwelle in dem Entfernungsbereich, wo die Strahlenmethode nicht anwendbar ist, hat sich Dr.Tschekin aus dem Moskauer Institut der Physik der Erde im Jahre 1964 beschäftigt [1]. Auf seiner Theorie ist auch ein beträchtlicher Teil der weiter angefürteten Ergebnisse begründet.

Im Falle eines starken Gradienten kann sich eine Kaustik bilden und dann treten die Umkehrpunkte auf der Laufzeitkurve auf. Im Falle eines schwachen Gradienten, den wir hier diskutieren, ist dieses nicht der Fall, und die Laufzeit ist dann eine eindeutige Funktion der Entfernung.

Wenn man einen Impuls benutzt, dessen Länge begrenzt ist, scheiden sich mit der wachsenden Herdentfernung aus dem Komplex der Interferenz-Tauchwelle, der Reihe nach, die einzelnen einfachen Tauchwellen. Als erste trennt sich diejenige, die ohne Reflexion von der Moho-Diskontinuität weiter verläuft. Diese Welle nennen wir reine Tauchwelle. Als zweite trennt sich diejenige, die nur einmal von der Moho-Diskontinuität reflektiert wird, usw. Die Herdentfernung der Trennung hängt, wenn andere Bedingungen dieselbe bleiben, von der Länge des Impulses ab. In diesem

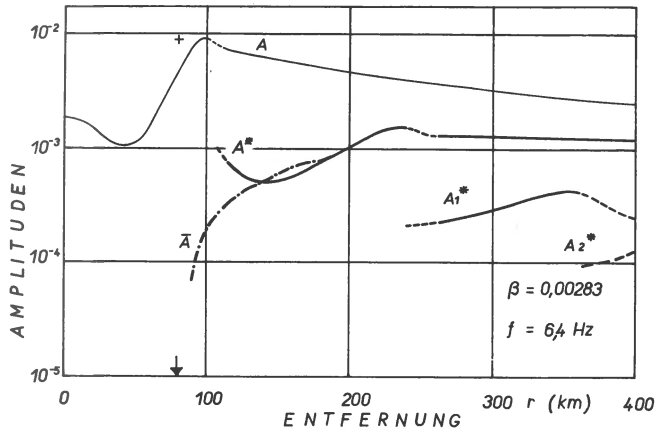

Abb. 2

Beitrag benutzen wir einen Impuls mit der Länge $\Delta t = \frac{1}{f}$, wo f die Frequenz ist.

Die Abbildung 2 zeigt die Amplitudenkurve A* der Tauchwelle, und zwar für den Gradienten $\beta = 0{,}00283\ km^{-1}$ und die Frequenz 6,4 Hz. Das Kreuz und der Pfeil zeigen die Lage des kritischen Punktes. Bis zur Entfernung 250 km ist diese Tauchwelle durch Interferenz von allen, beliebigemale von der Moho-Diskontinuität nach unten reflektierten Wellen gebildet. In dieser Entfernung trennt sich die reine Tauchwelle von dem Rest. Die Laufzeit dieses Restes ist grösser, als die Laufzeit der reinen Tauchwelle. Die Amplituden A_1^* des Restes sind wesentlich schwächer als die Amplituden A*. Ungefähr in der Entfernung 380 km trennt sich wieder eine einfache, und zwar einmal von der Moho-Diskontinuität nach unten reflektierte Tauchwelle. Der neue Rest hat die Amplituden A_2^*. Und so geht es weiter. Weil die Amplituden der Reste immer wesentlich schwächer sind als die Amplituden A*, werden wir weiter nur die Welle mit den Amplituden A* diskutieren. Diese Welle, die wir die Tauchwelle nennen, hat also anfangs einen Interferenzcharakter, weiter handelt es sich dann nur um die reine Tauchwelle. Für Vergleichszwecke zeigt diese Abbildung auch die entsprechende asymptotische Amplitudenkurve $\bar{A}$ der Inter-

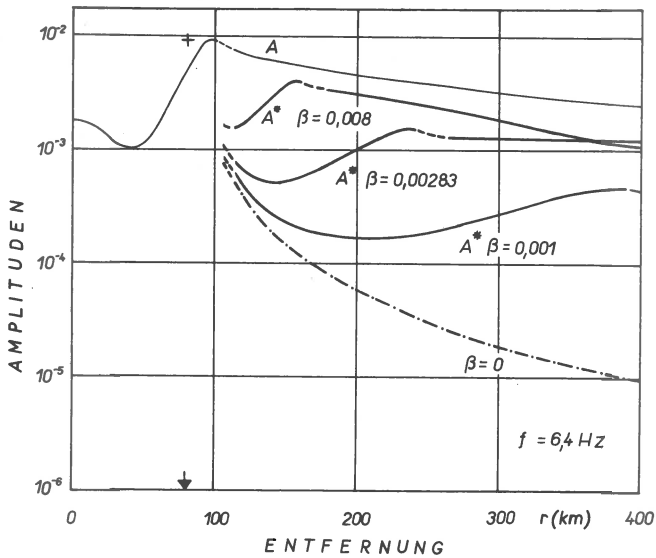

Abb. 3

ferenz-Tauchwelle (berechnet nach [2]) und die Amplitudenkurve A der von Moho-Diskontinuität nach oben reflektierten Reflexionswelle (berechnet nach [3]). Alle Trennintervalle (A von A*, A* von A_1^*, A_1^* von A_2^*) sind gestrichelt dargestellt. Unter "Amplituden" verstehen wir in diesem Beitrag die Amplituden des Potentials.

Die Abbildung 3 zeigt die Amplitudenkurven der Tauchwelle für die Frequenz 6,4 Hz und die Gradienten β = 0,008 km^{-1}, 0,00283 km^{-1} und 0,001 km^{-1}. Für den Vergleich sind im Bild auch die Amplitudenkurve der Kopfwelle (β = 0) und die Amplitudenkurve A der Reflexionswelle dargestellt. Man sieht, dass die Amplituden A* mit der Entfernung zuerst abnehmen, dann wachsen sie bis zu einem absoluten Maximum an und weiterhin nehmen sie langsam ab. Die Form der Amplitudenkurve der Tauchwelle und hauptsächlich die Lage und die Höhe des Maximums ändern sich mit dem Gradienten. Für alle unsere β sind die Amplituden der Tauchwelle beträchtlich grösser, als die Amplituden der Kopfwelle. Auch die Form der Amplitudenkurve der Tauchwelle

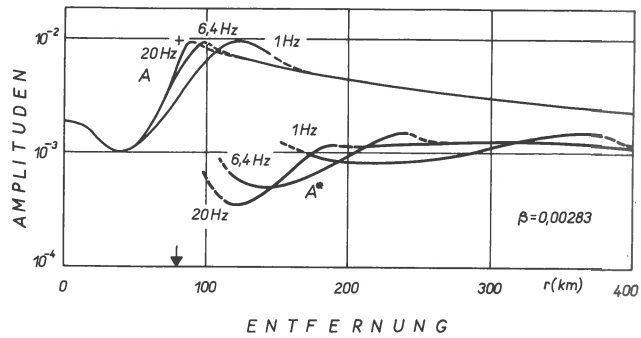

Abb. 4

unterscheidet sich mit ihrem charakteristischen Maximum wesentlich von derjenigen der Kopfwelle.

Die Abbildung 4 zeigt den Einfluss der Frequenz auf die Amplitudenkurve der Tauchwelle. Der Gradient ist in diesem Falle 0,00283 km^{-1} und die Frequenzen: 20 Hz, 6,4 Hz und 1 Hz. Je niedriger die Frequenz ist, um so mehr entfernt sich das Maximum vom Herdpunkt und die charakteristische Amplitudenerhöhung verläuft langsamer. Die absolute Höhe des Maximums ändert sich nicht viel. Wegen Vergleichs sind hier die Amplitudenkurven A der Reflexionswelle wiedergegeben. Diese ändern sich natürlich auch mit der Frequenz.

Das Maximum der Tauchwelle kann natürlich für geeignete Parameter auch grösser als das Maximum der Reflexionswelle werden.

Jetzt noch einige Bemerkungen zu dem Spektrum der Tauchwelle. Aus der Theorie ist bekannt, dass im Spektrum der Kopfwelle die überwiegende Frequenz niedriger ist als die im Spektrum der Reflexionswelle. In dem Fall der Existenz eines schwachen Gradienten unter der Moho-Diskontinuität erhalten wir ein abweichendes Ergebnis. Das Spektrum der Tauchwelle ändert sich diesmal so, dass die überwiegende Frequenz für einen Entfernungsbereich höher sein kann, als diejenige der Reflexionswelle.

Literaturangabe

[1] Chekin, B.S.: O vliyanii maloy neodnorodnosti prelomlyayushchey sredy na golovnuyu volnu. Izvest. Akad. Nauk USSR, Fizika Zemli, No.3 (1965), 1-10.

[2] Červený, V., Janský, J.: The amplitudes of seismic body waves propagating in the Earth's crust. Communication at the E.S.C.Meeting, Budapest 1964.

[3] Červený, V.: Simplified relations for amplitudes of spherical compressional harmonic waves reflected from plane interface. Studia geoph. et geod. 7 (1963), 337-352.

Yu.V.Riznichenko

EARTHQUAKES AS A DISPLAY OF THE EARTH'S CRUST AND MANTLE FLOW

Tectonic movements of the Earth's masses, if considered in a large space and time region, could be compared macroscopically to a flow of a viscous liquid. Really continuous elastic and plastic deformations of the Earth's masses are accompained by fracturing, breaks and faults, i.e. earthquakes of various magnitudes, from quite small up to catastrophic ones. They form together the microstructure of the "flow". Deformations released from a multiplicity of earthquakes constitute a substantial part of the macroscopic flow.

Perhaps, the first step on this way of thinking was done by H.Benioff [1-3]. His approach was widely used later on by many others ([4-7] and others). As a measure of deformation for a sequence of earthquakes $i = 1, 2, 3, \ldots, n$ Benioff used a sum like $\sum_{i=1}^{n} \sqrt{E_i}$, where the seismic energy of the earthquake-source of a shear type (Reid-Benioff's model [8])

$$E_i = \frac{\tau_{max}\, \varepsilon_{max}}{2} V_i = \frac{\mu \varepsilon_{max}^2}{2} V_i \quad , \qquad (1)$$

ε_{max}, τ_{max} = elastic strain and stress under brittle breakage (strength characteristics), μ = elastic shear modulus, V_i = volume of the source.

This presentation seems to be a reasonable one, at least as a zero approximation, when one describes a process of macroscopic shear deformation of a fault region and when the seismic process consists of a repetition of cracks along the fault, each of them being of the same magnitude. But already K.Tsuboi [9] and thereafter some others [10] pointed out that the physical meaning of a sum $\sqrt{E_i}$ as a

representation of some "strain" in a macroscopic region cannot be applied if one goes to summarise earthquakes of uneven magnitudes with various values of E_i and V_i.

Newly a large set of studies of seismic regime of regions has been conducted in the Sovjet Union, where a regime has been considered as a space and time multitude of earthquakes of various magnitudes $K = \log E$, K varying within large limits $-\infty < K \leq K_{max}$, and an average number N of earthquakes per unit of volume (or area) and time being established as a function of K from observations and known as a statistical "law of earthquake recurrence" $N = N(K)$ ([10-13] and others). For a seismic regime in this sense Benioff's approach fails and has to be replaced by another one.

Our first attempt to develope a more sound approach to the problem was described in [14, 15]. Among others the following assumptions were adopted there: 1) that the elastic shear strain energy accumulated by an earthquake's source before the break releases fully when breaking; 2) that all the energy dissipated by the macroscopic flow is a seismic energy. On our way to improve this approach a possibility is discussed below to eliminate these two limitations.

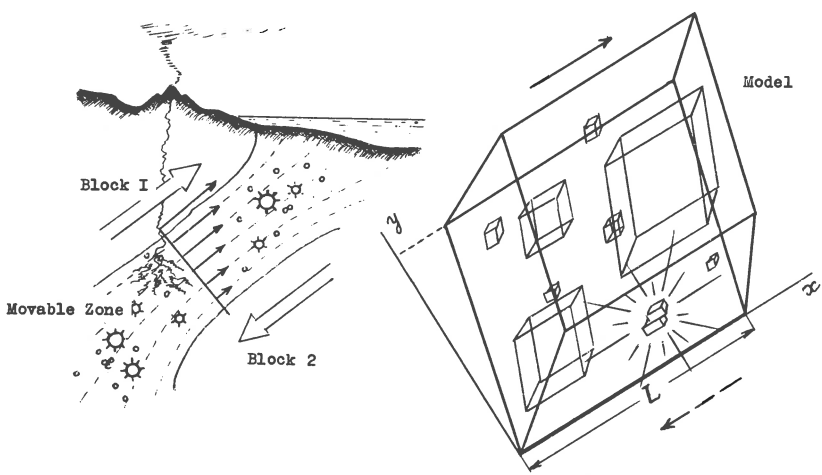

Fig. 1. Earth's flow and its model.

Here we take essentially the same model [14-16] of a medium where the seismic flow takes place (Fig. 1). It consists of a viscous material in which are intruded sporadically arising and disappearing elastic and brittly breakable elements - shear type earthquake sources [8] of various magnitudes K. They are distributed over K in accordance with the recurrence law N = N(K).

If the elastic energy of shear stress does not fully release then instead of (1) we must write

$$E_i = \frac{\tau_{max}\,\varepsilon_{max} - \tau_o\varepsilon_o}{2} V_i , \qquad (2)$$

where τ_o and ε_o are stress and strain remaining unreleased. By modifying the calculations [15] for this case we may find the part of the shear deformation of the macrovolume Fig. 1, which is due to displacements of masses (volumes) of the elastic elements. Density is supposed to be constant and the seismic regime stationary.

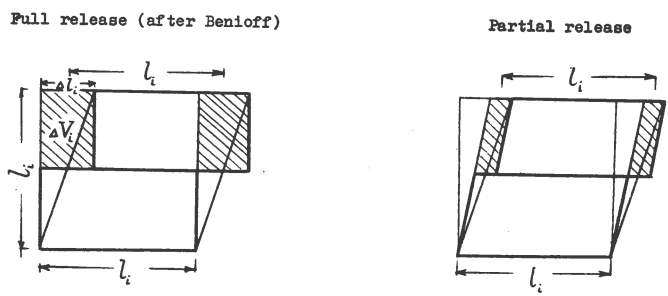

Fig. 2. Release of stress, strain and energy by an earthquake source.

Deformation and breaking at the source under a full release occurs as it is shown in Fig. 2. The volume shifted (it is shaded in Fig. 2) $\Delta V_i = (\varepsilon_{max}/2)l_i^3$, and the length of its transportation is l_i. When the release is not full, the transportation segment remains the same l_i, but the volume displaced converts into

$$V_i = \frac{\varepsilon_{max} - \varepsilon_o}{2} l_i^3 . \qquad (3)$$

The shift ΔL of the centre of masses of the macrovolume, due to shifts of masses in the sources, we find from

$$\Delta L = \frac{\sum \Delta V_i l_i}{V} , \qquad (4)$$

where $V = L^3$ (see Fig. 1), and $V_i = l_i^3$ (see Fig. 2). Assuming the shift ΔL to have happened during the time interval T, the velocity v of displacement of the centre of masses of the macrovolume, due to seismicity, equals $\Delta L/T$, and the velocity of shear deformation, or otherwise the gradient of the velocity of the flow, is $\dot{\varepsilon} = 2v/L$. We may put here $L = 1$ without reducing the plenitude of results. When inserting ΔV_i from (3) into (4) and taking into account (2), we find

$$\Delta L = \frac{1}{2V} \sum(\varepsilon_{max} - \varepsilon_o) l_i^4 = \frac{1}{2V} \sum(\varepsilon_{max} - \varepsilon_o) V_i^{4/3}$$

$$= \frac{1}{2V} \sum(\varepsilon_{max} - \varepsilon_o) \left[\frac{2 E_i}{\tau_{max}\varepsilon_{max} - \tau_o\varepsilon_o} \right]^{4/3} .$$

Whence, under all the assumptions made, the velocity of the shear deformation of the macrovolume is

$$\dot{\varepsilon} = \frac{2v}{L} = \frac{2\Delta L}{T} = \frac{1}{VT} \sum(\varepsilon_{max} - \varepsilon_o) \left[\frac{2 E_i}{\tau_{max}\varepsilon_{max} - \tau_o\varepsilon_o} \right]^{4/3} ,$$

or in an integral form

$$\dot{\varepsilon} = 2^{4/3} \int_{-\infty}^{K_{max}} \frac{(\varepsilon_{max} - \varepsilon_o)}{(\tau_{max}\varepsilon_{max} - \tau_o\varepsilon_o)^{4/3}} N E^{4/3} \, dK. \qquad (5)$$

And this is the final result as regards the value of the velocity of the shear deformation $\dot{\varepsilon}$ of the macrovolume, which is due to the "seismic flow" in it. The value $\dot{\varepsilon}$ is given here as a function of elastic and strength properties of the seismic elements (sources), and of parameters of the

seismic regime, which is defined by the occurrence law $N = N(K)$; $K = \log E$, where E is the seismic energy of a source and K_{max} is the value of a maximum possible earthquake in a given region.

In a particular case of full release, $\varepsilon_o = 0$, $\tau_o = 0$, formula (5) converts into one given in [14, 15]. In contrast to [14, 15] expressions with τ_{max}, ε_{max}, τ_o, ε_o are kept here under an integral sign, having in mind they may depend on K (τ_{max} and ε_{max} for great earthquakes could possibly be smaller that for weak ones; the share of deformation released $\varepsilon_o/\varepsilon_{max}$ may also depend on K).

If all the macroscopic flow of the Earth's material, that is its "tectonic flow", is due only to breaks, that is consists only of the seismic flow, then the value $\dot{\varepsilon}$, expressed by (5), may be, at least in principle, established strightly from geodetic, tiltmeter, geological, geomorphological or other similar measurements. But in the general case the velocity of deformation $\dot{\varepsilon}$, which is due to seismicity, may constitute only a certain part p ($0 \leqq p \leqq 1$) of the velocity of deformation $\dot{\varepsilon}_T$ of the complete tectonic flow, thus

$$\dot{\varepsilon} = p\dot{\varepsilon}_T \quad \text{or} \quad \dot{\varepsilon}_T = \dot{\varepsilon}/p\,. \tag{6}$$

This is due to the presence of a viscous material in our model of medium, in addition to elastic, brittly cracking elements, earthquake sources, belonging to it. In another variant the sources themselves might be supposed to be non-ideally elastic.

The role of seismicity in the motion of the Earth's material may be thought to increase with the rise of the total velocity of deformation, and not only absolutely but also relatively. The level of a seismic process may be characterized by the total flux of the seismic energy of earthquake sources per unit of space and time

$$w_S = \int_{-\infty}^{K_{max}} NE\, dK\,. \tag{7}$$

The coefficient p in (6) may be thought to increase with the rise of w_S.

Let us examine now the interrelations among deformation (5), (6) and energy (7) values on one hand, and on the other hand, the macroscopic shear stresses acting in the medium.

To model the tectonic flow of the medium as a whole by the viscous flow of a Newtonian liquid, we may write

$$\tau_T = \eta \dot{\varepsilon}_T , \tag{8}$$

where τ_T is an overall shear tectonic stress and η is an effective viscosity. An energy dissipated in course of the process is

$$w_T = \tau_T \dot{\varepsilon}_T . \tag{9}$$

Comparing (8) and (9) with the previous equations we may, under some additional suppositions, tie the seismic values with the macroscopic values of stress τ_T and viscosity η .

It is reasonable to regard the seismic energy w_S (7) as constituting some part q ($0 \leqq q \leqq 1$) of the total energy w_T (9) dissipated by the tectonic flow

$$w_S = q w_T \quad \text{or} \quad w_T = w_S/q . \tag{10}$$

The value q, as in the case of p, may be thought to increase with w_S (7).

From (9), (10) and (6) we get the value of the overall shear tectonic stress τ_T, expressed in terms of seismic indices

$$\tau_T = \frac{w_T}{\dot{\varepsilon}_T} = \frac{p}{q} \frac{w_S}{\dot{\varepsilon}} , \tag{11}$$

where w_S and $\dot{\varepsilon}$ are given by (7) and (5).

Finally, knowing τ_T from (11), and $\dot{\varepsilon}_T$ from (6) and (5), we may find from (8) the value of the effective macroscopic viscosity η of the medium

$$\eta = \frac{\tau_T}{\dot{\varepsilon}_T} \qquad (12)$$

expressed by the same indices. Maybe it is worth while to point out here that this value of viscosity η corresponds mainly to that separate part of the crust or upper mantle, where the observed seismic process takes place. Up to now geophysicists have known means to judge about viscosity mostly of much larger volumes, such as the mantle as a whole (in the case of earth-tide studies), or for large parts of it (as in case of the post-glacial uplift).

The equations (11), (12) for the macroscopic stress τ_T and viscosity η turn into those derived earlier [14, 15] in a special case when all the tectonic flow is supposed to consist of the seismic flow, i.e. when $p = q = 1$, and when the release is full $\varepsilon_o = 0$, $\tau_o = 0$.

Thus we found here, in frames of a definite model of construction and properties of a medium, some more general formulae connecting macroscopic indices of tectonic, especially seismic flow of the medium - the average velocity of deformation, the overall tectonic stress, the effective viscosity - with the properties of its elements, sources of future earthquakes, as well as with parametres of the seismic process, including the law of earthquake recurrence.

Formula (5) for the velocity of deformation at the seismic flow specifies an old aspiration of H.Benioff and others for estimation of the total deformation of the medium as a whole by summation of a sequence of deformations released in course of the seismic process.

The study presented here should help us in the attempts to solve the problem of evaluating tectonic stresses τ_T, and of calculating the maximum possible earthquakes K_{max} in a given region, on the basis of a joint use of seismological, geological, geodetic and some other data.

References

[1] Benioff, H. Earthquakes and rock creep. Bull.Seism. Soc.Am., 41, No.1, 31-62, 1951.

[2] Benioff, H. Global strain accumulation and release as revealed by great earthquakes. Bull.Geol.Soc.Am., 62, 331-338, 1951.

[3] Benioff, H. Crustal strain characteristics derived from the earthquake sequences. Trans.Am.Geophys.Un., 32, No.4, 1951.

[4] Ritsema, A.R. The seismicity of the Sunda arc in space and time. Indonesia Madjalah Ilmu Alam, 110, 41-49, 1954.

[5] Benioff, H. Mechanism and strain characteristics of the White Wolf fault as indicated by the aftershock sequence. Bull.California Div.Mines, 171, 199-202, 1955.

[6] Amand, P.,St. Two proposed measures of seismicity. Bull. Seism.Soc.Am., 46, No.1, 41-45, 1956.

[7] Allen, C.R., Amand, P.St., Richter, C.F. and Nordquist J.M. Relationship between seismicity and geologic structure in the Southern California region. Bull. Seism.Soc.Am., 55, No.4, 753-797, 1965.

[8] Benioff, H. Earthquake source mechanisms. Science, 143, No.3613, 1399-1406, 1964.

[9] Tsuboi, C. Earthquake energy, earthquake volume, aftershock area, and the strength of the earth's crust. Journ.Phys. of Earth (Tokyo), 63-66, 1956.

[10] Bune, V.I. and others. Methods of a detailed study of seismicity. (in Russian). Trudi Inst.fiziki Zemli Ac. Sci.USSR, No.9, 1960.

[11] Riznichenko Yu.V. On a study of the seismic regime (in Russian). Izvestiya Acad.Sci. USSR, Ser.geofiz., No.9, 1057-1074, 1958.

[12] Riznichenko, J.V. On quantitative determination and mapping of seismic activity. Annali di Geofisica (Roma), 12, No.2, 227-237, 1959.

[13] Riznichenko, Yu.V. and Nersessov, I.L. A detailed study of the seismic regime in the Garm epicentral region. Annali di Geofisica (Roma), 15, No.12, 173-186, 1961.

[14] Riznichenko, Yu.V. A dependance between the flow of earth's masses and seismicity, (in Russian). Dokladi Acad.Sci. USSR, 161, No.1, 97-99, 1965.

[15] Riznichenko, Yu.V. On seismic flow of the earth's masses (in Russian) in a book: Dinamika zemnoy kori. "Nauka", Moscow, 56-63, 1965.

[16] Riznichenko, Yu.V. On energy sense of the earthquake recurrence law (in Russian). Izvestiya Acad.Sci.USSR, Fizika Zemli, No.10, 7-16, 1965.

R.Schick and G.Schneider

THE PROPAGATION OF SEISMIC PULSES IN MEDIA WITH VARIABLE VELOCITY

Abstract

The propagation of ultrasonic pulses in paraffin plates is studied and compared with earthquake records. Paraffin is a suitable substance to realize velocity gradients and finely layered media, since the velocity of elastic waves depends strongly on temperature.

Introduction

There is quite some evidence now that the velocity distribution in the Earth's interior does not show only sharp discontinuities (as the Earth's core boundary for instance) but also transition zones where the velocity gradient has a finite value. For example: the transition layer between the inner and the outer part of the Earth's core, the low velocity layer in the upper mantle, and the velocity gradient in the uppermost part of the Variscean basement. It is still quite doubtful whether the "Moho" is a discontinuity of first or second order. Deciding between first and second order discontinuities is, however, just a matter of considering the relation between the used wave lengths and the thickness of the intermediate layer, which is embedded between two halfspaces of constant velocity.

In the case of thin transition layers it is very difficult to derive a velocity gradient from travel time measurements. Therefore, it should be useful to get some more information from the study of pulses after transmission or reflection from such a layer. Theoretical study of these processes is in the general case quite difficult and therefore we undertook some model seismic experiments concerning this problem.

Methods

There exist already some different techniques to realize the before-mentioned velocity distributions. J.Oliver (1956) used bimorphe two-dimensional models, which consisted of two wedges of varying thickness glued together. To avoid disturbances from air bubbles at the interface, another method was preferred. In paraffin the velocity of elastic waves depends strongly on temperature. Models of this kind were proposed by L.N.Rykunov and others (1961).

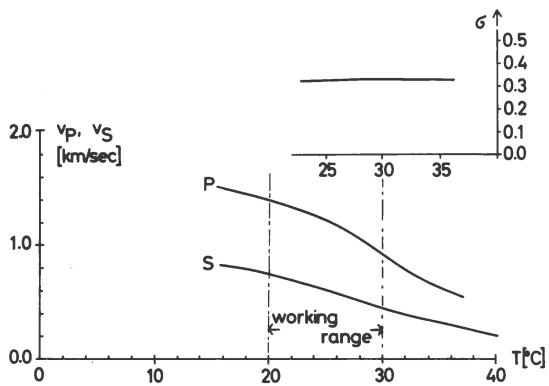

Fig. 1. Velocities in a Paraffin Plate.

In the first experiment the relation between temperature and velocity of P- and S-waves was studied (Fig. 1). We see from this figure that in the used temperature range between 20° and 30°C there is a velocity variation of about 40%. Poisson's number remains constant inside the used interval. For frequencies lower than 20 KHz the absorption coefficient is practically independent of temperature in the used working range. For frequencies up to 100 KHz the differences are less than 10%.

Electric heating and thermo-isolation plates were used to get the respective temperature fields, and accordingly the velocity distributions. Fig. 2 shows the experimental arrangement and some typical velocity profiles. To exclude and to check the effects caused by spherical wave fronts,

we used in addition a line source transducer for producing plane waves.

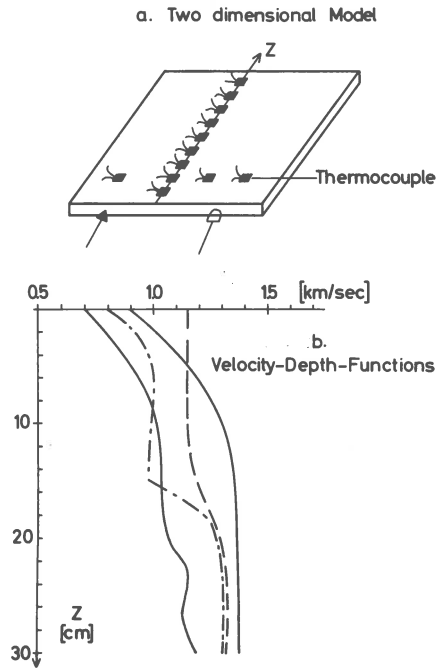

Fig. 2a and 2b.

Comparison between theory and model experiments for a one-dimensional case with normal ray incidence

Fig. 3a shows the relation between the values of reflection and transmission coefficients as a function of wave-number times layer thickness. For very short wave-lengths the reflection coefficient becomes zero and the transmission coefficient approaches one.

For very long wave lengths, both the reflection and transmission coefficient take on the value which can be expected for a sharp boundary.

As can be seen from Fig. 3b, there is only a small difference in the shape of pulses transmitted through a homogeneous halfspace and through a two-layered medium with the

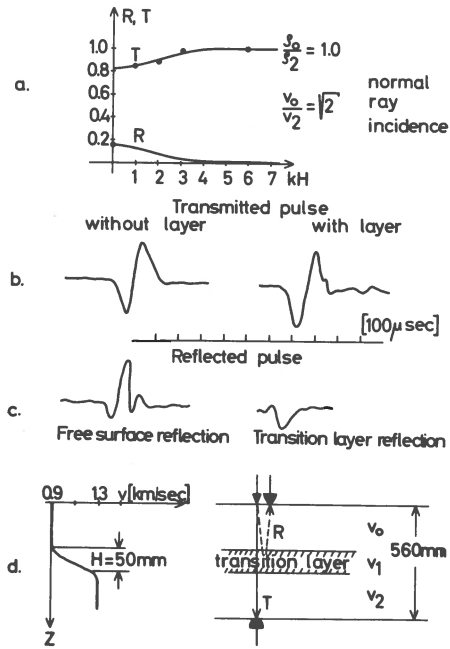

Fig. 3a, b, c and d.

given transition zone. This, however, is evident from Fig. 3a, where the measured coefficients for the different wave numbers in the frequency spectrum are plotted. Theoretical studies by I.Onda (1965) show that the dispersion of body waves only reaches measurable values in the case of a very high velocity contrast (for instance $\mu_1 : \mu_2 = 1:14$), or an accordingly long wave path (K.Sezawa and K.Kanai, 1935). On the other hand, in the case of a pulse reflected from a transition zone (Fig. 3c) there is a prominent, relative increase of low frequency amplitudes. The comparison of spectra was made with a free-surface reflection having travelled the same distance (Fig. 3c, left side). The behaviour of the reflection coefficient in Fig. 3a predicts clearly this effect.

Study of different inhomogeneous two-dimensional cases, with source and receiver both on the free surface

Starting with the homogeneous halfspace models, we see from Fig. 4 (left) that the model seismogram is adequate to Lamb's theoretical solution of the corresponding problem. Fig. 4 (centre and right side) makes it clear that in case of a slightly positive velocity gradient, there are the following differences compared with the homogeneous halfspace:

Firstly, there is no remarkable change in the shape of bodywave pulses.

Secondly, there is an increase of body-wave amplitudes caused by incidence angles becoming steeper in the inhomogeneous case.

Thirdly, the travel-time differences of body waves are less than 0.1 per cent compared to the homogeneous case.

Fourthly, the Rayleigh-waves are very strongly affected by even a small variation of the elastic parameters.

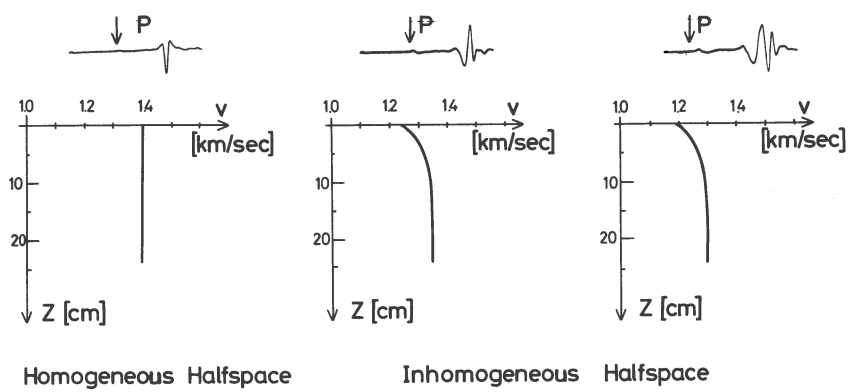

Fig. 4

It may be successful, therefore, to study the velocity gradient in the variscean basement not only by travel-times of body waves which require very accurate time measurements and high frequency pulses, but also by the dispersion of short-period surface-waves.

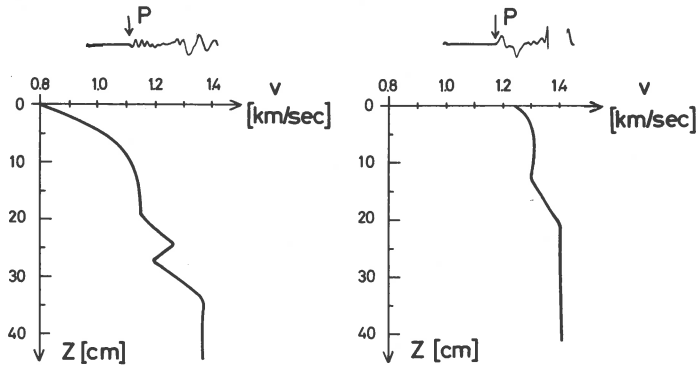

Fig. 5

Fig. 5 demonstrates more complicated velocity functions with depth. The resultant body-wave motions are of long duration and complex form, referring to the sharp and simple pulse shapes of Fig. 4.

A slight change from the monotonously increasing velocity function gives a quasi-multilayered structure with several pulses refracted along this second order discontinuities, and interfering with each other. Some interference patterns for pulses used in our models are shown in Fig.6. The third trace of this figure demonstrates that some care is necessary in interpreting second arrivals on refraction or near-earthquake seismograms. Sometimes these pulses may be the result of an interference pattern, caused by pulses having travelled through a complicated structure.

Final comparison with earthquake seismograms

1) On some near-earthquake seismograms, a pronounced reflection from the Moho-discontinuity has been recorded (Fig. 7). Comparing these reflections with a direct wave pulse that travelled the same distance as the reflected pulse, we find that the frequency content of vibrations up to about 10 Hz does not show any significant difference. Higher frequencies are unfortunately not recorded by the used seismographs. That means that the Moho-discontinuity in this region looks like a mirror for wave lengths longer

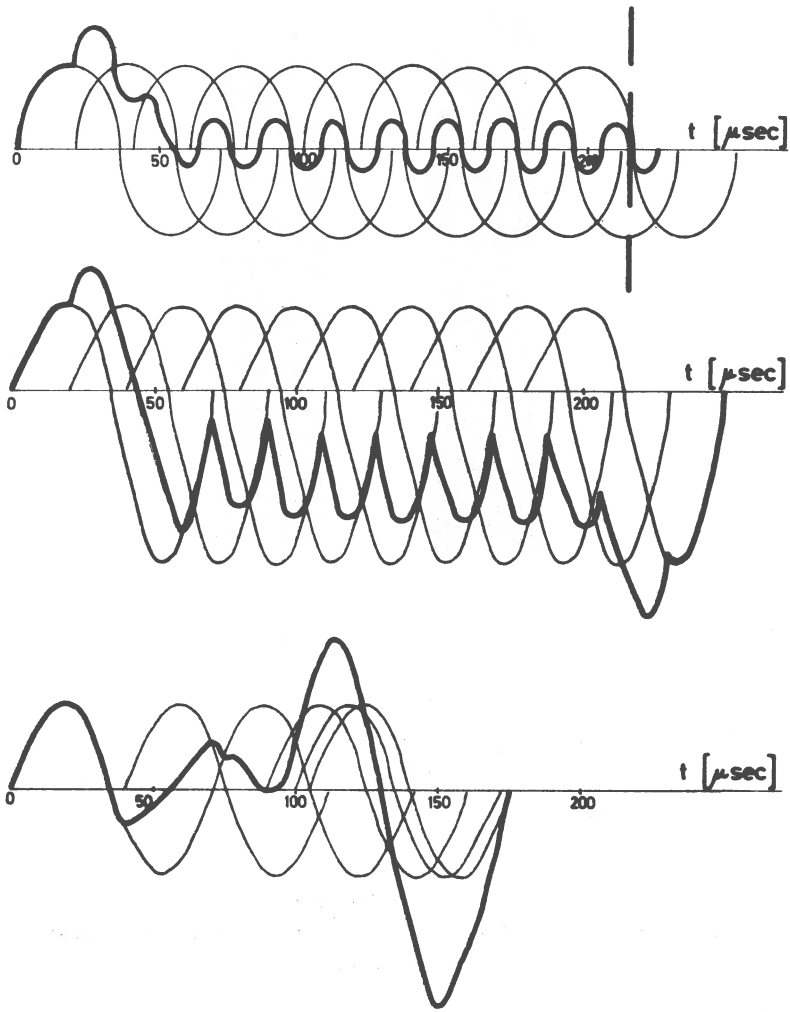

Fig. 6

than about 700 meters or in other words, the transition zone forming the "Moho" should be thinner than about 1 km.

2) First arrivals on seismograms recorded in epicentral distances between 140 and 150 degrees (Fig. 8a) show an oscillatory character which may be explained by a quasi staircase velocity function with depth in the transition zone of the Earth's core (Fig. 8b). Outside this 10°

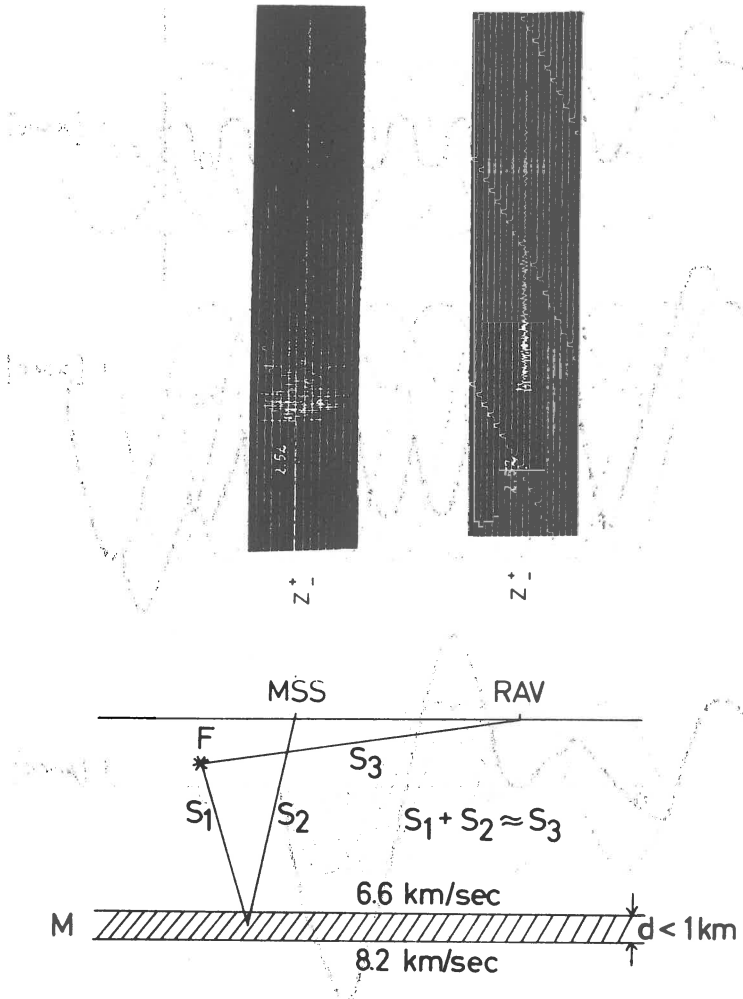

Fig. 7

interval, the PKP-phases are very simple pulses separated distinctly from one another. This behaviour of PKP could be found for all focal depths.

Acknowledgements

This report was sponsored by the Deutsche Forschungsgemeinschaft, Bad Godesberg.

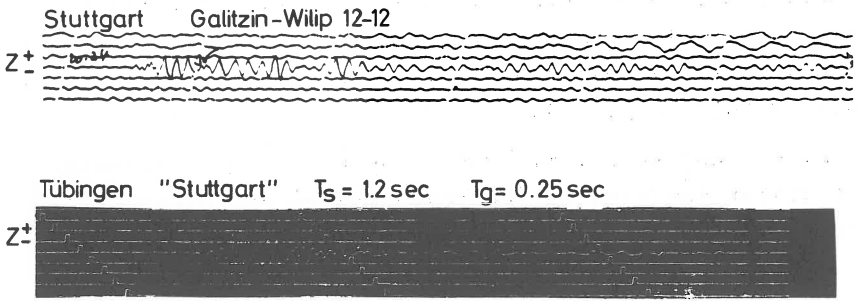

Fig. 8a

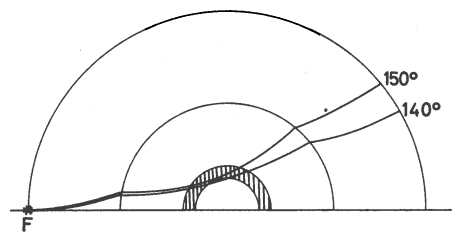

Rays through the Transition zone between Outer and Inner Core of the Earth

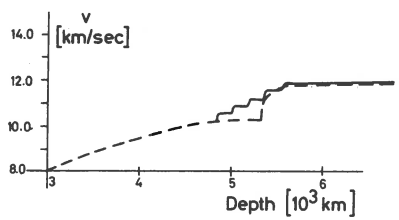

P-Velocities as a function of depth for the Earth's core after GUTENBERG and RICHTER (1951)

Fig. 8b

References

Oliver, J., 1956: Body waves in layered seismic models. Earthquake Notes 27, p.29-38.

Onda, I., 1965: Effects of intervenient boundaries on the elastic wave propagation. Bull.Earthqu.Res.Inst. 43, p.1-14.

Rykunov, L.N., Khorosheva, V.V., and Sedov, V.V., 1961: A two-dimensional model of a seismic waveguide with soft boundaries. Izvest.Akad.Sci., USSR, Geophys.Ser. Nr.11, p.1069-1071 (eng.ed.).

Sezawa, K., and Kanai, K. 1935: The effect of sharpness of discontinuities on the transmission and reflection of seismic waves. Bull.Earthqu.Res.Inst. 13, p.750-755.

Roman Teisseyre

CHAMP CONTINU DE DISLOCATION - LE PROBLEME DU PLI

Cet article traite de la méthode de solution des problèmes de déformation pour un milieu composé d'un système de couches parallèles très minces. Ce problème qui se conjugue avec le phénomène de plasticité a été résolu en se servant de la théorie du champ continu de dislocation. Cette théorie, qui est un exemple de théorie physique dans laquelle apparait la relation entre les grandeurs physiques et la géométrie, exige l'application de l'appareil mathématique de la géométrie non - Riemann avec la connexion affine avec la torsion. Au cas de répartition continue de la dislocation la non-continuité de déplacement en long d'un contour est définie par la formule

$$\Delta\vec{\xi} = \vec{i}_{\mu}\,\alpha^{\mu\nu}\,d\sigma_{\nu}$$

où: $\alpha^{\mu\nu}$ est le tenseur de densité de la dislocation donné par l'expression $\alpha^{\mu\nu} = \varepsilon^{\nu\alpha\beta}(S^{\mu}_{.\alpha\beta} + R^{\mu}_{.\alpha\eta\beta}\xi^{\eta})$; $S^{\mu}_{.\alpha\beta}$ est le tenseur de torsion, $R^{\mu}_{.\alpha\eta\beta}$ le tenseur de Riemann-Christoffel; $d\sigma_{\nu}$ - élément du surface. Dans la description de la déformation a été introduit le vecteur de déplacement élastique u_i ainsi que le tenseur de distorsion u_{ik}. Cette dernière grandeur est liée avec le tenseur de densité de dislocation par la relation qui emprunte dans l'approximation linéaire la forme:

$$\alpha_{mn} = \varepsilon_{kln}\,u_{m[k,l]}$$

La parenthèse carrée désigne l'alternance en rapport avec les index k,l. Il a été démontré que la partie antisymétrique du tenseur de distorsion $u_{[mk]}$ satisfait à l'équation de Laplace:

$$u_{[mk],ss} = 0$$

et que la partie symétrique $u_{(ki)}$ (la parenthèse arrondie désigne la symétrisation en rapport avec les index k,i) l'équation:

$$\lambda u_{(ss),i} + 2\mu u_{(ik),k} = 0$$

En s'appuyant sur le sens physique du tenseur de densité de dislocation α_{ik} on a défini le tenseur de densité des dislocations contournées Δ_{is} et on a trouvé la relation entre ces grandeurs:

$$\Delta_{is} = \varepsilon_{smk}\, \alpha_{ik,m}$$

On a démontré que cette formule est analoque à la formule connectant les fonctions subintégrales qui apparaissent dans les formules: de Burgers pour le champ de déplacement d'une dislocation unique contournée, exprimée par une intégrale de surface ainsi que de Peach-Koehler qui donne le champ de déplacements d'une dislocation unique au moyen d'une intégrale de contour.

On pourrait ainsi généraliser la formule de Nabarro entre le champ d'une infiniment petite dislocation unique contournée et le champ de deux dipôles avec un moment pour la répartition continue de dislocation, en définissant le tenseur de densité F_{iks} qui représente la répartition continue des dipôles avec moment et en analysant la dépendance de cette grandeur du champ de densité dislocations contournées Δ_{is}.

Les équations ont été adaptées au problème bi-dimensionnel du pli. On a supposé deux types des plis: le pli de type de l'anticlinal symétrique (the anticlinar concentric fold) pour lequel le déplacement élastique est présenté par la formule:

$$u = \beta\, x\, y \exp(-hr^2)$$

$$v = \beta\,(\varepsilon + |y|)\exp(-hr^2)$$

ainsi que le pli de type synclinal-anticlinal (the trough and ridge fold) représenté par la déformation élastique:

$$u = \beta x y \exp(-hr^2)$$

$$v = -\beta |y| x \exp(-hr^2)$$

Au cas d'une mince stratification du milieu la système de couches parallèles très minces définies par l'équation $d\xi_2 = 0$ pour la déformation connectée avec le déplacement en long des limites des couches on obtient le cas de répartition continue de la dislocation. En s'appuyant sur les formules précédentes, on a construit une solution pour la composante u_{11} du tenseur de distorsion, désignée dans le texte par:

$$u_{11} = \exp[A \exp(-hr^2)] \{1 - \Phi(\sqrt{\pi}\, r)\exp[C \exp(-hr^2)]\}$$

où

$$A = 2h\beta(\varepsilon + |y|)\left[y - \frac{\lambda}{\lambda + 2\mu}\frac{x^2}{y}\right], \qquad C = \frac{1}{\sqrt{h}\, r\Phi}$$

pour le pli d'anticlinal symétrique, ainsi que

$$A = 2\beta\, x|y|\left[-y + \frac{\lambda}{\lambda + 2\mu}\frac{x^2}{y}\right], \qquad C = \frac{1}{\sqrt{h}\, r\, \Phi}$$

pour le pli de type synclinal-anticlinal.

La fonction Φ présentée dans les formules est la fonction de Gauss connue dans la théorie des erreurs:

$$\Phi(z) = 2\int_0^z \exp(-t^2)dt\,.$$

Pour simplifier, on a supposé dans les calculs la condition $h \gg 1$. On a exprimé les composantes non évanescentes du tenseur de densité de dislocation α_{13} et α_{23} par la grandeur trouvée u_{11} et on a calculé le maximum conditionnel α_{13} en long de la ligne $d\xi_2 = 0$. Les résultats sont présentés dans les diagrammes. La fig. 1 représente un pli de type anticlinal symétrique et aussi un pli de type synclinal-anticlinal. Les lignes droites visibles sur les diagrammes sont les lignes des maxima de la composante α_{13}. Pour le pli de type d'anticlinal symétrique les lignes de maxima

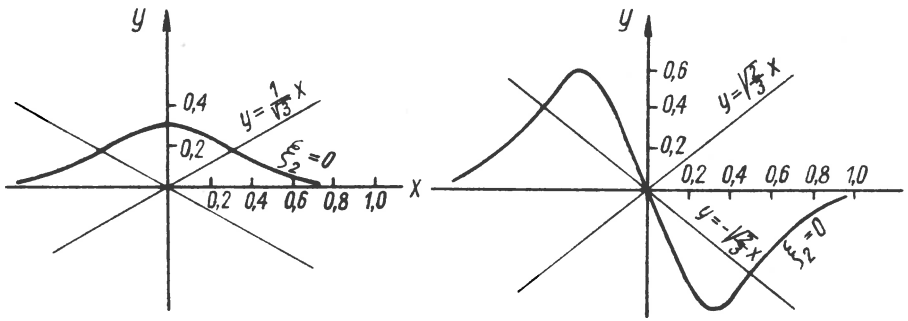

Fig. 1

sont séparées par un minimum déterminé par la droite $x = 0$. Au cas de pli de type anticlinal-synclinal les minima devraient être aussi situés à la plus élevée et la plus basse ligne de structure, c'est-à-dire avec les lignes $x = \pm \frac{1}{\sqrt{2h}}$, mais en considération de la condition $h \gg 1$ ces lignes sont déplacées vers l'axe $x = 0$. Pour la composante α_{23} on a déterminé que les maxima de cette grandeur sont des lignes verticales mais en considération de la condition $h \gg 1$ elles sont, comme plus haut, déplacées vers l'axe $x = 0$.

C'est une question de futures recherches qui pourraient élucider si les lignes des maxima peuvent se rapporter à certains plans hypocentraux des tremblements de terre.